Abstract

Gravitational and Electrostatic

Potential Fields and Dynamics of Non-spherical Systems

This thesis is devoted to several aspects of the n-body problem in the context of two models of interest: the gravitational n-body problem and the electrostatic n-body problem.

In the case of gravitational n-body problem, we study central configurations of three oblate bodies, the Hill approximation of the restricted four body problem with three oblate heavy bodies, and we find the equilibrium points of the Hill approximation and determine their linear stability. Also in the case of the gravitational n-body problem, we find equilibrium shapes of an irregular body, when the gravitational potential and the rotational potential balance each other. In particular, we find equilibrium dumbbell shapes.

In the context of the electrostatic n-body problem, we use variational methods to find approximate solutions of the Poisson-Boltzmann equation, representing the electrostatic potential produced by charged colloidal particles.

This research is motivated by applications to astrodynamics, dynamical astronomy and atomic force microscopy.

Gravitational and Electrostatic Potential Fields and Dynamics of Non-spherical Systems

by

Wai-Ting Lam

Submitted in partial fulfillment of the requirements

for the degree of

Doctor of Philosophy

in the Department of Mathematical Sciences

Yeshiva University

July, 2020

The committees for this doctoral dissertation consists of:

Marian Gidea, Ph.D, Chair of Mathematical Sciences at Stern College and Katz Graduate School; Chair of Division of Natural Sciences and Mathematics

Fredy Zypman, Ph.D, Chair of Physics at Yeshiva College and Katz Graduate School

Wenxiong Chen, Ph.D, Chair of Mathematics at Yeshiva College

Antonella Marini, Ph.D, Professor of Mathematics at Yeshiva College

Gabriel Cwilich, Ph.D, Professor of Physics at Yeshiva College; Division Coordinator of Natural and Mathmatical Sciences; Director of the Jay and Jeanie Schottenstein Honors Program

Edward Belbruno, Ph.D, Professor of Mathematics at Princeton University and Yeshiva College

Acknowledgments

I would like to express my sincere gratitude to both of my advisers Prof. Marian Gidea and Prof. Fredy Zypman for their continuous support of my Ph.D study and related researches, for their patience, guidance and timely help on preparing this thesis. Their inspiration, motivation and immense knowledge are indeed the most valuable academic resources to me and it has been my honor to have them as my mentors for my Ph.D study.

I would also like to thank Prof. Edward Belbruno , Prof. Morton Lowengrub, Prof. Pablo Roldán and the dissertation committees for sharing their prestige skills and professional knowledge with me. Their advice, discussions and comments elevate my skills to the next level.

Apart from the instructors at Yeshiva University, I would like to express my gratitude to my collaborators— Prof. Jaime Burgos-Garcia, Prof. Alessandra Celletti, Prof. Catalin Gales and Dr. Rodney Anderson, it has been one of the best learning experiences for me. Thank you for giving me insightful advice as always, and sharing ideas, suggestions and knowledge with me.

Albert Einstein said "In the middle of difficulty lies opportunity." Things and events in life are not always easy and smooth, but it is part of life. Nevertheless opportunity can knock at anytime in life; holding on to the opportunity and take it to one's fullest becomes hard. It's certainly not easy to remain focused or motivated to keep moving forward. Courage to face everything and keep everything moving is very important and I would not be able to do so without those who have assisted and motivated me throughout the years. I would not forget you all and I would take this very special moment to show them my gratitude.

To my mentors— Prof. Thomas Otway, Prof. Morton Lowengrub, Prof. Fredy Zypman and Prof. Marian Gidea, I say thank you. Thank you for seeing my potential when I didn't see it for myself. I am so grateful that the department gave me this opportunity to join the Ph.D program. Life is not easy, yet your words gave me the courage, the willpower and the tenacity to face and embrace life's hardships and keep on going with the researches. Thank you for shaping me as a research mathematician.

To my instructors— I say thank you. Thanks for your teaching. Your intellectual background made the contributions of each of you a valuable academic resource, I shall not forget the sweat and tears pooled by the mutual effort.

To the school staffs, I say thank you. Thanks for providing a great learning environment and being supportive. Without your help, my academic experience wouldn't be smooth and successful.

Of course, I would never forget about my friends and family. I say thank you. Thank you for your endless support. Thank you for always being there for me and encouraging me to strive forward. Words can not express how grateful I am to have you all in my life. Life is never easy and I thank you for your part in my journey. I truly do!

Table of Contents

Chapter 1

Introduction

This thesis is devoted to several aspects of the n-body problem in the context of the following models of interest: the gravitational n-body problem and the electrostatic n-body problem. The thesis is organized as follows. Chapter 2 includes some background information about Spherical Harmonics Expansion, which is a fundamental method to study the gravitational potential. An example of obtaining the Spherical Harmonics coefficients for an asteroid follows and we use it for the models we investigate in the later chapters in this thesis. In Chapter 3 Section 3.1.1, we recall some basic notions on central configuration. In Section 3.2, we show the existence and uniqueness of a scalene triangular central configurations of three oblate bodies, which is one of the main results in this thesis. Then we compute the positions of the bodies in such a central configuration relative to some rotating frame as a follow up. In Chapter 4, Section 4.3 we consider a restricted four-body problem, with a precise hierarchy between the bodies: two larger bodies and a smaller one, all three of oblate shape, and a fourth, infinitesimal body, in the neighborhood of the smaller of the three bodies. The three heavy bodies are assumed to move in a plane under their mutual gravity, and the fourth body to move in the 3-dimensional space under the gravitational influence of the three heavy bodies, but without affecting them. Then, assuming that these three bodies are in a scalene triangular central configuration as shown in Chapter 3, in Chapter 4 Section 4.4

we perform a Hill approximation of the equations of motion describing the dynamics of the infinitesimal body in a neighborhood of the smaller body. Through the use of Hill's variables and a limiting procedure, this approximation amounts to sending the two larger bodies to infinity. In the Section 4.5 for the Hill approximation of the four-body problem with three oblate bodies, we find the equilibrium points for the motion of the infinitesimal body and determine their linear stability. It provides another main result of this thesis. As a motivating example, we identify the three heavy bodies with the Sun, Jupiter, and the Jupiter's Trojan asteroid Hektor, which are assumed to move in a triangular central configuration.

In general the gravitational field of a body is described as a multipolar expansion involving spherical coordinates [Kau66]. Using spherical harmonic expansion leads to a very good approximation of the gravitational potential of spherical like shapes, as well as of more irregular shapes at points in space that are relatively far away from the body. However the spherical harmonic expansion does not give good approximation for the gravitational potential of irregular shaped bodies at points that are close to, or on the surface of irregular shaped bodies. Given that asteroids often have (very) irregular shapes, it is useful not only to assume that the asteroid is oblate, but also consider a more irregular shape, such as a dumbbell. We assume that the object can be modeled as an in-compressible fluid. This assumption is justify by the astronomical observation that many asteroids are 'rubble piles' formed by the aggregation of particles, which behave similarly to in-compressible fluids. In Chapter 5 we describe the shape in terms of cylindrical coordinates, which are most naturally adapted to the symmetry of the body, and we express the potential generated by the rotating body as a simple formula in terms of elliptic integrals. The equilibrium shapes that the body can attain are given by equipotential surfaces that correspond to the solution to an isoperimetric problem, which we solve via the variational method. We give an example where we apply this method to a two-parameter family of dumbbell shapes, and find approximate numerical solutions to the corresponding isoperimetric problem. We investigate the problem of determining the shape of a rotating celestial object- e.g., a comet or an asteroid- under its own gravitational field. We also describe the gravitational potential of an irregularly shaped body as a simple formula in terms of elliptic integrals. More specifically, we consider an object symmetric with respect to one axis- such as a dumbbell- that rotates around another axis which is perpendicular to the symmetry axis.

Finally in Chapter 5 we consider a special case of the electrostatic n-body problem that is described by the Poisson Boltzmann equation. We use the variational method to study the colloidal system formed by an Atomic Force Microscope Tip and a Charged Particle in Electrolyte. A variational principle to the nonlinear Poisson-Boltzmann equation in three dimensions is used to first obtain solutions to the electrostatic potential surrounding a pair of spherical colloidal particles, one of them modeling the tip of an Atomic Force Microscope. Specifically, we consider the Poisson Boltzmann action integral for the electrostatic potential produced by charged interacting colloidal particles and propose an analytical ansatz solution. This solution introduces the density and its corresponding electrostatic potential parametrically. The Poisson Boltzmann action is then minimized with respect to the parameter. Polynomial-exponential approximations for the parameters as functions of tip- particle separation and boundary electrostatic potential are obtained. With that information, tip-particle energy-separation curves are computed as well. Finally, based on the shape of the energy-separation curves, we study the stability properties predicted by this theory.

Throughout the thesis, there are works based on different models and the main results are listed as follows:

Main results of the thesis

Chapter 2

Consider a frame centered at the barycenter of the targeted body, the body rotates with the angular velocity Θ about its axis. The gravitational potential is of the form:

$$V(r,\theta,\phi) = \frac{GM}{r}\sum_{n=0}^{\infty}\left(\frac{R}{r}\right)^n \sum_{m=0}^{n} P_l^m(\sin\theta)C_{l,m}\cos(m(\phi+\Theta t)), \tag{1.1}$$

where Θ represents the frequency of the spin of Hektor. Notice that $C_{2,0}$ is time independent while $C_{2,2}$ is time dependent. However, it has averaging effect as zero if the targeted body spins fast and thus the higher order terms are neglected for the models in this thesis.

Chapter 3

We consider a system of three oblate bodies and describe the gravitational potential of each body in terms of spherical harmonics.We only retain the most significant ones, C_{20}^i (the C_{20} term for the i-body). The gravitational potential of each body in Cartesian coordinates is:

$$V_i(x,y,z) = \frac{m_i}{r} + \frac{m_i}{r}\left(\frac{R_i}{r}\right)^2\left(\frac{C_{20}^i}{2}\right)\left(3\left(\frac{z}{r}\right)^2 - 1\right) \tag{1.2}$$

where m_i is the normalized mass of the i-th body, r is the distance from an arbitrary point in space to m_i, R_i is its average radius in normalized units, and the gravitational constant is also normalized as $\mathscr{G} = 1$. Defining $C_i = {R_i}^2 C_{20}^i/2$ and $C_{ij} = C_i + C_j$, we obtain the following proposition.

Proposition 1.0.1. *In the three-body problem with all bodies oblate, for every fixed value $\bar{I}$ of the moment of inertia there exists a unique central configuration, which is in general a scalene triangle.*

Moreover, the body with the larger C_i is opposite to the longer side of the triangle, where the C_i's are assumed to satisfy some ordering e.g., $C_2 \leqslant C_1 \leqslant C_3$, then $r_{13} \leqslant r_{23} \leqslant r_{12}$.

Assuming one of the legs of the scalene triangle to be 1, we have the two legs to be uniquely determined and we denoted them having lengths of u and v. Together with the assumption of center of mass at origin and normalized mass, we have the following proposition.

Proposition 1.0.2. *In the synodic reference frame, the coordinates of the three bodies in the triangular central configuration, satisfying the constraints*

$$\begin{aligned}
(x_2-x_1)^2+(y_2-y_1)^2 &= 1,\\
(x_3-x_1)^2+(y_3-y_1)^2 &= u^2,\\
(x_3-x_2)^2+(y_3-y_2)^2 &= v^2,\\
m_1x_1+m_2x_2+m_3x_3 &= 0,\\
m_1y_1+m_2y_2+m_3y_3 &= 0,\\
m_1+m_2+m_3 &= 1,\\
y_1 &= 0,
\end{aligned}$$

are given by

$$\begin{aligned}
x_1 =& -\sqrt{m_2^2+wm_2m_3+u^2m_3^2},\\
y_1 =& 0,\\
x_2 =& \frac{-2m_2^2-2u^2m_3^2-2wm_2m_3+2m_2+wm_3}{2\sqrt{m_2^2+wm_2m_3+u^2m_3^2}},\\
y_2 =& -\frac{1}{2}\sqrt{\frac{(4u^2-w^2)m_3^2}{m_2^2+wm_2m_3+u^2m_3^2}},\\
x_3 =& \frac{-2m_2^2-2u^2m_3^2-2wm_2m_3+wm_2+2u^2m_3}{2\sqrt{m_2^2+wm_2m_3+u^2m_3^2}},\\
y_3 =& +\frac{1}{2}\sqrt{\frac{(4u^2-w^2)m_2^2}{m_2^2+wm_2m_3+u^2m_3^2}}.
\end{aligned} \tag{1.3}$$

Corollary 1.0.3. *Assume that only the body m_3 is oblate, i.e. $C_{20}^1 = C_{20}^2 = 0$. We obtain the following result: In the three-body problem with one oblate body m_3, for every fixed value $\bar{I}$ of the moment of inertia there exists a unique central configuration, which* *is an isosceles triangle with* $r_{13} = r_{23}$.

Corollary 1.0.4. *In the case when only the body of mass* m_3 *is oblate, by the Proposition we have* $r_{13} = u = r_{23} = v$, *so* $w = 1 + u^2 - v^2 = 1$, *so the formulas* (3.55) *become*

$$
\begin{aligned}
x_1 =& -\sqrt{m_2^2 + m_2 m_3 + u^2 m_3^2},\\
y_1 =& 0,\\
x_2 =& \frac{-2m_2^2 - 2u^2 m_3^2 - 2m_2 m_3 + 2m_2 + m_3}{2\sqrt{m_2^2 + m_2 m_3 + u^2 m_3^2}},\\
y_2 =& -\frac{1}{2}\sqrt{\frac{(4u^2-1)m_3^2}{m_2^2 + m_2 m_3 + u^2 m_3^2}},\\
x_3 =& \frac{-2m_2^2 - 2u^2 m_3^2 - 2m_2 m_3 + m_2 + 2u^2 m_3}{2\sqrt{m_2^2 + m_2 m_3 + u^2 m_3^2}},\\
y_3 =& \frac{1}{2}\sqrt{\frac{(4u^2-1)m_2^2}{m_2^2 + m_2 m_3 + u^2 m_3^2}}.
\end{aligned}
\tag{1.4}
$$

Chapter 4

The Hamiltonian for the restricted four-body problem is:

$$H = \frac{1}{2}(p_x^2 + p_y^2 + p_z^2) + yp_x - xp_y - \frac{1}{\omega^2}\sum_{i=1}^{3}\left(\frac{m_i}{r_i} + \frac{m_i}{r_i^3}C_i(3\frac{z}{r_i^2} - 1)\right),$$

where $C_i = {R_i}^2 C_{20}^i/2$, R_i is the average radius, C_{20}^i is the C_{20} coefficient of i-body and $r_i = ((x - x_i)^2 + (y - y_i)^2 + (z - z_i)^2)^{1/2}$. With masses $m_1 \geqslant m_2 \geqslant m_3$, we have

Theorem 1.0.5. *Transform the Hamiltonian as follows:*

(i) shift the origin of the reference frame so that it coincides with m_3*;*

(ii) perform a conformal symplectic scaling given by $(x, y, z, p_x, p_y, p_z) \to m_3^{1/3}(x, y, z, p_x, p_y, p_z)$*;*

(iii) rescale the average radius of each heavy body as $R_i = m_3^{1/3}\rho_i$ *for* $i = 1, 2, 3$*;*

(iv) expand the resulting Hamiltonian as a power series in $m_3^{1/3}$*, and*

(v) neglect all the terms of order $O(m_3^{1/3})$ in the expansion.

Then

$$
\begin{aligned}
H =& \frac{1}{2}(p_x^2 + p_y^2 + p_z^2) + yp_x - xp_y - \frac{1}{2}\Bigg[\Bigg(\frac{(1-\mu)\left(\frac{3w^2}{4} - 1\right)}{u^5} + \frac{\mu\left(\frac{3(2-w)^2}{4} - 1\right)}{v^5}\Bigg)x^2 \\
&+ \Bigg(\frac{(1-\mu)\left(\frac{3(4u^2-w^2)}{4} - 1\right)}{u^5} + \frac{\mu\left(\frac{3(4u^2-w^2)}{4} - 1\right)}{v^5}\Bigg)y^2 \\
&+ \Bigg(\frac{(1-\mu)\frac{6w\sqrt{4u^2-w^2}}{4}}{u^5} - \frac{\mu\frac{6(2-w)\sqrt{4u^2-w^2}}{4}}{v^5}\Bigg)xy - \left(\frac{(1-\mu)}{u^3} + \frac{\mu}{v^3}\right)z^2\Bigg] \\
&- \Bigg[\left(\frac{(1-\mu)c_1}{u^3}\right)\left(3\left(\frac{z}{u}\right)^2 - 1\right) + \left(\frac{\mu c_2}{v^3}\right)\left(3\left(\frac{z}{v}\right)^2 - 1\right) \\
&+ \frac{1}{(x^2+y^2+z^2)^{\frac{1}{2}}} + \frac{c_3}{(x^2+y^2+z^2)^{\frac{3}{2}}}\left(\frac{3z^2}{x^2+y^2+z^2} - 1\right)\Bigg],
\end{aligned}
\tag{1.5}
$$

where $1, u, v$ represent the sides of the triangular central configuration as shown, $w = 1 + u^2 - v^2$, $\mu = \frac{m_2}{m_1+m_2}$, and $c_i := \rho_i^2 C_{20}^i/2 = m_3^{-\frac{2}{3}} R_3^i C_{20}^i/2$, $i = 1, 2, 3$.

Numerical Results: We then obtain the equilibrium positions and their stability characters in the case of the Sun-Jupiter-Hektor system:

i) Eigenvalues of x-equilibria at $(\pm 0.6935267570, 0, 0)$

$$
\begin{aligned}
&2.5069424783, \quad -2.5069424783, \\
&2.0704830660i, \quad -2.0704830660i, \\
&1.9995877290i, \quad -1.9995877290i.
\end{aligned}
$$

Stability type: center $\times$ center $\times$ saddle.

ii) Eigenvalues of y-equilibria at $(0, \pm 7.7545750772, 0)$

$$\begin{array}{ll} 0.9890157325i, & -0.9890157325i, \\ 0.1403687326i, & -0.1403687326i, \\ 1.0013166944i, & -1.0013166944i \end{array}$$

Stability type: center × center × center.

iii) Eigenvalues of z-equilibria at $(0, 0, \pm 0.0008923544)$

$$\begin{array}{ll} -37514.04321 + 0.9999999997i, & -37514.04321 - 0.9999999997i, \\ 37514.04321 + 0.9999999997i, & 37514.04321 - 0.9999999997i, \\ 53052.86869i, & -53052.86869i, \end{array}$$

Stability type: center × complex saddle.

Analytical Results: With the tool of Hill's approximation, we are able to verify analytically the linear stability of the equilibrium positions in the case of the Sun-Jupiter-Hektor system.

Proposition 1.0.6. *Consider the equilibria on the z-axis. For $\mu \in (0, 1/2]$, one pair of eigenvalues is purely imaginary, and the two other pairs of eigenvalues are complex conjugate, with the imaginary part close to $\pm i$ for $c_1 = c_2 = 0$ and for c_3 negative and sufficiently small. The linear stability is of center × complex-saddle type.*

Proposition 1.0.7. *Consider the equilibria on the y-axis. For $\mu \in (0, 1/2]$ for $c_1 = c_2 = 0$ and for c_3 negative and sufficiently small, one pair of eigenvalues is always purely imaginary, and there exists μ_*, depending on c_3, where the other two pairs of eigenvalues change from being purely imaginary to being complex conjugate. The linear stability changes from center × center × center type to center × complex-saddle type.*

Proposition 1.0.8. *Consider the equilibria on the x-axis. For $\mu \in (0, 1/2]$, for $c_1 = c_2 =$*

0 *and for* c_3 *negative and sufficiently small, two pairs of eigenvalues are purely imaginary, and one pair of eigenvalues are real (one positive and one negative). The linear stability is of center* $\times$ *center* $\times$ *saddle type.*

Chapter 5

Consider a solid of revolution generated by $z \to f(z)$. The gravitational potential at an arbitrary point $\vec{r}$ of cylindrical coordinates (s, ϕ, z) is given by

$$U_G(\vec{r}) = -\int_{Body} \frac{G\rho}{|\vec{r} - \vec{r'}|} d^3\vec{r'}, \tag{1.6}$$

where $\vec{r'}$ is a generic point inside the body. Using the property of Bessel functions, we have

$$U_G = -2\pi G\rho \int_{-z_0}^{z_0} f(z')dz' \int_0^{+\infty} dk \frac{J_0(ks)J_1(kf(z'))}{k} e^{-k|z-z'|} \tag{1.7}$$

$$\text{Let } \mathbf{I}_{10}^{-1}(a, b, s) := \int_0^{\infty} x^{-1} J_1(ax) J_0(bx) e^{-sx} dx$$

Function $\mathbf{I}_{10}^{-1}$ is indeed known in a closed form in terms of Elliptical functions [KIB12] such that

$$\mathbf{I}_{10}^{-1}(a, b, s) = \frac{1}{\pi a}\left[\frac{2\sqrt{ab}}{\kappa}\mathbf{E} + (a^2 - b^2)\frac{\kappa}{2\sqrt{ab}}\mathbf{K}\right] + \frac{s}{\pi a} sgn(a-b)\Lambda - \frac{s}{a} H(a-b), \text{where} \tag{1.8}$$

$$\kappa = \tfrac{2\sqrt{ab}}{\sqrt{(a+b)^2+s^2}} \quad \nu = \tfrac{4ab}{(a+b)^2} \quad H(a-b) = \begin{cases} 0 & \text{if } a - b < 0 \\ 1 & \text{if } a - b \geqslant 0 \end{cases}$$

$$\mathbf{K} = \mathbf{K}(\kappa) \qquad \mathbf{E} = \mathbf{E}(\kappa) \quad \Lambda = \Lambda(\nu, \kappa) = \tfrac{|a-b|}{a+b} \tfrac{s}{\sqrt{(a+b)^2+s^2}} \mathbf{\Pi}(\nu, \kappa)$$

Proposition 1.0.9. *The gravitational potential at a point of cylindrical coordinates* (s, ϕ, z) *exerted by a body generated by revolving the graph of* $z \to f(z)$, $|z| \leqslant z_0$ *is* *given by*

$$U_G = -2\pi G\rho \int_{-z_0}^{z_0} dz'\, f(z')\boldsymbol{I}_{10}^{-1}(f(z'), s, |z - z'|). \tag{1.9}$$

Considering the rotation of the body about the s-axis, total potential is expressed as the sum of gravitational potential and a non-inertial rotational potential. Consider the family of shapes

$$f(z) = \gamma\sqrt{\left(1 - (z/z_0)^2\right)\left(1 + (\beta/(1-\beta))\,(z/z_0)^2\right)} \tag{1.10}$$

$$\begin{aligned} U_{Total} = &- 2\pi G\rho \int_{-z_0}^{z_0} dz'\, f(z')\mathbf{I}_{10}^{-1}(f(z'), f(z), |z - z'|) \\ &- \frac{1}{4}f^2(z)\omega^2 - \frac{1}{2}z^2\omega^2 \end{aligned}$$

For each ω we compute the potential at each location of z for fixed γ and β. We aim to find the nominally constant potential by comparing minimum values of the normalized standard deviation $\sigma/(|\mu|)$ for fixed γ and β.

For this isoperimetric problem, in Section 5.3, for $\omega = 0.1, 0.2, ..., 1.0$ we find the values at the parameters γ and β for which $\sigma/(|\mu|)$ attains relatively small values, and we generate the corresponding shapes.

Chapter 6

Consider a colloidal system, we aim to investigate the interaction energy, which is described by Poisson Boltzmann Equation, between two particles. With the charge density of the solvent, we have:

$$\bigtriangledown^2\Phi(R) = -(\frac{8\pi M e_c}{\epsilon})\sinh(\frac{e\Phi(\mathbf{r})}{k_B T}), \tag{1.11}$$

where M is the ion bulk concentration of electrolyte, T is the absolute temperature, e the ion charge magnitude of anions and cations, ϵ is the dielectric constant of the surrounding fluid and k_B is the Boltzmann's constant. Considering the dimensionless form: [McL89]

$$\bigtriangledown^2 \varphi = -\sinh \varphi \tag{1.12}$$

where φ represents the dimensionless electrostatic potential.Equation (5.91) can be derived from a variational principle, by applying Euler-Lagrange to the action

$$I = \int_{Space} [\frac{1}{2} \mid \bigtriangledown \varphi \mid^2 + \cosh(\varphi) - 1] dV \tag{1.13}$$

where V is the volume. The minimum of I occurs for the function φ that satisfies the Euler-Lagrange equation, which gives rise (5.91). We propose an ansatz for the density and corresponding electrostatic potential which depends on the parameter k,

$$\varphi(\eta, z) = \varphi_0 e^{-\frac{k}{2}[\sqrt{(z-\frac{d}{2})^2+\eta^2}-\frac{1}{2}][\sqrt{(z+\frac{d}{2})^2+\eta^2}-\frac{1}{2}]} \tag{1.14}$$

where φ_0 is the Dirichlet boundary condition, d is the center-to-center separation between the two spherical colloids and k is a constant refers to an inverse Debye length times the radius of the interacting particles. The functional forms for the k_{best}

$$k_{best} = (A(\varphi) - 0.1) e^{\frac{B(\varphi)}{A(\varphi)-0.1} d} + 0.1 \tag{1.15}$$

where $A(\varphi)$ is the polynomial approximation between the linear parameter-η-intercepts and φ_0, $B(\varphi)$ is the polynomial approximation between the other linear parameter-slope and φ_0, and d is the separation. Notice that $A(\varphi)$ and $B(\varphi)$ are known explicitly. Furthermore, we obtain the energy as a function of separation d [HC92]

$$E_\varphi(d) = \frac{1}{2} \int_{Space} dr \rho_\varphi(d) V_\varphi(d) \tag{1.16}$$

where to recall ρ is density and φ is voltage, which are now known from the previous section. For each boundary condition, the integral is performed for the corresponding optimal value of k and thus provides the sought sphere-sphere energy-separation curves. For each boundary condition, the integral in (6.16) is performed for the corresponding optimal value of k. Equation (1.16) then provides the sought sphere-sphere energy-separation curves as shown in Figure 1.1. Based on the shape of the curves, we can draw conclusions regarding the stability properties predicted by this theory.

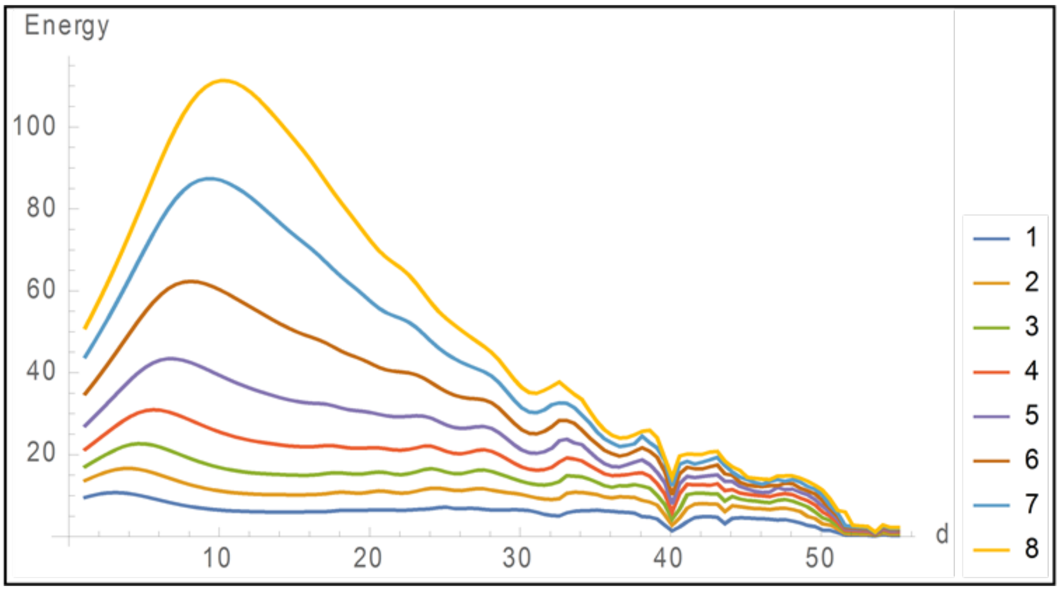

Figure 1.1: The energy-separation curves for φ_0 from 1 to 8.

Chapter 2

Gravitational Potential -Spherical Harmonics Expansion

This chapter is devoted to the exposition of some basic notions concerning the gravitational potential expressed in spherical harmonics expansion. We follow the exposition of [Boy97b] and [Bal94]. Then we use the Trojan asteroid— Hektor as an example to obtain its spherical harmonics coefficients.

2.1 Background

2.1.1 Gravitational Potential Expressed in Spherical coordinates

Consider two point masses m_1 and m_2, located at position vectors X_1 and X_2 in $\mathbb{R}^3$ moving under Newtonian gravitational law. That is, the force F between the two masses m_1 and m_2 separated by a distance r_{21} is given by

$$F = -\frac{Gm_1m_2}{r_{21}^2},$$

where $r_{21} = \|\vec{X}_2 - \vec{X}_1\|$. Since the negative sign of the force indicates only the direction, we choose to use the convension without the negative sign in the following work. By the

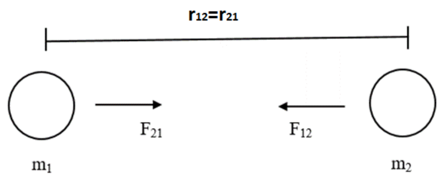

Figure 2.1: m_1 exerts a force F_{12} on m_2 while m_2 exerts a force F_{21} on m_1. F_{21} is equivalent to $-F_{21}$ by the Newton's third law.

Newton's second law, the acceleration a of an object is directly proportional to its mass m, i.e.

$$\vec{F} = m\vec{a}.$$

Therefore, the force exerted on m_1 is expressed as a vector form is given by

$$\vec{F} = m_1\vec{a} = \frac{Gm_1m_2}{r_{21}^2}\frac{\vec{X_2} - \vec{X_1}}{r_{21}}.$$

However, as is easily demonstrated

$$\frac{\vec{X_{2i}} - \vec{X_{1i}}}{r_{21}^3} = \frac{\partial}{\partial X_{1i}}\frac{1}{r_{21}},$$

where $\vec{X_{1i}}$ and $\vec{X_{2i}}$ are the $i-th$ components of $\vec{X_1}$ and $\vec{X_2}$ respectively. Hence,

$$\ddot{\vec{X}}_{1i} = Gm_2\frac{\partial}{\partial X_{1i}}(\frac{1}{r_{21}}), i = 1, 2, 3.$$

Since gravity is a conservative force, it follows that

$$\ddot{\vec{x_1}} = \nabla V$$

where $V = \frac{Gm_2}{r_{21}}$, which is known as the gravitational potential.

Definition 2.1.1 (Gravitational Potential energy)**.** Due to the gravitational force of attraction, any two objects with masses m_1 and m_2 located on a distance r_{21} apart perform work done and hence they have potential energy. The gravitational potential energy of the system of two bodies is defined as

$$U = \frac{Gm_1m_2}{r_{21}}.$$

Note that gravitational potential V, is directly related to gravitational potential energy U and the potential energy of mass m_1 as $U = m_1V$.

Now we consider a continuous mass distribution instead of a point mass in the standard

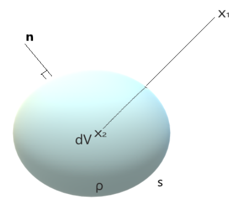

Figure 2.2: Continuous density distribution.

(x, y, z) Cartesian coordinate system, let the mass m_2 at $\vec{X_2}$ to be $\int_{V_{m_2}} \rho(\vec{X_2})d^3\vec{X_2}$, where $\rho(\vec{X_2})$ is the local mass density and $d^3\vec{X_2}$ represents a volume element. We have the gravitational potential at $\vec{X_1}$ as

$$V(\vec{X_1}) = \int_{V_{m_2}} \frac{G\rho(\vec{X_2})}{r_{21}} d^3\vec{X_2}, \tag{2.1}$$

where G is the gravitational constant. The gravitational potential field is a scalar field given by (2.1) where $V(\vec{X_1})$ is the gravitational potential energy of a unit mass in a gravitational field g. And g is the gradient of the potential energy $V(\vec{X_1})$, that is,

$$g = \nabla V = (\frac{\partial V}{\partial x}, \frac{\partial V}{\partial y}, \frac{\partial V}{\partial z}).$$

The divergence of the vector field g is defined as

$$\nabla \cdot \nabla V(\vec{X_1}) = \nabla^2 V = 4\pi G\rho(\vec{X_1})$$

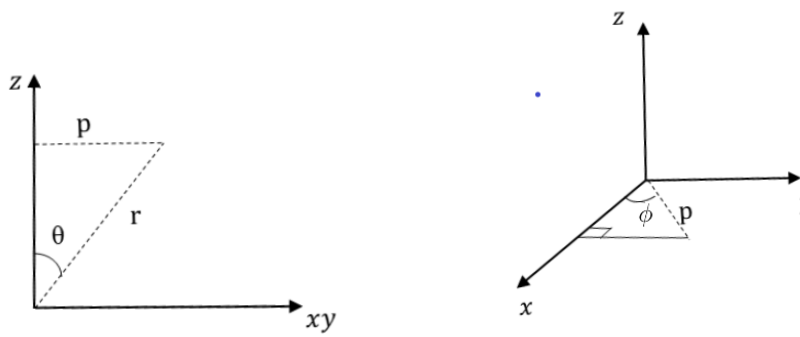

Figure 2.3: From Cartesian Coordinate (x, y, z) to Spherical Cooridinate (r, θ, ϕ).

by applying the differential form of Gauss's law for gravity. If the vector $\vec{X_1}$ is outside of the body of mass m_2, then we have $\rho(\vec{X_1}) = 0$. Thus we have the equation as $\nabla \cdot \nabla V(\vec{X_1}) = 0$, which is known as the Lapalce's equation. Consequently, the gravitation potential V satisfies the Laplace's equation, that is

$$\frac{\partial^2 V}{\partial x^2} + \frac{\partial^2 V}{\partial y^2} + \frac{\partial^2 V}{\partial z^2} = 0. \tag{2.2}$$

It is an important property of the potential energy which we will be using in later computation of spherical harmonics. Now, it is convenient to adopt spherical coordinates (r, θ, ϕ), aligned along the z-axis. These coordinates are related to the regular Cartesian coordinates for masses m_1 and m_2 as follows:

$$\begin{aligned} x &= r \sin\theta \cos\phi \\ y &= r \sin\theta \sin\phi \\ z &= r \cos\theta, \end{aligned} \tag{2.3}$$

where $0 \leqslant \phi \leqslant 2\pi$ is the azimuthal angle, $0 \leqslant \theta \leqslant \pi$ is the polar angle, and r is the radial distance of the point in the three-dimensional space. Let r_{21} be the distance between X_1 and X_2, $r = \mid \vec{X_1} \mid$ and $r' = \mid \vec{X_2} \mid$.

Now we have

$$\begin{aligned} V(\vec{X_1}) &= \int \frac{G}{r_{21}}\rho(\vec{X_2})d^3\vec{X_2} \\ &= \int \frac{G}{\sqrt{\mid \vec{X_2} \mid^2 -2\vec{X_1}\cdot\vec{X_2} + \mid \vec{X_1} \mid^2}}\rho(\vec{X_2})d^3\vec{X_2} \end{aligned} \tag{2.4}$$

Since $\vec{X_1}\cdot\vec{X_2} = rr'\cos\gamma$ where γ is the angle between the vectors and by the spherical law of cosine [Sve18], we have

$$\cos\gamma = \cos\theta\cos\theta' + \sin\theta\sin\theta'\cos(\phi-\phi').$$

Thus, we have

$$\vec{X_1}\cdot\vec{X_2} = rr'(\cos\theta\cos\theta' + \sin\theta\sin\theta'\cos(\phi-\phi')).$$

Let

$$\begin{aligned} \mathcal{F} &= \cos\gamma \\ &= \sin\theta\sin\theta'(\cos\phi\cos\phi' + \sin\phi\sin\phi') + \cos\theta\cos\theta' \\ &= \sin\theta\sin\theta'\cos(\phi-\phi') + \cos\theta\cos\theta'. \end{aligned} \tag{2.5}$$

Then

$$V(\vec{r}) = \frac{1}{r}\int_{V_{m_2}} \frac{G\rho(\vec{X_2})d^3\vec{X_2}}{\sqrt{(\frac{r'}{r})^2 - 2\frac{r'}{r}\mathcal{F} + 1}}.$$

Applying the Binomial Theorem, we obtain

$$\begin{aligned} (1-2\frac{r'}{r}\mathcal{F} + (\frac{r'}{r})^2)^{\frac{1}{2}} &= 1 + (-\frac{1}{2})(-\frac{r'}{r}\mathcal{F} + \frac{r'^2}{r^2}) + \frac{(\frac{1}{2})(-\frac{1}{2}-1)}{2!}(-2\frac{r'}{r}\mathcal{F} + (\frac{r'}{r})^2)^2 + \cdots \\ &= 1 + \frac{r'}{r}\mathcal{F} - \frac{r'^2}{2r^2} + \frac{3r'^2\mathcal{F}^2}{2r^2} \\ &= 1 + \frac{r'}{r}\mathcal{F} + \frac{1}{2}(\frac{r'}{r})^2(3\mathcal{F}^2 - 1) + O(\frac{r'^3}{r^3}). \end{aligned} \tag{2.6}$$

Notice that the above expansion coincides with Legendre Polynomials, which is an n-th degree polynomial expressed as:

$$\begin{aligned} P_n(x) &= \frac{1}{2^n n!}\frac{d^n}{dx^n}(x^2-1)^n, n = 0, 1, 2, ... \\ P_0(\mathcal{F}) &= 1 \\ P_1(\mathcal{F}) &= \frac{1}{2^1 1!}\frac{d}{d\mathcal{F}}(\mathcal{F}^2-1)^1 = \mathcal{F} \\ P_2(\mathcal{F}) &= \frac{1}{2^2 2!}\frac{d^2}{d\mathcal{F}^2}(\mathcal{F}^2-1)^2 = \frac{1}{8}\frac{d}{d\mathcal{F}}2(\mathcal{F}^2-1)(2\mathcal{F}) \\ &= \frac{1}{2}\frac{d}{d\mathcal{F}}(\mathcal{F}^3-\mathcal{F}) = \frac{1}{2}(3\mathcal{F}^2-1) \end{aligned} \tag{2.7}$$

We now have

$$\begin{aligned} V(\vec{X_1}) &= \frac{1}{r}\int_{V_{m_2}} G\rho(\vec{X_2})\sum_{l=0}^{\infty}(\frac{r'}{r})^l P_l(\mathcal{F})d\vec{X_2} \\ &= \frac{1}{r}\int_{V_{m_2}} G\rho(\vec{X_2})\sum_{l=0}^{\infty}(\frac{r'}{r})^l P_l(\cos\gamma)d\vec{X_2}. \end{aligned} \tag{2.8}$$

Consider the case without rotation, we have the difference between ϕ and ϕ' as 0. That is,

$$\begin{aligned} \mathcal{F} &= \cos\theta\cos\theta' + \sin\theta\sin\theta'\cos 0 \\ &= \cos\theta\cos\theta' + \sin\theta\sin\theta' \\ &= \cos(\theta-\theta') \end{aligned} \tag{2.9}$$

With $\gamma = \theta - \theta'$, we simply have the expansion with only Legendre polynomials, which define the zonal surface spherical harmonics. Instead of expanding the terms $P_l(\cos\gamma)$ with

$$\cos\gamma = \cos\theta\cos\theta' + \sin\theta\sin\theta'\cos(\phi-\phi')$$

in (2.8), we trace back to the general solutions to the Laplace's equation in spherical coordinates since the potential energy $V(\vec{X_1})$ satisfies the Laplace's equation as in equation

(2.2).

Starting with the spherical coordinates as in equations (2.3) The unit vectors in the spherical coordinate system are functions of position; it is convenient to express them in terms of the spherical coordinates:

$$\begin{aligned}
\hat{r} &= \frac{\vec{r}}{|\,\vec{r}\,|} = \frac{\vec{r}}{r} = \frac{x\hat{x} + y\hat{y} + z\hat{z}}{r} \\
&= \hat{x}\sin\theta\cos\phi + \hat{y}\sin\theta\sin\phi + \hat{z}\cos\theta \\
\hat{\phi} &= \frac{\frac{\partial\vec{r}}{\partial\phi}}{\|\,\frac{\partial\vec{r}}{\partial\phi}\,\|} = \frac{-\hat{x}\sin\phi\sin\theta + \hat{y}\sin\theta\cos\phi}{\sqrt{\sin^2\theta(\sin^2\phi + \cos^2\phi)}} \\
&= -\hat{x}\sin\phi + \hat{y}\cos\phi \\
\hat{\theta} &= \hat{\phi} \times \hat{r} \\
&= \hat{x}(\cos\phi\cos\theta) - \hat{y}(-\sin\phi\cos\theta) + \hat{z}(-\sin^2\phi\sin\theta - \sin\theta\cos^2\phi) \\
&= \hat{x}\cos\theta\cos\phi + \hat{y}\cos\theta\sin\phi - \hat{z}\sin\theta,
\end{aligned} \tag{2.10}$$

where $\hat{x}$, $\hat{y}$ and $\hat{z}$ are the orthogonal unit vectors associated with the Cartesian coordinate system and $\hat{r}$, $\hat{\phi}$ and $\hat{\theta}$ are the orthogonal unit vectors associated with the spherical coordinate system. Using the expressions obtained above, we can derive the following relationships:

$$
\begin{aligned}
\frac{\partial \hat{r}}{\partial r} &= 0 \\
\frac{\partial \hat{r}}{\partial \phi} &= -\hat{x}\sin\theta\sin\phi + \hat{y}\sin\theta\cos\phi \\
\frac{\partial \hat{r}}{\partial \theta} &= \hat{x}\cos\theta\cos\phi + \hat{y}\cos\theta\sin\phi - \hat{z}\sin\theta \\
\frac{\partial \hat{\phi}}{\partial r} &= 0 \\
\frac{\partial \hat{\phi}}{\partial \phi} &= -\hat{x}\cos\phi - \hat{y}\sin\phi = -(\hat{r}\sin\theta + \hat{\theta}\cos\theta) \\
\frac{\partial \hat{\phi}}{\partial \theta} &= 0 \\
\frac{\partial \hat{\theta}}{\partial r} &= 0 \\
\frac{\partial \hat{\theta}}{\partial \phi} &= -\hat{x}\sin\phi\cos\theta + \hat{y}\cos\phi\cos\theta = \hat{\phi}\cos\theta
\end{aligned}
\tag{2.11}
$$

2.1.2 Laplacian in Spherical Coordinates

The path increment $d\vec{r}$ can then be expressed in spherical coordinates as follows:

$$
\begin{aligned}
d\vec{r} &= d(r\vec{r}) \\
&= \hat{r}dr + rd\vec{r} \\
&= \hat{r}dr + r(\frac{\partial \hat{r}}{\partial r}dr + \frac{\partial \hat{r}}{\partial \theta}d\theta + \frac{\partial \hat{r}}{\partial \phi}d\phi) \\
&= \hat{r}dr + \theta r d\theta + \hat{\phi} r \sin\theta d\phi.
\end{aligned}
\tag{2.12}
$$

Consider any scalar field u as a function of the spherical coordinates r, θ and ϕ. Then we have

$$du = \frac{\partial u}{\partial r}dr + \frac{\partial u}{\partial \theta}d\theta + \frac{\partial u}{\partial \phi}d\phi$$

Note that we can express du as

$$du = \nabla u \cdot d\vec{r},$$

where the del operator ∇ represents gradient. Thus, we have

$$\begin{aligned} \frac{\partial u}{\partial r}dr + \frac{\partial u}{\partial \phi}d\phi + \frac{\partial u}{\partial \phi}d\phi &= \nabla u \cdot d\vec{r} \\ &= (\nabla u)_r dr + (\nabla u)_\theta r d\theta + (\nabla u)_\phi r \sin\theta d\phi \end{aligned} \tag{2.13}$$

And therefore, we obtained

$$\begin{aligned} (\nabla u)_r &= \frac{\partial u}{\partial r} \\ (\nabla u)_\theta &= \frac{1}{r}\frac{\partial u}{\partial \theta} \\ (\nabla u)_\phi &= \frac{1}{r\sin\theta}\frac{\partial u}{\partial \phi} \end{aligned} \tag{2.14}$$

and

$$\nabla = \hat{r}\frac{\partial}{\partial r} + \frac{\hat{\theta}}{r}\frac{\partial}{\partial \theta} + \frac{\hat{\phi}}{r\sin\theta}\frac{\partial}{\partial \phi}.$$

Now we have the Laplacian in spherical coordinates as

$$\begin{aligned} \nabla^2 u =& \nabla \cdot (\vec{\nabla u}) = (\hat{r}\frac{\partial}{\partial r} + \frac{\hat{\theta}}{r}\frac{\partial}{\partial \theta} + \frac{\hat{\phi}}{r\sin\theta}\frac{\partial}{\partial \phi}) \cdot (\hat{r}\frac{\partial u}{\partial r} + \frac{\hat{\theta}}{r}\frac{\partial u}{\partial \theta} + \frac{\hat{\phi}}{r\sin\theta}\frac{\partial u}{\partial \phi}) \\ =& \hat{r}\frac{\partial}{\partial r}(\hat{r}\frac{\partial u}{\partial r} + \frac{\hat{\theta}}{r}\frac{\partial u}{\partial \theta} + \frac{\hat{\phi}}{r\sin\theta}\frac{\partial u}{\partial \phi}) \\ &+ \frac{\hat{\theta}}{r}\frac{\partial}{\partial \theta}(\hat{r}\frac{\partial u}{\partial r} + \frac{\hat{\theta}}{r}\frac{\partial u}{\partial \theta} + \frac{\hat{\phi}}{r\sin\theta}\frac{\partial u}{\partial \phi}) \\ &+ \frac{\hat{\phi}}{r\sin\theta}\frac{\partial}{\partial \phi}(\hat{r}\frac{\partial u}{\partial r} + \frac{\hat{\theta}}{r}\frac{\partial u}{\partial \theta} + \frac{\hat{\phi}}{r\sin\theta}\frac{\partial u}{\partial \phi}) \end{aligned} \tag{2.15}$$

With the partial derivatives derived earlier, we have

$$\begin{aligned}
\nabla^2 u =& \hat{r}(\hat{r}\frac{\partial^2 u}{\partial r^2} - \frac{\hat{\theta}}{r^2}\frac{\partial u}{\partial \theta} + \frac{\hat{\theta}}{r}\frac{\partial^2 u}{\partial \theta \partial r} - \frac{\hat{\phi}}{r^2 \sin\theta}\frac{\partial u}{\partial \phi} + \frac{\hat{\phi}}{r \sin\theta}\frac{\partial^2 u}{\partial \phi \partial r}) \\
&+ \frac{\hat{\theta}}{r}(\hat{\theta}\frac{\partial u}{\partial r} + \hat{r}\frac{\partial^2 u}{\partial r \partial \theta} - \frac{\hat{r}}{r}\frac{\partial u}{\partial \theta} + \frac{\hat{\theta}}{r}\frac{\partial^2 u}{\partial \theta^2} - \frac{\hat{\theta}\cos\theta}{r \sin^2\theta}\frac{\partial u}{\partial \phi} + \frac{\hat{\phi}}{r \sin\theta}\frac{\partial^2 u}{\partial \phi \partial \theta}) \\
&+ \frac{\hat{\phi}}{r \sin\theta}(\hat{\phi}\sin\theta\frac{\partial u}{\partial r} + \hat{r}\frac{\partial^2 u}{\partial r \partial \phi} + \frac{\hat{\phi}\cos\theta}{r}\frac{\partial u}{\partial \theta} + \frac{\hat{\theta}}{r}\frac{\partial^2 u}{\partial \theta \partial \phi} \\
&- \frac{\hat{r}\sin\theta + \hat{\theta}\cos\theta}{r \sin\theta}\frac{\partial u}{\partial \phi} + \frac{\hat{\phi}}{r \sin\theta}\frac{\partial^2 u}{\partial \phi^2} \qquad (2.16) \\
=& (\frac{\partial^2 u}{\partial r^2}) + (\frac{1}{r}\frac{\partial u}{\partial r} + \frac{1}{r^2}\frac{\partial^2 u}{\partial \theta^2}) + (\frac{1}{r}\frac{\partial u}{\partial r} + \frac{\cos\theta}{r^2 \sin\theta}\frac{\partial u}{\partial \theta} + \frac{1}{r^2 \sin^2\theta}\frac{\partial^2 u}{\partial \phi^2}) \\
=& (\frac{\partial^2 u}{\partial r^2} + \frac{2}{r}\frac{\partial u}{\partial r}) + (\frac{1}{r^2}\frac{\partial^2 u}{\partial \theta} + \frac{\cos\theta}{r^2 \sin\theta}\frac{\partial u}{\partial \theta}) + (\frac{1}{r^2 \sin^2\theta}\frac{\partial^2 u}{\partial \phi^2}) \\
=& \frac{1}{r^2}\frac{\partial}{\partial r}(r^2\frac{\partial u}{\partial r}) + \frac{1}{r^2 \sin\theta}\frac{\partial}{\partial \theta}(\sin\theta\frac{\partial u}{\partial \theta}) + \frac{1}{r^2 \sin^2\theta}\frac{\partial^2 u}{\partial \phi^2}.
\end{aligned}$$

Therefore the Laplacian in Spherical coordinates can be expressed as

$$\nabla^2 = \frac{1}{r^2}\frac{\partial}{\partial r}(r^2\frac{\partial}{\partial r}) + \frac{1}{r^2 \sin\theta}\frac{\partial}{\partial \theta}(\sin\theta\frac{\partial}{\partial \theta}) + \frac{1}{r^2 \sin^2\theta}\frac{\partial^2}{\partial \phi^2}$$

2.1.3 Laplace's Equation

Laplace's equation is obtained by taking the divergence of the gradient of the potential, say ψ. It is a second order differential equation such that

$$\nabla^2 \psi = 0. \qquad (2.17)$$

As we have derived in Section 2.1.2, we have the Laplace's equation expressed in spherical coordinates as

$$\frac{\partial}{\partial r}(r^2\frac{\partial \psi}{\partial r}) + \frac{1}{\sin\theta}\frac{\partial}{\partial \theta}(\sin\theta\frac{\partial \psi}{\partial \theta}) + \frac{1}{\sin^2\theta}\frac{\partial^2 \psi}{\partial \phi^2} = 0 \qquad (2.18)$$

We note that this equation can be solved by separation of variables. Consider the potential expressed as a product of functions $R(r)$, $\Theta(\theta)$and $\Phi(\phi)$, that is

$$\psi(r, \theta, \phi) = R(r)\Theta(\theta)\Phi(\phi).$$

Substituting the product into the Laplace's equation (2.18), the derivatives are now the total derivatives as shown below.

$$\frac{d}{dr}(r^2\frac{dR(r)}{dr})\Theta(\theta)\Phi(\phi) + \frac{R(r)}{\sin\theta}\frac{d}{d\theta}(\sin\theta\frac{d\Theta(\theta)}{d\theta})\Phi(\phi) + \frac{R(r)\Theta(\theta)}{\sin^2\theta}\frac{d^2\Phi(\phi)}{d\phi^2} = 0 \qquad (2.19)$$

Dividing by $R(r)\Theta(\theta)\Phi(\phi)$ throughout the equation, we obtain

$$\frac{1}{R(r)}\frac{d}{dr}(r^2\frac{dR(r)}{dr}) + \frac{1}{\Theta(\theta)\sin\theta}\frac{d}{d\theta}(\sin\theta\frac{d\Theta(\theta)}{d\theta}) + \frac{1}{\Phi(\phi)\sin^2\theta}\frac{d^2\Theta(\theta)}{d\phi^2} = 0. \qquad (2.20)$$

The first term is now depending on r only and thus it must be a constant. We choose to have $l(l+1)$ to be the separation constant. This allows us to have the ordinary differential equation for $R(r)$ as:

$$\frac{1}{R(r)}\frac{d}{dr}(r^2\frac{dR(r)}{dr}) = l(l+1)$$

That is,

$$\frac{d}{dr}(r^2\frac{dR(r)}{dr}) - l(l+1)R(r) = 0.$$

This equation has the linearly independent solution of the form

$$Ar^l, Br^{-(l+1)}$$

such that

$$R(r) = Ar^l + Br^{-(l+1)}$$

where A and B are constants which will be determined by given boundary equation and/or conditions. Since the part of equation (2.20) that is associated with $R(r)$ is separated to be a constant, the remainder of the Laplace equation is

$$l(l+1) + \frac{1}{\Theta(\theta)\sin\theta}\frac{d}{d\theta}(\sin\theta\frac{d\Theta(\theta)}{d\theta}) + \frac{1}{\Phi(\phi)\sin^2\theta}\frac{d^2\Theta(\theta)}{d\phi^2} = 0.$$

Multiplying by $\sin^2\theta$, we obtain

$$l(l+1)\sin^2\theta + \frac{\sin\theta}{\Theta(\theta)}\frac{d}{d\theta}(\sin\theta\frac{d\Theta(\theta)}{d\theta}) + \frac{1}{\Phi(\phi)}\frac{d^2\Theta(\theta)}{d\phi^2} = 0$$

in which we see that the last term on the left hand side of the equation is a function depends only on ϕ. Similar to $R(r)$, the last term is now separable and it leads to the well-known Legendre and Associated Legendre Equations [AH12].

The separated equation for $\Phi(\phi)$ is

$$\frac{1}{\Phi(\phi)}\frac{d^2\Phi(\phi)}{d\phi^2} = const.$$

Similarly to the previous case, we will choose the constant to be $-m^2$. Since the solution of the equation has to be a single value, m is required to be either a positive or negative integer. The constant $-m^2$ allows us to justify the solution precisely:

$$\begin{aligned} \frac{1}{\Phi(\phi)}\frac{d^2\Phi(\phi)}{d\phi^2} &= -m^2 \\ \frac{d^2\Phi(\phi)}{d\phi^2} &= -m^2\Phi(\phi) \\ \frac{d^2\Phi(\phi)}{d\phi^2} + m^2\Phi(\phi) &= 0 \end{aligned} \tag{2.21}$$

The solution is of the form of $e^{\gamma t}$. Its characteristic equation is $(\gamma^2 + m^2) = 0$ and implies $\gamma = \pm mi$. Therefore we have the solution as

$$\Phi(\phi) = e^{\pm im\phi},$$

or the general solution as a sum of real functions

$$\Phi(\phi) = A_m \cos(m\phi) + B_m \sin(m\phi),$$

where A_m and B_m are some constants.

With separating the function for $\Phi(\phi)$ we have the original Laplace equation (2.18) left with $\Theta(\theta)$. Dividing

$$l(l+1)\sin^2\theta - m^2 + \sin\theta \frac{1}{\Theta(\theta)} \frac{d}{d\theta}(\sin\theta \frac{d\Theta(\theta)}{d\theta}) = 0$$

by $\Theta(\theta)$, we have

$$(l(l+1)\sin^2\theta - m^2)\Theta(\theta) + \sin\theta \frac{d}{d\theta}(\sin\theta \frac{d\Theta(\theta)}{d\theta}) = 0. \tag{2.22}$$

Let $u = \cos\theta$, then $\frac{du}{d\theta} = -\sin\theta$ and

$$\frac{d}{d\theta} = \frac{d}{du}\frac{du}{d\theta} = -\sin\theta \frac{d}{du}. \tag{2.23}$$

Substituting equation (2.23) into the Laplace equation 2.22, we obtain

$$(l(l+1)\sin^2\theta - m^2)\Theta + \sin^2\theta \frac{d}{du}(\sin^2\theta \frac{d\Theta}{du}) = 0$$

and thus we can now change the entire equation depending on u instead of θ:

$$(l(l+1)(1-u^2)-m^2)\Theta(u)+(1-u^2)\frac{d}{du}((1-u^2)\frac{d\Theta(u)}{du})=0. \tag{2.24}$$

2.1.4 Associated Legendre and Legendre Equations

The equation (2.24) derived from the Laplace equation (2.18) in the previous section can be written as follows by dividing the whole equation by $(1-u^2)$:

$$(1-u^2)\frac{d^2\Theta(u)}{du^2}-2u\frac{d\Theta(u)}{du}+(l(l+1)-\frac{m^2}{1-u^2})\Theta(u)=0. \tag{2.25}$$

This is known as the Associated Legendre equation. It is an equation expressed as a function of $\cos\theta$ and the solutions to the Associated Legendre equation are also polynomials, which are known as the Associated Legendre polynomials.

In the particular case of $m=0$, we obtain a simpler equation

$$(1-u^2)\frac{d^2\Theta(u)}{du^2}-2u\frac{d\Theta(u)}{du}+l(l+1)\Theta(u)=0. \tag{2.26}$$

This is known as the Legendre equation and the solutions to the Legendre equation are polynomials, which are known as the Legendre polynomials.

In this section, we start with solving the Legendre equation for Legendre polynomials. Then we make use of the Legendre polynomials to solve the associated Legendre equation for Associated Legendre polynomials.

To simplify the notation we let $g=\Theta(u)$, then the Legendre equation becomes

$$(1-u^2)\frac{d^2g}{du^2}-2u\frac{dg}{du}+l(l+1)g=0. \tag{2.27}$$

By the product rule of differentiation, we have

$$\frac{d}{du}((1-u^2)\frac{dg}{du}) + l(l+1)g = 0.$$

In order to give the general solution to the equation, we consider

$$y(u) = (u^2-1)^l.$$

Then we have

$$y' = 2lu(u^2-1)^{l-1}.$$

Multiplying by $1-u^2$ to y', we obtain

$$\begin{aligned}(1-u^2)y' &= -2lu(u^2-1)^l \\ &= -2luy\end{aligned} \tag{2.28}$$

Thus we can easily obtain

$$(1-u^2)y' + 2luy = 0$$

Now let $v = 1-u^2$ and performing k-times differentiation by using Leibniz rule, that is,

$$\frac{dk}{du^k}[vy'] = \sum_{j=0}^{k} \binom{k}{j} v^{(j)} y^{(k-j+1)}.$$

Since v is a second order polynomial, only three terms of the above sum will survive.

$$\begin{aligned}\frac{d^k}{du^k}[vy'] &= vy^{(k+1)} + kv'y^{(k)} + k(k-1)v^{(2)}y^{(k-1)} \\ &= (1-u^2)y^{(k+1)} - 2kuy^{(k)} - 2\frac{k(k-1)}{2}y^{(k-1)}\end{aligned} \tag{2.29}$$

Similarly, we apply the Leibniz rule on the product $2luy$.

$$\frac{d^k}{du^k}[2luy] = 2luy^{(k)} + 2lky^{(k-1)}$$

We now have

$$\frac{d^k}{du^k}[vy'] + \frac{d^k}{du^k}[2luy] = 0$$

becomes

$$(1-u^2)y^{(k+1)} - 2kuy^{(k)} - k(k-1)y^{(k-1)} + 2luy^{(k)} + 2nky^{(k-1)} = 0.$$

Let $k = l+1$, we have

$$(1-u^2)y^{(l+2)} - 2(l+1)uy^{(l+1)} - (l+1)(l)y^{(l)} + 2luy^{(l+1)} + 2l(l+1)y^{(l)} = 0$$

and it simplifies to

$$(1-u^2)y^{(l+2)} - 2uy^{(l+1)} + (l+1)(l)y^{(l)} = 0.$$

This is indeed the Legendre equation (2.27) with

$$g(u) = y^{(l)} = \frac{d^l}{du^l}(u^2-1)^l.$$

This shows that

$$c_l \frac{d^l}{du^l}(u^2-1)^l \tag{2.30}$$

where c_l is a constant satisfies the Legendre equation. For normalization, c_l is chosen to be $\frac{1}{2^l l!}$ such that expression (2.30) is 1 when u is 1 and thus

$$\frac{1}{2^l l!}\frac{d^l}{du^l}(u^2-1)^l \equiv P_l(u),$$

which is known as the Legendre polynomials (i.e. Rodrigues' formula). In the case of considering a m-times differentiation to the Legendre equation, we apply the Leibniz rule to the products vg'', $-2ug'$ and $(l(l+1)-m(m+1))g$ as follows:

$$\frac{d^m}{du^m}[vg''] = vg^{(m+2)} - 2mug^{(m+1)} - m(m-1)g^{(m)}$$

$$\frac{d^m}{du^m}[-2ug'] = -2ug^{(m+1)} - 2mg^{(m)}$$

$$\frac{d^m}{du^m}[l(l+1)g] = l(l+1)g^{(m)}$$

Thus we obtain a new differential equation

$$\left(1-u^2\right)(g^{(m)})'' - 2(m+1)u(g^{(m)})' + (l(l+1)-m(m+1))g^{(m)} = 0, \tag{2.31}$$

where $g^{(m)} \equiv \frac{d^m}{du^m}g(u)$. Now we consider

$$g^{(m)} = (1-u^2)^r f(u) \tag{2.32}$$

and we need to find such a function f. To determine r and the condition for f, we first computer the first and second derivative of the expression (2.32) as follows:

$$[g^{(m)}]' = -2ru(1-u^2)^{(r-1)}f + (1-u^2)^2 f' \tag{2.33}$$

$$[g^{(m)}]'' = \left(1-u^2\right)^r f'' - 4ru\left(1-u^2\right)^{r-1} f' - 2r\left(1-u^2\right)^{r-1} f + 4r(r-1)u^2\left(1-u^2\right)^{r-2} f. \tag{2.34}$$

Substitute the expressions (2.33) and (2.34) into equation (2.31), we have

$$(1-u^2)f'' - 2u(m+1+2r)f' + \left(l(l+1) - m(m+1) - 2r + \frac{4r(r-1)+4r(m+1)}{1-u^2}\right) f = 0 \tag{2.35}$$

Notice that with $r = \frac{-m}{2}$, we recover equation (2.25) with $\Theta(u) = f$. Therefore, the function

$$f(u) \equiv \left(1-u^2\right)^{\frac{m}{2}} \frac{d^m}{du^m} g(u), \tag{2.36}$$

where $g(u)$ is a solution to the Legendre equation (2.26). The solution to the Associated Legendre equation (2.25). With positive integers l and m is known as Associated Legendre polynomials and it is denoted as $P_l^m(u)$ such that

$$P_l^m(u) \equiv \left(1-u^2\right)^{\frac{m}{2}} \frac{d^m}{du^m} P_l(u). \tag{2.37}$$

Since we do not have computation for derivatives with negative index, we define $P_l^m(u)$ with positive m. However, we can use extend it to negative m by rewriting equation (2.37) with $P_l(u)$ defined through Rodrigues' formula. We have

$$\begin{aligned} P_l^m(u) &= \left(1-u^2\right)^{m/2} \frac{d^m}{du^m} \left(\frac{1}{2^l l!} \frac{d^l}{du^l} (u^2-1)^l \right) \\ &= \frac{1}{2^l l!} (1-u^2)^{\frac{m}{2}} \frac{d^{l+m}}{du^{l+m}} (u^2-1)^l \end{aligned} \tag{2.38}$$

Replacing m by $-m$ now, we obtain the extension to negative values of m:

$$\begin{aligned} P_l^{-m}(u) &= \frac{1}{2^l l!} (1-u^2)^{\frac{-m}{2}} \frac{d^{l-m}}{du^{l-m}} (u^2-1)^l \\ &= (-1)^m \frac{(l-m)!}{(l+m)!} P_l^m(u) \end{aligned} \tag{2.39}$$

Recall that $u = \cos\theta$, we have the solution to the Laplace's equation (2.17) as

$$\begin{aligned} \psi(r,\theta,\phi) &= R(r)\Theta(\theta)\Phi(\phi) \\ &= \sum_{l=0}^{\infty} \sum_{m=-l}^{l} \left(A_{l,m} r^l + B_{l,m} r^{-(l+1)}\right) \left(P_l^m(\cos\theta)\right) \left(e^{im\phi}\right) \\ &= \sum_{l=0}^{\infty} \sum_{m=-l}^{l} \left(A_{l,m} r^l + B_{l,m} r^{-(l+1)}\right) Y_l^m, \end{aligned} \tag{2.40}$$

where Y_l^m is the spherical harmonics that is defined in Section 2.1.5.

2.1.5 Spherical Harmonics

In general, the Associated Legendre polynomials is defined in the previous section 2.1.4

$$P_l^m(u) = (1-u^2)^{m/2}\frac{d^m}{du^m}(P_l(u)),$$

with $-1 \leqslant u \leqslant 1$, $m \geqslant 0$ and $l \geqslant m$.

Although differentiating a negative number of times is not defined, this problem does not occur in the Associated Legendre polynomials. As shown in Section 2.1.4, the Rodrigues' formula allows us to extend the range of m to $-l \leqslant m \leqslant l$. Hence the definition of P_l^m is also valid for negative m without loss of generality.

Assuming m is non-negative, we start with the Rodrigues' formula

$$\begin{aligned} P_l^m(u) &= \frac{1}{2^l l!}(1-u^2)^{m/2}\frac{d^{l+m}}{du^{l+m}}(u^2-1)^l \\ &= \frac{1}{2^l l!}(1-u^2)^{m/2}\frac{d^{l+m}}{du^{l+m}}[(u+1)^l(u-1)^l]. \end{aligned} \tag{2.41}$$

Now using the Leibniz rule to evaluate the derivative, it yields

$$P_l^m(u) = \frac{1}{2^l l!}(1-u^2)^{m/2}\sum_{r=0}^{l+m}\frac{(l+m)!}{r!(l+m-r)!}\frac{d^r(x+1)^l}{dx^r}\frac{d^{l+m-r}(x-1)^l}{dx^{l+m-r}}.$$

Considering the two derivative factors in a term in the summation, we note that the first is non-zero only for $r \leqslant l$ and the second is non-zero for $l+m-r \leqslant l$. These two conditions combine to yield $m \leqslant r \leqslant l$.

Performing the derivatives, we obtain

$$\begin{aligned} P_l^m(u) &= \frac{1}{2^l l!}(1-u^2)^{m/2}\sum_{r=0}^{l+m}\frac{(l+m)!}{r!(l+m-r)!}\frac{l!(u+1)^{l-r}}{(l-r)!}\frac{l!(u-1)^{r-m}}{(r-m)!} \\ &= (-1)^{m/2}\frac{l!(l+m)!}{2^l}\sum_{r=m}^{l}\frac{(u-1)^{l-r+m/2}(u-1)^{r-m/2}}{r!(l+m-r)!(l-r)!(r-m)!}. \end{aligned} \tag{2.42}$$

For the derivation of $P_l^{-m}(u)$, we perform the steps similarly as above

$$P_l^{-m}(u) = (-1)^{-m/2}\frac{l!(l-m)!}{2^l}\sum_{r=0}^{l-m}\frac{(u+1)^{l-r-\frac{m}{2}}(u-1)^{r+\frac{m}{2}}}{r!(l-m-r)!(l-r)!(r+m)!}$$

Let $\bar{r} = r + m$, we have

$$P_l^{-m}(u) = (-1)^{m/2}\frac{l!(l-m)!}{2^l}\sum_{\bar{r}=m}^{l}\frac{(u+1)^{l-\bar{r}+m/2}(u-1)^{\bar{r}-m/2}}{(\bar{r}-m)!(l-\bar{r})!(l+m-\bar{r})!\bar{r}!}.$$

In this case, we obtain the identity

$$P_l^{-m}(u) = (-1)^m\frac{(l-m)!}{(l+m)!}P_l^m(u). \tag{2.43}$$

It is now convenient to introduce Spherical Harmonics, which are special functions that define on the surface of a sphere. Spherical Harmonics form an orthogonal system, so they set up the base to the expansion of a general function on a sphere. A set of Spherical Harmonics are defined as

$$Y_l^m(\theta,\phi) \equiv \sqrt{\frac{2l+1}{4\pi}\frac{(l-m)!}{(l+m)!}}P_l^m(\cos\theta)e^{im\phi}$$

with $m = -l, -l+1, ..., l-1, l$ and $l = 0, 1, 2, ...$ Notice that

$$\begin{aligned}
Y_l^{-m}(\theta,\phi) &= \sqrt{\frac{2l+1}{4\pi}\frac{(l-m)!}{(l+m)!}}P_l^{-m}(\cos\theta)e^{-im\phi} \\
&= \sqrt{\frac{2l+1}{4\pi}\frac{(l-m)!}{(l+m)!}}(-1)^m\frac{(l-m)!}{(l+m)!}P_l^m(\cos\theta)e^{-im\phi} \\
&= (-1)^m\sqrt{\frac{2l+1}{4\pi}\frac{(l-m)!}{(l+m)!}}P_l^m(\cos\theta)e^{-im\phi} \\
&= (-1)^m\sqrt{\frac{2l+1}{4\pi}\frac{(l-m)!}{(l+m)!}}P_l^m(\cos\theta)\overline{e^{im\phi}} \\
&= (-1)^m\overline{Y_l^m(\theta,\phi)} \\
&\equiv (-1)^m Y_l^{m*}(\theta,\phi)
\end{aligned} \tag{2.44}$$

where $Y_l^{m*}(\theta,\phi)$ denotes the conjugate of $Y_l^m(\theta,\phi)$. The condition of the orthogonality is $l' \leqslant l$,

$$\int_0^{2\pi} d\phi \int_0^{\pi} \sin\theta d\theta Y_l^{m*}(\theta,\phi)Y_{l'}^{m'}(\theta,\phi) = \delta_{ll'}\delta_{mm'}. \tag{2.45}$$

A general function $g(\theta,\phi)$ is expanded in terms of the Spherical Harmonics as

$$g(\theta,\phi) = \sum_{l,m} A_l^m Y_l^m(\theta,\phi),$$

with

$$A_l^m = \int_0^{2\pi} d\phi \int_0^{\pi} d\theta \sin\theta g(\theta,\phi)Y_l^{m*}(\theta,\phi).$$

The angular part of the solutions to the Laplace equation is contained in the product of the azimuthal function $\Phi(\phi)$ and the polar function $\Theta(\theta)$. The azimuthal function comprise a complex exponential $e^{im\phi}$ and the polar function is a solution to the associated Legendre equation $P_l^m(\cos\theta)$.

Considering that most applications of spherical harmonics require only real-valued spherical functions, as the gravitational potential that we are working on, it is convenient for us to define the real-valued spherical harmonics function as follows:

$$Y_{l,m}(\theta,\phi) \equiv \begin{cases} \sqrt{2}\mathbf{Re}(Y_l^m) = \sqrt{2}K_l^m \cos(m\phi)P_l^m(\cos\theta) & \text{if } m > 0 \\ Y_l^0 = K_l^0 P_l^0(\cos\theta) & \text{if } m = 0 \\ \sqrt{2}\mathbf{Im}(Y_l^m) = \sqrt{2}K_l^{|m|} \sin(\mid m \mid \phi)P_l^{|m|}(\cos\theta) & \text{if } m < 0 \end{cases}$$

with $\sqrt{2}$ as a normalized factor and where

$$K_l^m = \sqrt{\frac{2l+1}{4\pi}\frac{(l-m)!}{(l+m)!}}.$$

The real functions $Y_{l,m}(\theta,\phi)$ are known in the literature as spherical harmonics of the first kind and they are divided into three categories:

(I) When $m = 0$, it is known as zonal harmonics.

(II) When $l = m$, it is known as sectorial harmonics.

(III) When $l \neq 0$ and $l \neq m$, it is known as tesseral harmonics.

The three types of surface harmonics represent different types of surface changes; graphical representation of the three types of surface harmonics is provided below.

Figure 2.4: Graphical views from the side of objects. The left and right picusre represent the zonal and tesseral harmonics respectively while the middle one represents sectorial harmonics.

Modeling an object by the zonal harmonics appear as a circle while viewing the described object from the top since the changes of the shape is happened to have some of the horizontal slides of the sphere cut off. This provides that zonal harmonics do not depend on longitudes. Modeling an object by sectorial harmonics appear as splitting as "triangles" while viewing from the top since the changes of the shape is sectional cut off of a sphere along longitude. Modeling an object by tesseral harmonics appear as a "checkerboard" while viewing from the top since the changes of the shape is cutting pieces out like a "checkerboard" in general.

Figure 2.5: Graphical views from the top of the objects. The left and right picusre represent the zonal and tesseral harmonics respectively while the middle one represents sectorial harmonics.

2.1.6 Gravitational Potential in Spherical Harmonics Expansion

Since the gravitational potential (2.1) satisfies the Laplace's equation as discussed, we have V in the form of equation (2.40). Remark that in the case of our interest, a potential in free space vanishing at infinity and thus $A_{l,m}$ must be zero in (2.40). Consider the gravitational potential V in spherical coordinates as an orthogonal expansion using spherical harmonics, we have

$$V(r,\theta,\phi) = \frac{GM}{r}\sum_{l=0}^{\infty}(\frac{r'}{r})^l \sum_{m=0}^{l} P_l^m(\cos\theta)[C_{l,m}\cos(m\phi) + S_{l,m}\sin(m\phi)] \tag{2.46}$$

where $C_{l,m}$ and $S_{l,m}$ are the spherical harmonics coefficients and M is the mass of the body. Note that in the case of gravity field, we adopt the convention to be real for the expansion functions.

2.1.7 Derivation of Spherical Harmonics Coefficients of a triaxial Ellipsoid

The solution to the Laplace's equation as in equation (2.40) is expressed by a series of spherical harmonics Y_l^m, which consists of two terms. The two terms are known as the spherical surface harmonics and defined as $Y_{l,m}^C$ and $Y_{l,m}^S$:

$$\begin{aligned} P_l^m(cos\theta)\cos(m\phi) &\equiv Y_{l,m}^C \\ P_l^m(cos\theta)\sin(m\phi) &\equiv Y_{l,m}^S. \end{aligned} \tag{2.47}$$

Note that the orthogonal property of the Spherical Harmonics is of use in the following text. In this thesis, we consider the shape of triaxial ellipsoid with semi-major axes $a > b > c$. Of our interest, the gravitational potential (2.46) has the the coefficients $S_{l,m}$ are all zeros due to the symmetry of triaxial ellipsoid. We have

$$V(r,\theta,\phi) = \frac{GM}{r}\sum_{l=0}^{\infty}(\frac{r'}{r})^l \sum_{m=0}^{l} P_l^m(\cos\theta)[C_{l,m}\cos(m\phi)]. \tag{2.48}$$

Consider

$$\beta = \sum_{l=0}^{\infty}\sum_{m=0}^{l} P_l^m(\cos\theta)C_{l,m}\cos(m\phi) \tag{2.49}$$

Multiply both sides of the equation by $P_{l'}^{m'}(\cos\theta)$ and $\cos(m'\phi)$ (i.e. $Y_{l',m'}^C$) , we have

$$\begin{aligned} \beta P_{l'}^{m'}(\cos\theta)\cos(m'\phi) &= \sum_{l=0}^{\infty}\sum_{m=0}^{l} P_l^m(\cos\theta)C_{l,m}\cos(m\phi)P_{l'}^{m'}(\cos\theta)\cos(m'\phi) \\ \Longrightarrow \beta\frac{(l-m)!}{(l+m)!}(2-\delta_{0m})\int_V P_{l'}^{m'}(\cos\theta)\cos(m'\phi)dV &= C_{l,m}. \end{aligned} \tag{2.50}$$

This provides us a way of determining the coefficient $C_{l,m}$ [Bal94]. With the symmetric property, we have $C_{2p+1,q} = 0$ and $C_{2p,2q+1} = 0$ and thus we only consider the even terms. As shown in equation (2.50), we use the property of orthogonality and normalization of spherical harmonics. Similarly, we obtain the coefficient $C_{2l,2m}$ of the gravitational potential (2.46) as in [Bal94] and [Boy97a]:

$$C_{2l,2m} = \frac{\beta}{Mr'^{2l}} \frac{(2l-2m)!}{(2l+2m)!}(2-\delta_{0m}) \int_V r^{2l+2} P_{2l}^{2m}(\cos\theta)\sin\theta\cos(2m\phi)drd\theta d\phi. \quad (2.51)$$

Considering $M = \frac{3}{4\pi abc\beta}$ [Bal94], we have

$$C_{2l,2m} = \frac{3}{4\pi abcr'^{2l}} \frac{(2l-2m)!}{(2l+2m)!}(2-\delta_{0m}) \int_V r^{2l+2} P_{2l}^{2m}(\cos\theta)\sin\theta\cos(2m\phi)drd\theta d\phi \quad (2.52)$$

where r is the radius of mass m while a,b and c are the semi-axes of the ellipsoid aligned with the x-, y- and z-axes respectively such that $a > b > c$.

The integral of (2.52) is given by [Boy97b]

$$\int_0^{2\pi}\int_0^{\pi}\int_0^{D(\theta,\phi)} r^{2l+2} P_{2l}^{2m}(\cos\theta)\sin\theta\cos(2m\phi)drd\theta d\phi.$$

Following the derivation of [Boy97b], we first integrate with respect to the radial coordinate r, then

$$\begin{aligned}\int_0^D r^{2l+2}dr &= \frac{D^{2l+3}}{2l+3} \\ &= \frac{1}{2l+3}[(\frac{\cos^2\phi}{a^2}+\frac{\sin^2\phi}{b^2})\sin^2\theta+\frac{\cos^2\theta}{c^2}]^{\frac{-(2l+3)}{2}} \\ &= \frac{1}{2l+3}\frac{1}{(A\sin^2\theta+B\cos^2\theta)^{\frac{-(2l+3)}{2}}}\end{aligned} \quad (2.53)$$

where $A = \frac{\cos^2\phi}{a^2} + \frac{\sin^2\phi}{b^2}$ and $B = \frac{1}{c^2}$.

Second, consider the integral with respect to the angle θ

$$\begin{aligned}&\int_0^{\pi} P_{2l}^{2m}(\cos\theta)\sin\theta\frac{1}{(A\sin^2\theta+B\cos^2\theta)^{\frac{l+3}{2}}}d\theta \\ =&(2l+2m)!\sum_{i=0}^{l-m}\frac{(-1)^i}{2^{2m+2i}(2l-2m-2i)!(2m+i)!i!}\int_0^{\pi}\frac{\cos^{2l-2m-2i}\theta\sin^{2m+2i+1}\theta}{(A\sin^2\theta+B\cos^2\theta)^{\frac{l+3}{2}}}d\theta\end{aligned} \quad (2.54)$$

by using another definition of the Legendre polynomial, that is,

$$P_l^m(u) = (l+m)! \sum_{i=0}^{int(\frac{l-m}{2})} \frac{(-1)^i (1-u^2)^{\frac{m}{2}+i} u^{l-m-2i}}{2^{m+2i}(l-m-2i)!(m+i)!i!}, \tag{2.55}$$

which differs from equation (2.42) by rewriting the combination of terms. Let $u \equiv \tan^2\theta$ and consider A and B as variables, we have

$$\begin{aligned}
&(2l+2m)! \sum_{i=0}^{l-m} \frac{(-1)^i}{2^{2m+2i}(2l-2m-2i)!(2m+i)!i!} \int_0^{\pi} \frac{\cos^{2l-2m-2i}\theta \sin^{2m+2i+1}\theta}{(A\sin^2\theta + B\cos^2\theta)^{\frac{l+3}{2}}} d\theta \\
=&(2l+2m)! \sum_{i=0}^{l-m} \frac{(-1)^i}{2^{2m+2i}(2l-2m-2i)!(2m+i)!i!} \\
&\qquad \cdot 2\frac{(-4)^l l!}{(2l+1)!} \frac{\partial^{l-m-i}}{\partial B^{l-m-i}} \frac{\partial^{m+i}}{\partial A^{m+i}} \int_0^{\frac{\pi}{2}} \frac{\sin\theta}{(A\sin^2\theta + B\cos^2\theta)^{\frac{l+3}{2}}} d\theta \\
=&(2l+2m)! \sum_{i=0}^{l-m} \frac{(-1)^i}{2^{2m+2i}(2l-2m-2i)!(2m+i)!i!} \\
&\qquad \cdot \frac{(-4)^l l!}{(2l+1)!} \frac{\partial^{l-m-i}}{\partial B^{l-m-i}} \frac{\partial^{m+i}}{\partial A^{m+i}} \int_0^{\infty} \frac{du}{(Au+B)^{\frac{3}{2}}} \\
=&(2l+2m)! \sum_{i=0}^{l-m} \frac{(-1)^i}{2^{2m+2i}(2l-2m-2i)!(2m+i)!i!} \frac{(-4)^l l!}{(2l+1)!} \frac{\partial^{l-m-i}}{\partial B^{l-m-i}} \frac{\partial^{m+i}}{\partial A^{m+i}} (\frac{2}{AB^{\frac{1}{2}}}) \\
=&2l! \frac{(2l+2m)!}{(2l+1)!} \sum_{i=0}^{l-m} \frac{K_{lmi}}{A^{m+i+1}}
\end{aligned} \tag{2.56}$$

where

$$K_{lmi} = (-1)^i \frac{(m+i)! c^{2l-2m-2i+1}}{(2m+i)!(l-m-i)!i!}.$$

Notice that A involves angle ϕ, which is the left over term to be considered in the integral (2.52). The last step for solving the integral, we take the integration with respect to ϕ.

Let $\phi = 2\psi$, we have

$$\begin{aligned}
&\int_0^{2\pi} \frac{\cos(2m\phi)d\phi}{A^{m+i+1}} \\
=&\int_0^{2\pi} \frac{\cos(2m\phi)d\phi}{(\frac{\cos^2\phi}{a^2}+\frac{\sin^2\phi}{b^2})^{m+i+1}} \\
=&\frac{(a^2b^2)^{m+i+1}}{(a^2b^2)^{m+i+1}} \int_0^{2\pi} \frac{\cos(2m\phi)d\phi}{(\frac{\cos^2\phi}{a^2}+\frac{\sin^2\phi}{b^2})^{m+i+1}} \\
=&(ab)^{2m+2i+2} \int_0^{2\pi} \frac{\cos 2m\phi}{(b^2\cos^2\phi + a^2\sin^2\phi)^{m+i+1}} d\phi \\
=&(ab)^{2m+2i+2} \int_0^{2\pi} \frac{\cos 2m\phi}{(\frac{a^2+b^2-a^2+b^2}{2}\cos^2\phi + \frac{a^2+b^2+a^2-b^2}{2}\sin^2\phi)^{m+i+1}} d\phi \\
=&(ab)^{2m+2i+2} \int_0^{2\pi} \frac{\cos 2m\phi}{(\frac{a^2+b^2}{2}(\cos^2\phi+\sin^2\phi) - \frac{a^2-b^2}{2}(\cos^2\phi-\sin^2\phi))^{m+i+1}} d\phi \\
=&(ab)^{2m+2i+2} \int_0^{2\pi} \frac{\cos 2m\phi}{(\frac{a^2+b^2}{2} - \frac{a^2-b^2}{2}(\cos(2\phi))^{m+i+1}} d\phi \\
=&2(ab)^{2m+2i+2} \int_0^{\pi} \frac{\cos m\psi}{(\frac{a^2+b^2}{2} - \frac{a^2-b^2}{2}(\cos(\psi))^{m+i+1}} d\psi \\
=&2(ab)^{2m+2i+2} \frac{1}{(ab)^{m+i+1}} \int_0^{\pi} \frac{\cos m\psi}{(\frac{a^2+b^2}{2ab} - \frac{a^2-b^2}{2ab}\cos\psi)^{m+i+1}} d\psi
\end{aligned} \tag{2.57}$$

Notice that the integral above is in fact the Laplace's second integral [MS]:

Definition 2.1.2 (Laplace's Second Integral for $P_n^m(x)$)**.** If n and m are positive integers and $m \leqslant n$,

$$P_n^m(x) = (-1)^m \frac{n!}{(n+m)!} \frac{1}{\pi} \int_0^{\pi} \frac{\cos m\phi}{(x+\sqrt{x^2-1}\cos\phi)^{n+1}} d\phi.$$

Now we let $\frac{a^2+b^2}{2ab} = x$ and $m+i=n$, we can easily express the integral in terms of associated Legendre polynomials

$$\begin{aligned}
\int_0^{\pi} \frac{\cos m\psi}{(\frac{a^2+b^2}{2ab} - \frac{a^2-b^2}{2ab}\cos\psi)^{m+i+1}} d\psi &= (-1)^{-m} \frac{(m+i-m)!}{(m+i)!} \pi P_{m+i}^m(\frac{a^2+b^2}{2ab}) \\
&= (-1)^m \frac{i!}{(m+i)!} \pi P_{m+i}^m(\frac{a^2+b^2}{2ab}).
\end{aligned} \tag{2.58}$$

We thus have

$$C_{2l,2m}$$
$$= \frac{3}{R^{2l}} \frac{l!(2l-2m)!}{(2m+i)(2l+1)!}(2-\delta_{0m}) \sum_{i=0}^{l-m} (-1)^{\frac{m}{2}+i} \frac{c^{2l-2m-2i}(ab)^{m+i}}{(2m+i)!(l-m-i)!} P_{m+i}^{m}(\frac{a^2+b^2}{2ab}). \tag{2.59}$$

Indeed, this expression could be further simplified by the idea of Ivory's theorem [Dan89]— instead of depending on the value of a, b and c, the gravitational field of a homogeneous triaxial ellipsoid at any exterior point depends only on its mass and any two of the quantities a^2-b^2, b^2-c^2 and a^2-c^2.

The Spherical harmonics form an orthogonal set of functions, so we can apply the Ivory's theorem such that each of the Harmonics coefficients depends only on $\alpha = a^2-c^2$ and $\beta = b^2-c^2$. It implies that for any two ellipsoids with different value of a, b and c but identical values of α, β and masses, their gravitational potentials are the same. We may reduce the terms of $C_{2l,2m}$ by applying the idea to an ellipsoid that is equivalent to the one in which we are interested but with the shortest axis as zero (i.e. $c=0$).

Now with $a=\sqrt{\alpha}$, $b=\sqrt{\beta}$ and $c=0$, we have only one non-zero term left from the series— when $i=l-m$.

$$C_{2l,2m} = \frac{3}{R^{2l}} \frac{l!(2l-2m)!}{(2l+3)(2l+1)!}(2-\delta_{0m})(-1)^{l-\frac{m}{2}} \frac{(\alpha\beta)^{\frac{l}{2}}}{(l+m)!} P_{lm}(\frac{\alpha+\beta}{2\sqrt{\alpha\beta}}). \tag{2.60}$$

Expanding the Legendre polynomial again as defined in (2.55), we have

$$\begin{aligned} P_{lm}(\frac{\alpha+\beta}{2\sqrt{\alpha\beta}}) &= (l+m)! \sum_{i=0}^{int(\frac{l-m}{2})} \frac{(-1)^i(1-(\frac{\alpha+\beta}{2\sqrt{\alpha\beta}})^2)^{\frac{m}{2}+i}(\frac{\alpha+\beta}{2\sqrt{\alpha\beta}})^{l-m-2i}}{2^{m+2i}(l-m-2i)!(m+i)!i!} \\ &= (l+m)! \sum_{i=0}^{int(\frac{l-m}{2})} \frac{(-1)^i(1-(\frac{\alpha+\beta}{2\sqrt{\alpha\beta}})^2)^{\frac{m}{2}+i}(\frac{\alpha+\beta}{2\sqrt{\alpha\beta}})^{l-m-2i}}{2^{m+2i}(l-m-2i)!(m+i)!i!} \\ &= (l+m)! \sum_{i=0}^{int(\frac{l-m}{2})} \frac{(-1)^i(-1)^{\frac{m}{2}+i}(\frac{\alpha-\beta}{2})^{m+2i}(-\frac{\alpha+\beta}{2})^{l-m-2i}}{2^{m+2i}(l-m-2i)!(m+i)!i!} \end{aligned} \tag{2.61}$$

$$
\begin{aligned}
C_{2l,2m} &= \frac{3}{R^{2l}} \frac{l!(2l-2m)!}{(2l+3)(2l+1)!}(2-\delta_{0m})(-1)^{l-\frac{m}{2}}(\alpha\beta)^{\frac{l}{2}} \\
&\qquad \cdot \sum_{i=0}^{int(\frac{l-m}{2})} \frac{(-1)^{-(\frac{m}{2}+2i)}(\frac{\alpha-\beta}{2})^{m+2i}(\frac{\alpha+\beta}{2})^{l-m-2i}}{2^{m+2i}(l-m-2i)!(m+i)!i!} \\
&= \frac{3}{R^{2l}} \frac{l!(2l-2m)!}{(2l+3)(2l+1)!}(2-\delta_{0m})(\alpha\beta)^{\frac{l}{2}} \sum_{i=0}^{int(\frac{l-m}{2})} \frac{(\frac{\alpha-\beta}{2})^{m+2i}(-\frac{\alpha+\beta}{2})^{l-m-2i}}{2^{m+2i}(l-m-2i)!(m+i)!i!} \\
&= \frac{3}{R^{2l}} \frac{l!(2l-2m)!}{(2l+3)(2l+1)!}(2-\delta_{0m}) \sum_{i=0}^{int(\frac{l-m}{2})} \frac{(\frac{\alpha-\beta}{2})^{m+2i}(-\frac{\alpha+\beta}{2})^{l-m-2i}}{2^{m+2i}(l-m-2i)!(m+i)!i!}
\end{aligned} \tag{2.62}
$$

Since this is the harmonic coefficient for the equivalent ellipsoid it must be the coefficient for the original ellipsoid and thus α and β can be rewritten in terms of a, b and c without loss of generosity.

$$
C_{2l,2m} = \frac{3}{r^{2l}} \frac{l!(2l-2m)!}{2^{2m}(2l+3)(2l+1)!}(2-\delta_{0m}) \sum_{i=0}^{int(\frac{l-m}{2})} \frac{(a^2-b^2)^{m+2i}[c^2-\frac{1}{2}(a^2+b^2)]^{l-m-2i}}{16^i(l-m-2i)!(m+i)!i!}. \tag{2.63}
$$

Notice that coefficients $C_{2l,2m}$ are all non-dimensional.

Remark 2.1.3. In the formula of $C_{2l,2m}$, variable r carries the unit of kilometers while the term a^2-b^2 carries the unit of square kilometer. In the first fraction of (2.63), we have r^{2l} as the denominator and thus it has the unit of $(km)^{2l}$ in the denominator. The numerator of the fraction of summation has the term $(a^2-b^2)^{m+2i}$, which carries the unit of $(km)^{2(m+2i)}$ while the term $[c^2-\frac{1}{2}(a^2+b^2)]^{l-m-2i}$ carries the unit of $(km)^{2(l-m-2i)}$. With the multiplication, it gives $(km)^{2(m+2i)+2(l-m-2i)} = (km)^{2l}$, which is the same as the unit we obtained from the denominator of the first fraction. A cancellation performed for simplification, we obtain a no-unit quantity as the coefficient $C_{2l,2m}$. Therefore, it is a non-dimensional quantity.

Other than the coefficients S_{lm} are all zeros, all the coefficients C_{lm} with either l or m as odd number are also zeros. Thus, the coefficients that contribute to the gravity as non-zeros terms are those of the form $C_{2l,2m}$ for $l, m = 0, 1, 2, ...$ [Sch16]. Since we consider a triaxial ellipsoid, the shape of its body is defined by the equation

$$\left(\frac{x}{a}\right)^2 + \left(\frac{y}{b}\right)^2 + \left(\frac{z}{c}\right)^2 \leqslant 1.$$

It follows that the first few terms of the spherical harmonics $C_{2l,2m}$ for $l, m = 0, 1, 2, ...$ can be written as the following explicit formula [Sch16]:

$$\begin{aligned} C_{20} &= \frac{1}{5R^2}\left(c^2 - \frac{a^2+b^2}{2}\right), \\ C_{22} &= \frac{1}{20R^2}\left(a^2 - b^2\right), \\ C_{40} &= \frac{15}{7}\left(C_{20}^2 + 2C_{22}^2\right), \\ C_{40} &= \frac{5}{7}\left(C_{20}^2 C_{22}^2\right), \\ C_{40} &= \frac{5}{28}C_{22}^2, \end{aligned} \tag{2.64}$$

where R is the normalized mean radius of the body.

2.2 Data of Trojan Asteroid 624 Hektor and its Spherical Harmonic Coefficients Computation

The spherical harmonic coefficients of a homogeneous tri-axial ellipsoid are given by:

$$C_{l,m} = \frac{3}{R_H^l}\frac{(l/2)!(l-m)!}{2^m(l+3)(l+1)!}(2-\delta_{0m})\sum_{i=0}^{int(\frac{l-m}{4})}\frac{(a^2-b^2)^{\frac{m+4i}{2}}\left[c^2-\frac{1}{2}(a^2+b^2)\right]^{\frac{l-m-4i}{2}}}{16^i(\frac{l-m-4i}{2})!(\frac{m+2i}{2})!i!}$$

where δ_{0m} is Kronecker symbol, a, b, c are the semi-major radius of the tri-axial ellipsoid and R_H is a scale length. According to the reference [Joh11] we have Hektor is approximately 416 × 131 × 120 km in size and the equivalent radius (i.e., the radius of a sphere with the same volume as the asteroid) is $R_H = 92$ km. Therefore $a = 208km$, $b = 65.5km$ and $c = 60km$; we take the scale length equal to the mean radius of Hektor, which is approximately $92km$.

Using the above formula, the following values for the first (non-zero) spherical harmonic coefficients are obtained:

$$
\begin{aligned}
&C_{2,0} = -0.4768, \quad C_{2,2} = \quad 0.2302, \\
&C_{4,0} = \quad 0.7143, \quad C_{4,2} = -0.0784, \quad C_{4,4} = \quad 0.0095, \\
&C_{6,0} = -1.5477, \quad C_{6,2} = \quad 0.0768, \quad C_{6,4} = -0.0025, \quad C_{6,6} = \quad 0.0002
\end{aligned}
$$

Among the above data, both C_{20} and C_{22} are significant to the gravitational potential. The sectional cut along the latitude of the body is described by the coefficient C_{22}. Due to the fact that Hektor spins as fast as $6.921 \pm 0h$ [Joh11], the averaging effect of the coefficient C_{22} is zero. While spinning fast, the effect of C_{22} can be considered as averaging out all the sectional cuts of the body. Therefore we opt out the effect of C_{22} in the following chapters.

Chapter 3

Central Configurations of Oblate bodies

This chapter is devoted to give some background information about central configuration as well as the derivation of the triangular central configurations of the model of three oblate bodies under mutual gravitational interaction. We will also consider the particular case when only one of the three bodies is oblate.

We note that there exist papers in the literature (e.g., [APHS16]), which consider systems of three bodies, with one of the bodies non-spherical, which are assumed to form an equilateral triangle central configuration. Such assumption, while it may lead to very good approximations, is not physically correct. Thus we aim to present the central configuration of the model that we are interested in.

3.1 Background

3.1.1 Central Configuration

The n–body problem study the motion of n–point masses in $\mathbb{R}^N$ moving under their mutual gravity, where $N = 1, 2$ or 3, assuming that the gravitational constant $G = 1$ the equations of motion can be written as

$$m_k \ddot{q}_k = \sum_{k=1,k\neq l}^{n} \frac{m_k m_l (q_k - q_l)}{\|q_k - q_l\|^3} = \nabla_k U = \frac{\partial U}{\partial q_k}, \tag{3.1}$$

where m_k is the body mass for $k = 1, 2, ..., n$, q_k is the position vector of the mass m_k, U is the Newtonian potential such that $U = \sum_{k<l} \frac{m_k m_l}{r_{lk}}$ and $r_{lk} = \|q_l - q_k\|$ for $l \neq k$. Notice that the potential U only depends on the mutual distances. Denote $\mathbf{q} = (q_1, q_2, q_3, ..., q_n)$, and $\mathbf{M} = Nn \times Nn$ diagonal matrix with N copies of each mass along the diagonal. Then equation (3.1) can be written as

$$\mathbf{M}\ddot{\mathbf{q}} = \nabla U(\mathbf{q}), \tag{3.2}$$

where ∇ is the Nn dimensional gradient given by $\nabla = (\nabla_1, ..., \nabla_n)$ where ∇_i is the N-dimensional gradient.

Definition 3.1.1 (Central Configuration)**.** A Central Configuration in the $n-$ body problem is a particular position of the $n-$ particles where the position and acceleration vectors are proportional, with the same constant of proportionality. In other words we have

$$\ddot{q}_k(t) = \gamma q_k(t), \tag{3.3}$$

for all t and $k = 1, 2, ..., n$.

Consider the center of mass is fixed at the origin, equation (3.3) says that all of the accelerations are pointing towards the center of mass, which is the origin, under our assumption. Multiplying both side of equation (3.3) by $m_k q_k$ and taking a summation over k, we have

$$\sum_k m_k q_k \cdot \ddot{q}_k = \gamma \sum_k m_k q_k^2, \tag{3.4}$$

where $\cdot$ refers to dot product in $\mathbb{R}^{\mathbb{N}}$. Thus, we have

$$\sum_k q_k \nabla_k U = \gamma \sum_k m_k q_k^2. \tag{3.5}$$

Next we introduce moment of inertia by the following definition:

Definition 3.1.2 (Moment of Inertia)**.** The moment of inertia is given by

$$I = \sum_{j=1}^{n} m_j q_j^2.$$

where m_j is the mass for the j^{th} body and q_j is the position vector of the mass m_j.

Now, the equation (3.4) becomes

$$\sum_k q_k \bigtriangledown_k U = \gamma I. \tag{3.6}$$

Furthermore, we have

$$\begin{aligned}
\sum_k q_k \nabla_k U &= \sum_k q_k \sum_{l \neq k} \frac{m_l m_k}{\|q_l - q_k\|^3}(q_l - q_k) \\
&= \sum_k q_k \sum_{l<k} \frac{m_l m_k}{\|q_l - q_k\|^3}(q_l - q_k) + \sum_k q_k \sum_{l>k} \frac{m_l m_k}{\|q_l - q_k\|^3}(q_l - q_k) \\
&= \sum_k q_k \sum_{l<k} \frac{m_i m_k (q_l - q_k)}{\|q_l - q_k\|^3} + \sum_l q_l \sum_{l<k} \frac{m_i m_k (q_k - q_l)}{\|q_l - q_k\|^3} \\
&= \sum_k \frac{m_l m_k (q_l - q_k)}{\|q_l - q_k\|^3}(q_k - q_l) \\
&= -\sum_k \frac{m_l m_k (q_l - q_k)^2}{\|q_l - q_k\|^3} \\
&= -U
\end{aligned} \tag{3.7}$$

The relationship above shows that the constant

$$\gamma = \frac{-U}{I}, \tag{3.8}$$

that introduces a negatively proportionality in a central configuration. Denote $M = m_1 + m_2 + \cdots + m_n$. Using the assumption of having the center of mass at origin, we have

$$\begin{aligned}\sum_{i,j} m_i m_j r_{ij}^2 &= \sum_{ij} m_i m_j \|q_i - q_j\|^2 \\ &= \sum_{i,j} m_i m_j \|q_i\|^2 - 2\sum_{i,j} m_i m_j q_i \cdot q_j + \sum_{ij} m_i m_j \|q_j\|^2 \\ &= MI - 2\sum_i m_i q_i \left(\sum_j m_j q_j\right) + MI \\ &= 2MI.\end{aligned} \tag{3.9}$$

Moreover,

$$\sum_{i,j} m_i m_j r_{ij}^2 = 2MI \iff 2\sum_{i<j} m_i m_j r_{ij}^2 = 2MI.$$

Thus the moment of inertial I can also be written as

$$I = \frac{1}{M}\sum_{i<j} m_i m_j r_{ij}^2. \tag{3.10}$$

As the moment of inertia I can be written in terms of the mutual distances, we can find its relation with the potential U easily. Using the equation of motion, we now obtain

$$\begin{aligned}\mathbf{M}\ddot{\mathbf{q}}(t) &= \gamma\mathbf{M}\mathbf{q}(t) = \gamma\sum_k m_k q_k = \frac{\gamma}{2}\sum_k \frac{\partial}{\partial q_k}(m_k q_k^2) \\ \nabla U(\mathbf{q}) &= \frac{1}{2}\gamma\nabla I(\mathbf{q})\end{aligned} \tag{3.11}$$

Since the central configurations are invariant under scaling, we may as well normalize the central configuration by setting I = 1, a normalized central configuration will be resulted in this case . We observe that equation (3.11) is a Lagrange multiplier problem, with γ as the Lagrange multiplier. It is well known that this delicate balancing of the gravitational forces in equation (3.8) gives rise to some remarkable solutions of the n-body problem. In this chapter, we found the scalene triangular central configuration as a solution to a

restricted four body problem with three heavy oblate bodies. In this thesis, the notion of Central Configuration and the results on this chapter are important for an application on the Hill approximation as shown in Chapter 4.
For instance, in the case of point masses, for $n = 3$, the only non-collinear central configuration is that the masses lie on the vertices of an equilateral triangle, which is known as the Lagrange central configuration. It is one of the first explicit solutions given in the three-body problem. We will consider this central configuration in the next section.

Definition 3.1.3 (Homographic solution)**.** A solution $\mathbf{q}(t) = (q_1(t), q_2(t), ..., q_n(t))$ of the n–body problem is called homographic if the configuration of the bodies remains similar with itself for all time t.

In other words, there exists a scalar function $P = P(t) > 0$ and an orthogonal matrix $\Omega(t) \in SO(3)$, such that $q_k(t) = P(t)\Omega(t)q_k(0)$, for $k = 1, 2, ..., n$, where $q_k(0) = (q_1(0), ..., q_N(0))$ in $\mathbb{R}^N$ is a central configuration. Homographic solutions are the configurations that are invariant under scaling and rotation and it is often called the self-similar configurations. A special class of homographic solutions consists of those for which the shape of the configuration remains unchanged.

Definition 3.1.4 (Relative equilibrium)**.** A solution of the n-body problem where the configuration formed by the bodies stays self-congruent is called a relative equilibrium.

In the following sections, we are particularly interested in obtaining the relative equilibrium solution for some special cases.

3.1.2 Central Configuration for the Three-Body Problem with All Three Point Masses the— Lagrange central configuration

Consider three point masses are interacting under the Newton's gravitational force such that $m_1 \geqslant m_2 \geqslant m_3$. We refer m_1 as the primary body, m_2 as the secondary, and m_3

as the tertiary. we obtain the following system of equations of motion. Below $q_1, q_2, q_3 \in \mathbb{R}^2 (N = 2)$:

$$
\begin{aligned}
m_1\ddot{q}_1 &= m_1m_2(q_2 - q_1)\frac{1}{\|q_2 - q_1\|^3} + m_1m_3(q_3 - q_1)\frac{1}{\|q_3 - q_1\|^3}, \\
m_2\ddot{q}_2 &= m_2m_1(q_1 - q_2)\frac{1}{\|q_1 - q_2\|^3} + m_2m_3(q_3 - q_2)\frac{1}{\|q_3 - q_2\|^3}, \\
m_3\ddot{q}_3 &= m_3m_1(q_1 - q_3)\frac{1}{\|q_2 - q_3\|^3} + m_1m_2(q_2 - q_1)\frac{1}{\|q_1 - q_3\|^3},
\end{aligned}
\tag{3.12}
$$

the gravitational constant is normalized to $G = 1$. Denote $r_{ij} = \|q_i - q_j\|$, for $i \neq j$, $\mathbf{q} = (q_1, q_2, q_3)$, and $\mathbf{M} = \operatorname{diag}(m_1, m_1, m_2, m_2, m_3, m_3)$ the 6×6 matrix with 2 copies of each mass along the diagonal. Then (3.12) can be written as

$$
\mathbf{M}\ddot{\mathbf{q}} = \nabla U(\mathbf{q}), \tag{3.13}
$$

where

$$
U(\mathbf{q}) = m_1m_2\left(\frac{1}{r_{12}}\right) + m_1m_3\left(\frac{1}{r_{13}}\right) + m_2m_3\left(\frac{1}{r_{23}}\right) \tag{3.14}
$$

is the potential for the three body problem. Assuming the center of mass is fixed at the origin, we have

$$
\mathbf{M}\mathbf{q} = \sum_{i=1}^{3} m_i q_i = 0, \tag{3.15}
$$

Following the notation and derivation in section 3.1.1, we have equation (3.8). As the moment of inertia I can be written in terms of the mutual distances, the conditions for U to have a critical point on the fixed $\bar{I}$ are

$$
\begin{aligned}
-\frac{m_1m_2}{r_{12}} &= \gamma m_1m_2r_{12}^2 \\
-\frac{m_2m_3}{r_{23}} &= \gamma m_2m_3r_{23}^2 \\
-\frac{m_3m_1}{r_{31}} &= \gamma m_3m_1r_{31}^2
\end{aligned}
\tag{3.16}
$$

which has the only solution of $r_{12} = r_{23} = r_{31} = \left(-\frac{1}{\gamma}\right)^{\frac{1}{3}}$. This solution is an equilateral triangle while γ is a scale parameter— one of the first explicit solutions given in the three-body problem was the Lagrange central configuration, where three bodies of different masses lie at the vertices of an equilateral triangle [Gei16,Eas93], with each body traveling along a specific Kepler orbit [Bel18].

Proposition 3.1.5 (Equilateral triangular centeral configuration)**.** *In the three-body problem with all three point masses, for every fixed value $\bar{I}$ of the moment of inertia there exists a unique central configuration, which is an equilateral triangle.*

3.1.3 Location of the Bodies in the Equilateral Triangular Central Configuration

We now compute the expression of the location of the three bodies in the equilateral triangular central configuration, relative to a synodic frame that rotates together with the bodies, with the center of mass fixed at origin, and the location of m_1 on the negative x-semi-axis. In $\mathbb{R}^3$ $(N = 3)$, we have $q_i = (x_i, y_i, z_i)$ as the position vector of the i^{th} body with mass m_i, for $i = 1, 2, 3$. Assuming the normalization of masses and the masses lie on the xy-plane, we have $\sum_{k=1}^{3} m_k = 1$, $z = 0$ for all bodies. Instead of fixing the value of the moment of inertia $\bar{I}$, we fixed the length of the equilateral triangle to be 1. It gives us the system of equations

$$(x_2 - x_1)^2 + (y_2 - y_1)^2 = 1, \tag{3.17}$$

$$(x_3 - x_1)^2 + (y_3 - y_1)^2 = 1, \tag{3.18}$$

$$(x_3 - x_2)^2 + (y_3 - y_2)^2 = 1, \tag{3.19}$$

$$m_1 x_1 + m_2 x_2 + m_3 x_3 = 0, \tag{3.20}$$

$$m_1 y_1 + m_2 y_2 + m_3 y_3 = 0, \tag{3.21}$$

$$m_1 + m_2 + m_3 = 1, \tag{3.22}$$

$$y_1 = 0 \tag{3.23}$$

Solving the system of equations, we obtain the location of the Lagrangian equilateral triangle central configuration and the positions of the vertices is given by the following formulas:

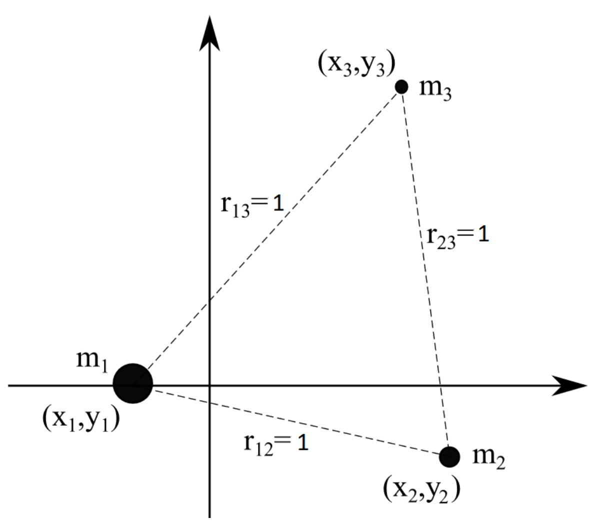

Figure 3.1: Equilarteral triangular central congfiguration.

$$
\begin{aligned}
x_1 &= \frac{-|K|\sqrt{m_2^2 + m_2 m_3 + m_3^2}}{K}, \\
y_1 &= 0, \\
z_1 &= 0, \\
x_2 &= \frac{|K|[(m_2 - m_3)m_3 + m_1(2m_2 + m_3)]}{2K\sqrt{m_2^2 + m_2 m_3 + m_3^2}}, \\
y_2 &= \frac{-\sqrt{3}m_3}{2m_2^{\frac{3}{2}}}\sqrt{\frac{m_2^3}{m_2^2 + m_2 m_3 + m_3^2}}, \\
z_2 &= 0, \\
x_3 &= \frac{|K|}{2\sqrt{m_2^2 + m_2 m_3 + m_3^2}}, \\
y_3 &= \frac{\sqrt{3}}{2m_2^{\frac{1}{2}}}\sqrt{\frac{m_2^3}{m_2^2 + m_2 m_3 + m_3^2}}, \\
z_3 &= 0,
\end{aligned}
\tag{3.24}
$$

where $K = m_2(m_3 - m_2) + m_1(m_2 + 2m_3)$. See [BP13]. We note that as m_3 goes to zero the limiting position of the three masses is given by:

$$
\begin{aligned}
x_1 &= -m_2, & y_1 &= 0, & z_1 &= 0, \\
x_2 &= 1 - m_2, & y_2 &= 0, & z_2 &= 0, \\
x_3 &= \tfrac{1-2m_2}{2}, & y_3 &= \tfrac{\sqrt{3}}{2}, & z_3 &= 0,
\end{aligned}
\tag{3.25}
$$

which represent the positions of the primaries and of the L_4 equilibrium point in the planar circular restricted three-body problem.

3.2 Central Configuration for the Three-Body Problem with All Three Oblate Bodies

In the case of an oblate body, we describe the gravitational potential of the body in terms of spherical harmonics as in Chapter 2, and we only retain the most significant one, that is the coefficient C_{20}, which is also denoted by $-J_2$.

We start by finding the triangular central configurations formed by the three heavy bodies m_1, m_2 and m_3. Consider three heavy, oblate bodies with normalized masses $m_1 \geqslant m_2 \geqslant m_3$ such that $\sum_{i=1}^{3} m_i = 1$. We denote the oblateness coefficient by C_{20}^i for each body m_i. The corresponding gravitational potential in Cartesian coordinates is:

$$V_i(x, y, z) = \frac{m_i}{r} + \frac{m_i}{r}\left(\frac{R_i}{r}\right)^2\left(\frac{C_{20}^i}{2}\right)\left(3\left(\frac{z}{r}\right)^2 - 1\right) \tag{3.26}$$

where m_i is the normalized mass of the i^{th} body, r is the distance from m_i, R_i is its average radius in normalized units, and the gravitational constant is also normalized as $G = 1$. When the bodies have oblate shapes, $C_{20}^i < 0$. The case of $C_{20}^i > 0$ corresponds to prolate shapes. Consider the rotating frame in the spherical coordinates, we have the approximation of the gravitational potential for the body of mass m_i to be expressed as

$$\begin{aligned} V_i(x, y, z) &= \frac{m_i}{r} - \frac{m_i}{r}\left(\frac{R_i}{r}\right)^2\left(\frac{C_{20}^i}{2}\right)\left(3\left(\frac{z}{r}\right)^2 - 1\right) \\ &= \frac{m_i}{r} - \frac{m_i}{r}\left(\frac{R_i}{r}\right)^2\left(\frac{C_{20}^i}{2}\right)\left(3\sin\phi^2 - 1\right), \end{aligned} \tag{3.27}$$

for $i = 1, 2, 3$, where m_i is the normalized mass of the i^{th} body (the sum of the three masses is the unit of mass), R_i is the average radius of the i^{th} body in normalized units, the gravitational constant is normalized to 1, $\sin\phi = z/r$. We want to find the triangular central configurations by following the approach in [APC13]. By the definition of central configuration, the three bodies lie in the same plane and therefore we set in the gravitational field (3.27). We obtain $z = 0$ (i.e.$\phi = 0$) and thus

$$V_i(q) = \frac{m_i}{r} + \frac{C_i m_i}{r^3}, \tag{3.28}$$

where $q = (x, y)$ is the position vector of an arbitrary point on the plane, $r = \|q\|$ is the distance from m_i, and we denote

$$C_i = R_i^2 J_{20}^i / 2 > 0. \tag{3.29}$$

Let q_i be the position vector of the mass m_i, for $i = 1, 2, 3$, in an inertial frame centered at the barycenter of the three bodies. The combination of the gravitational potentials (3.28) and the notation (3.29) yields the equations of motion of the three bodies:

$$\begin{aligned}
m_1\ddot{q}_1 &= m_1m_2(q_2 - q_1)\left[\frac{1}{\|q_2 - q_1\|^3} - \frac{3C_{12}}{\|q_2 - q_1\|^5}\right] + m_1m_3(q_3 - q_1)\left[\frac{1}{\|q_3 - q_1\|^3} - \frac{3C_{13}}{\|q_3 - q_1\|^5}\right],\\
m_2\ddot{q}_2 &= m_2m_1(q_1 - q_2)\left[\frac{1}{\|q_1 - q_2\|^3} - \frac{3C_{12}}{\|q_1 - q_2\|^5}\right] + m_2m_3(q_3 - q_2)\left[\frac{1}{\|q_3 - q_2\|^3} - \frac{3C_{23}}{\|q_3 - q_2\|^5}\right],\\
m_3\ddot{q}_3 &= m_3m_1(q_1 - q_3)\left[\frac{1}{\|q_3 - q_1\|^3} - \frac{3C_{13}}{\|q_3 - q_1\|^5}\right] + m_1m_2(q_2 - q_1)\left[\frac{1}{\|q_2 - q_1\|^3} - \frac{3C_{12}}{\|q_2 - q_1\|^5}\right],
\end{aligned} \tag{3.30}$$

where the terms C_{ij} represents the sum of C for the i^{th} and j^{th} bodies, that is,

$$C_{ij} = C_i + C_j \text{ for } i \neq j \in \{1, 2, 3\}. \tag{3.31}$$

and the gravitational constant is normalized to $G = 1$. With $r_{ij} = \|q_i - q_j\|$, for $i \neq j$, $\mathbf{q} = (q_1, q_2, q_3)$, and $\mathbf{M} = \text{diag}(m_1, m_1, m_2, m_2, m_3, m_3)$ the 6×6 matrix with 2 copies of each mass along the diagonal, equation (3.30) can be written as a compact form:

$$\mathbf{M}\ddot{\mathbf{q}} = \nabla U(\mathbf{q}), \tag{3.32}$$

where

$$U(\mathbf{q}) = m_1m_2\left(\frac{1}{r_{12}} - \frac{C_{12}}{r_{12}^3}\right) + m_1m_3\left(\frac{1}{r_{13}} - \frac{C_{13}}{r_{13}^3}\right) + m_2m_3\left(\frac{1}{r_{23}} - \frac{C_{23}}{r_{23}^3}\right) \tag{3.33}$$

is the potential for the system of three oblate bodies problem. Assuming the center of mass fixed at the origin, we have

$$\mathbf{Mq} = \sum_{i=1}^{3} m_i q_i = 0. \tag{3.34}$$

Relative equilibrium solutions for the motion of the three bodies are of interest. Note that they are characterized by the fact they become equilibrium points in a uniformly rotating frame.

The 6×6 block diagonal matrix that consists of 3 diagonal blocks is denoted by $R(\theta)$; it takes the form

$$\begin{pmatrix} \cos(\theta) & -\sin(\theta) \\ \sin(\theta) & \cos(\theta) \end{pmatrix} \in SO(2).$$

Consider $\mathbf{q}(t) = R(\omega t)\mathbf{z}(t)$ for some $\omega \in \mathbb{R}$ where $\mathbf{z} = (z_1, z_2, z_3) \in \mathbb{R}^6$, we have,

$$\begin{aligned} \dot{q} &= \omega \dot{R}\mathbf{z}(t) + R\dot{\mathbf{z}(t)} \\ \ddot{q} &= \omega^2 \ddot{R}\mathbf{z}(t) + \omega \dot{R}\dot{\mathbf{z}(t)} + \omega \dot{R}\dot{\mathbf{z}(t)} + R\ddot{\mathbf{z}(t)} \\ &= \omega^2 \ddot{R}\mathbf{z}(t) + 2\omega \dot{R}\dot{\mathbf{z}(t)} + R\ddot{\mathbf{z}(t)}, \end{aligned} \tag{3.35}$$

where

$$R = \begin{pmatrix} \cos(\omega t) & -\sin(\omega t) \\ \sin(\omega t) & \cos(\omega t) \end{pmatrix}, \text{ and} \tag{3.36}$$

$$\dot{R} = \begin{pmatrix} -\sin(\omega t) & -\cos(\omega t) \\ \cos(\omega t) & -\sin(\omega t) \end{pmatrix}, \ddot{R} = \begin{pmatrix} -\cos(\omega t) & \sin(\omega t) \\ -\sin(\omega t) & -\cos(\omega t). \end{pmatrix} \tag{3.37}$$

When $\theta = 0$, we have $R(\theta) = Id$. And thus we follow with using $\theta = 0$ to evaluate R, $\dot{R}$ and $\ddot{R}$. We obtain

$$\dot{R} = \begin{pmatrix} 0 & -1 \\ 1 & 0 \end{pmatrix}, \ddot{R} = \begin{pmatrix} -1 & 0 \\ 0 & -1 \end{pmatrix} = -Id \tag{3.38}$$

Substituting $\ddot{\mathbf{q}}(t) = \ddot{\mathbf{z}} + 2\omega J\dot{\mathbf{z}} - \omega^2\mathbf{z}$ in equation (3.32), we obtain

$$\mathbf{M}\left(\ddot{\mathbf{z}} + 2\omega J\dot{\mathbf{z}} - \omega^2\mathbf{z}\right) = \nabla U,$$

where $\mathbf{J}$ is the block diagonal matrix consisting of 3 diagonal blocks of the form

$$J = \begin{pmatrix} 0 & -1 \\ 1 & 0 \end{pmatrix}. \tag{3.39}$$

The condition for an equilibrium point of (3.27) such that $\dot{\mathbf{z}} = 0$ and $\ddot{\mathbf{z}} = 0$ yields the algebraic equation

$$\nabla U(\mathbf{z}) + \omega^2\mathbf{M}\mathbf{z} = 0. \tag{3.40}$$

A solution $\mathbf{z}$ of the three-body problem satisfying (3.40) is referred to as a *central configuration.* This is equivalent to $\ddot{z}_i = -\omega^2 z_i$, for $i = 1, 2, 3$, which means that the accelerations of the three masses are proportional to their corresponding position vectors, and all accelerations are pointing towards the center of mass. Hence, the solution $\mathbf{q}(t)$ is a relative equilibrium solution if and only if $\mathbf{q}(t) = R(\omega t)\mathbf{z}(t)$ with $\mathbf{z}(t)$ being a central configuration solution. Note that the rotation $R(\omega t)$ is a circular solution of the Kepler's problem. Let $I(\mathbf{z}) = \mathbf{z}^T M\mathbf{z} = \sum_i m_i\|z_i\|^2$ be the moment of inertia. Since it is in a quadratic form, we have gradient $\nabla I(\mathbf{z}) = (M^T + M)\mathbf{z}$. Notice that M is a diagonal matrix, and thus it is symmetric $(M^T = M)$. We then obtain $\nabla I(\mathbf{z}) = 2M\mathbf{z}$. It is easy to see that this is a conserved quantity for the motion, that is, $I(\mathbf{z}(t)) = \bar{I}$ for some $\bar{I}$ for all t. With $\mathbf{M}\mathbf{z} = 0$, normalization on masses such that $\sum_{i=1}^{3} m_i = 1$ and following the derivation shown in Section 3.1.1 as in equation (3.10), we have the moment of inertia can be written as:

$$I(\mathbf{z}) = \sum_{1\leqslant i<j\leqslant 3} m_i m_j \|z_i - z_j\|^2 := \sum_{1\leqslant i<j\leqslant 3} m_i m_j r_{ij}^2. \tag{3.41}$$

Alternatively, we can use Lagrange's second identity to show the above relationship (see, e.g., [GN12]). In conclusion, central configurations correspond to critical points of the potential U on the sphere $\mathbf{z}^T M\mathbf{z} = 1$, which can be obtained by solving the Lagrange multiplier problem

$$\nabla f(\mathbf{z}) = 0, \qquad I(\mathbf{z}) - \bar{I} = 0, \tag{3.42}$$

where $f(\mathbf{z}) = U(\mathbf{z}) + \frac{1}{2}\omega^2(I(\mathbf{z}) - \bar{I})$. In the above, we used the fact that $\nabla I(\mathbf{z}) = 2\mathbf{M}\mathbf{z}$.

Since both U and I can be written in terms of $r_{ij} = \|z_i - z_j\|$ for $1 \leqslant i < j \leqslant 3$, we solve the problem (3.42) in these variables. This reduces the dimension of the system (3.42) from 7 equations to 4 equations. Denote $\mathbf{r} = (r_{12}, r_{13}, r_{23})$, and let $\tilde{f}(\mathbf{r})$ be the function f expressed in the variable $\mathbf{r}$, that is $\tilde{f}(\mathbf{r}(\mathbf{z})) = f(\mathbf{z})$. Using the chain rule, we have $\nabla_r \tilde{f} \cdot \left(\frac{\partial \mathbf{r}}{\partial \mathbf{z}}\right) = \nabla_{\mathbf{z}} f(\mathbf{z})$. For z_1, z_2, z_3 are not collinear, it is easy to see that the rank of the matrix $\left(\frac{\partial \mathbf{r}}{\partial \mathbf{z}}\right)$ is maximal (for details, see [CLPC04, APC13]). As we are looking for triangular central configurations, this condition is satisfied. Thus, $\nabla_r \tilde{f}(\mathbf{r}) = 0$ if and only if $\nabla_{\mathbf{z}} f(\mathbf{z}) = 0$. In addition, we recall the moment of inertia as in equation (3.10). We can now solve the system (3.42) in the variable $\mathbf{r}$. We obtain

$$\begin{cases} \frac{1}{r_{12}^2} - \frac{3C_{12}}{r_{12}^4} - \omega^2 r_{12} = 0, \\ \frac{1}{r_{13}^2} - \frac{3C_{13}}{r_{13}^4} - \omega^2 r_{13} = 0, \\ \frac{1}{r_{23}^2} - \frac{3C_{23}}{r_{23}^4} - \omega^2 r_{23} = 0, \\ m_1 m_2 r_{12}^2 + m_1 m_3 r_{13}^2 + m_2 m_3 r_{23}^2 = \bar{I}. \end{cases}$$

It gives us the system of equations

$$\begin{cases} \frac{1}{r_{12}^3} - \frac{3C_{12}}{r_{12}^5} = \omega^2, \\ \frac{1}{r_{13}^3} - \frac{3C_{13}}{r_{13}^5} = \omega^2, \\ \frac{1}{r_{23}^3} - \frac{3C_{23}}{r_{23}^5} = \omega^2, \\ m_1 m_2 r_{12}^2 + m_1 m_3 r_{13}^2 + m_2 m_3 r_{23}^2 = \bar{I}. \end{cases} \tag{3.43}$$

Note that the function

$$h(r) = \frac{1}{r^3} - \frac{3C}{r^5} - \omega^2 \tag{3.44}$$

has negative derivative

$$h'(r) = -\frac{3}{r^4} + \frac{15C}{r^6} < 0$$

for $r > 0$ and $C < 0$, and thus h is injective as a function of r. In addition, we note that $\lim_{r\to 0} h(r) = +\infty$ and $\lim_{r\to\infty} = -\omega^2 < 0$. And therefore, for each of the first three equations in the system (3.43), and for a fixed ω, there exists a unique solution $r_{ij} = r_{ij}(\omega)$. Consider the first equation of the system (3.43). Taking implicit differentiation with respect to ω, we have

$$\begin{aligned} &\frac{3}{r_{12}^4}\frac{dr_{12}}{d\omega} - \frac{15C_{12}}{r_{12}^6}\frac{dr_{12}}{d\omega} = -2\omega, \\ \Longrightarrow &\frac{dr_{12}}{d\omega} = \frac{-2\omega}{\frac{3}{r_{12}^4} - \frac{15C_{12}}{r_{12}^6}}. \end{aligned} \tag{3.45}$$

For $r_{12} > 0$ and $C_{12} < 0$, we have $\frac{dr_{12}}{d\omega} < 0$, provided $\omega > 0$. Similarly, we obtain $\frac{dr_{13}}{d\omega} < 0$, and $\frac{dr_{23}}{d\omega} < 0$.

Consider the right-hand side of the last equation in the system (3.43) as a function of ω. We denote it as $F(\omega)$, that is

$$F(\omega) = m_1m_2r_{12}^2(\omega) + m_2m_3r_{23}^2(\omega) + m_1m_3r_{13}^2(\omega) \tag{3.46}$$

and its derivative with respect to ω is

$$F'(\omega) = 2m_1m_2r_{12}\frac{dr_{12}}{d\omega} + 2m_1m_3r_{13}\frac{dr_{13}}{d\omega} + 2m_2m_3r_{23}\frac{dr_{23}}{d\omega}. \tag{3.47}$$

Recall that $\frac{dr_{ij}}{d\omega} < 0$, we thus have $F'(\omega) < 0$. Therefore, there exists a unique ω such that $F(\omega) = \bar{I}$. Next, we study the dependence on the unique solution r_{ij} on C_{ij}. Consider r

as the unique solution of

$$\frac{1}{r^3} - \frac{3C}{r^5} = \omega^2,$$

the implicit differentiation with respect to C yields

$$\frac{dr}{dC} = -\frac{r}{r^2 - 5C} < 0.$$

It shows that r is a decreasing function in C. If the C_i's satisfy some ordering such as $C_2 \leqslant C_1 \leqslant C_3$, then $C_{12} \leqslant C_{23} \leqslant C_{13}$, and hence $r_{13} \leqslant r_{23} \leqslant r_{12}$. Thus, we have proved the following result:

Proposition 3.2.1. *In the three-body problem with all bodies oblate, for every fixed value $\bar{I}$ of the moment of inertia there exists a unique central configuration, which is in general a scalene triangle.*

Furthermore, the body with the larger C_i is opposite to the longer side of the triangle.

Remark 3.2.2. The last statement of Proposition 3.2.1 is similar to the elementary geometry theorem saying that, in a triangle, the largest angle is opposite the longest side.

Surprisingly, the masses of the bodies do not play a role in the ordering of the sides.

Remark 3.2.3. The triangular central configurations corresponding to different values of ω are not similar to one another, as shown by the following counterexample. Let $C_{12} = -0.1$, $C_{13} = -0.2$, and $C_{23} = -0.3$. For $\omega = 1$ solving (3.43) yields $r_{12} = 1.07937$, $r_{13} = 1.13577$, $r_{23} = 1.18063$. For $\bar{\omega} = 2$ solving (3.43) yields $\bar{r}_{12} = 0.730867$, $\bar{r}_{13} = 0.788914$, $\bar{r}_{23} = 0.831688$. We have

$$\frac{r_{12}}{\bar{r}_{12}} = 1.47683, \frac{r_{13}}{\bar{r}_{13}} = 1.43967, \frac{r_{23}}{\bar{r}_{23}} = 1.41956.$$

This situation is very different from the case of point masses (no oblateness), when all triangular central configurations are equilateral triangles.

Remark 3.2.4. If the unit of distance is rescaled by a factor of α, that is, the quantities r_{ij} and R_i get rescaled by a factor of α, then C_i and C_{ij} get rescaled by a factor of α^2 due to (3.29) and (3.31). Therefore ω gets rescaled by a factor of $\alpha^{-3/2}$, and $\bar{I}$ gets rescaled by a factor of α^2 due to (3.43).

3.3 Location of the Bodies in the Scalene Triangular Central Configuration

In this section we compute the expressions of the locations of the three bodies in the scalene triangular central configuration, relative to a synodic frame that rotates together with the bodies. Assuming the center of mass at the origin, and the location of m_1 on the negative x-semi-axis. In addition we assume that the masses lie on the plane such that $z = 0$. Instead of fixing $\bar{I}$ the moment of inertia, we fix one of the leg of the triangular configuration to be one without loss of generality. It simplifies further computation of the exact location of the vertices of the triangular central configuration in later computation. We fix $r_{12} = 1$, and let $r_{13} = u$, and $r_{23} = v$, where u and v are uniquely determined by the system (3.43). For convenience, we denote $w = 1 + u^2 - v^2$ to yield the following result:

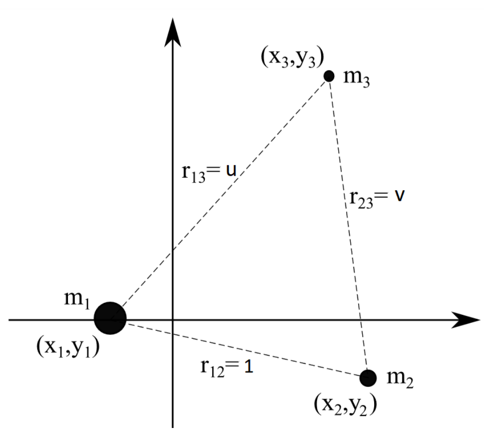

Figure 3.2: Scalene triangular central configuration.

Proposition 3.3.1. *In the synodic reference frame, the coordinates of the three bodies in the triangular central configuration, satisfying the constraints*

$$\begin{aligned}
(x_2 - x_1)^2 + (y_2 - y_1)^2 &= 1, && (3.48)\\
(x_3 - x_1)^2 + (y_3 - y_1)^2 &= u^2, && (3.49)\\
(x_3 - x_2)^2 + (y_3 - y_2)^2 &= v^2, && (3.50)\\
m_1x_1 + m_2x_2 + m_3x_3 &= 0, && (3.51)\\
m_1y_1 + m_2y_2 + m_3y_3 &= 0, && (3.52)\\
m_1 + m_2 + m_3 &= 1, && (3.53)\\
y_1 &= 0, && (3.54)
\end{aligned}$$

are given by

$$\begin{aligned}
x_1 =& -\sqrt{m_2^2 + wm_2m_3 + u^2m_3^2},\\
y_1 =& 0,\\
x_2 =& \frac{-2m_2^2 - 2u^2m_3^2 - 2wm_2m_3 + 2m_2 + wm_3}{2\sqrt{m_2^2 + wm_2m_3 + u^2m_3^2}},\\
y_2 =& -\frac{1}{2}\sqrt{\frac{(4u^2 - w^2)m_3^2}{m_2^2 + wm_2m_3 + u^2m_3^2}},\\
x_3 =& \frac{-2m_2^2 - 2u^2m_3^2 - 2wm_2m_3 + wm_2 + 2u^2m_3}{2\sqrt{m_2^2 + wm_2m_3 + u^2m_3^2}},\\
y_3 =& +\frac{1}{2}\sqrt{\frac{(4u^2 - w^2)m_2^2}{m_2^2 + wm_2m_3 + u^2m_3^2}}.
\end{aligned} \tag{3.55}$$

Proof. With the assumptions introduced in Section 3.2 and 3.3, we begin with the following system

$$\begin{cases} m_1 + m_2 + m_3 = 1, & (1) \\ m_1x_1 + m_2x_2 + m_3x_3 = 0, & (2) \\ m_1y_1 + m_2y_2 + m_3y_3 = 0, & (3) \\ (x_2 - x_1)^2 + (y_2 - y_1)^2 = 1, & (4) \\ (x_3 - x_1)^2 + (y_3 - y_1)^2 = u^2, & (5) \\ (x_3 - x_2)^2 + (y_3 - y_2)^2 = v^2, & (6) \\ y_1 = 0. & (7) \end{cases} \tag{3.56}$$

Since (3) and (7) implies

$$y_2 = -\frac{m_3}{m_2} y_3, \tag{3.57}$$

and thus we have equations (4) and (5) become

$$\begin{cases} (x_1 - x_2)^2 + y_2^2 = 1, & (A) \\ (x_3 - x_1)^2 + y_3^2 = u^2, & (B) \end{cases}$$

With straightforward computation we have equations (A) and (B) become

$$\begin{cases} (x_1 - x_2)^2 = 1 - \frac{m_3^2}{m_2^2} y_3^2, & (A') \\ (x_3 - x_1)^2 = u^2 - y_3^2, & (B') \end{cases}$$

And thus

$$\begin{aligned} x_1 - x_2 + x_3 - x_1 &= \sqrt{1 - \frac{m_3^2}{m_2^2} y_3^2} - \sqrt{u^2 - y_3^2} \\ x_3 - x_1 &= \sqrt{1 - \frac{m_3^2}{m_2^2} y_3^2} - \sqrt{u^2 - y_3^2} \end{aligned} \tag{3.58}$$

On the other hand, the equation (7) in the system (3.56) yields

$$\begin{aligned}(x_3 - x_2)^2 &= v^2 - (y_3 - y_2)^2 \\ &= v^2 - y_3^2(1 + \frac{m_3}{m_2})^2\end{aligned} \tag{3.59}$$

And thus we have

$$\begin{aligned}&\sqrt{1 - \frac{m_3^2}{m_2^2}y_3^2} - \sqrt{u^2 - y_3^2} = v^2 - y_3^2(1 + \frac{m_3}{m_2})^2 \\ &\Longrightarrow 1 - \frac{m_3^2}{m_2^2}y_3^2 - 2\sqrt{1 - \frac{m_3^2}{m_2^2}y_3^2}\sqrt{u^2 - y_3^2} + u^2 - y_3^2 = v^2 - y_3^2(1 + \frac{m_3}{m_2})^2 \\ &\Longrightarrow 1 - \frac{m_3^2}{m_2^2}y_3^2 - 2\sqrt{u^2 - y_3^2 - u^2\frac{m_3^2}{m_2^2}y_3^2 + \frac{m_3^2}{m_2^2}y_3^2} + u^2 - y_3^2 = v^2 - y_3^2(1 + 2\frac{m_3}{m_2} + \frac{m_3^2}{m_2^2}) \\ &\Longrightarrow -2\sqrt{u^2 - y_3^2 - u^2\frac{m_3^2}{m_2^2}y_3^2 + \frac{m_3^2}{m_2^2}y_3^4} = v^2 - 2\frac{m_3}{m_2}y_3^2 - 1 - u^2 \\ &\Longrightarrow 4(u^2 - y_3^2 - u^2\frac{m_3^2}{m_2^2}y_3^2 + \frac{m_3^2}{m_2^2}y_3^4) = 4\frac{m_3^2}{m_2^2}y_3^4 - 4(\frac{m_3}{m_2}y_3^2)(v^2 - 1 - u^2) + (v^2 - 1 - u^2)^2\end{aligned} \tag{3.60}$$

$$\begin{aligned}&\Longrightarrow 4\frac{m_3}{m_2}(v^2 - 1 - u^2)y_3^2 - 4y_3^2 - 4u^2\frac{m_3^2}{m_2^2}y_3^2 = (v^2 - 1 - u^2)^2 - 4u^2 \\ &\Longrightarrow y_3^2(4\frac{m_3}{m_2}(v^2 - 1 - u^2) - 4 - 4u^2\frac{m_3^2}{m_2^2}) = (v^2 - 1 - u^2)^2 - 4u^2 \\ &\Longrightarrow y_3^2 = \frac{(v^2 - 1 - u^2)^2 - 4u^2}{4\frac{m_3}{m_2}(v^2 - 1 - u^2) - 4 - 4u^2\frac{m_3^2}{m_2^2}} \\ &\Longrightarrow y_3 = \sqrt{\frac{(v^2 - 1 - u^2)^2 - 4u^2}{4\frac{m_3}{m_2}(v^2 - 1 - u^2) - 4 - 4u^2\frac{m_3^2}{m_2^2}}}\end{aligned} \tag{3.61}$$

and

$$y_2 = -\frac{m_3}{m_2}\sqrt{\frac{(v^2 - 1 - u^2)^2 - 4u^2}{4\frac{m_3}{m_2}(v^2 - 1 - u^2) - 4 - 4u^2\frac{m_3^2}{m_2^2}}}. \tag{3.62}$$

Now we will make use of the equation (1) of the system (3.56). Let

$$\begin{aligned} A &= x_1 - x_2 = \sqrt{1 - y_2^2}, \\ B &= x_3 - x_1 = \sqrt{u^2 - y_3^2}. \end{aligned} \tag{3.63}$$

Then we have

$$\begin{aligned} x_2 &= x_1 - A, \\ x_3 &= x_1 + B. \end{aligned} \tag{3.64}$$

Thus we have

$$\begin{aligned} & m_1 x_1 + m_2(x_1 - A) + m_3(x_1 + B) = 0 \\ \Longrightarrow\ & m_1 x_1 + m_2 x_1 + m_3 x_1 = m_2 A - m_3 B \\ \Longrightarrow\ & x_1(m_1 + m_2 + m_3) = m_2 A - m_3 B, \end{aligned} \tag{3.65}$$

and since one of our assumptions is $m_1 + m_2 + m_3 = 1$, we have

$$\begin{aligned} & x_1 = m_2 A - m_3 B \\ \Longrightarrow\ & x_1 = m_2\sqrt{1 - y_2^2} - m_2\sqrt{u^2 - y_3^2} \\ \Longrightarrow\ & = m_2\sqrt{1 - \frac{m_3^2[(v^2 - 1 - u^2)^2 - 4u^2]}{m_2^2[4\frac{m_3}{m_2}(v^2 - 1 - u^2) - 4 - 4u^2\frac{m_3^2}{m_2^2}]}} \\ & \qquad - m_3\sqrt{u^2 - \frac{(v^2 - 1 - u^2)^2 - 4u^2}{4\frac{m_3}{m_2}(v^2 - 1 - u^2) - 4 - 4u^2\frac{m_3^2}{m_2^2}}} \\ \Longrightarrow\ & = m_2\sqrt{\frac{m_2^2[4\frac{m_3}{m_2}(v^2 - 1 - u^2) - 4 - 4u^2\frac{m_3^2}{m_2^2}] - m_3^2[(v^2 - 1 - u^2)^2 - 4u^2]}{m_2^2[4\frac{m_3}{m_2}(v^2 - 1 - u^2) - 4 - 4u^2\frac{m_3^2}{m_2^2}]}} \\ & \qquad - m_3\sqrt{\frac{u^2 m_2^2[4\frac{m_3}{m_2}(v^2 - 1 - u^2) - 4 - 4u^2\frac{m_3^2}{m_2^2}] - m_2^2[(v^2 - 1 - u^2)^2 - 4u^2]}{m_2^2[4\frac{m_3}{m_2}(v^2 - 1 - u^2) - 4 - 4u^2\frac{m_3^2}{m_2^2}]}} \end{aligned} \tag{3.66}$$

$$\begin{aligned}
&\implies = \frac{m_2\sqrt{-(2m_2 - m_3(v^2-1-u^2))^2} - m_3\sqrt{-(2u^2m_3 - m_2(v^2-1-u^2))^2}}{\sqrt{4m_2m_3(v^2-1-u^2) - 4m_2^2 - 4u^2m_3^2}} \\
&\implies = \frac{m_2(m_3(v^2-1-u^2) - 2m_2) - m_3(2u^2m_3 - m_2(v^2-1-u^2))}{2\sqrt{m_2^2 + u^2m_3^2 - m_2m_3(v^2-1-u^2)}} \\
&\implies = \frac{-2m_2^2 + 2m_2m_3(v^2-1-u^2) - 2u^2m_3^2}{2\sqrt{m_2^2 + u^2m_3^2 - m_2m_3(v^2-1-u^2)}} \\
&\implies = \frac{-m_2^2 + m_2m_3(v^2-1-u^2) - u^2m_3^2}{\sqrt{m_2^2 + u^2m_3^2 - m_2m_3(v^2-1-u^2)}} \\
&\implies = \frac{-(m_2^2 - m_2m_3(v^2-1-u^2) + u^2m_3^2)}{\sqrt{m_2^2 + u^2m_3^2 - m_2m_3(v^2-1-u^2)}}
\end{aligned} \tag{3.67}$$

We are now getting the expression of x_2 and x_3.

$$\begin{aligned}
&x_2 = x_1 - A \\
&\implies x_2 = \frac{-(m_2^2 - m_2m_3(v^2-1-u^2) + u^2m_3^2)}{\sqrt{m_2^2 + u^2m_3^2 - m_2m_3(v^2-1-u^2)}} \\
&\qquad - \sqrt{1 - \frac{m_3^2[(v^2-1-u^2)^2 - 4u^2]}{m_2^2[4\frac{m_3}{m_2}(v^2-1-u^2) - 4 - 4u^2\frac{m_3^2}{m_2^2}]}} \\
&\implies = \frac{-(m_2^2 - m_2m_3(v^2-1-u^2) + u^2m_3^2)}{\sqrt{m_2^2 + u^2m_3^2 - m_2m_3(v^2-1-u^2)}} \\
&\qquad - \sqrt{\frac{4m_2m_3(v^2-1-u^2) - 4m_2^2 - 4u^2m_3^2 - m_3^2(v^2-1-u^2)^2 + 4u^2m_3^2}{4(m_2m_3(v^2-1-u^2) - m_2^2 - u^2m_3^2)}} \\
&\implies = \frac{-2(m_2^2 - m_2m_3(v^2-1-u^2) + u^2m_3^2) - (2m_2 - m_3(v^2-1-u^2))}{2\sqrt{m_2^2 + u^2m_3^2 - m_2m_3(v^2-1-u^2)}} \\
&\implies = \frac{-(2m_2^2 - 2m_2m_3(v^2-1-u^2) + 2u^2m_3^2 + 2m_2 + m_3(v^2-1-u^2))}{2\sqrt{m_2^2 + u^2m_3^2 - m_2m_3(v^2-1-u^2)}}
\end{aligned} \tag{3.68}$$

and

$$\begin{aligned}
&x_3 = x_1 + B \\
&\implies x_3 = \frac{-(m_2^2 - m_2m_3(v^2-1-u^2) + u^2m_3^2)}{\sqrt{m_2^2 + u^2m_3^2 - m_2m_3(v^2-1-u^2)}} \\
&\qquad + \sqrt{u^2 - \frac{[(v^2-1-u^2)^2 - 4u^2]}{[4\frac{m_3}{m_2}(v^2-1-u^2) - 4 - 4u^2\frac{m_3^2}{m_2^2}]}}
\end{aligned} \tag{3.69}$$

$$\begin{aligned}
\Longrightarrow &= \frac{-(m_2^2 - m_2m_3(v^2-1-u^2) + u^2m_3^2)}{\sqrt{m_2^2 + u^2m_3^2 - m_2m_3(v^2-1-u^2)}} \\
&+ \sqrt{\frac{4m_2m_3u^2(v^2-1-u^2) - 4u^4m_3^2 - m_2^2(v^2-1-u^2)^2}{4(m_2m_3(v^2-1-u^2) - m_2^2 - u^2m_3^2)}} \\
\Longrightarrow &= \frac{-2(m_2^2 - m_2m_3(v^2-1-u^2) + u^2m_3^2) + (2u^2m_3 - m_2(v^2-1-u^2))}{2\sqrt{m_2^2 + u^2m_3^2 - m_2m_3(v^2-1-u^2)}} \\
\Longrightarrow &= \frac{-(2m_2^2 - 2m_2m_3(v^2-1-u^2) + 2u^2m_3^2 - 2u^2m_3 + m_2(v^2-1-u^2))}{2\sqrt{m_2^2 + u^2m_3^2 - m_2m_3(v^2-1-u^2)}}
\end{aligned} \tag{3.70}$$

For convenience, we now denote $w = 1+u^2-v^2$ and substitute w for the above cooridates. We obtain the formulas (3.55). □

Remark 3.3.2. For future reference, we note that if we let $m_3 \to 0$ in (3.55), we obtain

$$\begin{aligned}
x_1 &= -m_2, & y_1 &= 0, \\
x_2 &= -m_2 + 1, & y_2 &= 0, \\
x_3 &= -m_2 + \tfrac{w}{2}, & y_3 &= \tfrac{1}{2}\sqrt{4u^2 - w^2}.
\end{aligned} \tag{3.71}$$

3.4 Central Configurations for the Three-Body Problem with One Oblate Body

In this section, we consider three heavy bodies, of masses $m_1 \geqslant m_2 \geqslant m_3$, with only the tertiary body with mass m_3 being oblate, in which we only take into account the term corresponding to $C_{20} = -J_2$ in the potential (3.27) as in section 3.2 for $i = 3$. It implies the assumption that$C_{20}^1 = C_{20}^2 = 0$. We write the approximation of the gravitational potential of the tertiary in both Cartesian and spherical coordinates in the frame of the tertiary and rotating together with the body:

$$\begin{aligned}
V_3(x,y,z) &= \frac{m_3}{r} - \frac{m_3}{r}\left(\frac{R_3}{r}\right)^2 \left(\frac{J_2}{2}\right)\left(3\left(\frac{z}{r}\right)^2 - 1\right) \\
&= \frac{m_3}{r} + \frac{m_3}{r}\left(\frac{R_3}{r}\right)^2 \left(\frac{C_{20}}{2}\right)\left(3\sin\phi^2 - 1\right),
\end{aligned} \tag{3.72}$$

where m_3 is the normalized mass of the tertiary body with the sum of the three masses as the unit of mass, R_3 is the average radius of mass m_3 in normalized units with the distance between m_1 and m_3 as the unit of distance, the gravitational constant G is again normalized to 1, and $\sin\phi = z/r$. And the potential for the primary and secondary bodies with normalized masses m_1 and m_2 are

$$V_1(x,y,z) = \frac{m_1}{r} \text{ and } V_2(x,y,z) = \frac{m_2}{r} \tag{3.73}$$

respectively. Similar to Section 3.2 we want to find the triangular central configurations formed by the masses m_1, m_2 and m_3. Following the notations in Section 3.2, we note that in the special case when $C_1 = C_2$ we have $C_{13} = C_1 + C_3 = C_2 + C_3 = C_{23}$. In this case, the second and third equations of the system (3.43) are identical, and, since the function h defined in the equation (3.44) is injective as a function of r, it follows that $r_{13} = r_{23}$. Thus the central configuration is an isosceles triangle. This situation occurs, for example, if we assume that only the body m_3 is oblate, i.e. $C_{20}^1 = C_{20}^2 = 0$ and therefore we have obtained the following:

Corollary 3.4.1. *In the three-body problem with one oblate tertiary body with mass m_3, for every fixed value $\bar{I}$ of the moment of inertia there exists a unique central configuration, which is an isosceles triangle with $r_{13} = r_{23}$.*

We note that, while [APC13] studies central configurations of three oblate bodies (as well as of three bodies under Schwarzschild metric), the isosceles central configuration found above is not explicitly shown there (see Theorem 4 in [APC13]).

In order to put this in quantitative perspective, we use the data from Section 2.2 in equation(3.29) and we obtain $C_{20}^3 = 3.329215 \times 10^{-15}$. Letting $u = r_{13} = r_{23} = 1$, we obtain $v = r_{12} = 0.9999999999999967 = 1.0 - 3.3 \times 10^{-15}$ from the system (3.43). Practically, this isosceles triangular central configuration is almost an equilateral triangle.

3.5 Location of the Bodies in the Isosceles Triangular Central Configuration

We now compute the expressions of the locations of the three bodies in the isosceles triangular central configuration, relative to a synodic frame that rotates together with the bodies. With the center of mass fixed at the origin, and the primary body located on the negative x-semi-axis and the assumption that the masses lie in the $z = 0$ plane, we have the following result.

Remark 3.5.1. Similar to Section 3.3 we want to find the location of the isosceles triangular central configurations formed by the masses m_1, m_2 and m_3. Following the notations in Section 3.3, in the case when only the tertiary body with mass m_3 is oblate, by Proposition 3.3.1 we have $r_{13} = u = r_{23} = v$, so $w = 1 + u^2 - v^2 = 1$, and thus the formulas (3.55) become

$$\begin{aligned}
x_1 =& -\sqrt{m_2^2 + m_2 m_3 + u^2 m_3^2},\\
y_1 =& 0,\\
x_2 =& \frac{-2m_2^2 - 2u^2 m_3^2 - 2m_2 m_3 + 2m_2 + m_3}{2\sqrt{m_2^2 + m_2 m_3 + u^2 m_3^2}},\\
y_2 =& -\frac{1}{2}\sqrt{\frac{(4u^2-1)m_3^2}{m_2^2 + m_2 m_3 + u^2 m_3^2}},\\
x_3 =& \frac{-2m_2^2 - 2u^2 m_3^2 - 2m_2 m_3 + m_2 + 2u^2 m_3}{2\sqrt{m_2^2 + m_2 m_3 + u^2 m_3^2}},\\
y_3 =& \frac{1}{2}\sqrt{\frac{(4u^2-1)m_2^2}{m_2^2 + m_2 m_3 + u^2 m_3^2}}.
\end{aligned} \tag{3.74}$$

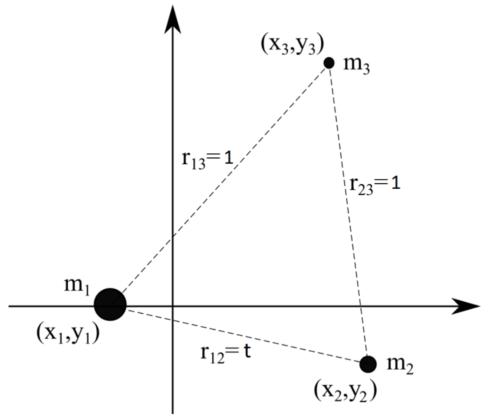

Figure 3.3: Isosceles triangular central configuration.

3.6 Location of the Bodies in the Equilateral Triangular Central Configuration

With the oblateness coefficient C_{20} to be zero for all three bodies, we have the case in terms of point masses. We follow the computations in Section 3.3 and we have $u = 1$ and $v = 1$, we want to recover the locations of vertices of the equilateral triangular central configuration as shown in Section 3.1.3 equation (3.24)

Remark 3.6.1. In the case when none of the bodies are oblate we have $u = v = 1$ and $w = 1$. From the system (3.74) we obtain the Lagrangian equilateral triangle central configuration $r_{12} = r_{23} = r_{13} = 1$. The position given (3.74) are equivalent to the following formulas (see, e.g., [BP13]):

$$
\begin{aligned}
x_1 &= \frac{-|K|\sqrt{m_2^2 + m_2 m_3 + m_3^2}}{K}, \\
y_1 &= 0, \\
x_2 &= \frac{|K|[(m_2 - m_3)m_3 + m_1(2m_2 + m_3)]}{2K\sqrt{m_2^2 + m_2 m_3 + m_3^2}}, \\
y_2 &= -\frac{\sqrt{3}m_3}{2\sqrt{m_2^2 + m_2 m_3 + m_3^2}}, \\
x_3 &= \frac{|K|}{2\sqrt{m_2^2 + m_2 m_3 + m_3^2}}, \\
y_3 &= \frac{\sqrt{3}m_2}{2\sqrt{m_2^2 + m_2 m_3 + m_3^2}},
\end{aligned}
\tag{3.75}
$$

where $K = m_2(m_3 - m_2) + m_1(m_2 + 2m_3)$. Notice that the coordinates of the locations in equations (3.75) are expressed in terms of m_1, m_2 and m_3, while the formulas in (3.55) are expressed in terms of m_2, m_3. Using the assumption of the normalization of masses, we have the relation $\sum_{m=1}^{3} = 1$ and thus we can make a substitution of $m_1 = 1 - m_2 - m_3$ in formulas (3.75). It follows that the corresponding expressions are equivalent. One minor difference is that in formulas (3.75) the position of x_1 is not constrained to be on the negative x-semi-axis, as we assumed for formulas (3.55). Note that the position of x_1 in formulas (3.75) depends on the quantity $\text{sign}(K)$. When $\text{sign}(K) > 0$, we have $|K|/K = 1$, and the equations (3.55) become equivalent with the formulas (3.75).

As a reference, when $m_3 \to 0$, we have the limiting position of the three masses in formulas (3.75) given by:

$$
\begin{aligned}
&x_1 = -m_2, && y_1 = 0, && z_1 = 0, \\
&x_2 = 1 - m_2, && y_2 = 0, && z_2 = 0, \\
&x_3 = \tfrac{1-2m_2}{2}, && y_3 = \tfrac{\sqrt{3}}{2}, && z_3 = 0,
\end{aligned}
\tag{3.76}
$$

with (x_1, y_1) and (x_2, y_2) representing the position of the primary and secondary bodies, respectively, and (x_3, y_3) representing the position of the equilibrium point L_4 in the planar circular restricted three-body problem. Note that when $m_3 = 0$ and $m_2 := \mu$, we recover the coordinates (3.24) of L_4 in the restricted three body problem with one mass at $(x_1, y_1, z_1) = (-\mu, 0, 0)$, a second mass at $(x_2, y_2, z_2) = (1 - \mu, 0, 0)$ and the L_3 equilibrium point at $(x_3, y_3, z_3) = (\frac{1}{2} - \mu, \frac{\sqrt{3}}{2}, 0)$.

3.7 Conclusions

In this chapter, we consider the three-body problems with different conditions— three oblate bodies, one oblate body and three point masses — and we obtain their corresponding triangular central configuration. It is well known that for the restricted three-body problem (with three point-masses) the only non colinear central configuration is given by an equilateral triangle. This is one of the first explicit solutions given in the three-body problem was the Lagrange central configuration, where three bodies of different masses lie at the vertices of an equilateral triangle. To begin this chapter, we first consider the three-body problem with three heavy oblate bodies and we find that the corresponding triangular central configurations is given by a scalene triangle. Furthermore, we find the locations of the vertices of the scalene triangular central configurations formed by the three oblate bodies. The results of the scalene triangular central configurations (i.e. the case for three oblate bodies) allow us to reduce to the special case of having only one oblate body in the three-body problem. In the three-body problem with one oblate body, there exists a unique central configuration, which is an isosceles triangle. In addition, we find the locations of the vertices of such an isosceles triangular central configurations. At the end of this chapter, we are able to recover the equilateral triangular central configuration and the locations for its vertices in the absence of oblateness on the three-body problem (i.e. the case for three point masses).

Chapter 4

Hill Four-Body Problem with Three Oblate Bodies

Hill approximation of the lunar problem is a classical approximation of the restricted three body problem, which has been used to write accurate series solutions for the motion of the Moon. Similarly on a restricted four body problem [BGG15], we perform a symplectic scaling, in which we aim to send the two massive bodies to infinity, we then expand the potential as a power series in m_3, and take a limit as m_3 goes to zero. As a motivating example, we consider the dynamics of the moonlet Skamandrios of Jupiter's Trojan asteroid Hektor. Other than the moonlet, we can also consider the small body as a spacecraft orbiting Hektor. The system Sun-Jupiter-Hektor-Skamandrios plays a relevant role for several reasons. Being the largest Jupiter Trojan, Hektor has one of the most elongated shapes among the bodies of its size in the Solar system. And it is one of the few Trojan asteroids to possess a moonlet (see, e.g., [DLZ12] for stability regions of Trojans around the Earth and [LC15] for dissipative effects around the triangular Lagrangian points). Astrodynamics is another motivation for us to study the dynamics of a small body near a Trojan asteroid. NASA is preparing the first mission to the Jupiter's Trojans— Lucy is planned to be launched in October 2021 to flyby and visit seven different asteroids including Trojans asteroids.

4.1 Background

4.1.1 Hill's approximation on a Restricted Four-Body Problem

The model of a restricted four-bodies problem

Consider an equilateral triangular central configuration with three point masses located on the vertices while moving under mutual Newtonian gravitational attraction in circular periodic orbits around their center of mass at origin. A fourth body of infinitesimal mass is moving under the gravitational attraction of the three bodies, without affecting their motion. This model is known as the equilateral restricted four body problem [Bel18], in which we assume that the three masses are $m_1 \geqslant m_2 \geqslant m_3$, where m_1 refer to the primary body, m_2 the secondary, and m_3 the tertiary. With dimensionless coordinates, the equations of motion of the infinitesimal body relative to a synodic frame of reference that rotates together with the three point masses are:

$$\ddot{x} - 2\dot{y} = \Omega_x$$

$$\ddot{y} - 2\dot{x} = \Omega_y$$

$$\ddot{z} = \Omega_z$$

where

$$\Omega(x, y, z) = \frac{1}{2}(x^2 + y^2) + \sum_{i=1}^{3} \frac{m_i}{r_i}$$

$$r_i = \sqrt{(x - x_i)^2 + (y - y_i)^2 + z^2}, i = 1, 2, 3$$

and (x_i, y_i) denotes the $xy-$coordinates of the body mass m_i for $i = 1, 2, 3$. Multiplying the equations by $2\dot{x}$, $2\dot{y}$ and $2\dot{z}$ respectively, we have

$$2\dot{x}\ddot{x} - 4\dot{x}\dot{y} = 2\dot{x}\Omega_x$$

$$2\dot{y}\ddot{y} + 4\dot{x}\dot{y} = 2\dot{y}\Omega_y$$

$$2\dot{z}\ddot{z} = 2\dot{z}\Omega_z$$

Summing the equations, we have

$$2\dot{x}\ddot{x} + 2\dot{y}\ddot{y} + 2\dot{z}\ddot{z} = 2\dot{x}\Omega_x + 2\dot{y}\Omega_y + 2\dot{z}\Omega_y$$
$$\Rightarrow \dot{x}^2 + \dot{y}^2 + \dot{z}^2 = 2\Omega - C$$
$$\Rightarrow C = 2\Omega - (\dot{x}^2 + \dot{y}^2 + \dot{z}^2)$$
$$\Rightarrow H = -\Omega + \tfrac{1}{2}(\dot{x}^2 + \dot{y}^2 + \dot{z}^2)$$

$$\Rightarrow H = \frac{1}{2}(\dot{x}^2 + \dot{y}^2 + \dot{z}^2) - \frac{1}{2}(x^2 + y^2) - \sum_{i=1}^{3} \frac{m_i}{r_i}$$

Performing the transformation $\dot{x} = p_x + y$, $\dot{y} = p_y - x$, $\dot{z} = p_z$, we have the Hamiltonian

$$\begin{aligned} H &= \frac{1}{2}((p_x + y)^2 + (p_y - x)^2 + (p_z)^2) - \frac{1}{2}(x^2 + y^2) - \sum_{i=1}^{3} \frac{m_i}{r_i} \\ &= \frac{1}{2}p_x^2 + p_y^2 + p_z^2 + yp_x - xp_y - \sum_{i=1}^{3} \frac{m_i}{r_i} \end{aligned} \tag{4.1}$$

with respect to the standard symplectic form $\varpi = dp_x \wedge dx + dp_y \wedge dy + dp_z \wedge dz$ on $T^*\bar{\Omega}$ where $\bar{\Omega} = (x, y, z, p_x, p_y, p_z) : (x, y, z) \neq (x_1, y_1, z_1), (x_2, y_2, z_2), (x_3, y_3, z_3)$. This symplectic structure allows us to rewrite the Hamiltonian equations as $\dot{x} = J \bigtriangledown H(x)$, where

$$J = \begin{pmatrix} 0 & Id \\ -Id & 0 \end{pmatrix}, \tag{4.2}$$

and $x = (x, y, z, p_x, p_y, p_z)$. Notice that $H(x, y, z, p_x, p_y, p_z) = H(x, y, z, \dot{x}, \dot{y}, \dot{z})$.

Hill's Approximation Applied to a Restricted Four-Body Problem

In this section we will study the limiting Hamiltonian of the restricted four body problem when $m_3 \to 0$. We use a procedure similar to that in [BGG15], by performing a symplectic scaling depending on $m_3^{1/3}$, expanding the Hamiltonian as a power series in $m_3^{1/3}$ in a neighborhood of the small mass m_3, and neglecting all terms of order $O(m_3^{\frac{1}{3}})$ or higher. Then we obtain a limiting Hamiltonian, which is a three-degree of freedom system. The resulting Hamiltonian depends on a parameter μ which becomes equal to the mass of the secondary m_2 in normalized units i.e. $\mu = \frac{m_2}{m_1+m_2}$.

Consider the Hamiltonian of the restricted four body problem with the center of mass coordinates at m_3, we have equation (4.1). We first make the change of coordinates as follow:

$$\begin{aligned} x \to x + x_3, \quad & y \to y + y_3, \quad z \to z \\ p_x \to p_x - y_3, \quad & p_y \to p_y + x_3, \quad p_z \to p_z. \end{aligned} \tag{4.3}$$

We obtain the Hamiltonian

$$\begin{aligned} H &= \frac{1}{2}[(p_x - y_3)^2 + (p_y + x_3)^2 + p_z^2] + (y + y_3)(p_x - y_3) - (x + x_3)(p_y + x_3) \\ &\quad - \sum_{i=1}^{3} \frac{m_i}{r_i} \\ &= \frac{1}{2}[(p_x^2 - 2p_x y_3 + y_3^2) + (p_y^2 + 2p_y x_3 + x_3^2) + p_z^2] + yp_x - yy_3 + y_3 p_x - y_3^2 \\ &\quad - xp_y - xx_3 - x_3 p_y - x_3^2 - \sum_{i=1}^{3} \frac{m_i}{r_i} \\ &= \frac{1}{2}(p_x^2 + p_y^2 + p_z^2) + yp_x - xp_y - (xx_3 + yy_3) - \sum_{i=1}^{3} \frac{m_i}{r_i} - \frac{1}{2}(x_3^2 + y_3^2) \end{aligned} \tag{4.4}$$

Since the term of $\frac{1}{2}(x_3^2 + y_3^2)$ is a constant, we drop it in the computation and we obtain

$$H = \frac{1}{2}(p_x^2 + p_y^2 + p_z^2) + yp_x - xp_y - (x_3 x + y_3 y) - \sum_{i=1}^{3} \frac{m_i}{\bar{r_i}}, \tag{4.5}$$

where $\bar{r_i}^2 = (x + x_3 - x_i)^2 + (y + y_3 - y_i)^2 + z^2 := (x + \bar{x}_i)^2 + (y + \bar{y}_i)^2 + z^2$ for $i = 1, 2, 3$. Expanding the terms $\frac{1}{r_1}$ and $\frac{1}{r_2}$ in Taylor series round the new origin of coordinates, we obtain

$$
\begin{aligned}
f^1 &:= \frac{1}{\bar{r_1}} = \sum_{k\geqslant 0} P_k^1(x,y,z) \\
f^2 &:= \frac{1}{\bar{r_2}} = \sum_{k\geqslant 0} P_k^2(x,y,z)
\end{aligned}
\tag{4.6}
$$

where $P_k^j(x,y,z)$ is a homogenous polynomial of degree k for $j = 1,2$. Notice that we neglect the constant terms. With some computations, we have

$$
P_0^i = (\bar{x_i}^2 + \bar{y_i}^2)^{-\frac{1}{2}} = r_{i3}^{-1} \tag{4.7}
$$

for $i = 1,2$, where $r_{13} = ((x_1 - x_3)^2 + (y_1 - y_3)^2)^{1/2}$, and $r_{23} = ((x_2 - x_3)^2 + (y_2 - y_3)^2)^{1/2}$.

Notice that P_0^1 and P_0^2 are constant terms and play no role in the Hamiltonian equations, so they will be dropped in the following calculations. Now we perform the following symplectic scaling $x \to m_3^{\frac{1}{3}}x$, $y \to m_3^{\frac{1}{3}}y$, $z \to m_3^{\frac{1}{3}}z$, $p_x \to m_3^{\frac{1}{3}}p_x$, $p_y \to m_3^{\frac{1}{3}}p_y$ and $p_z \to m_3^{\frac{1}{3}}p_z$ with multiplier $m_3^{-\frac{2}{3}}$, obtaining

$$
\begin{aligned}
H = m_3^{-\frac{2}{3}}[&\frac{1}{2}[(m_3^{\frac{1}{3}}p_x)^2 + (m_3^{\frac{1}{3}}p_y)^2 + (m_3^{\frac{1}{3}}p_z)^2 + m_3^{\frac{1}{3}}y m_3^{\frac{1}{3}}p_x - m_3^{\frac{1}{3}}x m_3^{\frac{1}{3}}p_y - m_3^{\frac{1}{3}}xx_3 \\
&+ m_3^{\frac{1}{3}}yy_3 - m_3^{\frac{1}{3}}\sum_{k\geqslant 1} m_1 P_k^1(x,y,z) - m_3^{\frac{1}{3}}\sum_{k\geqslant 1} m_2 P_k^2(x,y,z) - \frac{m_3}{m_3^{\frac{1}{3}}\bar{r_3}}] \\
=& \frac{1}{2}(p_x^2 + p_y^2 + p_z^2) + yp_x - xp_y - m_3^{-\frac{1}{3}}xx_3 + m_3^{-\frac{1}{3}}yy_3 - m_3^{-\frac{1}{3}}P_1^1 - m_3^{-\frac{1}{3}}P_1^2 \\
&- \sum_{k\geqslant 2} m_3^{\frac{k-2}{3}} m_1 P_k^1(x,y,z) - \sum_{k\geqslant 2} m_3^{\frac{k-2}{3}} m_2 P_k^2(x,y,z) - \frac{1}{\bar{r_3}} \\
=& \frac{1}{2}(p_x^2 + p_y^2 + p_z^2) + yp_x - xp_y - m_3^{-\frac{1}{3}}(xx_3 + yy_3 + m_1 P_1^1 + m_2 P_1^2) \\
&- \sum_{k\geqslant 2} m_3^{\frac{k-2}{3}} m_1 P_k^1(x,y,z) - \sum_{k\geqslant 2} m_3^{\frac{k-2}{3}} m_2 P_k^2(x,y,z) - \frac{1}{\bar{r_3}}
\end{aligned}
\tag{4.8}
$$

where

$$
\begin{aligned}
P_1^1 &= \frac{\partial f^1}{\partial x}(0,0,0)x + \frac{\partial f^1}{\partial y}(0,0,0)y + \frac{\partial f^1}{\partial z}(0,0,0)z \\
&= \frac{x_1 - x_3}{\bar{r_1}^3}x + \frac{y_1 - y_3}{\bar{r_1}^3}y
\end{aligned}
\tag{4.9}
$$

and similarly we have

$$\begin{aligned} P_1^2 &= \frac{\partial f^2}{\partial x}(0,0,0)x + \frac{\partial f^2}{\partial y}(0,0,0)y + \frac{\partial f^2}{\partial z}(0,0,0)z \\ &= \frac{x_2 - x_3}{\bar{r_2}^3}x + \frac{y_2 - y_3}{\bar{r_2}^3}y \end{aligned} \tag{4.10}$$

where $\bar{r_i} = \sqrt{(x_3 - x_i)^2 + (y_3 - y_i)^2}$. Note that the first partial derivative with respect to the variable z is given by

$$f_z^i = -\tfrac{z}{\bar{r_i}^3} \text{ for } i = 1, 2.$$

Therefore, we obtain

$$f_z^i(0,0,0) = f_{xz}^i(0,0,0) = f_{yz}^i(0,0,0) = 0 \text{ and } f_{zz}^i(0,0,0) = -1.$$

Recall that the three bodies form an equilateral triangle configuration with length equal to 1 by assumption and thus we have the relation on $m_1 = 1 - m_2 - m_3$.

$$\begin{aligned} & m_3^{-\frac{1}{3}}(x_3 x + y_3 y + m_1 P_1^1 + m_2 P_1^2) \\ &= m_3^{-\frac{1}{3}}[x_3 x + y_3 y + (1 - m_2 - m_3)\frac{(x_1 - x_3)}{\bar{r_1}^3}x + (1 - m_2 - m_3)\frac{(y_1 - y_3)}{\bar{r_1}^3}y \\ &\quad + m_2\frac{(x_2 - x_3)}{\bar{r_2}^3}x + m_2\frac{(y_2 - y_3)}{\bar{r_2}^3}y] \\ &= m_3^{-\frac{1}{3}}[x_3 + \frac{(x_1 - x_3)}{\bar{r_1}^3} - m_2\frac{(x_1 - x_3)}{\bar{r_1}^3} - m_3\frac{(x_1 - x_3)}{\bar{r_1}^3} + m_2\frac{(x_2 - x_3)}{\bar{r_2}^3}]x + m_3^{-\frac{1}{3}}[y_3 \\ &\quad + \frac{(y_1 - y_3)}{\bar{r_1}^3} - m_2\frac{(y_1 - y_3)}{\bar{r_1}^3} - m_3\frac{(y_1 - y_3)}{\bar{r_1}^3} + m_2\frac{(y_2 - y_3)}{\bar{r_2}^3}]y \\ &= m_3^{-\frac{1}{3}}[x_1 + m_2(x_2 - x_1) - m_3(x_1 - x_3)]x + m_3^{-\frac{1}{3}}[y_1 + m_2(y_2 - y_1) - m_3(y_1 - y_3)]y \end{aligned} \tag{4.11}$$

Together with the general expressions of the coordinates of the three bodies that are given by equation (3.24), we obtain

$$
\begin{aligned}
&m_3^{-\frac{1}{3}}[y_1 + m_1(y_2 - y_1) - m_3(y_1 - y_3)] \\
&= m_3^{-\frac{1}{3}}[m_2(\frac{-\sqrt{3}m_3}{2m_2^{\frac{3}{2}}}\sqrt{\frac{m_2^3}{m_2^2 + m_2m_3 + m_3^2}}) + m_3(\frac{\sqrt{3}}{2m_2^{\frac{1}{2}}}\sqrt{\frac{m_2^3}{m_2^2 + m_2m_3 + m_3^2}})] \\
&= m_3^{\frac{2}{3}}m_2(\frac{-\sqrt{3}}{2})\sqrt{\frac{1}{m_2^2 + m_2m_3 + m_3^2}} + m_3^{\frac{2}{3}}(\frac{\sqrt{3}}{2}\frac{m_2}{\sqrt{m_2^2 + m_2m_3 + m_3^2}}).
\end{aligned}
\tag{4.12}
$$

Similarly, we have

$$
\begin{aligned}
&m_3^{-\frac{1}{3}}[x_1 + m_2(x_2 - x_1) - m_3(x_1 - x_3)] \\
&= m_3^{-\frac{1}{3}}[x_1(1 - m_2) + m_2x_2 - m_3x_1 + x_3m_3] \\
&= m_3^{-\frac{1}{3}}[x_1m_1 + x_2m_2 + x_3m_3] \\
&= 0.
\end{aligned}
\tag{4.13}
$$

Thus the Hamiltonian becomes

$$
H = \frac{1}{2}(p_x^2 + p_y^2 + p_z^2) + yp_x - xp_y - \frac{1}{\bar{r}_3} - m_1P_2^1 - m_2P_2^2 + O(m_3^{\frac{1}{3}}). \tag{4.14}
$$

Neglecting the terms of order $O(m_3^{\frac{1}{3}})$ by taking the limit $m_3 \to 0$; we mean to send the primary and the secondary bodies at an infinity distance and their total mass becomes infinite.

For the computation of P_1^1, we have

$$
\begin{aligned}
P_2^1 &= \frac{1}{2}[x^2f_{xx}(0,0,0) + xyf_{yx}(0,0,0) + xzf_{zx}(0,0,0) + xyf_{xy}(0,0,0) + y^2f_{yy}(0,0,0) \\
&\quad + yzf_{zy}(0,0,0) + xzf_{xz}(0,0,0) + yzf_{yz}(0,0,0) + z^2f_{zz}(0,0,0)] \\
&= \frac{1}{2}[x^2f_{xx}(0,0,0) + 2xyf_{xy}(0,0,0) + y^2f_{yy}(0,0,0) + z^2f_{zz}(0,0,0)]
\end{aligned}
\tag{4.15}
$$

Recall from Section 3.6 we have that when $m_3 = 0$ and $m_2 := \mu$, restricted three body problem with one mass at $(x_1, y_1, z_1) = (-\mu, 0, 0)$, a second mass at $(x_2, y_2, z_2) = (1 - \mu, 0, 0)$ and the third oneat $(x_3, y_3, z_3) = (\frac{1}{2} - \mu, \frac{\sqrt{3}}{2}, 0)$ and thus we have

$$\begin{aligned} P_2^1 &= \frac{1}{2}[x^2 \frac{3(x_1 - x_3)^2}{\bar{r_1}^5} + 2xy \frac{3y_3(x_3 - x_1)}{\bar{r_1}^5} + y^2 \frac{3y_3^2}{\bar{r_1}^5} + z^2(-1)] \\ &= \frac{3}{8}x^2 + xy\frac{3\sqrt{3}}{4} + y^2\frac{9}{8} - \frac{1}{2}z^2. \end{aligned} \tag{4.16}$$

Similarly, we have

$$\begin{aligned} P_2^2 &= \frac{1}{2}[x^2 f_{xx}|_{(0,0,0)} + xyf_{yx}|_{(0,0,0)} + xzf_{zx}|_{(0,0,0)} + xyf_{xy}|_{(0,0,0)} + y^2 f_{yy}|_{(0,0,0)} \\ &\quad + yzf_{zy}|_{(0,0,0)} + xzf_{xz}|_{(0,0,0)} + yzf_{yz}|_{(0,0,0)} + z^2 f_{zz}|_{(0,0,0)}] \\ &= \frac{1}{2}[x^2 f_{xx}|_{(0,0,0)} + 2xyf_{xy}|_{(0,0,0)} + y^2 f_{yy}|_{(0,0,0)} + z^2 f_{zz}|_{(0,0,0)}] \\ &= \frac{1}{2}[x^2 \frac{3(x_2 - x_3)^2}{\bar{r_2}^5} + 2xy \frac{3(y_2 - y_3)(x_2 - x_3)}{\bar{r_2}^5} + y^2 \frac{3(y_2 - y_3)^2}{\bar{r_2}^5} + z^2(-1)] \\ &= \frac{3}{8}x^2 - xy\frac{3\sqrt{3}}{4} + y^2\frac{9}{8} - \frac{1}{2}z^2 \end{aligned} \tag{4.17}$$

With the above computations, the limiting Hamiltonian

$$H = \frac{1}{2}(p_x^2 + p_y^2 + p_z^2) + yp_x - xp_y - \frac{1}{\bar{r_3}} - m_1 P_2^1 - m_2 P_2^2 \tag{4.18}$$

becomes

$$\begin{aligned} H &= \frac{1}{2}(p_x^2 + p_y^2 + p_z^2) + yp_x - xp_y - \frac{1}{\sqrt{x^2 + y^2 + z^2}} - (1 - \mu) \\ &\quad (\frac{3}{8}x^2 + xy\frac{3\sqrt{3}}{4} + y^2\frac{9}{8} - \frac{1}{2}z^2) - \mu(\frac{3}{8}x^2 - xy\frac{3\sqrt{3}}{4} + y^2\frac{9}{8} - \frac{1}{2}z^2) \\ &= \frac{1}{2}(p_x^2 + p_y^2 + p_z^2) + yp_x - xp_y - [\frac{3}{8}x^2 + (1 - 2\mu)xy\frac{3\sqrt{3}}{4} + \frac{9}{8}y^2 - \frac{1}{2}z^2 \\ &\quad + \frac{1}{\sqrt{x^2 + y^2 + z^2}}]. \end{aligned} \tag{4.19}$$

4.2 Data on the Sun-Jupiter-Hektor-Skamandrios system

The application for the model that we develop below is the case of the Sun-Jupiter-Hektor-Skamandrios system. Since we will demostrate the application in this chapter, it will be useful to extract some data for this system from [JPL, MDCR$^+$14, Des15]. Our target asteroid — Hektor is the largest Trojan asteroid that is approximately located at the Lagrangian point L_4 of the Sun-Jupiter system. According to [Des15], Hektor's size is is approximately $416 \times 131 \times 120$ km, while the equivalent radius ,that is, the radius of a sphere with the same volume as the asteroid, is $R_H = 92$ km[1]. It is observed that Hektor's shape can be approximated by a dumb-bell figure. Furthermore, Hektor spins very fast that it has a rotation period of approximately 6.92 hours (see the JPL Solar System Dynamics archive [JPL]).

The moonlet with 12 ± 3km diameter, which is known as Skamandrios, was detected orbiting around Hektor at a distance of approximately 957.5 km, with an orbital period of 2.965079 days; see [Des15]. The orbit is observed to be highly inclined, at approximately $50.1°$ with respect to the orbit of Hektor, which justifies the system refers to as a model of the spatial restricted four-body problem rather than the planar one; see [MDCR$^+$14].

According to [JPL], the inclination of Hektor is approximately $18.17°$. Although a more refined model should include a non-zero inclination, we will consider that Sun-Jupiter-Hektor move in the same plane, due to the assumption is needed in order for the three bodies to form a central configuration. Furthermore, we assume that the axis of rotation of Hektor is perpendicular to the plane of motion.

In this work, we use the values of $m_1 = 1.989 \times 10^{30}$ kg, $m_2 = 1.898 \times 10^{27}$, and $m_3 = 7.91 \times 10^{18}$ kg for the masses of Sun, Jupiter and Hektor respectively. Having Sun-Jupiter as the average distance, we use the value 778.5×10^6 km.

[1] Note that [Des15] claims that there are some typos in the values reported in [MDCR$^+$14].

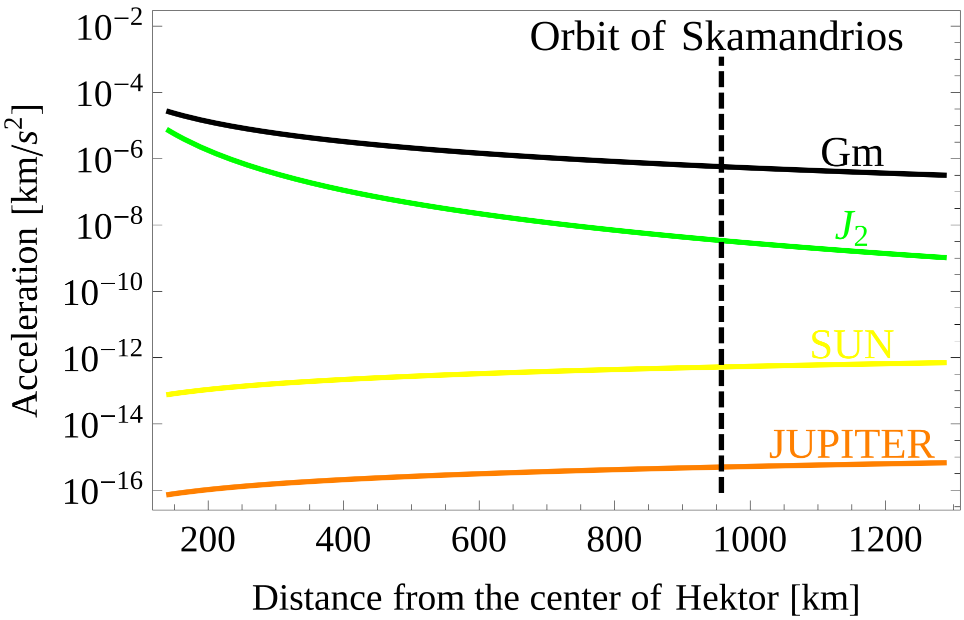

Figure 4.1: Order of magnitude of the different perturbations acting on the moonlet as a function of its distance from Hektor. The terms Gm, Sun and Jupiter denote, respectively, the monopole terms of the gravitational influence of Hektor, the attraction of the Sun and that of Jupiter. J_2 represents the perturbation due to the non-spherical shape of Hektor. The actual distance of the moonlet is indicated by a vertical line.

In Figure 4.1 we show the comparison between the strength of different forces acting on the moonlet: the Newtonian gravitational attraction of Hektor, Sun, Jupiter, and the effect of the non-spherical shape of the asteroid, limited to the so-called J_2 coefficient, which will be introduced in Section 4.2.1.

4.2.1 The gravitational field of a non-spherical body

It is well known that the gravitational potential of a general (non-spherical) shape can be expanded in terms of spherical harmonics (see, e.g., [CG18]). In this thesis, we will only use the truncation up to the second order, which is known as the zonal harmonics due to the reasons provide in Chapter 2. In other words, we are approximating the body by an an oblate shape (i.e., an ellipsoid of revolution obtained by rotating an ellipse about its minor axis). Relative to a reference frame centered at the barycenter of the body, this potential is given in spherical coordinates (r, ϕ, θ) as in Section 3.2 equation (3.27).

Recall that C_{20} is a negative number for an oblate body C_{20} and notice that the positive quantity $-C_{20}$ is often denoted by J_2, and the study of the motion of particle relative to the gravitational field (3.27) is referred to as the J_2 problem.

In the case of an ellipsoid of semi-axes $a \geqslant b \geqslant c$, we have the explicit formula ([Boy97a]) for C_{20} as in Section 2.1.7 equation (2.64). Recall the dimensions of Hektor from Section 2.2, we have $a = 208$ km, $b = 65.5$ km, $c = 60$ km and $R_H = 92$ km, as in [Des15]. We obtain

$$C_{20}^3 = -0.476775$$

as the zonal coefficient for Hektor (see Section 2.2). Consider the value of C_{20}^3 computed from Section 2.2 being different from the corresponding value of 0.15 reported in [MDCR$^+$14]. We note that it is due to the different estimates for the size of Hektor, following [Des15]. We note that the oblateness for the Sun is a subject of active debate, and several different values can be found in the literature. In this thesis, we use the measurements from [KBES12], that is $C_{20}^1 = -5.00 \times 10^{-6}$ for the oblateness coefficient of Sun. For Jupiter's oblateness coefficient we use the value $C_{20}^2 = -14,736 \times 10^{-6}$.

4.3 Equations of motion for the restricted four-body problem with three oblate bodies

Similar to the first part of Section 4.1.1, in this section we consider the dynamics of an infinitesimal mass under the influence of the three heavy oblate bodies. A fourth body of infinitesimal mass, such as the moonlet Skamandrios or a spacecraft, is moving under the gravitational attraction of the three bodies, without affecting their motion. The dynamics of the fourth body is modeled by the spatial, circular, restricted four-body problem. It means that the moonlet is moving under the gravitational attraction of Hektor, Jupiter and the Sun, without affecting their motion which remains on circular orbits and forming a triangular central configuration as in Section 3.2. With (x_i, y_i, z_i) representing the (x, y, z)-coordinates in the synodic reference frame of the body of mass m_i, the equations of motion of the infinitesimal mass relative to a synodic frame of reference that rotates together with the three heavy oblate bodies is given by

$$\begin{aligned} \ddot{x} - 2\omega\dot{y} &= \frac{\partial\tilde{\Omega}}{\partial x} = \tilde{\Omega}_x \\ \ddot{y} + 2\omega\dot{x} &= \frac{\partial\tilde{\Omega}}{\partial x} = \tilde{\Omega}_y \\ \ddot{z} &= \frac{\partial\tilde{\Omega}}{\partial z} = \tilde{\Omega}_z, \end{aligned} \tag{4.20}$$

where the effective potential $\tilde{\Omega} = \tilde{\Omega}(x, y, z)$ is given by

$$\tilde{\Omega} = \frac{1}{2}\omega^2(x^2 + y^2) + \sum_{i=1}^{3}\left(\frac{m_i}{r_i} + \frac{m_i}{r_i}\left(\frac{R_i}{r_i}\right)^2\left(\frac{C_{20}^i}{2}\right)(3\sin^2\phi_i - 1)\right)$$

where $r_i = ((x - x_i)^2 + (y - y_i)^2 + z^2)^{\frac{1}{2}}$ is the distance from the infinitesimal body to the mass m_i, $\sin\phi_i = z/r_i$, ω is the angular velocity of the system of three bodies around the center of mass, and C_{20}^i is the oblateness coefficient of mass m_i, for $i = 1, 2, 3$. We notice that ω depends on the oblateness parameters. Following the notation in Section 3.3 equations (3.48), (3.49) and (3.50) we have $r_{12} = 1$, $r_{13} = u$ and $r_{23} = v$. With the relations shown in equation (3.43) we have that the angular velocity is given by

$$\omega = \sqrt{1 - 3C_{12}}, \tag{4.21}$$

where we recall from Section 3.2 equation (3.31) that $C_{12} = C_1 + C_2 = R_1^2 C_{20}^1/2 + R_2^2 C_{20}^2/2$. Rescaling the time $t = \frac{s}{\omega}$, we have the relative to the new time s the mean motion is normalized to 1. Thus we obtain

$$\begin{aligned} \ddot{x} - 2\dot{y} &= \frac{\partial \Omega}{\partial x} = \Omega_x, \\ \ddot{y} + 2\dot{x} &= \frac{\partial \Omega}{\partial y} = \Omega_y, \\ \ddot{z} &= \frac{\partial \Omega}{\partial z} = \Omega_z, \end{aligned} \tag{4.22}$$

with the effective potential $\Omega = \Omega(x, y, z)$ given by

$$\Omega = \frac{1}{2}(x^2 + y^2) + \frac{1}{\omega^2} \sum_{i=1}^{3} \left(\frac{m_i}{r_i} + \frac{m_i}{r_i} \left(\frac{R_i}{r_i} \right)^2 \left(\frac{C_{20}^i}{2} \right) (3 \sin^2 \phi_i - 1) \right). \tag{4.23}$$

The equations of motion (4.22) have the total energy H defined as a conserved quantity:

$$\begin{aligned} H =& \frac{1}{2}(\dot{x}^2 + \dot{y}^2 + \dot{z}^2) - \Omega, \\ =& \frac{1}{2}(\dot{x}^2 + \dot{y}^2 + \dot{z}^2) \\ & - \left[\frac{1}{2}(x^2 + y^2) + \frac{1}{\omega^2} \sum_{i=1}^{3} \left(\frac{m_i}{r_i} + \frac{m_i}{r_i} \left(\frac{R_i}{r_i} \right)^2 \left(\frac{C_{20}^i}{2} \right) (3 \sin^2 \phi_i - 1) \right) \right]. \end{aligned}$$

Performing the transformation $\dot{x} = p_x + y$, $\dot{y} = p_y - x$ and $\dot{z} = p_z$, we now switch to the Hamiltonian setting And thus the Hamiltonian passes to have the symplectic coordinates (x, y, z, p_x, p_y, p_z) relative to the symplectic form $\varpi = x \wedge p_x + y \wedge p_y + z \wedge p_z$. We obtain

$$\begin{aligned} H =& \frac{1}{2}((p_x + y)^2 + (p_y - x)^2 + p_z^2) - \frac{1}{2}(x^2 + y^2) \\ & - \frac{1}{\omega^2} \left(\sum_{i=1}^{3} \frac{m_i}{r_i} + \frac{m_i}{r_i} \left(\frac{R_i}{r_i} \right)^2 \left(\frac{C_{20}^i}{2} \right) (3 \sin^2 \phi_i - 1) \right) \\ =& \frac{1}{2}(p_x^2 + p_y^2 + p_z^2) + y p_x - x p_y \\ & - \frac{1}{\omega^2} \sum_{i=1}^{3} \left(\frac{m_i}{r_i} + \frac{m_i}{r_i^3} C_i (3 \sin^2 \phi_i - 1) \right), \end{aligned} \tag{4.24}$$

where $C_i = {R_i}^2 C_{20}^i / 2$. Thus, the equations of motion (4.20) are equivalent to Hamilton's equations for the Hamiltonian given by (4.24).

Remark 4.3.1. In the special case when $m_3 = 0$ and only the mass m_2 is oblate we have

$$\omega = \sqrt{1 - 3C_{20}^2} = \sqrt{1 - \frac{3R_2^2 C_{20}^2}{2}}.$$

The resulting model is the circular restricted three-body problem with one oblate body, and the above formula agrees with the one in [McC63, SR76, AGST12]. Furthermore, if m_2 has no oblateness, i.e. $C_{20}^2 = 0$, we have $\omega = 1$, and the resulting model is the classical circular restricted three-body problem. There are other models of the restricted three-body problems are studied such as the ones withoblate primaries, relativistic and radiation effects in [BS16, BU18].

4.4 Hill four-body problem with three oblate bodies

In this section we perform the Hill approximation on the spatial, circular, restricted four-body problem with oblate bodies in shifted coordinates. Using rescaled variables and a limiting procedure, the masses m_1 and m_2 are 'sent to infinite distance' and thus a neighborhood of m_3 can be studied in detail.

4.4.1 Hill's approximation

The main result is as follows:

Theorem 4.4.1. *Transform the Hamiltonian* (4.24) *with the following procedures:*

(i) shift the origin of the reference frame such that it coincides with m_3*;*

(ii) perform a conformal symplectic scaling which is given by

$$(x, y, z, p_x, p_y, p_z) \to m_3^{1/3}(x, y, z, p_x, p_y, p_z);$$

(iii) rescale the average radius of each heavy body as $R_i = m_3^{1/3}\rho_i$ *for* $i = 1, 2, 3$*;*

(iv) expand the resulting Hamiltonian as a power series in $m_3^{1/3}$*, and*

(v) neglect all the terms of order $O(m_3^{1/3})$ *in the expansion.*

Then, we obtain the following Hamiltonian describing the Hill four-body problem with three oblate bodies:

$$
\begin{aligned}
H =& \frac{1}{2}(p_x^2 + p_y^2 + p_z^2) + yp_x - xp_y \\
& - \frac{1}{2}\left[\left(\frac{(1-\mu)\left(\frac{3w^2}{4} - 1\right)}{u^5} + \frac{\mu\left(\frac{3(2-w)^2}{4} - 1\right)}{v^5} \right) x^2 \right. \\
& + \left(\frac{(1-\mu)\left(\frac{3(4u^2-w^2)}{4} - 1\right)}{u^5} + \frac{\mu\left(\frac{3(4u^2-w^2)}{4} - 1\right)}{v^5} \right) y^2 \\
& \left. + \left(\frac{(1-\mu)\frac{6w\sqrt{4u^2-w^2}}{4}}{u^5} - \frac{\mu\frac{6(2-w)\sqrt{4u^2-w^2}}{4}}{v^5} \right) xy - \left(\frac{(1-\mu)}{u^3} + \frac{\mu}{v^3} \right) z^2 \right] \\
& - \left[\left(\frac{(1-\mu)c_1}{u^3} \right) \left(3\left(\frac{z}{u}\right)^2 - 1 \right) + \left(\frac{\mu c_2}{v^3} \right) \left(3\left(\frac{z}{v}\right)^2 - 1 \right) \right. \\
& \left. + \frac{1}{(x^2+y^2+z^2)^{\frac{1}{2}}} + \frac{c_3}{(x^2+y^2+z^2)^{\frac{3}{2}}} \left(\frac{3z^2}{x^2+y^2+z^2} - 1 \right) \right],
\end{aligned}
\tag{4.25}
$$

where $1, u, v$ *represent the sides of the triangular central configuration as in Section 3.3,* $w = 1 + u^2 - v^2$*,* $\mu = \frac{m_2}{m_1+m_2}$*, and* $c_i := \rho_i^2 C_{20}^i/2 = m_3^{-\frac{2}{3}} R_3^i C_{20}^i/2$*, for* $i = 1, 2, 3$*.*

Proof. We begin with the Hamiltonian (4.24), we first shift the origin of the coordinate system (x, y, z) to the location of the mass m_3 (i.e. Hektor), via the following change of coordinates

$$
\begin{aligned}
&\xi = x - x_3, \quad \eta = y - y_3, \quad \zeta = z, \\
&p_\xi = p_x + y_3, \quad p_\eta = p_y - x_3, \quad p_\zeta = p_z.
\end{aligned}
$$

And the Hamiltonian becomes

$$\begin{aligned}
H =& \frac{1}{2}\left((p_\xi - y_3)^2 + (p_\eta + x_3)^2 + p_\zeta^2\right) \\
&+ (\eta + y_3)(p_\xi - y_3) - (\xi + x_3)(p_\eta + x_3) \\
&- \frac{1}{\omega^2}\sum_{i=1}^{3}\left(\frac{m_i}{\bar{r}_i} + \frac{m_i}{\bar{r}_i}\left(\frac{R_i}{\bar{r}_i}\right)^2\left(\frac{C_{20}^i}{2}\right)(3\sin^2\phi_i - 1)\right) \\
=& \frac{1}{2}(p_\xi^2 + p_\eta^2 + p_\zeta^2) + \eta p_\xi - \xi p_\eta - (\xi x_3 + \eta y_3) - \frac{1}{2}(x_3^2 + y_3^2) \\
&- \frac{1}{\omega^2}\sum_{i=1}^{3}\left(\frac{m_i}{\bar{r}_i} + \frac{m_i}{\bar{r}_i}\left(\frac{R_i}{\bar{r}_i}\right)^2\left(\frac{C_{20}^i}{2}\right)(3\sin^2\phi_i - 1)\right),
\end{aligned} \tag{4.26}$$

where $\bar{r}_i^2 = (\xi - \bar{x}_i)^2 + (\eta - \bar{y}_i)^2 + \zeta^2 = (\xi + x_3 - x_i)^2 + (\eta + y_3 - y_i)^2 + \zeta^2$, with $\bar{x}_i = x_i - x_3$, $\bar{y}_i = y_i - y_3$. Note that $\bar{r}_3 = r_3$. Being a constant term, $-\frac{1}{2}(x_3^2 + y_3^2)$ plays no role in the Hamiltonian equations and it will be dropped in the following computation. Since $\sin\phi_i = \frac{\zeta}{\bar{r}_i}$ for each mass m_i, we have

$$\begin{aligned}
H =& \frac{1}{2}(p_\xi^2 + p_\eta^2 + p_\zeta^2) + \eta p_\xi - \xi p_\eta - (\xi x_3 + \eta y_3) \\
&- \frac{1}{\omega^2}\sum_{i=1}^{3}\left[\frac{m_i}{\bar{r}_i} + \frac{m_i}{\bar{r}_i}\left(\frac{R_i}{\bar{r}_i}\right)^2\left(\frac{C_{20}^i}{2}\right)\left(3\left(\frac{\zeta}{\bar{r}_i}\right)^2 - 1\right)\right].
\end{aligned} \tag{4.27}$$

Expanding the terms $\dfrac{1}{\bar{r}_1}$ and $\dfrac{1}{\bar{r}_2}$ in Taylor series around the new origin of coordinates, we obtain

$$\begin{aligned}
f^1 &:= \frac{1}{\bar{r}_1} = \sum_{k\geqslant 0} P_k^1(\xi, \eta, \zeta), \\
f^2 &:= \frac{1}{\bar{r}_2} = \sum_{k\geqslant 0} P_k^2(\xi, \eta, \zeta),
\end{aligned}$$

where $P_k^j(\xi, \eta, \zeta)$ is a homogeneous polynomial of degree k, for $j = 1, 2$. With some computations and simplifications, we obtain

$$\begin{aligned}
P_0^i =&(\bar{x}_i{}^2+\bar{y}_i{}^2)^{-\frac{1}{2}} = r_{i3}^{-1},\\
P_1^i =&\frac{\bar{x}_i}{r_{i3}^3}\xi+\frac{\bar{y}_i}{r_{i3}^3}\eta\\
P_2^i =&\frac{1}{2}\left(\frac{3\bar{x}_i^2}{r_{i3}^5}-\frac{1}{r_{i3}^3}\right)\xi^2+\frac{1}{2}\left(\frac{3\bar{y}_i^2}{r_{i3}^5}-\frac{1}{r_{i3}^3}\right)\eta^2+\frac{1}{2}\left(-\frac{1}{r_{i3}^3}\right)\zeta^2\\
&+\left(\frac{3\bar{x}_i\bar{y}_i}{r_{i3}^5}\right)\xi\eta,
\end{aligned}\tag{4.28}$$

for $i = 1,2$, where $r_{13} = ((x_1-x_3)^2+(y_1-y_3)^2)^{1/2} = u$, and $r_{23} = ((x_2-x_3)^2+(y_2-y_3)^2)^{1/2} = v$. Similar to that in the case of restricted four body problem in Section 4.1.1, we notice that P_0^1 and P_0^2 are constant terms and play no role in the Hamiltonian equations, so they will be dropped from equation (4.27) in the following calculations. We now perform the following conformal symplectic scaling with multiplier $m_3^{-2/3}$, given by

$$\begin{aligned}
\xi &= m_3^{\frac{1}{3}}x\ , \qquad \eta = m_3^{\frac{1}{3}}y\ , \qquad \zeta = m_3^{\frac{1}{3}}z,\\
p_\xi &= m_3^{\frac{1}{3}}p_x\ , \qquad p_\eta = m_3^{\frac{1}{3}}p_y\ , \qquad p_\zeta = m_3^{\frac{1}{3}}p_z,
\end{aligned}\tag{4.29}$$

where, with an abuse of notation, we call again the new variables x, y, z, p_x, p_y and p_z. Being consistent with the scale change, it is necessary to introduce the scaling transformation of the average radius of the three bodies as follows

$$R_i^2 = (m_3^{1/3}\rho_i)^2 = m_3^{2/3}\rho_i^2, \text{ with } \rho_i = m_3^{-1/3}R_i, \text{ for } i = 1,2,3. \tag{4.30}$$

The motivation of the choice of the power of m_3 is driven by the fact that in this way the gravitational force becomes of the same order of the centrifugal and Coriolis forces (see, e.g., [MS82]). Conformal symplectic scaling with multiplier $m_3^{-2/3}$ yields the following the Hamiltonian in the new variables, which we still denote by H:

$$H(x,y,z,p_x,p_y,p_z) = m_3^{-2/3}H(m_3^{\frac{1}{3}}x, m_3^{\frac{1}{3}}y, m_3^{\frac{1}{3}}z, m_3^{\frac{1}{3}}p_x, m_3^{\frac{1}{3}}p_y, m_3^{\frac{1}{3}}p_z).$$

The resulting Hamiltonian H is now in the form:

$$\begin{aligned}
H =& m_3^{-\frac{2}{3}}\Bigg[\frac{1}{2}(m_3^{\frac{2}{3}}p_x^2 + m_3^{\frac{2}{3}}p_y^2 + m_3^{\frac{2}{3}}p_z^2)\\
&+ m_3^{\frac{2}{3}}yp_x - m_3^{\frac{2}{3}}xp_y - m_3^{\frac{1}{3}}xx_3 - m_3^{\frac{1}{3}}yy_3\\
&- \frac{1}{\omega^2}\Bigg(\sum_{k\geqslant 1} m_1 m_3^{\frac{k}{3}} P_k^1(x,y,z) + \sum_{k\geqslant 1} m_2 m_3^{\frac{k}{3}} P_k^2(x,y,z)\\
&+ \frac{m_1 m_3^{\frac{2}{3}}}{\bar{r}_1}\left(\frac{\rho_1}{\bar{r}_1}\right)^2\left(\frac{C_{20}^1}{2}\right)\left(3\left(\frac{z}{\bar{r}_1}\right)^2 - 1\right)\\
&+ \frac{m_2 m_3^{\frac{2}{3}}}{\bar{r}_2}\left(\frac{\rho_2}{\bar{r}_2}\right)^2\left(\frac{C_{20}^2}{2}\right)\left(3\left(\frac{z}{\bar{r}_2}\right)^2 - 1\right)\\
&+ \frac{m_3^{\frac{2}{3}}}{\bar{r}_3} + \frac{m_3^{\frac{2}{3}}}{\bar{r}_3}\left(\frac{\rho_3}{\bar{r}_3}\right)^2\left(\frac{C_{20}^3}{2}\right)\left(3\left(\frac{z}{\bar{r}_3}\right)^2 - 1\right)\Bigg)\Bigg].
\end{aligned}$$

After cancellations we obtain

$$\begin{aligned}
H =& \frac{1}{2}(p_x^2 + p_y^2 + p_z^2) + yp_x - xp_y - m_3^{-\frac{1}{3}}xx_3 - m_3^{-\frac{1}{3}}yy_3\\
&- \frac{1}{\omega^2}\Bigg(m_3^{-\frac{1}{3}} m_1 P_1^1(x,y,z) + m_3^{-\frac{1}{3}} m_2 P_1^2(x,y,z)\\
&+ \sum_{k\geqslant 2} m_3^{\frac{k-2}{3}} m_1 P_k^1(x,y,z) + \sum_{k\geqslant 2} m_3^{\frac{k-2}{3}} m_2 P_k^2(x,y,z)\\
&+ \frac{m_1}{\bar{r}_1}\left(\frac{\rho_1}{\bar{r}_1}\right)^2\left(\frac{C_{20}^1}{2}\right)\left(3\left(\frac{z}{\bar{r}_1}\right)^2 - 1\right)\\
&+ \frac{m_2}{\bar{r}_2}\left(\frac{\rho_2}{\bar{r}_2}\right)^2\left(\frac{C_{20}^2}{2}\right)\left(3\left(\frac{z}{\bar{r}_2}\right)^2 - 1\right)\\
&+ \frac{1}{\bar{r}_3} + \frac{1}{\bar{r}_3}\left(\frac{\rho_3^2}{\bar{r}_3^2}\right)\left(\frac{C_{20}^3}{2}\right)\left(3\left(\frac{z}{\bar{r}_3}\right)^2 - 1\right)\Bigg).
\end{aligned} \tag{4.31}$$

Following the expansion of the resulting Hamiltonian as a power series in $m_3^{1/3}$, we will then neglect all the terms of order $O(m_3^{1/3})$ in the expansion, as in the classical Hill theory of lunar motion ([MS82]).

To compute the contribution of the different terms in (4.31), we make use of equations

(4.28) and (3.43). Thus, we obtain

$$\begin{aligned}
&-m_3^{-\frac{1}{3}}\left[xx_3 + yy_3 + \frac{m_1 P_1^1}{\omega^2} + \frac{m_2 P_1^2}{\omega^2}\right] \\
&\quad = -m_3^{-\frac{1}{3}}\left[\left(x_3 + \frac{m_1\bar{x}_1}{\omega^2 u^3} + \frac{m_2\bar{x}_2}{\omega^2 v^3}\right)x + \left(y_3 + \frac{m_1\bar{y}_1}{\omega^2 u^3} + \frac{m_2\bar{y}_2}{\omega^2 v^3}\right)y\right] \\
&\quad = -m_3^{-\frac{1}{3}}\left[\left(x_3 + m_1\bar{x}_1\left(1 + \frac{3C_{13}}{\omega^2 u^5}\right) + m_2\bar{x}_2\left(1 + \frac{3C_{23}}{\omega^2 v^5}\right)\right)x\right. \\
&\qquad\qquad \left. + \left(y_3 + m_1\bar{y}_1\left(1 + \frac{3C_{13}}{\omega^2 u^5}\right) + m_2\bar{y}_2\left(1 + \frac{3C_{23}}{\omega^2 v^5}\right)\right)y\right] \\
&\quad = -m_3^{-\frac{1}{3}}\left[\left(x_3 + m_1\bar{x}_1 + m_2\bar{x}_2 + m_1\bar{x}_1\frac{3C_{13}}{\omega^2 u^5} + m_2\bar{x}_2\frac{3C_{23}}{\omega^2 v^5}\right)x\right. \\
&\qquad\qquad \left. + \left(y_3 + m_1\bar{y}_1 + m_2\bar{y}_2 + m_1\bar{y}_1\frac{3C_{13}}{\omega^2 u^5} + m_2\bar{y}_2\frac{3C_{23}}{\omega^2 v^5}\right)y\right].
\end{aligned} \tag{4.32}$$

Using equations (3.51) and (3.53) we have

$$x_3 + m_1\bar{x}_1 + m_2\bar{x}_2 = x_3 + m_1(x_1 - x_3) + m_2(x_2 - x_3) = 0 \tag{4.33}$$

and similarly, using equations (3.52) and (3.53) we have

$$y_3 + m_1\bar{y}_1 + m_2\bar{y}_2 = 0.$$

Thus equation (4.32) becomes

$$-m_3^{-\frac{1}{3}}\left[\left(m_1\bar{x}_1\frac{3C_{13}}{\omega^2 u^5} + m_2\bar{x}_2\frac{3C_{23}}{\omega^2 v^5}\right)x + \left(m_1\bar{y}_1\frac{3C_{13}}{\omega^2 u^5} + m_2\bar{y}_2\frac{3C_{23}}{\omega^2 v^5}\right)y\right]. \tag{4.34}$$

Recalling the C_{ij} notation, we obtain

$$\begin{aligned}
C_{ij} =& C_i + C_j = \left(\frac{R_i^2 C_{20}^i}{2} + \frac{R_j^2 C_{20}^j}{2}\right) = m_3^{\frac{2}{3}}\left(\frac{\rho_i^2 C_{20}^i}{2} + \frac{\rho_j^2 C_{20}^j}{2}\right) \\
:=& m_3^{\frac{2}{3}} K_{ij}
\end{aligned} \tag{4.35}$$

for $i \neq j$.

From equation (3.43), $\omega^2 = 1 - 3C_{12} = 1 - m_3^{\frac{2}{3}} K_{12}$ and thus

$$\frac{1}{\omega^2} = \frac{1}{1 - m_3^{\frac{2}{3}} K_{12}} = 1 + m_3^{\frac{2}{3}} K_{12} + O(m_3^{\frac{4}{3}}). \tag{4.36}$$

Now we neglect the higher order terms in equation (4.36) and equation (4.34) becomes

$$\begin{aligned} m_3^{-\frac{1}{3}} \Bigg[& \left(m_1 \bar{x}_1 \frac{3m_3^{\frac{2}{3}} K_{13}}{u^5} + m_2 \bar{x}_2 \frac{3m_3^{\frac{2}{3}} K_{23}}{v^5} \right) x \\ & + \left(m_1 \bar{y}_1 \frac{3m_3^{\frac{2}{3}} K_{13}}{u^5} + m_2 \bar{y}_2 \frac{3m_3^{\frac{2}{3}} K_{23}}{v^5} \right) y \Bigg]. \end{aligned} \tag{4.37}$$

Since in the procedures of Hill approximation, we are neglecting all terms of order of $m_3^{1/3}$. It follows that the expressions (4.37) and (4.32) will be neglected. Combining the corresponding terms for the second-degree polynomials P_2^i in the Hamiltonian (4.31) and using (4.36), we obtain

$$\begin{aligned} & -\frac{1}{\omega^2} \left(m_1 P_2^1 + m_2 P_2^2 \right) \\ & = -\frac{1}{\omega^2} \Bigg[\frac{m_1}{2} \left(\frac{3\bar{x}_1^2}{r_{13}^5} - \frac{1}{r_{13}^3} \right) x^2 + \frac{m_1}{2} \left(\frac{3\bar{y}_1^2}{r_{13}^5} - \frac{1}{r_{13}^3} \right) y^2 \\ & \quad + \frac{m_1}{2} \left(-\frac{1}{r_{13}^3} \right) z^2 + m_1 \left(\frac{3\bar{x}_1 \bar{y}_1}{r_{13}^5} \right) xy \\ & \quad + \frac{m_2}{2} \left(\frac{3\bar{x}_2^2}{r_{23}^5} - \frac{1}{r_{23}^3} \right) x^2 + \frac{m_2}{2} \left(\frac{3\bar{y}_2^2}{r_{23}^5} - \frac{1}{r_{23}^3} \right) y^2 \\ & \quad + \frac{m_2}{2} \left(-\frac{1}{r_{23}^3} \right) z^2 + m_2 \left(\frac{3\bar{x}_2 \bar{y}_2}{r_{23}^5} \right) xy \Bigg] \\ & = -\frac{1}{2} \Bigg[\left(\frac{3m_1 \bar{x}_1^2}{u^5} + \frac{3m_2 \bar{x}_2^2}{v^5} - \frac{m_1}{u^5} - \frac{m_2}{v^5} \right) x^2 \\ & \quad + \left(\frac{3m_1 \bar{y}_1^2}{u^5} + \frac{3m_2 \bar{y}_2^2}{v^5} - \frac{m_1}{u^5} - \frac{m_2}{v^5} \right) y^2 \\ & \quad + \left(\frac{6m_1 \bar{x}_1 \bar{y}_1}{u^5} + \frac{6m_2 \bar{x}_2 \bar{y}_2}{v^5} \right) xy + \left(-\frac{m_1}{u^3} - \frac{m_2}{v^3} \right) z^2 \Bigg]. \end{aligned} \tag{4.38}$$

Notice that quadratic polynomial consists of the quantities $\bar{x}_1$, $\bar{x}_2$, $\bar{y}_1$ and $\bar{y}_2$ that depend on m_3. While the terms of order of $m_3^{1/3}$ are neglected, we use equation (3.71) to evaluate the corresponding quantities:

$$\bar{x}_1 = -\frac{w}{2},\ \bar{x}_2 = \frac{2-w}{2},\ \bar{y}_1 = \bar{y}_2 = -\frac{1}{2}\sqrt{4u^2 - w^2}, \tag{4.39}$$

where we recall that $w = 1 + u^2 - v^2$. Thus, the quadratic polynomial (4.38) becomes

$$\begin{aligned} -\frac{1}{2}\Bigg[& \left(\frac{m_1\left(\frac{3w^2}{4} - 1\right)}{u^5} + \frac{m_2\left(\frac{3(2-w)^2}{4} - 1\right)}{v^5} \right) x^2 \\ & + \left(\frac{m_1\left(\frac{3(4u^2-w^2)}{4} - 1\right)}{u^5} + \frac{m_2\left(\frac{3(4u^2-w^2)}{4} - 1\right)}{v^5} \right) y^2 \\ & + \left(\frac{m_1\frac{6w\sqrt{4u^2-w^2}}{4}}{u^5} - \frac{m_2\frac{6(2-w)\sqrt{4u^2-w^2}}{4}}{v^5} \right) xy - \left(\frac{m_1}{u^3} + \frac{m_2}{v^3} \right) z^2 \Bigg]. \end{aligned} \tag{4.40}$$

In the Taylor expansions f^i, for $i = 1, 2$, the expressions of order $k \geqslant 3$ in the Hamiltonian are of the form

$$\sum_{k\geqslant 3} m_3^{\frac{k-2}{3}} m_1 P_k^1(x, y, z) + \sum_{k\geqslant 3} m_3^{\frac{k-2}{3}} m_2 P_k^2(x, y, z).$$

Since they can be written in terms of positive exponents of $m_3^{1/3}$, they are neglected in the Hill approximation. The terms that are left in the Hamiltonian (4.31) are

$$\begin{aligned} -\Bigg[& \left(\frac{m_1\rho_1^2}{\bar{r}_1^3} \right) \left(\frac{C_{20}^1}{2} \right) \left(3\left(\frac{z}{\bar{r}_1} \right)^2 - 1 \right) + \left(\frac{m_2\rho_2^2}{\bar{r}_2^3} \right) \left(\frac{C_{20}^2}{2} \right) \left(3\left(\frac{z}{\bar{r}_2} \right)^2 - 1 \right) \\ & + \frac{1}{\bar{r}_3} + \left(\frac{\rho_3^2}{\bar{r}_3^3} \right) \left(\frac{C_{20}^3}{2} \right) \left(3\left(\frac{z}{\bar{r}_3} \right)^2 - 1 \right) \Bigg]. \end{aligned} \tag{4.41}$$

Notice that the terms $\bar{r}_1$, and $\bar{r}_2$ also depend on m_3. Let $m_3 \to 0$, we have $\bar{r}_1 \to u$ and $\bar{r}_2 \to v$. Also, we recall $\bar{r}_3 = r_3 = (x^2 + y^2 + z^2)^{\frac{1}{2}}$ which we now denote by r. When all terms of order $m_3^{\frac{1}{3}}$ are neglected in equation (4.31), we obtain the Hamiltonian as

$$
\begin{aligned}
H =& \frac{1}{2}(p_x^2 + p_y^2 + p_z^2) + yp_x - xp_y \\
& - \Bigg[\left(\frac{(1-\mu)\left(\frac{3w^2}{4} - 1\right)}{u^5} + \frac{\mu\left(\frac{3(2-w)^2}{4} - 1\right)}{v^5} \right) \frac{x^2}{2} \\
& \quad + \left(\frac{(1-\mu)\left(\frac{3(4u^2-w^2)}{4} - 1\right)}{u^5} + \frac{\mu\left(\frac{3(4u^2-w^2)}{4} - 1\right)}{v^5} \right) \frac{y^2}{2} \\
& \quad + \left(\frac{(1-\mu)\frac{6w\sqrt{4u^2-w^2}}{4}}{u^5} - \frac{\mu\frac{6(2-w)\sqrt{4u^2-w^2}}{4}}{v^5} \right) \frac{xy}{2} \\
& \quad - \left(\frac{(1-\mu)}{u^3} + \frac{\mu}{v^3} \right) \frac{z^2}{2} \\
& \quad + \left(\frac{(1-\mu)c_1}{u^3} \right) \left(3\left(\frac{z}{u}\right)^2 - 1 \right) + \left(\frac{\mu c_2}{v^3} \right) \left(3\left(\frac{z}{v}\right)^2 - 1 \right) \\
& \quad + \frac{1}{r} + \left(\frac{c_3}{r^3} \right) \left(3\left(\frac{z}{r}\right)^2 - 1 \right) \Bigg],
\end{aligned}
\tag{4.42}
$$

where we denote $\mu = m_2/(m_1+m_2)$, $r = (x^2+y^2+z^2)^{\frac{1}{2}}$, and $c_i := \rho_i^2 C_{20}^i/2 = m_3^{-\frac{2}{3}} R_3^i C_{20}^i/2$.

□

We refer to the Hamiltonian (4.42) as the *Hill's approximation*. It can be thought of as the limiting Hamiltonian, when the primary and the secondary are sent at an infinite distance. The approximation allows us to study the motion of the infinitesimal particle in an $O(m_3^{1/3})$ neighborhood of m_3. Remarkably, the angular velocity ω associated to the triangular central configuration does not appear in the limiting Hamiltonian. We introduce the gravitational potential as

$$
\begin{aligned}
\widehat{U}(x,y,z) = {} & \left(\frac{(1-\mu)\left(\frac{3w^2}{4}-1\right)}{u^5} + \frac{\mu\left(\frac{3(2-w)^2}{4}-1\right)}{v^5}\right)\frac{x^2}{2} \\
& + \left(\frac{(1-\mu)\left(\frac{3(4u^2-w^2)}{4}-1\right)}{u^5} + \frac{\mu\left(\frac{3(4u^2-w^2)}{4}-1\right)}{v^5}\right)\frac{y^2}{2} \\
& + \left(\frac{(1-\mu)\frac{6w\sqrt{4u^2-w^2}}{4}}{u^5} - \frac{\mu\frac{6(2-w)\sqrt{4u^2-w^2}}{4}}{v^5}\right)\frac{xy}{2} \\
& - \left(\frac{(1-\mu)}{u^3} + \frac{\mu}{v^3}\right)\frac{z^2}{2} \\
& + \left(\frac{(1-\mu)c_1}{u^3}\right)\left(3\left(\frac{z}{u}\right)^2 - 1\right) + \left(\frac{\mu c_2}{v^3}\right)\left(3\left(\frac{z}{v}\right)^2 - 1\right) \\
& + \frac{1}{r} + \left(\frac{c_3}{r^3}\right)\left(3\left(\frac{z}{r}\right)^2 - 1\right)
\end{aligned}
\tag{4.43}
$$

and the effective potential as

$$
\widehat{\Omega}(x,y,z) = \frac{1}{2}(x^2+y^2) + \widehat{U}(x,y,z). \tag{4.44}
$$

The equations of motion associated to (4.42) can thus be written as:

$$
\begin{aligned}
\ddot{x} - 2\dot{y} &= \widehat{\Omega}_x, \\
\ddot{y} + 2\dot{x} &= \widehat{\Omega}_y, \\
\ddot{z} &= \widehat{\Omega}_z.
\end{aligned}
$$

Remark 4.4.2. One of the main advantages of the Hill approximation is that it yields a much simpler Hamiltonian than for the circular restricted four-body problem. Particallt, the effective potential (4.23) has three singularities, corresponding to the positions of the three heavy bodies in the latter.while there is only one singularity, corresponding to the position of the tertiary in the former. Furthermore, the effect of the primary and the secondary are included in the effective potential (4.44) is represented by a quadratic polynomial in x, y, z.

Remark 4.4.3. In the case when $C_{20}^i = 0$ for $i = 1, 2, 3$, we have that $u = v = w = 1$ and the Hamiltonian in (4.42) is the same as the one obtained in Section 4.1.1 [BGG15]. Furthermore, its quadratic part coincides with the quadratic part of the expansion of the Hamiltonian of the restricted three-body problem centered at the Lagrange libration point L_4. Notice that in the case of $\mu = 0$, we obtain the classical lunar Hill problem, after some rotation of the coordinate axes as in Section 4.4.2.

Remark 4.4.4. Our model is an extension of the classical Hill's approximation of the restricted three-body problem, with the major differences that we consider a four-body problem which takes into account the effect of the oblateness coefficients C_{20}^i, $i = 1, 2, 3$; compare with [Hil78, MS82, BGG15]. We remark that an approach similar to ours was adopted in [MRPD01], where a Hill's three body problem with oblate primaries has been considered.

4.4.2 Hill's approximation applied to the Sun-Jupiter-Hektor system

Consider the Sun-Jupiter-Hektor system, we use the following data (see Section 2.2):

	C_{20}	Average radius(km)	Mass(kg)
Sun	$C_{20}^1 = -5.00 \times 10^{-6}$	$R_1 = 695,700$	$M_1 = 1.989 \times 10^{30}$
Jupiter	$C_{20}^2 = -14,736 \times 10^{-6}$	$R_2 = 69,911$	$M_2 = 1.898 \times 10^{27}$
Hektor	$C_{20}^3 = -0.476775$	$R_3 = 92$	$M_3 = 7.91 \times 10^{18}$

For the normalized units, we use the average distance Sun-Jupiter 778.5×10^6 km as the unit of distance, while the mass of Sun-Jupiter-Hektor 1.990898×10^{30} kg as the unit of mass. With these unit quantities, we have the average radius $R_1 = 8.936416 \times 10^{-4}$, $R_2 = 8.980218 \times 10^{-5}$, $R_3 = 1.18176 \times 10^{-7}$, masses $m_1 = 0.9990467$, $m_2 = 9.533386 \times 10^{-4}$ and $m_3 = 3.97308 \times 10^{-12}$. Let $r_{12} = 1$, we obtain $r_{13} = u = 1 - 5.94154 \times 10^{-11}$ and $r_{23} =$

$v = 1 - 1.99318 \times 10^{-12}$ from the system (3.43). In terms of the unit distance $r_{12} = 1$ (the Sun-Jupiter distance is 778.5×10^6 km), the difference between the distances r_{13} and r_{12} is 0.0462549 km, while the difference between the distances r_{23} and r_{12} is 0.00155169 km. Practically, the scalene triangle central configuration is almost an equilateral triangle. The parameters that appear in the Hamiltonian (4.42) are

$$\begin{aligned} c_1 =& m_3^{-\frac{2}{3}} R_1^2 C_{20}^1/2 = -7.958816 \times 10^{-5}, \\ c_2 =& m_3^{-\frac{2}{3}} R_2^2 C_{20}^2/2 = -2.368673 \times 10^{-3}, \\ c_3 =& m_3^{-\frac{2}{3}} R_3^2 C_{20}^3/2 = -1.327161 \times 10^{-7}. \end{aligned} \tag{4.45}$$

The mass ratio that appears in the Hill approximation is $\mu = m_2/(m_1+m_2) = 0.0009533386$. We note that for the case of considering the restricted four-body problem (without the Hill approximation) described by the Hamiltonian (4.24), the oblateness effect is given by the coefficients

$$\begin{aligned} C_1 =& R_1^2 C_{20}^1/2 = -1.996488 \times 10^{-12}, \\ C_2 =& R_2^2 C_{20}^2/2 = -5.941874 \times 10^{-11}, \\ C_3 =& R_3^2 C_{20}^3/2 = -3.32921544 \times 10^{-15}, \end{aligned} \tag{4.46}$$

which are much smaller then the corresponding normalized values c_i, for $i = 1, 2, 3$ as in (4.45). By means of having the numerical values of the parameters involved to be relatively larger, the Hill approximation is more convenient to use for numerical computations. We also note that we have the ordering

$$C_2 < C_1 < C_3,$$

with the corresponding ordering of length

$$r_{13} = u < r_{23} = v < r_{12} = 1.$$

The analogy here between these two orderings agree with Proposition 3.2.1.

4.4.3 Hill's approximation in rotated coordinates

In this section we consider the Hamiltonian of the Hill approximation in a rotated reference frame, and thus the quadratic part of the effective potential (4.44) is diagonalized.

Corollary 4.4.5. *The Hamiltonian* (4.25) *is equivalent, via a rotation of the coordinate axes that diagonalizes the quadratic part of the effective potential, to the Hamiltonian*

$$\begin{aligned} H = {} & \frac{1}{2}(p_x^2 + p_y^2 + p_z^2) + yp_x - xp_y \\ & + \left(\frac{1-\lambda_2}{2}\right)x^2 + \left(\frac{1-\lambda_1}{2}\right)y^2 + \frac{1}{2}\left(\frac{(1-\mu)}{u^3} + \frac{\mu}{v^3}\right)z^2 \\ & - \left(\frac{(1-\mu)c_1}{u^3}\right)\left(3\left(\frac{z}{u}\right)^2 - 1\right) - \left(\frac{\mu c_2}{v^3}\right)\left(3\left(\frac{z}{v}\right)^2 - 1\right) \\ & - \frac{1}{(x^2+y^2+z^2)^{1/2}} - \frac{c_3}{(x^2+y^2+z^2)^{3/2}}\left(\frac{3z^2}{x^2+y^2+z^2} - 1\right), \end{aligned} \tag{4.47}$$

where λ_2 and λ_1 are the eigenvalues corresponding to the rotation transformation in the xy-plane, given by (4.50).

Proof. With a rotation on the xy-plane, we re-write the Hamiltonian in equation (4.25) in the rotated coordinates, which are more suitable for the further analysis. We adopt the following notation

$$\begin{aligned} & U = \frac{3w^2}{4} - 1, \quad V = \frac{3(2-w)^2}{4} - 1, \quad Z = \frac{3(4u^2 - w^2)}{4} - 1, \\ & W_1 = \frac{6w\sqrt{4u^2 - w^2}}{4}, \quad W_2 = \frac{6(2-w)\sqrt{4u^2 - w^2}}{4}. \end{aligned} \tag{4.48}$$

The planar effective potential restricted to the xy-plane (i.e., $z = 0$) is given by

$$\begin{aligned}\widehat{\Omega}(x,y) = &\left(1 + \frac{(1-\mu)U}{u^5} + \frac{\mu V}{v^5}\right)\frac{x^2}{2} + \left(1 + \frac{(1-\mu)Z}{u^5} + \frac{\mu Z}{v^5}\right)\frac{y^2}{2} \\ &+ \left(\frac{(1-\mu)W_1}{u^5} - \frac{\mu W_2}{v^5}\right)\frac{xy}{2} \\ &- \left(\frac{(1-\mu)c_1}{u^3}\right) - \left(\frac{\mu c_2}{v^3}\right) + \frac{1}{r} - \left(\frac{c_3}{r^3}\right),\end{aligned}$$

which can be written in matrix notation as

$$\widehat{\Omega} = \frac{1}{2}q^T M q - \left(\frac{(1-\mu)c_1}{u^3}\right) - \left(\frac{\mu c_2}{v^3}\right) + \frac{1}{\|q\|} - \frac{c_3}{\|q\|^3},$$

where $q = (x, y)^T$ and

$$M = \begin{pmatrix} 1 + \frac{(1-\mu)U}{u^5} + \frac{\mu V}{v^5} & \frac{1}{2}\left(\frac{(1-\mu)W_1}{u^5} - \frac{\mu W_2}{v^5}\right) \\ \frac{1}{2}\left(\frac{(1-\mu)W_1}{u^5} - \frac{\mu W_2}{v^5}\right) & 1 + \frac{(1-\mu)Z}{u^5} + \frac{\mu Z}{v^5} \end{pmatrix}. \tag{4.49}$$

In order to obtain the eigenvalues of M, we solve the characteristic equation $\det(M - \lambda I) = 0$, which yields

$$\begin{aligned}\lambda^2 &- \left(2 + \frac{(1-\mu)(U+Z)}{u^5} + \frac{\mu(V+Z)}{v^5}\right)\lambda \\ &+ \left(1 + \frac{(1-\mu)U}{u^5} + \frac{\mu V}{v^5}\right)\left(1 + \frac{(1-\mu)Z}{u^5} + \frac{\mu Z}{v^5}\right) \\ &- \frac{1}{4}\left(\frac{(1-\mu)W_1}{u^5} - \frac{\mu W_2}{v^5}\right)^2 = 0, \qquad (4.50) \\ \lambda_1 &= \frac{1}{2}\left(2 - \frac{2(1-\mu)}{u^5} - \frac{2\mu}{v^5} + \frac{3(1-\mu)}{u^3} + \frac{3\mu}{v^3} - \frac{3}{u^3v^3}\sqrt{\Delta}\right), \\ \lambda_2 &= \frac{1}{2}\left(2 - \frac{2(1-\mu)}{u^5} - \frac{2\mu}{v^5} + \frac{3(1-\mu)}{u^3} + \frac{3\mu}{v^3} + \frac{3}{u^3v^3}\sqrt{\Delta}\right).\end{aligned}$$

where

$$\Delta = (\mu u^3 + (1-\mu)v^3)^2 - \mu(1-\mu)uv\left(-u^4 - v^4 + 2u^2 + 2v^2 + 2u^2v^2 - 1\right).$$

When u and v approach 1, which is the case when c_1, c_2, c_3 approach 0, we have $\lambda_1, \lambda_2 > 0$ and $\lambda_1 \neq \lambda_2$.

Since the matrix M is symmetric, its eigenvalues λ_1 and λ_2 are real. Notice that the corresponding eigenvectors of λ_1 and λ_2 are orthogonal. Let v_1 and v_2 be the unit eigenvectos for λ_1 and λ_2 respectively (i.e. $Mv_1 = \lambda_1 v_1$ and $Mv_2 = \lambda_2 v_2$). These eigenvalues are given explicitly in Section 4.4.4. The associated matrix $C = \mathrm{col}(v_2, v_1)$ is orthogonal, i.e., $C^T = C^{-1}$. Hence, C defines a rotation in the xy-plane. Now we can express the equations of motion for the planar case as

$$\ddot{q} - 2J\dot{q} = Mq - \frac{q}{\|q\|^3} + \frac{3c_3 q}{\|q\|^5},$$

where

$$J = \begin{pmatrix} 0 & 1 \\ -1 & 0 \end{pmatrix}.$$

Substituting the linear change of variable $q = C\bar{q}$ with $\bar{q} = (\bar{x}, \bar{y})^T$ and multiplying C^{-1} from the left, we obtain

$$C^{-1}C\ddot{\bar{q}} - 2C^{-1}JC\dot{\bar{q}} = C^{-1}MC\bar{q} - \frac{C^{-1}C\bar{q}}{\|\bar{q}\|^3} + \frac{3c_3 C^{-1}C\bar{q}}{\|\bar{q}\|^5}.$$

The matrix $D = C^{-1}MC$ is in fact a diagonal matrix such that $D = \mathrm{diag}(\lambda_2, \lambda_1)$, that is $\|C\bar{q}\|^3 = \|\bar{q}\|^3$. And therefore the equation becomes

$$\ddot{\bar{q}} - 2C^{-1}JC\dot{\bar{q}} = D\bar{q} - \frac{\bar{q}}{\|\bar{q}\|^3} + \frac{3c_3\bar{q}}{\|\bar{q}\|^5}.$$

Recall that $v_1 = (v_{11}, v_{12})^T$, $v_2 = (v_{21}, v_{22})^T$ and $C = \mathrm{col}(v_2, v_1)$. Since C is unitary, we have $C^{-1} = C^T$. Furthermore, we have

$$C^{-1}JC = \begin{pmatrix} 0 & v_{12}v_{21} - v_{11}v_{22} \\ -(v_{12}v_{21} - v_{11}v_{22}) & 0 \end{pmatrix}.$$

A straightforward computation shows that $v_{12}v_{21} - v_{11}v_{22} = 1$, which implies $C^{-1}JC = J$. The relation $C^{-1}JC = C^TJC = J$ shows that the matrix C is symplectic by definition. Hence, the change of coordinates is symplectic. Thus, the equations of motion can be written as

$$\ddot{\bar{q}} - 2J\dot{\bar{q}} = D\bar{q} - \frac{\bar{q}}{\|\bar{q}\|^3} + \frac{3c_3\bar{q}}{\|\bar{q}\|^5}.$$

For $\mu \in [0, \frac{1}{2})$, we obtain the equations

$$\begin{aligned} \ddot{\bar{x}} - 2\dot{\bar{y}} &= \bar{\Omega}_{\bar{x}} \\ \ddot{\bar{y}} + 2\dot{\bar{x}} &= \bar{\Omega}_{\bar{y}} \end{aligned} \tag{4.51}$$

with

$$\bar{\Omega}(\bar{x}, \bar{y}) = \frac{1}{2}(\lambda_2\bar{x}^2 + \lambda_1\bar{y}^2) - \frac{(1-\mu)c_1}{u^3} - \frac{\mu c_2}{v^3} + \frac{1}{\|\bar{q}\|} - \frac{c_3}{\|\bar{q}\|^3}. \tag{4.52}$$

We remark the symmetry properties from the expressions for $\bar{\Omega}_{\bar{x}}$ and $\bar{\Omega}_{\bar{y}}$ as:

$$\bar{\Omega}_{\bar{x}}(\bar{x}, -\bar{y}) = \bar{\Omega}_{\bar{x}}(\bar{x}, \bar{y}) , \qquad \bar{\Omega}_{\bar{y}}(\bar{x}, -\bar{y}) = -\bar{\Omega}_{\bar{x}}(\bar{x}, \bar{y}).$$

Using these properties, we observe that the equations (4.51) are invariant under the transformations of $\bar{x} \to \bar{x}$, $\bar{y} \to -\bar{y}$, $\dot{\bar{x}} \to -\dot{\bar{x}}$, $\dot{\bar{y}} \to \dot{\bar{y}}$, $\ddot{\bar{x}} \to \ddot{\bar{x}}$ and $\ddot{\bar{y}} \to -\ddot{\bar{y}}$. If we now return back to the spatial problem, we need to replace $\bar{\Omega}$ by

$$\begin{aligned}\bar{\Omega}(\bar{x},\bar{y},\bar{z}) =& \frac{1}{2}(\lambda_2\bar{x}^2+\lambda_1\bar{y}^2) - \frac{1}{2}\left(\frac{(1-\mu)}{u^3}+\frac{\mu}{v^3}\right)\bar{z}^2 \\ &+ \left(\frac{(1-\mu)c_1}{u^3}\right)\left(3\left(\frac{\bar{z}}{u}\right)^2-1\right) + \left(\frac{\mu c_2}{v^3}\right)\left(3\left(\frac{\bar{z}}{v}\right)^2-1\right) \\ &+ \frac{1}{r} + \left(\frac{c_3}{r^3}\right)\left(3\left(\frac{\bar{z}}{r}\right)^2-1\right).\end{aligned} \tag{4.53}$$

Furthermore, we can write $\bar{\Omega}(\bar{x},\bar{y},\bar{z}) = \frac{1}{2}\bar{x}^2 + \frac{1}{2}\bar{y}^2 + \bar{U}(\bar{x},\bar{y},\bar{z})$, where

$$\begin{aligned}\bar{U}(\bar{x},\bar{y},\bar{z}) =& \left(\frac{\lambda_2-1}{2}\right)\bar{x}^2 + \left(\frac{\lambda_1-1}{2}\right)\bar{y}^2 - \frac{1}{2}\left(\frac{(1-\mu)}{u^3}+\frac{\mu}{v^3}\right)\bar{z}^2 \\ &+ \left(\frac{(1-\mu)c_1}{u^3}\right)\left(3\left(\frac{\bar{z}}{u}\right)^2-1\right) + \left(\frac{\mu c_2}{v^3}\right)\left(3\left(\frac{\bar{z}}{v}\right)^2-1\right) \\ &+ \frac{1}{r} - \frac{c_3}{r^3} + \frac{3c_3\bar{z}^2}{r^5}.\end{aligned} \tag{4.54}$$

In conclusion, the Hamiltonian in the new coordinates is now given by (note that we omit the bars for x, y and z for simplification of notations):

$$\begin{aligned}H(x,y,z,p_x,p_y,p_z) =& \frac{1}{2}(p_x^2+p_y^2+p_z^2) + yp_x - xp_y \\ &+ \left(\frac{1-\lambda_2}{2}\right)x^2 + \left(\frac{1-\lambda_1}{2}\right)y^2 + \frac{1}{2}\left(\frac{(1-\mu)}{u^3}+\frac{\mu}{v^3}\right)z^2 \\ &- \left(\frac{(1-\mu)c_1}{u^3}\right)\left(3\left(\frac{z}{u}\right)^2-1\right) - \left(\frac{\mu c_2}{v^3}\right)\left(3\left(\frac{z}{v}\right)^2-1\right) \\ &- \frac{1}{r} + \frac{c_3}{r^3} - \frac{3c_3z^2}{r^5}.\end{aligned}$$

With the substitution of $r = (x^2+y^2+z^2)^{\frac{1}{2}}$, we obtain (4.47). □

Remark 4.4.6. In the case of having $C_{20}^i = 0$ for $i = 1,2,3$ and $\mu = 0$ in (4.47), we obtain the Hamiltonian for the classical lunar Hill problem, see, e.g., [MS82].

4.4.4 Expressions for the eigenvectors of the rotated Monodromy matrix M

With the martix (4.49), the explicit expressions of the eigenvectors v_1, v_2 associated to the eigenvalues (4.50), respectively are shown below. Let

$$\Theta := \sqrt{-u^4 - v^4 + 2u^2 + 2v^2 + 2u^2v^2 - 1},$$

we have

$$\begin{aligned}
v_1 = \Big[&- \big((1-\mu)(-v^7 + (1+u^2)v^5) - \mu(-u^7 + (1+v^2)u^5)\big)\,\Theta, \\
&(1-\mu)(v^9 - 2(1+u^2)v^7 + v^5(1+u^4)) \\
&+ \mu(u^9 - 2(1+v^2)u^7 + u^5(1+v^4)) \\
&- \sqrt{2}u^2v^2\sqrt{((1-\mu)v^3 + \mu u^3)^2 - \mu(1-\mu)uv\Theta^2}\Big], \\
v_2 = \Big[&- \big((1-\mu)(-v^7 + (1+u^2)v^5) - \mu(-u^7 + (1+v^2)u^5)\big)\,\Theta, \\
&(1-\mu)(v^9 - 2(1+u^2)v^7 + v^5(1+u^4)) \\
&+ \mu(u^9 - 2(1+v^2)u^7 + u^5(1+v^4)) \\
&+ \sqrt{2}u^2v^2\sqrt{((1-\mu)v^3 + \mu u^3)^2 - \mu(1-\mu)uv\Theta^2}\Big].
\end{aligned} \tag{4.55}$$

4.5 Linear stability analysis of the Hill four-body problem with oblate bodies

In this section we aim to obtain the equilibrium points, which are associated to the potential in equation (4.53) for our model of Hill four-body problem with oblate bodies. Furthermore, we analyze their linear stability.

4.5.1 The equilibrium points of the system

In order to find the equilibrium points of equation (4.47), we have to solve the following system:

$$\left.\begin{array}{l}\Omega_x = 0\\ \Omega_y = 0\\ \Omega_z = 0\end{array}\right\} \Rightarrow \left.\begin{array}{l}\left(\lambda_2 - \dfrac{1}{r^3} + \dfrac{3c_3}{r^5} - \dfrac{15c_3 z^2}{r^7}\right) x := Ax = 0\\ \left(\lambda_1 - \dfrac{1}{r^3} + \dfrac{3c_3}{r^5} - \dfrac{15c_3 z^2}{r^7}\right) y := By = 0\\ \left(\gamma - \dfrac{1}{r^3} + \dfrac{9c_3}{r^5} - \dfrac{15c_3 z^2}{r^7}\right) z := Cz = 0\end{array}\right\}$$

where Ω is the effective potential (4.53) (again we omit the bars), and

$$\gamma := -\left[\frac{(1-\mu)}{u^3} + \frac{\mu}{v^3}\right] + \frac{6(1-\mu)c_1}{u^5} + \frac{6\mu c_2}{v^5}. \tag{4.56}$$

We first note that the expressions A and B cannot simultaneously equal to 0 due to the relations

$$A - B = \lambda_2 - \lambda_1$$

and $\lambda_1 \neq \lambda_2$. Since $c_i \leqslant 0$ for $i = 1, 2, 3$ and $\lambda_1 \neq \lambda_2$, we have

$$A - C = \lambda_2 + \frac{(1-\mu)}{u^3} + \frac{\mu}{v^3} - \frac{6(1-\mu)c_1}{u^5} - \frac{6\mu c_2}{v^5} - \frac{6c_3}{r^5} > 0$$

and hence the expressions A and C or B and C in the above system cannot simultaneously equal to 0. A similar argument holds for expressions B and C. This implies that, for example, if $A = 0$, then $B \neq 0$ and $C \neq 0$, so $y = z = 0$ and x is given by the equation $A = 0$; the same reasoning applies for the other combinations of variables. Consequently, we have all equilibrium points must lie on the x-, y-, z-coordinate axes. Precisely, we have the following results.

(i) Equilibrium points on the x-axis In the case $A = 0$, $B \neq 0$, $C \neq 0$, we must have $y = z = 0$. From $A = 0$ and $z = 0$ we infer

$$h_A(r) := \lambda_2 - \frac{1}{r^3} + \frac{3c_3}{r^5} = 0.$$

We have $h'_A(r) = \dfrac{3}{r^4} - \dfrac{15c_3}{r^6} > 0$, since $c_3 < 0$; also, $\lim_{r\to 0} h_A(r) = -\infty$ and $\lim_{r\to\infty} h_A(r) = \lambda_2 > 0$. Hence, the equation $h_A(r) = 0$ has a unique solution $r^*_x > 0$, yielding the equilibrium points $(\pm r^*_x, 0, 0)$.

(ii) Equilibrium points on the y-axis In the case $B = 0$, $A \neq 0$, $C \neq 0$, we must have $x = z = 0$. From $B = 0$ and $z = 0$ we infer

$$h_B(r) := \lambda_1 - \frac{1}{r^3} + \frac{3c_3}{r^5} = 0.$$

We have $h'_B(r) = \dfrac{3}{r^4} - \dfrac{15c_3}{r^6} > 0$, since $c_3 < 0$; also, $\lim_{r\to 0} h_B(r) = -\infty$ and $\lim_{r\to\infty} h_B(r) = \lambda_1 > 0$. Hence, the equation $h_B(r) = 0$ has a unique solution $r^*_y > 0$, yielding the equilibrium points $(0, \pm r^*_y, 0)$.

(iii) Equilibrium points on the z-axis In the case $C = 0$, $A \neq 0$, $B \neq 0$, we must have $x = y = 0$, so $z = \pm r$. Hence $C = 0$ implies

$$\gamma - \frac{1}{r^3} - \frac{6c_3}{r^5} = \frac{\gamma r^5 - r^2 - 6c_3}{r^5} = 0.$$

Since $c_1, c_2 \leqslant 0$ we have that $\gamma < 0$. Let $h_C(r) = \gamma r^5 - r^2 - 6c_3$. We have $h'_C(r) = 5\gamma r^4 - 2r < 0$; also, $\lim_{r\to 0} h_C(r) = -6c_3 > 0$ and $\lim_{r\to+\infty} h_C(r) = -\infty$. Hence, the equation $h_C(r) = 0$ has a unique solution $r^*_z > 0$, yielding the equilibrium points $(0, 0, \pm r^*_z)$.

In the case of the Sun-Jupiter-Hektor system, in normalized units, we obtain $\lambda_1 = 0.002144499689960222$, $\lambda_2 = 2.9978555002506795$ and the equilibrium points location are given as follows:

	x	y	z
x-equilibria	± 0.6935267570	0	0
y-equilibria	0	± 7.7545750772	0
z-equilibria	0	0	± 0.0008923544

Note that the x-equilibria and the y-equilibria also exist in the case of the Hill's redistricted four body problem (i.e., without oblateness), as in [BGG15]. The locations of the equilibria, in the case of Hektor, are very close to the ones as in the case of an oblate tertiary. Precisely, we have the following

	x	y	z
x-equilibria	± 0.6935265657	0	0
y-equilibria	0	± 7.7545747024	0

In conclusion, the x-equilibria and the y-equilibria are the ones inherits from the Hill's restricted four body problem (with non-oblate bodies). In other words, the Hill's problem with oblate bodies are continuations of the ones for the Hill's restricted four body problem. Contrarily, the z-equilibria do not exist for the Hill's restricted four body problem. Nevertheless, these z-equilibria are a continuation of the equilibria that appear in the J_2-problem; see Section 4.2.1. For the J_2-problem, we can compute the distance from the z-equilibria to the center, as $\hat{r}_z = R_3(-3C_{20})^{1/2}$. Applying this formula for the Hektor's case, the numerical result is very close to the one found from the approximation in this section. To summarize, the Hill restricted three-body problem has 2 equilibrium points while the Hill's restricted four-body problem has 4 equilibrium points, and the Hill four-body problem with oblate bodies has 6 equilibrium points.

Notice that there is a rescaling procedure performed in the Hill's approximation. In order to compute the distance of the equilibrium points from the barycenter in real unit, we need to multiply by $m_3^{1/3}$ and the unit of distance (i.e. Sun-Jupiter). Consequently, the x-equilibrium points, the y-equilibrium points and the z-equilibrium points are located at a distance of $85,512.774$ km, $956,149.451$ km and 110.028 km from the barycenter of Hektor respectively. Recall the dimension of Hektor, the smallest semi-minor axis is 60 km. Subsequently, we have the z-equilibrium points are located outside but very close to the body of the asteroid. The computation of the distances uses the value of $C_{20}^3 = -0.476775$, which is obtained from Section 4.2.1. If we use $C_{20}^3 = -0.15$, as provided by [MDCR+14] instead, we obtain that the z-equilibrium points are at 62 km from the barycenter. It follows that the z-equilibrium points are located right at the surface of the asteroid.

Since the shape of an asteroid is not known, it is difficult to determine the asteroid's oblateness and thus, it is worth studying the effect of a range of values of the oblateness parameter. In order to understand the effect, we plot the dependence on the C_{20}^3, within the range of -0.001 and -0.95, of the distance from the z-equilibrium point to the barycenter (in km). We remark that for some values, the z-equilibrium points are outside the Brillouin sphere (which is the smallest sphere that contains the body), while for some others they are inside. The z-equilibria that are outside are an artifact of the model, as they do not make physical sense. However, the z-equilibria that are inside the Brillouin sphere of the asteroid are physically possible. See Section 4.7 for further information.

4.5.2 Linear stability of the equilibrium points

In this section, we study the linear stability of the equilibrium points that found in Section 4.5 in the case of Hektor.

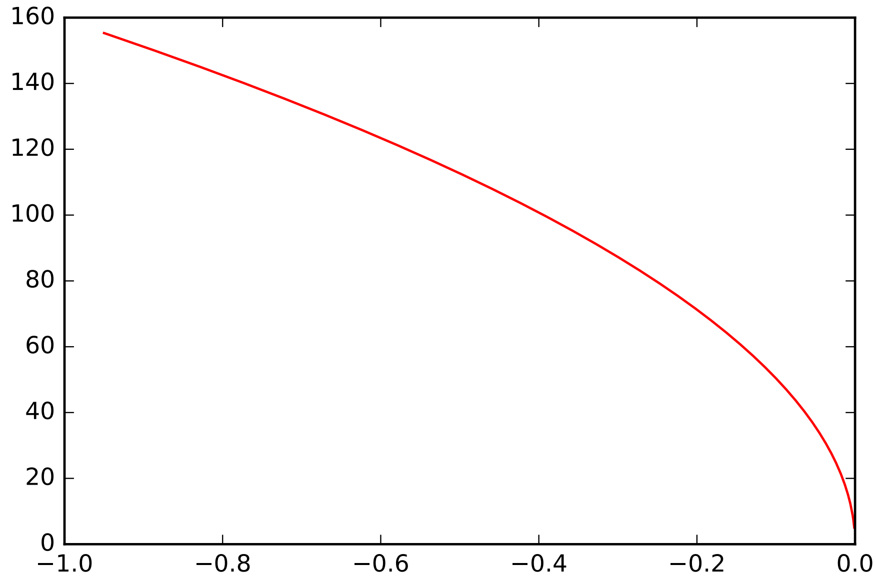

Figure 4.2: The dependence of the z-equilibrium point distance on C_{20}^3.

The Hamiltonian (4.47) yields the following system of equations

$$\dot{x} = v_x, \quad \dot{v}_x = 2v_y + \Omega_x,$$

$$\dot{y} = v_y, \quad \dot{v}_y = -v_x + \Omega_y,$$

$$\dot{z} = v_z, \quad \dot{v}_z = \Omega_z,$$

where Ω is the effective potential given by (4.53) (again, we omit the overline bar on the variables). The second order derivatives of Ω are given by

$$\begin{aligned}
\Omega_{xx} =& \lambda_2 - \frac{1}{r^3} + \frac{3x^2}{r^5} + \frac{3c_3}{r^5} - \frac{15c_3x^2}{r^7} - \frac{15c_3z^2}{r^7} + \frac{105c_3z^2x^2}{r^9}, \\
\Omega_{yy} =& \lambda_1 - \frac{1}{r^3} + \frac{3y^2}{r^5} + \frac{3c_3}{r^5} - \frac{15c_3y^2}{r^7} - \frac{15c_3z^2}{r^7} + \frac{105c_3z^2y^2}{r^9}, \\
\Omega_{zz} =& \gamma - \frac{1}{r^3} + \frac{3z^2}{r^5} + \frac{9c_3}{r^5} - \frac{90c_3z^2}{r^7} + \frac{105c_3z^4}{r^9}, \\
\Omega_{xy} =& \frac{3xy}{r^5} - \frac{15c_3xy}{r^7} + \frac{105c_3z^2xy}{r^9}, \\
\Omega_{xz} =& \frac{3xz}{r^5} - \frac{45c_3xz}{r^7} + \frac{105c_3z^3x}{r^9}, \\
\Omega_{yz} =& \frac{3yz}{r^5} - \frac{45c_3yz}{r^7} + \frac{105c_3z^3y}{r^9}.
\end{aligned} \tag{4.57}$$

To describe the linearized system, we consider the Jacobain such that

$$\mathcal{J} = \begin{pmatrix} 0 & 0 & 0 & 1 & 0 & 0 \\ 0 & 0 & 0 & 0 & 1 & 0 \\ 0 & 0 & 0 & 0 & 0 & 1 \\ \Omega_{xx} & \Omega_{xy} & \Omega_{xz} & 0 & 2 & 0 \\ \Omega_{yx} & \Omega_{yy} & \Omega_{yz} & -2 & 0 & 0 \\ \Omega_{zx} & \Omega_{zy} & \Omega_{zz} & 0 & 0 & 0 \end{pmatrix}. \tag{4.58}$$

With the nature that the equilibria are on the x-axis, y-axis and z-axis, the equilibria are of the form $(\pm r_x^*, 0, 0)$, $(0, \pm r_y^*, 0)$, $(0, 0, \pm r_z^*)$. In addition, we have the mixed second order partial derivatives Ω_{xy}, Ω_{xz}, Ω_{yz} vanish at each of the equilibrium points. Hence the Jacobian matrix (4.58) evaluated at the equilibria is of the form:

$$\mathcal{J} = \begin{pmatrix} 0 & 0 & 0 & 1 & 0 & 0 \\ 0 & 0 & 0 & 0 & 1 & 0 \\ 0 & 0 & 0 & 0 & 0 & 1 \\ \Omega_{xx} & 0 & 0 & 0 & 2 & 0 \\ 0 & \Omega_{yy} & 0 & -2 & 0 & 0 \\ 0 & 0 & \Omega_{zz} & 0 & 0 & 0 \end{pmatrix}, \tag{4.59}$$

Furthermore, the matrix (4.59) has the characteristic equation as

$$(\rho^2 - \Omega_{zz})(\rho^4 + (4 - \Omega_{xx} - \Omega_{yy})\rho^2 + \Omega_{xx}\Omega_{yy}) = 0. \tag{4.60}$$

The signs of expressions Ω_{xx}, A, B and D determine the stability of the equalibria. In the case of the Sun-Jupiter-Hektor system, we obtain the following stability character of the equilibrium positions numerically:

i) **Eigenvalues of x-equilibria at** $(\pm 0.6935267570, 0, 0)$

$$\begin{array}{cc} 2.5069424783 & -2.5069424783, \\ 2.0704830660i, & -2.0704830660i, \\ 1.9995877290i, & -1.9995877290i. \end{array}$$

Stability type: center × center × saddle.

ii) **Eigenvalues of y-equilibria at** $(0, \pm 7.7545750772, 0)$

$$\begin{array}{cc} 0.9890157325i, & -0.9890157325i, \\ 0.1403687326i, & -0.1403687326i, \\ 1.0013166944i, & -1.0013166944i \end{array}$$

Stability type: center × center × center.

iii) **Eigenvalues of z-equilibria at** $(0, 0, \pm 0.0008923544)$

$$
\begin{array}{cc}
-37514.04321 + 0.9999999997i & -37514.04321 - 0.9999999997i \\
37514.04321 + 0.9999999997i & 37514.04321 - 0.9999999997i \\
53052.86869i & -53052.86869i
\end{array}
$$

Stability type: center × complex saddle.

We notice that the imaginary part of the 'Krein quartet' of eigenvalues of the z-equilibria is approximately ± 1, meaning that the motion of the infinitesimal mass around the equilibrium point is close to the $1:1$ resonance relative with the rotation of the primary and the secondary. In Fig. 4.3 we show the behavior of the real part and the imaginary part of the 'Krein quartet' of eigenvalues for a range of r_z^* values between $z = 0.0008923544$ (corresponding to the value for Hektor $c_3 = -1.327161 \times 10^{-7}$) and $z = 0.009999$ (corresponding to $c_3 = -1.666271 \times 10^{-5}$).Note that the imaginary part remains close to ± 1. In Section 4.5.3 we will show an analytic approach and argument that the real part of the 'Krein quartet' of eigenvalues is always non-zero, while the imaginary part is close to ± 1 for r_z^* sufficiently small. The analytical results help us to further understand and explain the behavior of both the real and the complex parts of the 'Krein quartet' of eigenvalues observed in Fig. 4.3.

4.5.3 Analytical Results on the Linear Stability of Equilibria

In this section, we consider analytical approaches. Due to the performance of the Hill's approximation, we are able to provide some analytical arguments for the linear stability of the equilibria. Notice that the problem refers to the three parameters, c_1, c_2 and c_3, which make the analysis quite complicated. To simplify the complication, in this section

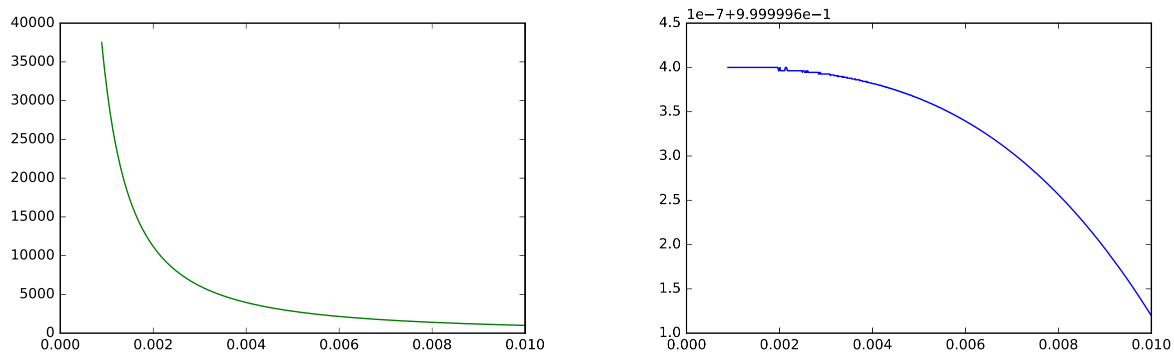

Figure 4.3: The dependence of the real part (left) and imaginary part (right) of the Krein quartet of eigenvalues on the z-equilibrium point. The horizontal axis represents the distance r_z^* from the equilibrium point to the origin, the vertical axis the real part (left), and the absolute value of the imaginary part (right) of the eigenvalues. The former never changes sign, and the latter stays within 4×10^{-7} from 1.

we will assume that $c_1 = c_2 = 0$ and study the stability of the equilibria for varying c_3 for $c_3 < 0$. The justification of this simplifying assumption refers to the contribution to the gravitational potential (4.43) as in the Hill problem. The contribution to the gravitational potential (4.43) from the term containing c_3 in a small neighborhood of the tertiary, that is, for $r \ll 1$, is much bigger than the contributions from the terms containing c_1 and c_2. In addition, we rescale the sides of the triangular central configuration (3.43) differently, namely $r_{13} = r_{23} = 1$ and $r_{12} = \upsilon$. Referring to the Remark 3.2.4, we note that rescaling the unit of distance, the triangular central configuration does not change. Instead, only the constant c_3 get rescaled by a factor. With this rescaling, the computations is made to be somewhat easier. In this case, the eigenvalues of the matrix M in (4.49) becomes

$$\begin{aligned}\lambda_1 =& \frac{3}{2}\left[1 - \sqrt{1 - (\mu - \mu^2)\upsilon^2(4 - \upsilon^2)}\right], \\ \lambda_2 =& \frac{3}{2}\left[1 + \sqrt{1 - (\mu - \mu^2)\upsilon^2(4 - \upsilon^2)}\right],\end{aligned} \tag{4.61}$$

and the constant γ in (4.56) becomes $\gamma = -1$.

Linear stability of the equilibria on the z-axis

The z-equilibrium points are of the form $(0, 0, \pm r_z^*)$, with

$$-(r_z^*)^5 - (r_z^*)^2 - 6c_3 = 0, \tag{4.62}$$

which yields

$$c_3 = \frac{-(r_z^*)^2 - (r_z^*)^5}{6}. \tag{4.63}$$

Evaluating Ω_{xx}, Ω_{yy}, Ω_{zz} at the equilibrium point yields:

$$\begin{aligned}
\Omega_{xx} =& \lambda_2 - (r_z^*)^{-3} - 12c_3(r_z^*)^{-5}, \\
\Omega_{yy} =& \lambda_1 - (r_z^*)^{-3} - 12c_3(r_z^*)^{-5}, \\
\Omega_{zz} =& -1 + 2(r_z^*)^{-3} + 24c_3(r_z^*)^{-5}.
\end{aligned}$$

Substituting (4.63) we obtain

$$\begin{aligned}
\Omega_{xx} &= 2 + \lambda_2 + (r_z^*)^{-3}, \\
\Omega_{yy} &= 2 + \lambda_1 + (r_z^*)^{-3}, \\
\Omega_{zz} &= -5 - 2(r_z^*)^{-3}.
\end{aligned} \tag{4.64}$$

Using (4.50) and denoting $d := \sqrt{1 - (\mu - \mu^2)v^2(4 - v^2)}$ we can write

$$\begin{aligned}
\lambda_1 &= \frac{3}{2}(1 - d), \\
\lambda_2 &= \frac{3}{2}(1 + d).
\end{aligned} \tag{4.65}$$

Also for $c_3 = 0$ we have $d_0 = \sqrt{1 - 3(\mu - \mu^2)}$ and

$$\begin{aligned}
\lambda_{10} =& \frac{3}{2}(1 - d_0), \\
\lambda_{20} =& \frac{3}{2}(1 + d_0).
\end{aligned} \tag{4.66}$$

Note that this is the same as the results shown in [BGG15]. For future reference, we expand d as a power series in the parameter c_3 as

$$d = d_0 + d_1 c_3 + O(c_3^2), \tag{4.67}$$

where the coefficient d_1 can be obtained from the Taylor's theorem around $c_3 = 0$ as

$$d_1 = -\frac{2(\mu - \mu^2)}{d_0}. \tag{4.68}$$

With the characteristic equation given by the equation (4.60) and the condition $\Omega_{zz} < 0$ as in equation (4.64), we obtain that the pair of eigenvalues $\rho_{1,2} = \pm(\Omega_{zz})^{1/2}$ is purely imaginary.The 'Krein quartet' eigenvalues are given by

$$\rho_{3,4,5,6} = \pm\sqrt{\frac{-A \pm \sqrt{A^2 - 4B}}{2}}, \tag{4.69}$$

where

$$\begin{aligned} A &= 4 - \Omega_{xx} - \Omega_{yy} &&= -3 - \tfrac{2}{(r_z^*)^3}, \\ B &= \Omega_{xx}\Omega_{yy} &&= 10 + \frac{9}{4}\upsilon^2(4 - \upsilon^2)(\mu - \mu^2) + \frac{7}{(r_z^*)^3} + \frac{1}{(r_z^*)^6}. \end{aligned}$$

Then we have

$$D := A^2 - 4B = d^2 - 40 - \frac{16}{(r_z^*)^3} = -31 - 9\upsilon^2(4 - \upsilon^2)(\mu - \mu^2) - \frac{16}{(r_z^*)^3} < 0.$$

Provided that $-A > 0$ and $D < 0$, we obtain that the eigenvalues $\rho_{3,4,5,6}$ as complex numbers, non-real, non-purely-imaginary, for all parameter values. Now we let $\rho = a + ib$

be such that $\rho^2 = -\frac{A}{2} \pm \frac{\sqrt{4B-A^2}}{2} i := \alpha + i\beta$, we have the expression

$$a + ib = \left(\frac{(\alpha^2 + \beta^2)^{\frac{1}{2}} + \alpha}{2} \right)^{\frac{1}{2}} + \operatorname{sign}(\beta) \left(\frac{(\alpha^2 + \beta^2)^{\frac{1}{2}} - \alpha}{2} \right)^{\frac{1}{2}} i.$$

To show that b is approximately ± 1, or $b^2 \approx 1$, for $r_z^* \approx 0$, note that

$$\begin{aligned} b^2 =& \frac{(\alpha^2 + \beta^2)^{\frac{1}{2}} - \alpha}{2} = \frac{A}{4} + \frac{\sqrt{B}}{2} \\ =& -\frac{3}{4} + \frac{1}{2} \left[\left(10 + \frac{9}{4}\Upsilon + \frac{7}{(r_z^*)^3} + \frac{1}{(r_z^*)^6} \right)^{\frac{1}{2}} - \frac{1}{(r_z^*)^3} \right] \\ =& -\frac{3}{4} + \frac{1}{2} \frac{10 + \frac{9}{4}\Upsilon + \frac{7}{(r_z^*)^3} + \frac{1}{(r_z^*)^6} - \frac{1}{(r_z^*)^6}}{\left(10 + \frac{9}{4}\Upsilon + \frac{7}{(r_z^*)^3} + \frac{1}{(r_z^*)^6} \right)^{\frac{1}{2}} + \frac{1}{(r_z^*)^3}} \\ =& -\frac{3}{4} + \frac{1}{2} \frac{10 + \frac{9}{4}\Upsilon + \frac{7}{(r_z^*)^3}}{\left(10 + \frac{9}{4}\Upsilon + \frac{7}{(r_z^*)^3} + \frac{1}{(r_z^*)^6} \right)^{\frac{1}{2}} + \frac{1}{(r_z^*)^3}}, \end{aligned}$$

where $\Upsilon := \upsilon^2(4 - \upsilon^2)(\mu - \mu^2)$. Since

$$\lim_{r_z^* \to 0} \frac{10 + \frac{9}{4}\Upsilon + \frac{7}{(r_z^*)^3}}{\left(10 + \frac{9}{4}\Upsilon + \frac{7}{(r_z^*)^3} + \frac{1}{(r_z^*)^6} \right)^{\frac{1}{2}} + \frac{1}{(r_z^*)^3}} = \frac{7}{2},$$

we have that $\lim_{r_z^* \to 0} b^2 = -\frac{3}{4} + \frac{7}{4} = 1$, and so $b^2 \approx 1$ for $r_z^* \approx 0$, as in the case of Hektor. We obtain the following result:

Proposition 4.5.1. *Consider the equilibria on the z-axis. For $\mu \in (0, 1/2]$, Ω_{zz}, A and D are negative. Consequently, one pair of eigenvalues is purely imaginary, and the two other pairs of eigenvalues are complex conjugate, with the imaginary part close to $\pm i$ for $c_1 = c_2 = 0$ and for c_3 negative and sufficiently small. The linear stability is of center $\times$ complex-saddle type.*

Linear stability of the equilibria on the y-axis

The y-equilibrium points are of the form $(0, \pm r_y^*, 0)$, with

$$\lambda_1 (r_y^*)^5 - (r_y^*)^2 + 3c_3 = 0, \tag{4.70}$$

which yields

$$c_3 = \frac{(r_y^*)^2 - \lambda_1 (r_y^*)^5}{3}. \tag{4.71}$$

Evaluating Ω_{xx}, Ω_{yy}, Ω_{zz} at the equilibrium point yields:

$$\begin{aligned} \Omega_{xx} =& \lambda_2 - \frac{1}{(r_y^*)^3} + \frac{3c_3}{(r_y^*)^5}, \\ \Omega_{yy} =& \lambda_1 + \frac{2}{(r_y^*)^3} - \frac{12c_3}{(r_y^*)^5}, \\ \Omega_{zz} =& -1 - \frac{1}{(r_y^*)^3} + \frac{9c_3}{(r_y^*)^5}. \end{aligned} \tag{4.72}$$

Substituting c_3 from (4.71) we obtain

$$\begin{aligned} \Omega_{xx} =& \lambda_2 - \lambda_1, \\ \Omega_{yy} =& 5\lambda_1 - \frac{2}{(r_y^*)^3}, \\ \Omega_{zz} =& -1 - 3\lambda_1 + \frac{2}{(r_y^*)^3}, \end{aligned} \tag{4.73}$$

$$\begin{aligned} A &= 1 - 3\lambda_1 + \tfrac{2}{(r_y^*)^3} && = \tfrac{9d}{2} - \tfrac{7}{2} + \tfrac{2}{(r_y^*)^3}, \\ B &= (\lambda_2 - \lambda_1)\left(5\lambda_1 - \tfrac{2}{(r_y^*)^3}\right) && = (3d)\left(\tfrac{15}{2} - \tfrac{15d}{2} - \tfrac{2}{(r_y^*)^3}\right). \end{aligned} \tag{4.74}$$

Expanding r_y^* as a power series in the parameter c_3 as

$$r_y^* = r_{y0} + r_{y1}c_3 + O(c_3^2), \tag{4.75}$$

where $\pm r_{y0}$ is the position of the y-equilibrium in the case when $c_3 = 0$, which is given by $r_{y0}^3 = 1/\lambda_{10}$; this agrees with the result in [BGG15]. And we have the computation of r_{y1} yields

$$r_{y1} = \frac{-1 + (1/2)d_1 r_{y0}^5}{r_{y0}}, \tag{4.76}$$

with d_1 as in formula (4.68). We will also need to expand $\frac{1}{(r_y^*)^3}$ as a power series in the parameter c_3 as follows

$$\frac{1}{(r_y^*)^3} = \alpha + \beta c_3 + O(c_3^2). \tag{4.77}$$

A straightforward calculation yields

$$\begin{aligned} \alpha &= \frac{1}{r_{y0}^3}, \\ \beta &= -\frac{3r_{y1}}{r_{y0}^4}. \end{aligned} \tag{4.78}$$

Note that we have $d_0 = \frac{1}{2}$, $\lambda_{10} = \frac{3}{4}$, $d_1 = -m_3^{2/3}$, $r_{y0} = \left(\frac{4}{3}\right)^{1/3}$ for $\mu = 1/2$. It is easy to see that dominant part d_0 of d is a strictly decreasing function with respect to $\mu \in (0, 1/2]$ and takes values in $[1/2, 1)$. The dominant part λ_{10} of λ_1 is increasing with respect to $\mu \in (0, 1/2]$ and takes values in $(0, 3/4]$. Furthermore, the dominant part r_{y0} of r_y^* is a strictly decreasing function for $\mu \in (0, 1/2]$, where $r_{y0}(1/2) = \sqrt[3]{4/3}$ and $r_{y0} \to \infty$ when $\mu \to 0$. Consequently,the values of r_{y0} are in the interval $[\sqrt[3]{4/3}, \infty)$. From equation (4.72) we have

$$\begin{aligned} \Omega_{zz} &= -1 - \frac{1}{(r_y^*)^3} + \frac{9c_3}{(r_y^*)^5} \\ &= -\frac{1}{(r_y^*)^5}((r_y^*)^5 + (r_y^*)^2 - 9c_3) \\ &< 0 \end{aligned}$$

since $r_y^* > 0$ and c_3 is negative. Therefore, $\Omega_{zz} < 0$ for all admissible values of μ.

Using the formulas (4.66) and the expansions (4.67) and (4.77) and for $A = 4 - \Omega_{xx} -$

Ω_{yy}, we obtain

$$\begin{aligned} A &= 1 - 3\lambda_1 + \frac{2}{(r_y^*)^3} \\ &= 1 - 3\lambda_{10} + \frac{2}{(r_{y0})^3} + O(c_3) \\ &= 1 - 3\lambda_{10} + 2\lambda_{10} + O(c_3) \\ &> 0 \end{aligned}$$

for c_3 small. Similarly with the formulas (4.66) and the expansions (4.67) and (4.77) and for $B = \Omega_{xx}\Omega_{yy}$ using, we obtain

$$\begin{aligned} B &= (\lambda_2 - \lambda_1)\left(5\lambda_1 - \frac{2}{(r_y^*)^3}\right) \\ &= (3d)\left(\frac{15}{2} - \frac{15d}{2} - \frac{2}{(r_y^*)^3}\right) \\ &= (3d_0)\left(5\lambda_{10} - \frac{2}{r_{y0}^3}\right) + O(c_3) \\ &= (3d_0)\left(5\lambda_{10} - 2\lambda_{10}\right) + O(c_3) \\ &> 0 \end{aligned}$$

for c_3 small. Lastly, using the formulas (4.66) and the expansions (4.67) and (4.77) and for $D = A^2 - 4B$, we have

$$\begin{aligned} D &= \left(1 - 3\lambda_{10} + \frac{2}{r_{y0}^3}\right)^2 - 4(3d_0)\left(5\lambda_{10} - \frac{2}{r_{y0}^3}\right) + O(c_3) \\ &= (1 - \lambda_{10})^2 - 12(3 - 2\lambda_{10})\lambda_{10} + O(c_3). \end{aligned}$$

Note that we have $D \approx 1 + O(c_3)$ for $\mu \approx 0$ and we have $D = -\frac{215}{16} + O(c_3)$ for $\mu = 1/2$. By the intermediate value theorem and thus D changes its sign from positive to negative for $\mu \in (0, 1/2]$, provided c_3 is small. We have proved the following result:

Proposition 4.5.2. *Consider the equilibria on the y-axis. For $\mu \in (0, 1/2]$ for $c_1 = c_2 = 0$*

and for c_3 negative and sufficiently small, Ω_{zz} is always negative, the coefficients A and B are always positive, and the value of the discriminant D changes from positive to negative values. Consequently, one pair of eigenvalues is always purely imaginary, and there exists μ_*, depending on c_3, where the other two pairs of eigenvalues change from being purely imaginary to being complex conjugate. The linear stability changes from center $\times$ center $\times$ center type to center $\times$ complex-saddle type.

Linear stability of the equilibria on the x-axis

The x-equilibrium points are of the form $(\pm r_x^*, 0, 0)$, with

$$\lambda_2(r_x^*)^5 - (r_x^*)^2 + 3c_3 = 0, \tag{4.79}$$

which yields

$$c_3 = \frac{(r_x^*)^2 - \lambda_2(r_x^*)^5}{3}. \tag{4.80}$$

Evaluating Ω_{xx}, Ω_{yy}, Ω_{zz} at the equilibrium point yields:

$$\begin{aligned} \Omega_{xx} =& \lambda_2 + \frac{2}{(r_x^*)^3} - \frac{12c_3}{(r_x^*)^5}, \\ \Omega_{yy} =& \lambda_1 - \frac{1}{(r_x^*)^3} + \frac{3c_3}{(r_x^*)^5}, \\ \Omega_{zz} =& -1 - \frac{1}{(r_x^*)^3} + \frac{9c_3}{(r_x^*)^5}. \end{aligned} \tag{4.81}$$

Substituting c_3 from (4.80) we obtain

$$\begin{aligned} \Omega_{xx} =& 5\lambda_2 - \frac{2}{(r_x^*)^3}, \\ \Omega_{yy} =& \lambda_1 - \lambda_2, \\ \Omega_{zz} =& -1 - 3\lambda_2 + \frac{2}{(r_x^*)^3}, \end{aligned} \tag{4.82}$$

Expanding r_x^* as a power series in the parameter c_3 as

$$r_x^* = r_{x0} + r_{x1}c_3 + O(c_3^2), \tag{4.83}$$

where $\pm r_{x0}$ is the position of the x-equilibrium in the case when $c_3 = 0$, which is given by $r_{x0}^3 = 1/\lambda_{20}$ as in [BGG15]. With some computations, we have

$$r_{x1} = \frac{-1 - (1/2)d_1 r_{x0}^5}{r_{x0}}. \tag{4.84}$$

Next, we expand $\frac{1}{(r_x^*)^3}$ as a power series in the parameter c_3

$$\frac{1}{(r_x^*)^3} = \alpha' + \beta' c_3 + O(c_3^2), \tag{4.85}$$

and with a simple calculation, we have the expressions

$$\begin{aligned} \alpha' &= \frac{1}{r_{x0}^3}, \\ \beta' &= -\frac{3r_{x1}}{r_{x0}^4}. \end{aligned} \tag{4.86}$$

Consider the expression for Ω_{zz} in equation (4.81) we have

$$\begin{aligned} \Omega_{zz} &= -1 - \frac{1}{(r_x^*)^3} + \frac{9c_3}{(r_x^*)^5} \\ &= -\frac{1}{(r_x^*)^5}((r_x^*)^5 + (r_x^*)^2 - 9c_3) \\ &< 0 \end{aligned}$$

with $r_x^* > 0$ and $c_3 < 0$. Therefore, $\Omega_{zz} < 0$ for all admissible values of μ. Using the formula (4.66) and the expansions (4.67) and (4.85) and for $A = 4 - \Omega_{xx} - \Omega_{yy}$, we obtain

$$\begin{aligned} A &= 1 - 3\lambda_{20} + \frac{2}{(r_{x0})^3} + O(c_3) \\ &= 1 - \lambda_{20} + O(c_3) \\ &= -\frac{1}{2} - \frac{3}{2}d_0 + O(c_3) \\ &< 0 \end{aligned}$$

for c_3 small. Similarly sing the formula (4.66) and the expansions (4.67) and (4.85) and for $B = \Omega_{xx}\Omega_{yy}$, we obtain

$$\begin{aligned} B &= -(3d_0)\left(5\lambda_{20} - \frac{2}{r_{x0}^3}\right) + O(c_3) \\ &= -(3d_0)\left(5\lambda_{20} - 2\lambda_{20}\right) + O(c_3) \\ &= -9d_0\left(\frac{3}{2} + \frac{3}{2}d_0\right) \\ &< 0 \end{aligned}$$

for c_3 small.

Lastly, with the formula (4.66) and the expansions (4.67) and (4.85) and for $D = A^2 - 4B$, we have

$$\begin{aligned} D &= (1 - \lambda_{20})^2 + 36d_0\lambda_{20} + O(c_3) \\ &> 0. \end{aligned}$$

for c_3 small and thus we have proved the following result:

Proposition 4.5.3. *Consider the equilibria on the x-axis. For $\mu \in (0, 1/2]$, for $c_1 = c_2 = 0$ and for c_3 negative and sufficiently small, Ω_{zz} is negative, A and B are negative, and the value of the discriminant D is always positive. Consequently, two pairs of eigenvalues are purely imaginary, and one pair of eigenvalues are real (one positive and one negative). The linear stability is of center $\times$ center $\times$ saddle type.*

4.6 Non-linear Stability

Recall that, in the case of the Sun-Jupiter-Hektor system, as well as for $c_1 = c_2 = 0$ and c_3 sufficiently small, the linear stability of the $x-$equilibria is of center-center-saddle type, the linear stability of the $y-$equilibria is of the center-center-center type (for μ less than some critical value μ_c), and the linear stability of the $z-$equilibria is of the center-complex saddle type. See Sections 4.5.2 and 4.5.3. We now discuss the non-linear stability.

4.6.1 The $x-$equilibria

The eigenvalues of the linearization of the $x-$equilibria are of the form $\pm\lambda$, $\pm i\omega_1$ and $\pm i\omega_2$. We can use the Lyapunov center theorem as shown below to conclude the existence of some families of periodic orbits near these points.

Theorem 4.6.1 (Lyapunov Center Theorem)**.** *[Eas93] Assume that H is a Hamiltonian function with associated Hamiltonian system:*

$$\dot{x} = J\nabla H(x),\ x \in \mathbb{R}^{2n}. \tag{4.87}$$

Assume that the system has an equilibrium point with exponents $\pm\lambda_1$, $\pm\lambda_2$, ..., $\pm\lambda_n$, where $\pm\lambda_1 = \pm i\omega \neq 0$ is pure imaginary. Assume that none of the ratios $\frac{\lambda_2}{\lambda_1}$, $\frac{\lambda_3}{\lambda_1}$,..., $\frac{\lambda_n}{\lambda_1}$ is an integer. Then there exists a one-parameter family of periodic solutions emanating from the equilibrium point, whose periods tend to $\frac{2\pi}{\omega}$ when approaching the equilibrium point along the family.

In our case we have two imaginary frequencies $\pm i\omega_1$, $\pm i\omega_2$ and one pair of real eigenvalues $\pm\lambda$. It follows that, unless $\frac{\omega_2}{\omega_1}$ is an integer, then there must exist two families of periodic orbits, a 'planar' family of Lyapunov orbits and a 'vertical' family of Lyapunov orbits. An example of a planar Lyapunov orbit is shown in Figure 4.5.

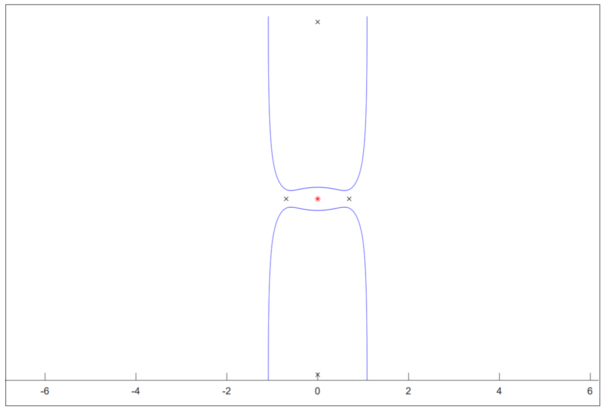

Figure 4.4: Zero velocity curves bounding the Hill regions.

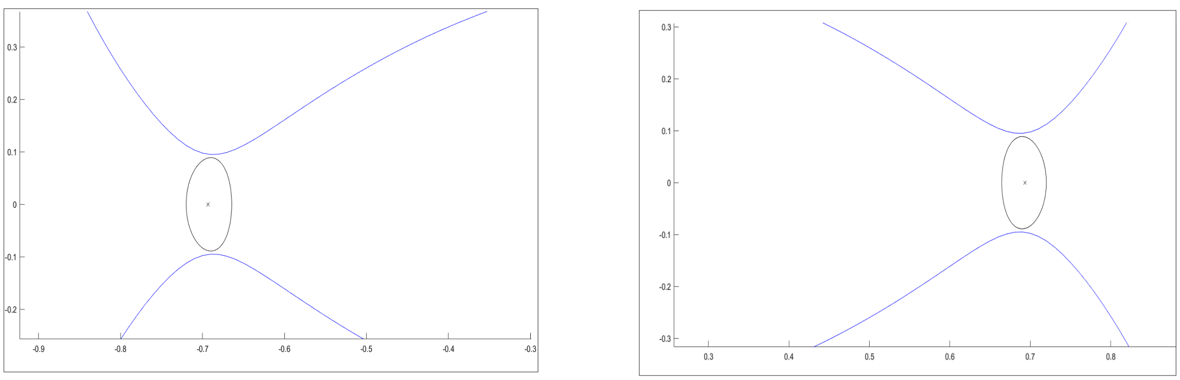

(a) Around the negative $x-$ equilibria. (b) Around the positive $x-$ equilibria.

Figure 4.5: Planar Lyapunov orbits around the $x-$ equilibria.

Theorem 4.6.2 (Center Manifold Theorem)**.** *[Mei07] Suppose that f is a C^k vector field, $k \geqslant 1$, with a fixed point at the origin. Let the eigenspaces of $Df(0) = A$ be written $E^u \bigoplus E^c \bigoplus E^s$. Then there is a neighborhood of the origin in where there exist C^k invariant manifolds: the local stable manifold, W^s_{loc}, tangent to E^s, on which $|x(t)| \to 0$ as $t \to \infty$, the local unstable manifold W^u_{loc}, tangent to E^u, on which $|x(t)| \to 0$ as $t \to -\infty$, and a local center manifold W^c, tangent to E^c.*

Moreover, we can invoke the Center Manifold Theorem to establish the existence of a $4-$dimensional center manifold that is tangent to the vector space spanned by the eigenvectors corresponding to $\pm i\omega_1$, $\pm i\omega_2$. Sufficiently close to the equilibrium point, we can find a Cantor families of 2−dimensional tori whose frequencies approach ω_1 and ω_2 when approaching the equilibrium point. The existence of these families of tori follows from the KAM Theorem (for instance, [JV97] and [Cel10]). Due to the real eigenvalues $\pm\lambda$, the Lyapunov orbits have 2−dimensional stable and unstable manifolds, and the 2−dimensional tori have 3−dimensional stable and unstable manifolds. Thus, the x−equilibrium points are unstable. Each of the stable and unstable manifolds have branches inside the region of the tertiary (i.e., towards Hektor), as well as the branches in the exterior region (i.e.,towards the Sun and Jupiter). See Figure 4.6 and 4.7.

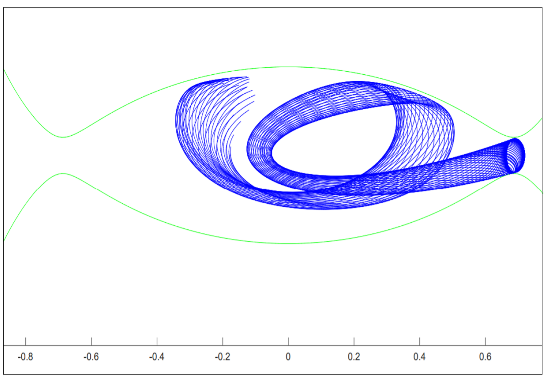

(a) Inside the region.

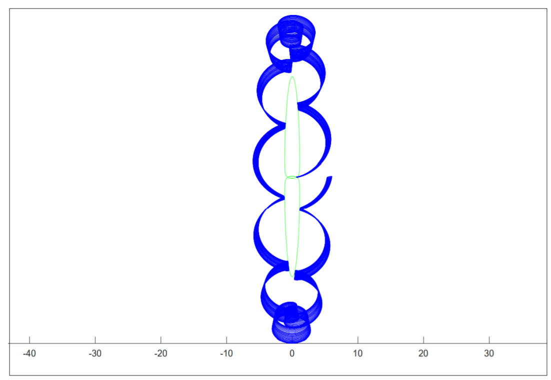

(b) Outside the region.

Figure 4.6: Projection of the stable manifold on the xy−plane, and projections of the zero velocity surface.

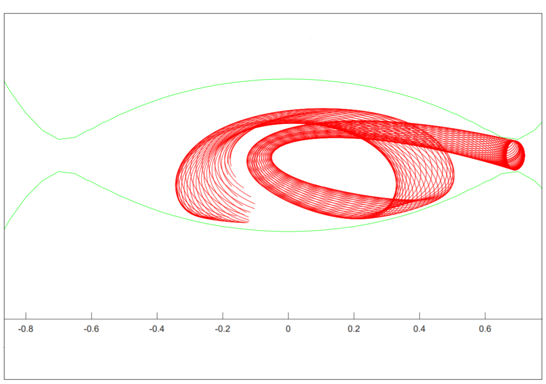

(a) Inside the region.

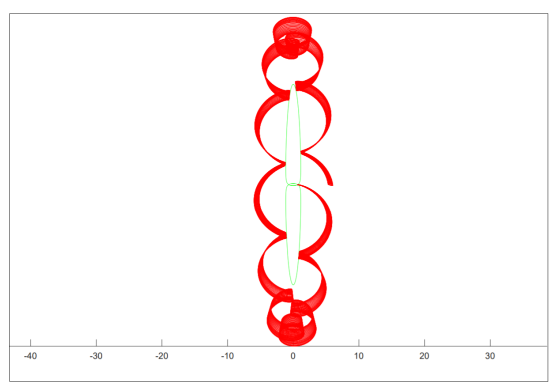

(b) Outside the region.

Figure 4.7: Projection of the unstable manifold on the xy−plane.

The projection of these stable and unstable manifolds onto the $xy-$plane are confined by the Hill regions. The Hill region as shown in Figure 4.4 represents the projection of the energy manifold $\{H = h\}$ onto the configuration space. The boundary of the Hill region is the zero velocity surface. We observe the exterior branches of the stable and unstable manifolds go around the Hill regions. Based on the numerical experiments, we expect the existence of transverse homoclinic connection for each of the equilibrium points, as well as of the transverse heteroclinic connections between the two equilibrium points. By the Smale Birkhoff Theorem [Bel18], the existence of transverse homoclinic and heteroclinic connections implies the existence of chaotic dynamics (symbolic dynamics). In practical applications, the stable and unstable manifolds of periodic orbits or of invariant tori can be used to design spacescraft trajectories that come from the exterior region, enter the interior region and orbit around it for some number of turns, and then leave the interir region and return to the exterior region. Such trajectories require low energy. For references to applications of invariant manifolds to space mission design see [Bel18], [PA13].

4.6.2 The $y-$equilibria

The eigenvalues of the linearized system at the $y-$equilibria are of the form $\pm i\omega_1$, $\pm i\omega_2$ and $\pm i\omega_3$ (for μ sufficiently small). The KAM Theorem can be used to show the existence of Cantor families of $3-$dimensional tori in a vicinity of these equilibrium points. These tori are filled with quasi-periodic orbits. An example of a quasi-periodic orbit is shown in Figure 4.8. We note that in the spatial problem, the existence of the $3-$dimensional KAM tori does not imply stability. This is because the energy manifold is $5-$dimensional (in the $6-$dimensional phase space), and the $3-$dimensional tori do not separate the $5-$dimensional energy manifold into disjoint connected components. In the planar case, the KAM tori are $2-$dimensional and the energy manifold is $3-$dimensional (in the $4-$dimensional phase space). In this case the existence of $2-$dimensional KAM tori implies stability.

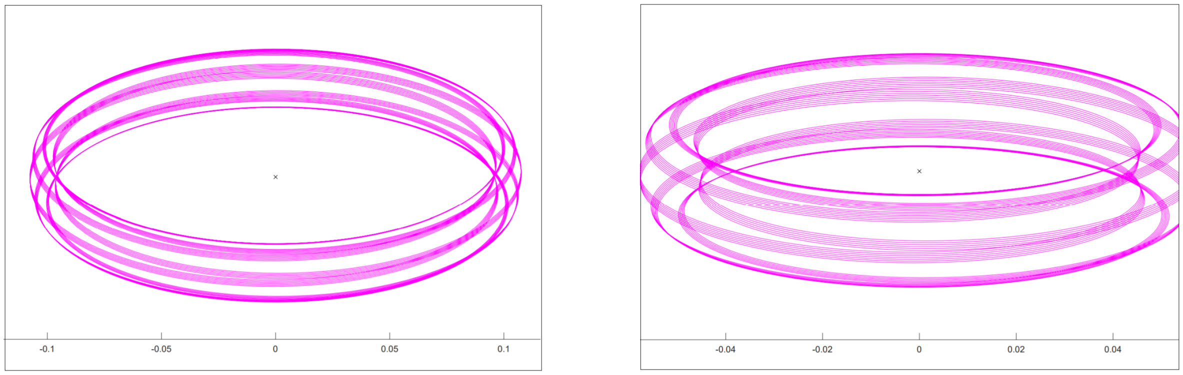

Figure 4.8: Quasi-periodic orbits around the $y-$equilibria.

4.6.3 The $z-$ equilibria

The eigenvalues of the linearized system of the $z-$equilibria are of the form $\pm i\omega$, and $\pm\alpha \pm i\beta$. We can invoke again the Lyapunov Center Theorem to assert the existence of a family of periodic orbits near each equilibrium point. Each periodic orbit has $3-$dimensional stable and unstable manifolds. Thus, these equilibrium points are unstable. One problem that requires future investigation is the existence of transverse homoclinic and heteroclinic connections associated to these manifolds. An example of an orbit in the neighborhood of one of the $z-$equilibrium points is shown in Figure 4.9 and 4.10.

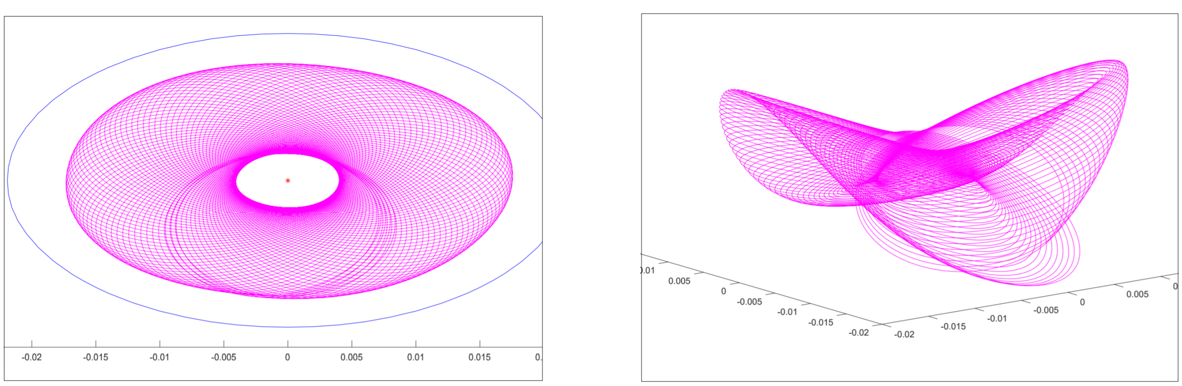

(a) Viewing from above, i.e. in 2D. (b) In 3D.

Figure 4.9: Example of an orbit in the neighborhood of $z-$equilibrium.

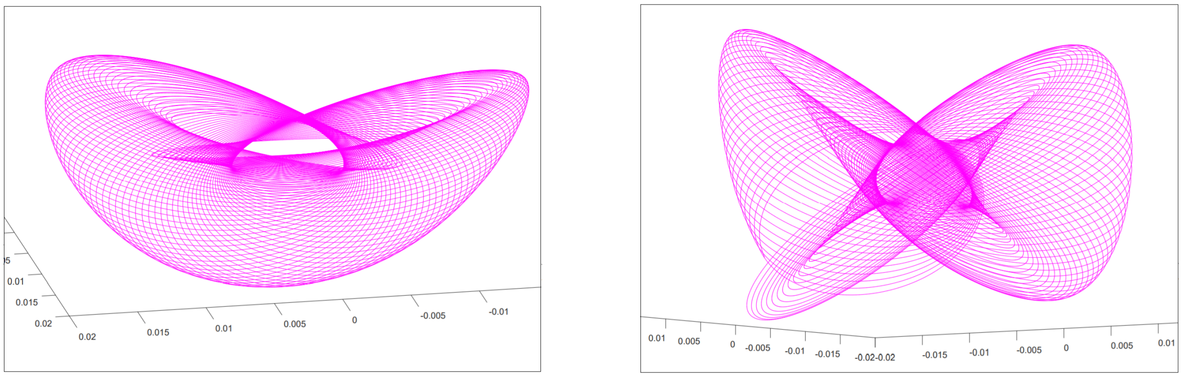

Figure 4.10: Three-dimentional views of an orbit in the neighborhood of $z-$equilibrium.

4.7 Existence of 'out-of plane' equilibria

The existence of 'out-of-plane' equilibria near an oblate asteroid does not agree with the physical intuition. The z-equilibrium points found in Section 4.5.2 is one of the examples of 'out-of-plane' equilibria since it seems that the combined gravitational force acting on the infinitesimal mass must be pointing towards the plane of $z = 0$. Such kind of 'out-of-plane' equilibria appear due to the J_2-approximation of the gravitational potential. The J_2-approximation refers to a truncation of the spherical harmonic series expansion of the gravitational potential. Such expansion is known to be convergent outside the Brillouin sphere, which is the smallest sphere that contains the body. However, in general the nature of the series within the Brillouin sphere is unknown in general. For certain shapes, such as ellipsoids, the series is divergent inside the Brillouin sphere. The paper [WWZ18] shows analytically that for a restricted three-body problem with one primary as a rotational ellipsoid,'out-of-plane' equilibrium points do not physically exist. They further note that the same conclusion can be drawn if both primary and secondary are rotational ellipsoids. We note that their argument can also be carried out for the Hill four-body problem with the three heavy bodies as rotational ellipsoids. However we shall remark that for non-convex shapes, 'out-of-plane' equilibria are physically possible. Here in this section we show a 'rubble pile'-model which has true 'out-of-plane' equilibria.

The model consists of six balls— four identical larger balls of radius R and two identical smaller balls of radius r. They are arranged as in the left-side of Fig. 4.11. The centers of the larger and smaller balls are at $(\pm 1, 0, \pm R)$ and $(\pm r, 0, 0)$ respectively. The condition that the balls in the configuration are tangent is $r = 1/(2(1 + R))$. With numerical integration, we compute the gravitational force along the $z-$axis and plot as in the right side of Fig. 4.11. In the plot, the intersections of the graph and the horizontal axis correspond to the z-values of the 'out-of-plane' equilibria. Note that such 'out-of-plane' equilibria exist only for certain ranges of values of R, and disappear through a saddle-node bifurcation. We plan to study families of such configurations in future works;

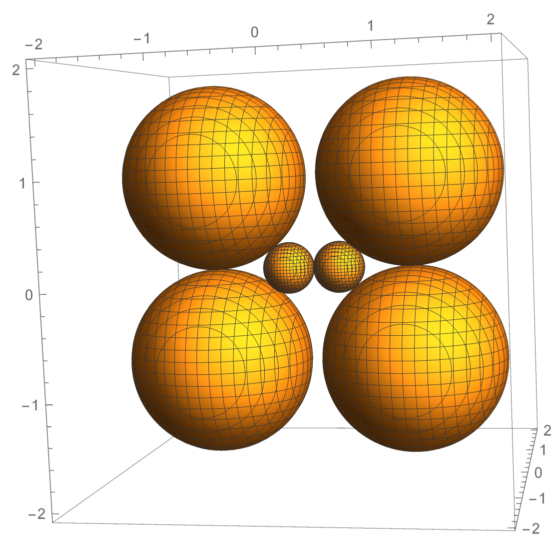

(a) Six-balls 'rubble-pile' model.

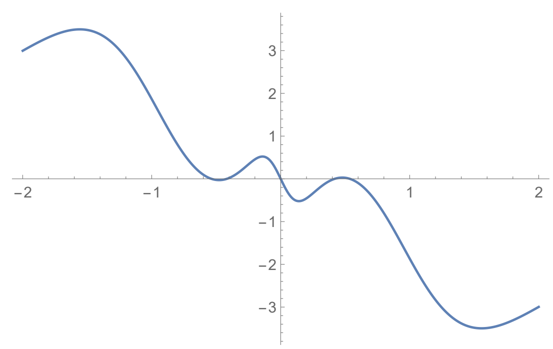

(b) The gravitational force along the z-axis.

Figure 4.11: Example model for existence of 'out-of plane' equilibria.

many small bodies in the solar system are believed to be formed as 'rubble piles', consisting of smaller elements separated by voids. Therefore, many known asteroids are observed to have very irregular shapes. With possible applications to space missions that target asteroids, the study of 'out-of-plane' equilibria for asteroids become an interesting problem.

4.8 Conclusions

In this chapter we consider a Hill four-body problem with oblate bodies and develop a rigorous mathematical model for the problem that can be used for analytical studies. In Chapter 3 we study and determine the triangular central configurations of three-body problem with different conditions. In particular, we study and determine the triangular central configurations of three-body problem with oblateness in Section 3.2. In Proposition 3.2.1 we determined the triangular central configurations of three oblate bodies to be scalene triangles. Moreover, the triangles corresponding to different moments of inertia are not necessarily similar to one another. This situation is very different from the case of having three point-masses, that the central configurations are equilateral triangles. Assuming that the three heavy bodies are in such a scalene triangular central configurations, we begin with the spatial circular restricted four-body problem with three oblate bodies and perform the Hill approximation. Our Hill approximation and result in Theorem 4.4.1 are different from the one in the case of three point-masses, due to the different type of triangular central configuration and of the oblateness effects. The Hill approximation acts like a 'magnifying glass' to 'zoom' into a neighborhood of the smallest body, by sending the two larger bodies at infinite distance via a limiting procedure. The resulting Hamiltonian encounter the effect of the two larger bodies is represented in the Hamiltonian by a quadratic polynomial, while in the restricted four-body problem their effect is represented by singular terms. The Hamiltonian resulted from the Hill approximation provides us a simpler form that allows us to study the equilibrium points and their stability analytically, as in Proposition 4.5.1, Proposition 4.5.3, and Proposition 4.5.2. Contrarily, in the restricted four-body problem it is only possible to have such a study numerically. An interesting result of our model is the presence of 'out-of-plane' equilibria. These may be physically possible only when they are very close to the barycenter of the smallest body, and only for certain shapes. At the end of this chapter in Section 4.7 we further describe a toy-model that has true ‘out-of-plane’ equilibria.

Chapter 5

Gravitational Potential for Dumb-bell shaped Body

According to the observational data, mostly optical, the shape of asteroid is typically non-spherical. The Jupiter's Trojan 624 Hektor is one example; it can be well approximated by a dumb-bell shape [MBW$^+$06], which can be well approximated by explicit functions. In the context of the n-body problem [Taf85], the gravitational field of a homogeneous celestial object is usually described as a a multipolar expansion naturally involving spherical coordinates [Kau66]. In this thesis we describe the shape in terms of cylindrical coordinates instead and we make use of Bessel and Elliptic Functions to express the gravitational potential generated by the rotating body as a simple formula in terms of elliptic integrals. This chapter is devoted to provide an overview of Bessel Functions, Elliptic Integrals as well as the applications of variational principle to the gravitational potential for a body with any shape in cylindrical coordinate system.

5.1 Background

5.1.1 Bessel Functions of the First Kind

In this section, we consider a class of functions known as Bessel functions [BDVV+04], which are the canonical solutions of the Bessel's differential equation,

$$x^2\frac{d^2y}{dx^2}+x\frac{dy}{dx}+(x^2-\alpha^2)y=0 \tag{5.1}$$

for an arbitrary complex number α, which refers as the order of the Bessel function. With order α as integers, the Bessel functions are known as the cylindrical functions or cylindrical harmonics since they are the solutions to the Laplace's equation in cylindrical coordinates (s,ϕ,z), that is,

$$\bigtriangledown^2 V=\frac{1}{s}\frac{\partial}{\partial s}(s\frac{\partial V}{\partial s})+\frac{1}{s^2}\frac{\partial^2 V}{\partial \phi^2}+\frac{\partial^2 V}{\partial z^2}=0. \tag{5.2}$$

Consider the following generating function with complex variables t and z

$$g(z,t)=e^{\frac{1}{2}z(t-\frac{1}{t})} \qquad \forall z,t\neq 0$$

expanded by the Laurent's theorem in a series with both positive and negative powers of t. Denote the coefficient of t^n for $n\in\mathbb{Z}$ by $J_n(z)$. Then we obtain

$$\begin{aligned} e^{\frac{1}{2}z(t-\frac{1}{t})} &= \sum_{n=-\infty}^{\infty} J_n(z)t^n \\ &= \cdots + J_{-1}(z)t^{-1}+J_1(z)t+J_2(z)t^2+J_3(z)t^3+\cdots, \end{aligned} \tag{5.3}$$

where

$$J_n(z)=\frac{1}{2\pi i}\int_C u^{-n-1}e^{\frac{1}{2}z(u-\frac{1}{u})}du$$

and C represents the contour as an unit circle enclosing the origin.

Definition 5.1.1 (Bessel coefficient)**.** The Bessel coefficient of order $n \in \mathbb{Z}$, denoted as $J_n(z)$ is given by

$$J_n(z) = \frac{1}{2\pi i}(\frac{z}{2})^n \int_C u^{-n-1} e^{u-\frac{z^2}{4u}} du,$$

where C is any closed contour encircling the origin once counterclockwise.

Let $u = \frac{2t}{z}$, we can easily express $J_n(z)$ as a power series in z as

$$J_n(z) = \frac{1}{2\pi i}(\frac{z}{2})^n \int_C t^{-n-1} e^{t-\frac{z^2}{4t}} dt. \tag{5.4}$$

We can further expand the exponential function in the integrand as a power series of z as follows:

$$\begin{aligned} J_n(z) &= \frac{1}{2\pi i}\left(\frac{z}{2}\right)^n \int_C t^{-n-1} e^t e^{-(\frac{z}{2\sqrt{t}})^2} dt \\ &= \frac{1}{2\pi i}(\frac{z}{2})^n \int_C t^{-n-1} e^t \sum_{r=0}^{\infty} (-1)^r \frac{(\frac{z}{2\sqrt{t}})^{2r}}{r!} dt. \end{aligned} \tag{5.5}$$

With the contour C as an unit circle centered at origin, in which the integrand is uniformly convergent [AW99], we have

$$J_n(z) = \frac{1}{2\pi i} \sum_{r=0}^{\infty} (\frac{z}{2})^{n+2r} \frac{(-1)^r}{r!} \int_C t^{-n-1-r} e^t dt \tag{5.6}$$

Let $f(t) = \frac{e^t}{t^{n+1+r}}$. Since the contour is a positively oriented simple closed curve in the complex plane and f is analytic except for $t = 0$, then by the Residue Theorem we have

$$\int_C f(t)dt = 2\pi i \sum_{k=1}^{n} Res(f, t_k). \tag{5.7}$$

At $t = 0$, the residue of $f(t)$ is

$$Res(f, t_k) = \begin{cases} \frac{1}{(n+r)!} & \text{if } n + r \geqslant 0 \text{ and } n + r \in \mathbb{Z} \\ 0 & \text{if } n + r < 0 \text{ and } n + r \in \mathbb{Z}. \end{cases} \tag{5.8}$$

Therefore, if $n \geqslant 0$ and $n \in \mathbb{Z}$, we have

$$J_n(z) = \sum_{r=0}^{\infty} \frac{(-1)^r (\frac{z}{r})^{n+2r}}{r!(n+r)!}. \tag{5.9}$$

Definition 5.1.2 (Bessel function of the first kind with order of positive integer)**.** The Bessel function of the first kind with order $n \in \mathbb{Z}$ and $n \geqslant 0$ is defined by the equation

$$J_n(z) = (\frac{z}{2})^n \sum_{r=0}^{\infty} \frac{(-1)^r}{r!\Gamma(n+r+1)} (\frac{z}{2})^{2r}.$$

By an index shift, we can easily extend the expansion of $J_n(z)$ for having the order n as a negative integer, say $-m$, then

$$\begin{aligned} J_{-m}(z) &= \sum_{r=m}^{\infty} \frac{(-1)^r (\frac{z}{2})^{2r-m}}{r!(r-m)!} \\ &= \sum_{s=0}^{\infty} \frac{(-1)^{m+s} (\frac{z}{s})^{m+2s}}{(m+s)!s!}. \end{aligned} \tag{5.10}$$

Thus, $J_n(z) = (-1)^m J_m(z)$. By the above definition, we may show that $J_n(z)$ is a solution of the linear differential equation (5.2) in variable z. Dividing the equation by z^2, we have

$$\frac{d^2y}{dz^2} + \frac{1}{z}\frac{dy}{dz} + (1 - \frac{n^2}{z^2})y = 0, \tag{5.11}$$

which is known as the Bessel's equation for functions of integer order n. Since $J_n(z)$ possesses a Riemann integral with respect to t and note that $\frac{\partial f}{\partial z}$ of the function $f(t) = t^{-n-1}e^{t-\frac{z^2}{4t}}$ is continuous for both variables z and t, we carry out the following differentiations with respect to z:

$$\begin{aligned}&\frac{1}{z}\frac{d}{dz}J_n(z)\\=&\frac{1}{z}\frac{n}{2\pi i}\frac{z^{n-1}}{z^n}\int_C t^{-n-1}e^{(t-\frac{z^2}{4t})}dt+\frac{1}{z}\frac{1}{2\pi i}\frac{z^n}{2^n}\int_C t^{-n-1}e^{(t-\frac{z^2}{4t})}(-\frac{2z}{4t})dt\end{aligned}\tag{5.12}$$

and

$$\begin{aligned}&\frac{d^2}{dz^2}J_n(z)\\=&\frac{1}{2\pi i}\frac{n(n-1)z^{n-2}}{2^n}\int_C t^{-n-1}e^{(t-\frac{z^2}{4t})}dt+\frac{1}{2\pi i}\frac{nz^{n-1}}{2^n}\int_C t^{-n-1}e^{t-\frac{z^2}{4t}}(-\frac{2z}{4t})dt\\&+\frac{1}{2\pi i}\frac{nz^{n-1}}{2^n}\int_C t^{-n-1}e^{t-\frac{z^2}{4t}}(-\frac{2z}{4t})dt+\frac{1}{2\pi i}(\frac{z}{2})^n\int_C t^{-n-1}e^{t-\frac{z^2}{4t}}(-\frac{2z}{4t})^2dt\\&+\frac{1}{2\pi i}(\frac{z}{2})^n\int_C t^{-n-1}e^{t-\frac{z^2}{4t}}(-\frac{2z}{4t})dt\end{aligned}\tag{5.13}$$

while we have

$$\begin{aligned}&(1-\frac{n^2}{z^2})J_n(z)\\=&\frac{1}{2\pi i}(\frac{z}{2})^n\int_C t^{-n-1}e^{(t-\frac{z^2}{4t})}dt-\frac{n^2}{2\pi i}\frac{z^{n-2}}{2^n}\int_C t^{-n-1}e^{(t-\frac{z^2}{4t})}dt.\end{aligned}\tag{5.14}$$

Thus,

$$\begin{aligned}&\frac{d^2J_n(z)}{dz^2}+\frac{1}{z}\frac{dJ_n(z)}{dz}+(1-\frac{n^2}{z^2})J_n(z)\\=&\frac{1}{2\pi i}(\frac{z}{2})^n\int_C t^{-n-1}(1-\frac{n+1}{t}+\frac{z^2}{4t^2})e^{(t-\frac{z^2}{4t})}dt\\=&\frac{1}{2\pi i}(\frac{z}{2})^n\int_C\frac{d}{dt}(t^{-n-1}e^{(t-\frac{z^2}{4t})})dt\\=&0\end{aligned}\tag{5.15}$$

since $t^{-n-1}e^{(t-\frac{z^2}{4t})}$ is one-valued. We have proved that

$$\frac{d^2J_n(z)}{dz^2}+\frac{1}{z}\frac{dJ_n(z)}{dz}+(1-\frac{n^2}{z^2})J_n(z)=0\tag{5.16}$$

In fact, it is not necessary to have n as an integer for the solution of the Bessel's equation. In order to extend the definition of $J_n(z)$ to the case for n being any number, real or complex, we will need the following definitions.

Definition 5.1.3 (Euler's Gamma Function)**.** Euler's expression of the Gamma's function $\Gamma(z)$ as an infinite integral is defined by

$$\Gamma(z) = \int_0^{\infty} t^{z-1}e^{-t}dt$$

for $t \in \mathbb{C}$ and $\mathbf{Re}(z) > 0$.

Definition 5.1.4 (Hankel's Gamma Function)**.** Hankel's expression of the Gamma's function $\Gamma(z)$ as a contour integral is defined by

$$\frac{1}{\Gamma(z)} = \frac{i}{2\pi}\int_C (-t)^{-z}e^{-t}dt$$

where C is the path starts at 'infinity' on the real axis, encircles the origin in the positive direction and returns to the starting point. That is,

$$\frac{1}{\Gamma(z)} = \frac{i}{2\pi}\int_{\infty}^{(0+)} (-t)^{-z}e^{-t}dt.$$

where $(0+)$ represents the positively oriented path that encircles the origin.

As shown before in equations (5.12), (5.13) and (5.14), for all values of n, the equation (5.16) is satisfied by the integral of the form

$$y = z^n\int_C t^{-n-1}e^{t-\frac{z^2}{4t}}dt$$

provided that the integrand resumes its initial value after following the contour C and that differentiation under the sign of integration are justified [WW02]. And thus we have extended $J_n(z)$ as

$$J_n(z) = \frac{1}{2\pi i}(\frac{z}{2})^n \int_{\infty}^{(0+)} t^{-n-1} e^{(t-\frac{z^2}{4t})} dt, \tag{5.17}$$

provided that there is a branch point at $z = 0$. The principal branch of $J_n(z)$ is given by the principal value of $\left(\frac{z}{2}\right)^n$ and is analytic in the $z-$ plane along the interval $(-\infty, 0]$. Similarly, we can express the integral (5.17) as a power series and notice that it is an analytic function of z. Again, we may obtain the coefficients from the Taylor's series in the powers of z by differentiating under the sign of integration. That is, $J_n(z)$ can be expressed in terms of Gamma functions as [Kre09]

$$\begin{aligned} J_n(z) =& \frac{1}{2\pi i}(\frac{z}{2})^n \sum_{r=0}^{\infty} \frac{(-1)^r}{r!}(\frac{z}{2})^{2r} \int_{-\infty}^{(0+)} e^t t^{-n-r-1} dt \\ =& \sum_{r=0}^{\infty} \frac{(-1)^r}{r!}(\frac{z}{2})^{n+2r} \frac{1}{\Gamma(n+r+1)} \end{aligned} \tag{5.18}$$

for any general values of n.

Definition 5.1.5 (Bessel function of the first kind with order of any general number)**.** The Bessel function of the first kind with order n is defined by the equation

$$J_n(z) = (\frac{z}{2})^n \sum_{r=0}^{\infty} \frac{(-1)^r}{r!\Gamma(n+r+1)}(\frac{z}{2})^{2r}.$$

This function $J_n(z)$, which is known as Bessel function of the first kind, reduces to a Bessel coefficient when n is an integer. In general, Bessel functions of the first kind, denoted as $J_n(x)$ are the solutions of Bessel's differential equation (5.1). The functions $J_n(x)$ are finite at the origin (i.e. $x = 0$) for integer or positive order n and diverge as $x \to 0$ for negative or non-integer n. To obtain the recurrance relationsip of Bessel's fucntion, we consider the following derivative [Kre09]

$$\begin{aligned}
\frac{d}{dz}\left[z^{-s}J_s(z)\right] &= \frac{1}{2^s}\frac{d}{dz}\sum_{k=0}^{\infty}\frac{(-1)^k}{k!\Gamma(s+k+1)}\left(\frac{z}{2}\right)^{2k} \\
&= \frac{1}{2^s}\sum_{k=1}^{\infty}\frac{(-1)^k}{k!\Gamma(s+k+1)}2k\left(\frac{z}{4}\right)\left(\frac{z}{2}\right)^{2(k-1)} \\
&= -\frac{z}{2^{s+1}}\sum_{k=0}^{\infty}\frac{(-1)^k}{k!\Gamma(s+k+2)}\left(\frac{z}{2}\right)^{2k}.
\end{aligned} \tag{5.19}$$

Multiplying the equation by z^s, we obtain

$$z^s\frac{d}{dz}\left[z^{-s}J_s(z)\right] = -J_{s+1}(z) \tag{5.20}$$

or

$$\begin{aligned}
J_{s+1}(z) &= \frac{s}{z}J_s(z) - J_s'(z) \\
\implies J_s'(z) &= \frac{s}{z}J_s(z) - J_{s+1}(z).
\end{aligned} \tag{5.21}$$

The following plot shows $J_n(x)$ for $n = 0, 1, 2, 3, ..., 10$.

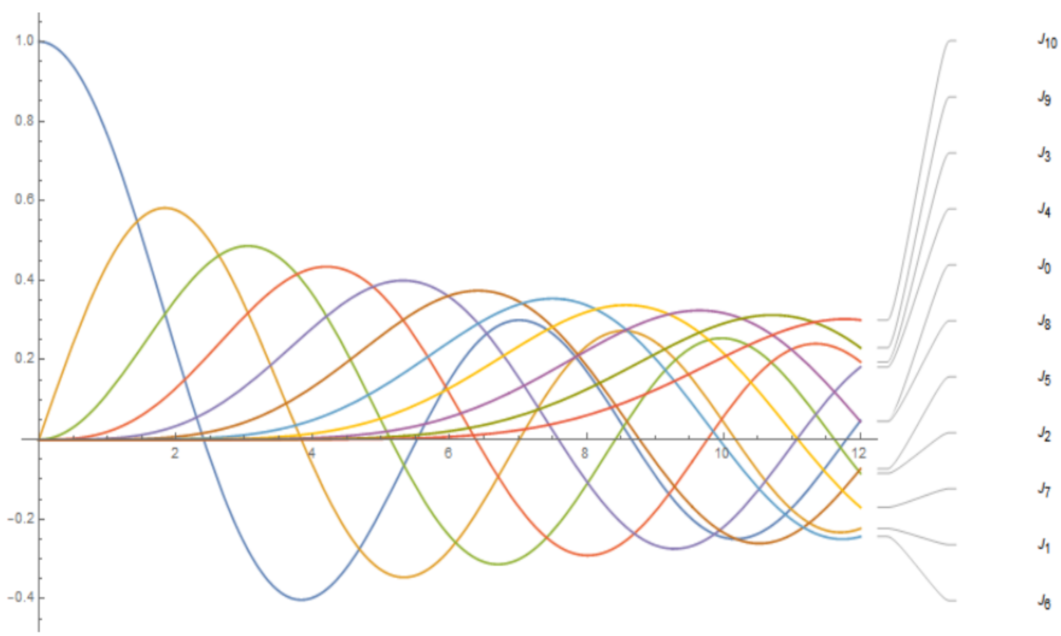

Figure 5.1: Bessel functions of the first kind.

5.1.2 Elliptical Integrals

Let $R(x, y)$ be a rational function of x and y, the integral

$$\int R(x, y)dx$$

can be evaluated in terms of elementary functions of the form $y = \sqrt{ax + b}$ or $y = \sqrt{ax^2 + bx + c}$ [Hal95]. However, the integral is not easy to evaluate when y^2 is a cubic or quartic polynomial. This difficulty leads to the following definition.

Definition 5.1.6 (Elliptic Integral)**.** Let $R(x, y)$ be a rational function of x and y such that y^2 is a cubic or quartic polynomial of x (i.e. $y^2 = ax^3 + bx^2 + cx + d$ or $y^2 = ax^4 + bx^3 + cx^2 + dx + e$). Then the integral

$$\int R(x, y)dx$$

is called an elliptic integral.

Elliptical integrals were originally investigated in the study of arc length of ellipses and they can be considered as generalizations of inverse trigonometric functions. The general form of an elliptic integral is written as

$$f(x) = \int \frac{A(x) + B(x)}{C(x) + D(x)\sqrt{S(x)}}dx, \tag{5.22}$$

where $A(x)$, $B(x)$, $C(x)$ and $D(x)$ are polynomials in x and $S(x)$ is a polynomial of degree 3 or 4. In this section, we are going to provide an overview of the elliptic integrals of the first, second and third kind. In Legendre's notation, we have the following definitions [BF13].

Definition 5.1.7 (Elliptic Integral of the first kind)**.** Let the modulus k be such that

$0 < k^2 < 1$. The incomplete elliptic integral of the first kind is defined as

$$K(\phi, k) = \int_0^\phi \frac{d\theta}{\sqrt{1 - k^2 \sin^2 \theta}}.$$

Definition 5.1.8 (Elliptic Integral of the second kind)**.** Let the modulus k be such that $0 < k^2 < 1$. The incomplete elliptic integral of the second kind is defined as

$$E(\phi, k) = \int_0^\phi \sqrt{1 - k^2 \sin^2 \theta} d\theta.$$

Definition 5.1.9 (Elliptic Integral of the third kind)**.** Let the modulus k be such that $0 < k^2 < 1$. The incomplete elliptic integral of the third kind is defined as

$$\Pi(\phi, n, k) = \int_0^\phi \frac{d\theta}{(1 + n \sin^2 \theta)\sqrt{1 - k^2 \sin^2 \theta}}.$$

Substituting $x = \sin \theta$, the above elliptic integrals take the Jacobi's form as

$$\begin{aligned}
&\text{The frist kind: } K(x, k) = \int_0^x \frac{dx}{\sqrt{(1 - x^2)(1 - k^2 x^2)}} \\
&\text{The second kind: } E(x, k) = \int_0^x \sqrt{\frac{1 - k^2 x^2}{1 - x^2}} dx \\
&\text{The third kind: } \Pi(x, n, k) = \int_0^x \frac{dx}{(1 + n x^2)\sqrt{(1 - x^2)(1 - k^2 x^2)}}.
\end{aligned} \tag{5.23}$$

Notice that the above elliptic integrals are referred as complete when $\phi = \frac{\pi}{2}$ in the Legendre's notation or $x = 1$ in the Jacobi's form.

The complete elliptic integral of the first kind in fact arises the problem of simple pendulum [Hal95]. Consider finding the period of a pendulum without the small angle assumption. Let L be the length of the pendulum, g be the gravitational acceleration, and θ be the angle of the displacement of the pendulum from the vertical axis. The motion of the pendulum is governed by the differential equation

$$\theta'' = -\frac{g}{L}\sin\theta(t). \tag{5.24}$$

Writing the equation in the Hamiltonian form, we note that the above equation integrates and yields

$$\frac{1}{2}(\theta')^2 - \frac{g}{L}\cos\theta = C, \tag{5.25}$$

where C is a constant. Assume the pendulum has a maximal displacement of angle α such that $\theta'(\alpha) = 0$ so that we have

$$\frac{1}{2}\theta'^2 = \frac{g}{L}(\cos\theta - \cos\alpha),$$

and thus

$$\theta' = \pm\frac{g}{L}\sqrt{2(\cos\theta - \cos\alpha)}.$$

Taking the positive value and integrate, we obtain

$$\begin{aligned} \frac{g}{L}t &= \int_0^\theta \frac{d\phi}{\sqrt{2(\cos\phi - \cos\alpha)}} \\ &= \frac{1}{2}\int_0^\theta \frac{d\phi}{\sqrt{\sin^2\frac{\alpha}{2} - \sin^2\frac{\phi}{2}}}. \end{aligned} \tag{5.26}$$

With the substitution of

$$x = \frac{\sin\frac{\phi}{2}}{\sin\frac{\alpha}{2}}, \quad \rho = \frac{\sin\frac{\theta}{2}}{\sin\frac{\alpha}{2}}, \quad k = \sin\tfrac{\alpha}{2} \in [0, 1) \tag{5.27}$$

we obtain

$$\sqrt{\frac{g}{L}}t = \int_0^\rho \frac{dx}{\sqrt{(1-x^2)(1-k^2x^2)}}. \tag{5.28}$$

At the maximal displacement we have $\rho = 1$ and $\frac{2\pi}{T}t = \frac{\pi}{2}$, that is $t = \frac{T}{4}$. So the maximal displacement happens for the first time when

$$\frac{T}{4} = \sqrt{\frac{L}{g}} \int_0^1 \frac{dx}{\sqrt{(1-x^2)(1-k^2x^2)}}, \tag{5.29}$$

where T is the period of the oscillation. This application on the simple pendulum arises the elliptic integral of the first kind.

In order to rewrite the integral as a power series expansion, we start with the one in Legendre's notation

$$K(k) = \int_0^{\frac{\pi}{2}} \frac{d\phi}{\sqrt{1-k^2\sin^2\phi}}. \tag{5.30}$$

By the Binomial theorem, we have

$$\begin{aligned} K(k) &= \int_0^{\frac{\pi}{2}} \sum_{m=0}^{\infty} \binom{-\frac{1}{2}}{m} (-1)^m k^{2m} \sin^{2m}\phi d\phi \\ &= \sum_{m-0}^{\infty} \binom{-\frac{1}{2}}{m} (-1)^m k^{2m} \int_0^{\frac{\pi}{2}} \sin^{2m}\phi d\phi. \end{aligned} \tag{5.31}$$

In order to evaluate the integral term by term, we have to recall the expansion of the binomial coefficient in terms of Gamma functions, that is

$$\binom{-\frac{1}{2}}{m} = \frac{\Gamma(\frac{1}{2})}{m!\Gamma(\frac{1}{2}-m)} \tag{5.32}$$

as well as the definition of the Beta function

$$B(\alpha,\beta) = \frac{\Gamma(\alpha)\Gamma(\beta)}{\Gamma(\alpha+\beta)} = 2\int_0^{\frac{\pi}{2}} \cos^{2\alpha-1}\phi \sin^{2\beta-1}\phi d\phi. \tag{5.33}$$

With $\alpha = \frac{1}{2}$ and $\beta = m + \frac{1}{2}$, we have

$$K(k) = \sum_{m=0}^{\infty} \frac{(-1)^m\Gamma(\frac{1}{2})}{m!\Gamma(\frac{1}{2}-m)} \frac{\Gamma(\frac{1}{2})\Gamma(\frac{1}{2}+m)}{2m!} k^{2m}. \tag{5.34}$$

Applying Euler's reflection identity, that is

$$\Gamma(z)\Gamma(1-z) = \frac{\pi}{\sin(\pi z)}, \tag{5.35}$$

then taking $z = \frac{1}{2} + m$, the Gamma functions on the numerator in the equation (5.33) could be written as

$$\Gamma(\frac{1}{2}+m)\Gamma(\frac{1}{2}-m) = \frac{\pi}{\sin(\pi(\frac{1}{2}+m))}. \tag{5.36}$$

The series (5.33) become

$$\begin{aligned} K(k) &= \sum_{m=0}^{\infty} \frac{(-1)^m\Gamma(\frac{1}{2})}{m!\frac{\pi}{\Gamma(\frac{1}{2}+m)\sin(\pi(\frac{1}{2}+m))}} \frac{\Gamma(\frac{1}{2})\Gamma(\frac{1}{2}+m)}{2m!} k^{2m} \\ &= \sum_{m=0}^{\infty} \frac{(-1)^m\Gamma(\frac{1}{2})\Gamma(\frac{1}{2}+m)\sin(\pi(\frac{1}{2}+m))}{m!\pi} \frac{\Gamma(\frac{1}{2})\Gamma(\frac{1}{2}+m)}{2m!} k^{2m} \\ &= \frac{\pi}{2}\sum_{m=0}^{\infty} \frac{\Gamma^2(\frac{1}{2}+m)}{\pi(m!)^2} k^{2m}. \end{aligned} \tag{5.37}$$

By the following identity

$$(2m-1)!! = \frac{2^m\Gamma(\frac{1}{2}+m)}{\sqrt{\pi}}, \tag{5.38}$$

we obtain

$$\begin{aligned} K(k) &= \frac{\pi}{2}\sum_{m=0}^{\infty} \left(\frac{(2m-1)!!}{2^m m!}\right)^2 k^{2m} \\ &= \frac{\pi}{2}\sum_{m=0}^{\infty} \left(\frac{(2m-1)!!}{(2m)!!}\right)^2 k^{2m}. \end{aligned} \tag{5.39}$$

For the elliptic integral of the second kind, we consider an ellipse having the equation

$$\frac{x^2}{a^2} + \frac{y^2}{b^2} = 1 \tag{5.40}$$

with $a < b$. In parametric form, we have the equations

$$x = a\cos\theta \text{ and } y = b\sin\theta. \tag{5.41}$$

And we have the circumference C such that

$$\begin{aligned} C &= 4\int_0^{\frac{\pi}{2}} \sqrt{a^2\sin^2\theta + b^2\cos^2\theta d\theta} \\ &= 4b\int_0^{\frac{\pi}{2}} \sqrt{1-(1-\frac{a^2}{b^2})\sin^2\theta d\theta} \\ &= 4b\int_0^{\frac{\pi}{2}} \sqrt{1-k^2\sin^2\theta d\theta}, \end{aligned} \tag{5.42}$$

where $k^2 = 1 - \frac{a^2}{b^2}$. Notice that the integral is in the form of elliptic integral of the second kind.

Similar to the above computation for solving elliptic integral of the first kind, we obtain

$$E(k) = \frac{\pi}{2}\sum_{m=0}^{\infty}\left(\frac{(2m-1)!!}{(2m)!!}\right)^2 \frac{k^{2m}}{1-2m} \tag{5.43}$$

as the power series for the complete elliptic integral of the second kind. Above we provided the motivational examples for the elliptic integral of the first and second kinds, and computed in terms of power series. However, the applications for the elliptic integral of the third kind are relatively complicated.

In general, we evaluate elliptic integrals in a systematic way as follows. Since the general form of elliptic integral is as shown in (5.22) where $A(x)$,$B(x)$,$C(x)$ and $D(x)$ are polynomials in x, we have

$$\begin{aligned} R(x,\sqrt{S(x)}) &= (\frac{A(x)+B(x)}{C(x)+D(x)\sqrt{S(x)}})(\frac{C(x)-D(x)\sqrt{S(x)}}{C(x)-D(x)\sqrt{S(x)}}) \\ &= \frac{A(x)C(x)+B(x)C(x)}{C^2(x)-D^2(x)S(x)} + \frac{-A(x)D(x)-B(x)D(x)}{C^2(x)-D^2(x)S(x)}\sqrt{S(x)}. \end{aligned} \tag{5.44}$$

Hence, we have

$$R(x, \sqrt{S(x)}) = R_1(x) + \frac{R_2(x)}{\sqrt{S(x)}}, \tag{5.45}$$

where R_1 and R_2 are two rational functions of x only. Focusing on the fraction of $R_2(x)$ over $\sqrt{S(x)}$, we recall that $S(x)$ is a cubic or quartic polynomial in x. Then it would be convenient to consider the following theorem for factorization.

Theorem 5.1.10. *Any quartic polynomial in x with no repeated factors can be written in the form*

$$[a_1(x-c_1)^2 + b_1(x-c_2)^2][a_2(x-c_1)^2 + b_2(x-c_2)^2].$$

The constants a_1, b_1, a_2, b_2, c_1 and c_2 are all real for the coefficients in the quartic polynomial are real.

Proof. Let $Q(x)$ as any quartic polynomial such that

$$Q(x) = F_1(x)F_2(x),$$

where $F_1(x)$ and $F_2(x)$ are quadratic polynomials.

Note that the complex roots (if any) of $Q(x)$ occurs in conjugate pairs, and thus it leads to the following three cases:

CASE I— Four Real Roots

Let r_i, $i = 1, 2, 3, 4$ be the real roots of $Q(x)$ such that $r_1 < r_2 < r_3 < r_4$.

Let

$$F_1(x) = (x - r_1)(x - r_2)$$

and

$$F_2(x) = (x - r_3)(x - r_4)$$

. Note that an appropriate constant coefficient would be necessary in case the leading coefficient of $Q(x)$ is not one.

CASE II— Two Real Roots and Two Complex Roots

Let r_i, $i = 1, 2$ be the real roots of $Q(x)$ and $\rho_1 \pm \rho_2 i$ be the complex roots.

Let

$$F_1(x) = (x - r_1)(x - r_2)$$

and

$$F_2(x) = x^2 - 2\rho_1 x + (\rho_1^2 + \rho_2^2).$$

CASE III— Four Complex Roots

Let $\rho_1 \pm \rho_2 i$ and $\rho_3 \pm \rho_4 i$ be the complex roots of $Q(x)$.

Let

$$F_1(x) = x^2 - 2\rho_1 x + (\rho_1^2 + \rho_2^2)$$

and

$$F_2(x) = x^2 - 2\rho_3 x + (\rho_3^2 + \rho_4^2).$$

In general, we have $F_1(x)$ and $F_2(x)$ as quadratic polynomials, which are expressed as

$$F_1(x) = a_1 x^2 + 2b_1 x + c_1$$

and

$$F_2(x) = a_2 x^2 + 2b_2 x + c_2.$$

Consider a constant α such that $F_1(x) - \alpha F_2(x)$ is a perfect square. Since $F_1(x) - \alpha F_2(x)$ is simply a quadratic polynomial in x, it is a perfect square if and only if the discriminant is zero, that is,

$$\begin{aligned} (2b_1 - 2\alpha b_2)^2 - 4(a_1 - \alpha a_2)(c_1 - \alpha c_2) = 0 \\ \Longrightarrow (b_1 - \alpha b_2)^2 - (a_1 - \alpha a_2)(c_1 - \alpha c_2) = 0. \end{aligned} \tag{5.46}$$

This discriminant is indeed a quadratic in α and has two roots α_1 and α_2. Thus, we get

$$\begin{aligned} F_1(x) - \alpha_1 F_2(x) &= (a_1 - \alpha_1 a_2)[x + \frac{b_1 - \alpha_1 b_2}{a_1 - \alpha_1 b_2}]^2 \\ &= (a_1 - \alpha_1 a_2)(x - K_1)^2, \end{aligned} \tag{5.47}$$

$$\begin{aligned} F_2(x) - \alpha_2 F_2(x) &= (a_1 - \alpha_2 a_2)[x + \frac{b_1 - \alpha_2 b_2}{a_1 - \alpha_2 b_2}]^2 \\ &= (a_1 - \alpha_2 a_2)(x - K_2)^2, \end{aligned} \tag{5.48}$$

where $K_1 = \frac{b_1 - \alpha_1 b_2}{a_1 - \alpha_1 b_2}$ and $K_2 = -\frac{b_1 - \alpha b_2}{b_1 - \alpha_2 b_2}$. Lastly, solving the above equations for $F_1(x)$ and $F_2(x)$ would obtain the required form. □

In regard to the integral

$$\int \frac{R_1(x)}{\sqrt{S(x)}} dx, \tag{5.49}$$

we consider the substitution $t = \frac{x-\alpha}{x-\beta}$. Hence, we have

$$\begin{aligned} x &= \frac{-\beta t + \alpha}{1 - t} \\ \frac{dx}{dt} &= \frac{(x-\beta)^2}{\alpha - \beta}. \end{aligned} \tag{5.50}$$

This yields

$$\begin{aligned} S(x) &= [A_1(x-\alpha)^2 + B_1(x-\beta)^2][A_2(x-\alpha)^2 + B_2(x-\beta)^2] \\ &= (x-\beta)^4 \frac{[A_1(x-\alpha)^2 + B_1(x-\beta)^2]}{(x-\beta)^2} \frac{[A_2(x-\alpha)^2 + B_2(x-\beta)^2]}{(x-\beta)^2} \\ &= (x-\beta)^4 (A_1 t^2 + B_1)(A_2 t^2 + B_2) \end{aligned} \tag{5.51}$$

Now the integrand of (5.49) becomes

$$R_1(x)[\frac{(\alpha-\beta)^{-1} dt}{\sqrt{(A_1 t^2 + B_1)(A_2 t^2 + B_2)}}]$$

and $R_1(x)$ can now be written as

$$\pm(\alpha - \beta)R_3(t),$$

where $R_3(t)$ is a rational function of t.

Theorem 5.1.11 (Lemma)**.** *There exist rational functions R_4 and R_5 such that*

$$R_3(t) + R_3(-t) = 2R_4(t^2)$$

and

$$R_3(-t) = 2tR_5(t^2).$$

Thus, $R_3(t) = R_4(t^2) + tR_5(t^2)$.

The above lemma is introduced to further reduce the integral (5.49) to

$$\int \frac{R_4(t^2)}{\sqrt{(A_1t^2 + B_1)(A_2t^2 + B_2)}}dt + \int \frac{tR_5(t^2)}{\sqrt{(A_1t^2 + B_1)(A_2t^2 + B_2)}}dt.$$

Let $u = t^2$, the second integral would be in terms of elementary functions for further evaluation. Expanding $R_4(t^2)$ in partial fractions, allows us to reduce the first integral to the sums of the following:

$$I = \int t^{2m}[(A_1t^2 + B_1)(A_2t^2 + B_2)]^{-\frac{1}{2}}dt,$$

where m is an integer and

$$II = \int (1 + Nt)^{-n}[(A_1t^2 + B_1)(A_2t^2 + B_2)]^{-\frac{1}{2}}dt,$$

where n is a positive integer and $N \neq 0$.

Reduction formulas can be further done to reduce I and II to a combination of known functions and integral in canonical forms as follow

$$\begin{aligned} i.&\int[(A_1t^2+B_1)(A_2t^2+B_2)]^{-\frac{1}{2}}dt \\ ii.&\int t^2[(A_1t^2+B_1)(A_2t^2+B_2)]^{-\frac{1}{2}}dt \\ iii.&\int(1+Nt)^{-1}[(A_1t^2+B_1)(A_2t^2+B_2)]^{-\frac{1}{2}}dt, \end{aligned} \tag{5.52}$$

which are known as the **elliptic integrals of the first, second and third kinds** respectively. They form an important class of special functions [Hal95]; a class of integrals and functions that are particularly applicable for classical mechanics and engineering. Conveniently, general form of elliptic integral can be reduced to a closed expression in terms of the three special form, namely the Legendre elliptic integrals of the first, second and third kinds.

5.2 Gravitational Potential in Terms of Elliptic Integrals

In this section, we are interested in modeling the gravitational fields produced by non-spherical celestial bodies. We note that many asteroids and/or comets have very irregular shapes; many small bodies in the solar system are observed to be rubble piles meaning that the small fragments accumulated to form an aggregate body. There are models that analyze in detail the granular structure of asteroids, and study the tidal stress corresponding to different particle shapes as in [G$^+$09]. Numerical simulations show that such granular structures preferentially assume shapes that are close to fluid equilibrium shapes [T$^+$09]. However the perfect fluid equilibrium shapes are not attained due to inter-particle friction. Assumig that the object can be modeled as an incompressible fluid, which is regarded as a first approximation of an aggregate of particles. The problem of a roatating fluid object brings us to a classical problem in fluid mechanics. We consider a self-gravitating in-compressible liquid body floating in space and rotating uniformly about some fixed axis, which passes through its center of mass. The shape of the self-gravitating rotating liquid body depends on the pressure from the fluid, its gravity and the rotational (i.e. in its reference frame, centrifugal) force. Since the fluid has its weigth, the weight of the fluid exert a pressure from gravity. In addition, the relative movement (i.e. acceleration) of a liquid produces pressure. Fluid pressure refers to the force acting on particles in the fluid and it will be neglected in this work since we would consider rotation around x- axis. Physically, fluid spins as if it were a solid body [WB06]. Centrifugal force (i.e. the force perpendicular to the axis of rotation) opposes gravity [Abr90] while rotating.

It is easy to prove that the body forms a spherical shape in the absence of rotation. We would expect rotation to cause changes on the shape of the liquid body— there is an expansion in the plane perpendicular to the axis of rotation while there is a contraction occurs along the axis of rotation; the picture is shown on Figure 5.2. In Chapter 2, we

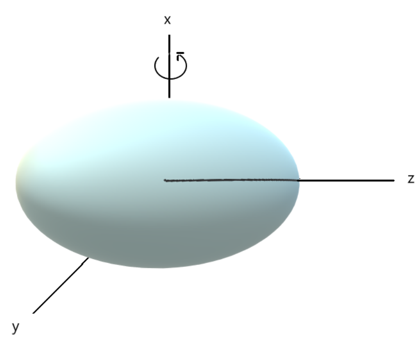

Figure 5.2: A liquid body is rotating along the x-axis.

consider the gravitational potential Φ such that

$$\Phi(r, \mu, \phi) = -G\rho \int d^3\vec{r'} \frac{\rho}{\mid \vec{r} - \vec{r'} \mid} \tag{5.53}$$

where

ρ is the density of the celestial body

$\vec{r'}$ is the vector from the origin to the surface of the celestial body

$\vec{r}$ is the vector from the origin to an arbitrary point in space.

Instead of a spherical coordinate system and having the negative sign to be dropped as in Chapter 2, we switch to a cylindrical coordinate system and we keep the negative sign for the gravitational potential in this chapter. We now consider the points $\vec{r'}$ inside the body produce a gravitational potential at a point $\vec{r} = z\ \hat{z} + f\,(z)\,\hat{r}$ on the surface. Using the notation from Section 2.1.1, we have the gravitational potential as equation (2.1)

$$\Phi(\vec{X_1}) = -\int_{V_{m_2}} \frac{G\rho(\vec{X_2})}{r_{21}} d^3X_2, \tag{5.54}$$

we recall $r_{12} = |\vec{x_1} - \vec{x_2}|$. We now consider the cylindrical coordinate system as follows.

$$\begin{aligned} x &= r\cos\phi \\ y &= r\sin\phi \\ z &= z, \end{aligned} \tag{5.55}$$

With this cylindrical coordinate frame (r, ϕ, z), consider the points $\vec{r'}$ inside the body produce a gravitational potential at a point $\vec{r} = z\ \hat{z} + f\,(z)\,\hat{r}$ on the surface and $\Phi(\vec{X_1})$

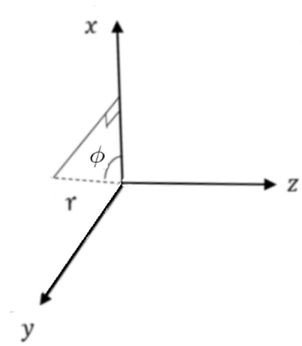

Figure 5.3: From Cartesian Coordinate to Cylindrical Cooridinate (r, ϕ, z).

is expressed as

$$\begin{aligned}\Phi(\vec{X_1}) &= -\int \frac{G}{\sqrt{\sum_{i=1}^{3}(x_{2i}-x_{1i})^2}}\rho(\vec{X_2})d^3\vec{X_2} \\ &= -\int \frac{G}{\sqrt{r^2+r'^2-2rr'(\cos\phi\cos\phi'+\sin\phi\sin\phi')+(z-z')^2}}\cdot\rho(\vec{X_2})d^3\vec{X_2}. \\ &= -\int \frac{G\rho(\vec{X_2})d^3\vec{X_2}}{\sqrt{r^2+r'^2+2rr'\cos(\phi-\phi')+(z-z')^2}}.\end{aligned} \tag{5.56}$$

Applying the Lipschitz integral, that is

$$\int_0^\infty J_0(ka)e^{-k|b|}dk = \frac{1}{\sqrt{a^2+b^2}},$$

and we let

$$\begin{aligned} a &= \sqrt{r^2+r'^2+2rr'\cos(\phi-\phi')} \\ b &= (z-z')^2. \end{aligned} \tag{5.57}$$

Then

$$\begin{aligned}&\frac{1}{\sqrt{r^2+r'^2+2rr'\cos(\phi-\phi')+(z-z')^2}}\\&=\int_0^\infty J_0(k\sqrt{r^2+r'^2+2rr'\cos(\phi-\phi')})e^{-k|z-z'|}dk\end{aligned} \tag{5.58}$$

where J_0 is the order zero Bessel function of the first kind. We have shown that the term of $\frac{1}{\sqrt{\sum_{i=1}^{3}(x_{2i}-x_{1i})^2}}$ can be expressed in terms of the integral of Lipschitz. Furthermore, we can apply the Neumann's addition theorem for Bessel functions. The order zero Bessel function of the first kind can then be written as a Fourier series expansion over Bessel functions of varying order, that is

$$\sum_{m=-\infty}^{\infty} J_m(kr)J_m(kr')e^{im(\phi-\phi')} = J_0(k\sqrt{r^2+r'^2-2rr'\cos(\phi-\phi')}) \tag{5.59}$$

where J_m is the order m Bessel function of the first kind. Therefore

$$\begin{aligned}\frac{1}{\sqrt{r^2+r'^2+2rr'\cos(\phi-\phi')+(z-z')^2}} &= \int_0^\infty J_0(k\sqrt{r^2+r'^2-2rr'\cos(\phi-\phi')})e^{-k|z-z'|}dk\\&= \int_0^\infty \sum_{m=-\infty}^{\infty} J_m(kr)J_m(kr')e^{im(\phi-\phi')}e^{-k|z-z'|}.\end{aligned} \tag{5.60}$$

It follows that

$$\Phi(\vec{X_1}) = -G\rho\int r'dz'dr'd\phi' \sum_{m=-\infty}^{\infty}\int_0^\infty dk e^{im(\phi-\phi')}J_m(kr)J_m(kr')e^{-k|z-z'|}. \tag{5.61}$$

Consider the cylindrical system as in Figure 5.3 with rotation around the x-axis, the total potential is the sum of the gravitational and rotational potentials. For a given angular velocity, ω, the equilibrium condition on the fluid shape is that the total potential should remain constant everywhere on the surface. It is expressed as

$$\begin{aligned} U(r,z,\phi) &= \Phi - \frac{1}{2}I\omega^2 \\ &= C, \end{aligned} \tag{5.62}$$

where Φ refers as the gravitational potential, $\frac{1}{2}I\omega^2$ refers as the rotational potential, which will be justified later and C is a constant. In addition, we introduce the notation

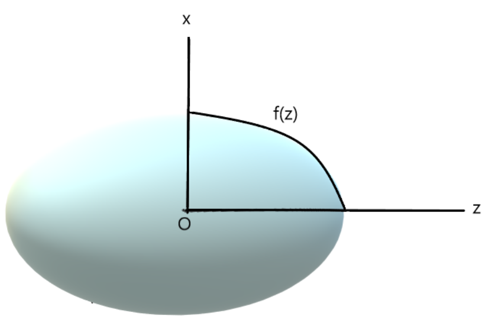

(a) A generis shape is shown.

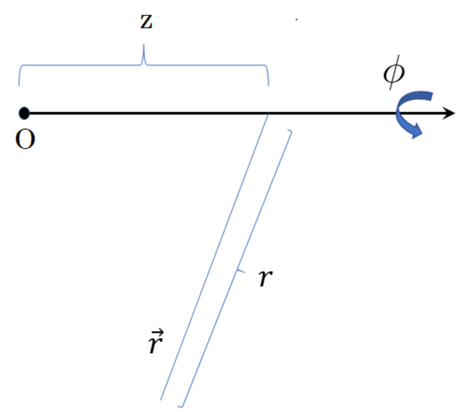

(b) Notation for the shape that is interested in; $-z_0$ and z_0 are the endpoints of the planet on $z-$axis where $f(z)$ is the function that generates the shape of the planet via revolution on $z-$axis.

Figure 5.4: In general, the optimal shape of the body is not necessarily to be a dumbbell.

as shown in Figure 5.4.

Integrating with respect to ϕ' first, we will then obtain a simplified integral

$$\Phi = -G\rho \sum_{m=-\infty}^{\infty} \int_0^{\infty} dk \int_{-z_0}^{z_0} dz' e^{-k|z-z'|} \int_0^{f(z')} dr' J_m(kr') J_m(kr) r' \int_0^{2\pi} d\phi' e^{im(\phi-\phi')}.$$

Note that

$$\int_0^{2\pi} d\phi' e^{im(\phi'-\phi)} = 2\pi\delta_{m0},$$

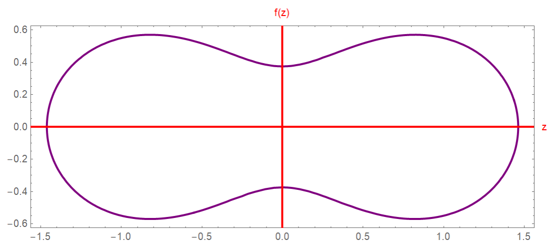

(a) The function $f(z)$ (i.e. F(z) for dimension).

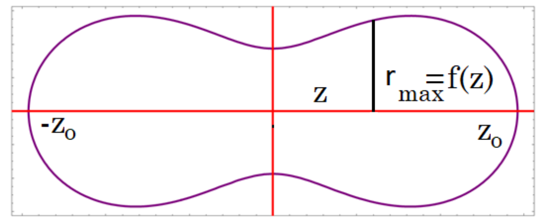

(b) Notation for position vectors and its distance.

Figure 5.5: Definition for position and function $f(z)$.

where δ is a Kronecker function such that

$$\delta_{m0} = \begin{cases} 0 & \text{if } m = 0 \\ 1 & \text{if } m \neq 0 \end{cases} \tag{5.63}$$

and thus the Bessel functions collapse to order zero. That is,

$$\Phi = -2\pi\rho G \int_0^\infty dk \int_{-z_0}^{z_0} dz' e^{-k|z-z'|} \int_0^{f(z')} J_0(kr')J_0(kr)r'dr'.$$

Using the following identity of the Bessel function

$$\begin{aligned} \frac{1}{k}\frac{d}{ds'}[s'J_1(ks')] &= \frac{1}{k}[J_1(ks') + s'kJ_1'(ks')] \\ &= \frac{1}{k}[J_1(ks') + (s'kJ_0(ks') - J_1(ks'))] \\ &= s'J_0(ks') \end{aligned} \tag{5.64}$$

We now have

$$\begin{aligned} \Phi &= -2\pi\rho G \int_0^\infty dk \int_{-z_0}^{z_0} dz' e^{-k|z-z'|} \int_0^{f(z')} J_0(ks)\frac{1}{k}\frac{d}{dr'}[r'J_1(kr')]dr' \\ &= -2\pi\rho G \int_0^\infty dk \int_{-z_0}^{z_0} dz' e^{-k|z-z'|} \frac{J_0(kr)}{k} f(r')J_1(kf(r')) \\ &= -2\pi\rho G \int_0^\infty dk e^{-k|z-z'|} \frac{J_0(kr)J_1(kr')}{k} \int_{-z_0}^{z_0} f(z')dz'. \end{aligned} \tag{5.65}$$

Let $z' = z_0\eta'$, $z = z_0\eta$ and $k = \frac{K}{z_0}$, then we have the dimensionless case

$$\Phi = -2\pi\rho G z_0 \int_0^\infty dK e^{-K|\eta-\eta'|} \frac{J_0(\frac{K}{z_0}r)J_1(\frac{K}{z_0}r')}{K} \int_{-1}^1 f(\eta')d\eta'. \tag{5.66}$$

Now let $x = K \mid \eta - \eta' \mid$ and $K = \frac{x}{|\eta-\eta'|}$, we obtain

$$\Phi = -2\pi\rho G z_0 \int_0^\infty \frac{dx}{x} e^{-x} J_0(\frac{1}{z_0}\frac{x}{\mid \eta-\eta' \mid}r) J_1(\frac{1}{z_0}\frac{x}{\mid \eta-\eta' \mid}r') \int_{-1}^1 f(\eta')d\eta' \tag{5.67}$$

Since we are interested in the potential Φ at the surface that is defined by the function f, we consider the replacement of r as $f(\eta)$ and r' as $f(\eta')$.

$$\Phi = -2\pi\rho G z_0 \int_0^\infty \frac{dx}{x} e^{-x} J_0(\frac{1}{z_0}\frac{x}{\mid \eta-\eta' \mid}f(\eta)) J_1(\frac{1}{z_0}\frac{x}{\mid \eta-\eta' \mid}f(\eta')) \int_{-1}^1 f(\eta')d\eta' \tag{5.68}$$

Notice that the integral with respect to x is known as the Laplace Transform of the Bessel/rational integrand. By the equation (2.1) of [KIB12]

$$I_{10}^{-1}(a, b, s) := \int_0^\infty x^{-1} J_1(ax) J_0(bx) e^{-sx} dx$$

with

$$a = \frac{f(\eta')}{z_0|\eta-\eta'|}, \quad b = \frac{f(\eta)}{z_0|\eta-\eta'|}, \quad s = 1.$$

The function I_{10}^{-1} is indeed known in a closed form in terms of Elliptical functions [KIB12]. That is,

$$\Phi = -2\pi\rho G z_0 \int_{-1}^1 d\eta' f(\eta') I_{10}^{-1}(f(\eta'), f(\eta), 1) \tag{5.69}$$

where

$$I_{10}^{-1}(a, b, s) = \frac{1}{\pi a}\left[\frac{2\sqrt{ab}}{\kappa}\mathbf{E} + (a^2 - b^2)\frac{\kappa}{2\sqrt{ab}}\mathbf{K}\right] + \frac{s}{\pi a} sgn(a-b)\Lambda - \frac{s}{a}H(a-b) \tag{5.70}$$

and

$$\kappa = \frac{2\sqrt{ab}}{\sqrt{(a+b)^2+s^2}} \quad \nu = \frac{4ab}{(a+b)^2} \quad H(a-b) = \begin{cases} 0 & \text{if } a-b<0 \\ 1 & \text{if } a-b \geqslant 0 \end{cases}.$$

$$\mathbf{K} = \mathbf{K}(\kappa) \qquad \mathbf{E} = \mathbf{E}(\kappa) \quad \Lambda = \Lambda(\nu, \kappa)$$
$$= \frac{|a-b|}{a+b} \frac{s}{\sqrt{(a+b)^2+s^2}} \mathbf{\Pi}(\nu, \kappa)$$

And thus equation (5.69) shows the case in dimensionless notation. With the non-dimensionless notation, we obtain the following:

Proposition 5.2.1. *The gravitational potential at a point of cylindrical coordinates* $(f(z), \phi, z)$ *on the surface of a body generated by revolving the graph of* $f(z)$, $|z| \leqslant z_0$ *is given by*

$$\Phi = -2\pi G\rho \int_{-z_0}^{z_0} dz'\, f(z') I_{10}^{-1}(f(z'), f(z), |z-z'|). \tag{5.71}$$

The expression I_{10}^{-1} for the Proposition 5.2.1 above has the explicit form as follows:

$$\begin{aligned} I_{10}^{-1}(f(z'), f(z), |z-z'|) = & \frac{\sqrt{(z'-z)^2 + (f(z)+f(z'))^2}}{\pi f(z')} \\ & \cdot \mathbf{E}(\frac{4f(z)f(z')}{(z'-z)^2 + (f(Z)+f(z'))^2}) \\ & + \frac{f(z')^2 - f(z)^2}{\pi f(z')\sqrt{(z'-z)^2 + (f(z)+f(z'))^2}} \\ & \cdot \mathbf{K}(\frac{4f(z)f(z')}{(z'-z)^2 + (f(z)+f(z'))^2})(z'-z)^2 \\ & + \frac{(f(z'-f(z))}{\pi f(z')(f(z)+f(z'))\sqrt{(z'-z)^2 + (f(z)+f(z'))^2}} \\ & \cdot \mathbf{\Pi}(\frac{4f(z)f(z')}{(f(z)+f(z'))^2} \frac{4f(z)f(z')}{(z'-z)^2 + (f(z)+f(z'))^2})) \\ & - \frac{|z'-z|}{f(z')} \mathbf{\Theta}(f(z') - f(z)) \end{aligned} \tag{5.72}$$

For a given body shape generated by the profile function $f(z)$, equation (5.71) gives the gravitational potential Φ as a function of z at any point of the surface. In addition, equation (5.71) can be easily modified to obtain the exact gravitational potential at any point in space, as follows:

Corollary 5.2.2. *The gravitational potential at a point in space of cylindrical coordinates* (s, ϕ, z)*, exerted by a body generated by revolving the graph of* $z \mapsto f(z)$*,* $|z| \leqslant z_0$*, is given by*

$$\Phi = -2\pi G\rho \int_{-z_0}^{z_0} dz'\, f(z') I_{10}^{-1}(f(z'), s, |z - z'|). \tag{5.73}$$

We remark that the formulas (5.71) and (5.73) are very general that they are applicable for any solid of revolution. They give the gravitational potential in terms of a simple 1-dimensional integral with combination of elliptic functions. As shown in Section 5.1.2, it is known that the elliptic functions have expansions in power series that are convergent, thus (5.71) and (5.73) can themselves be expanded in convergent power series [BF13]. Note that many numerical computation software packages have been created numerical computation for elliptic functions. Since the definition of the arguments does not follow a uniform convention, we must pay attention to the arguments of the function when using the elliptic functions from standard programming languages such as C, Python, Matlab, Mathematica. We notice that the definition of elliptic integral can be written as the function

$$\begin{aligned} F(a, b) &= \frac{2}{\pi} \int_0^{\frac{\pi}{2}} \frac{d\theta}{\sqrt{a^2 \cos^2\theta + b^2 \sin^2\theta}} \\ &= \frac{2}{\pi} \int_0^{\frac{\pi}{2}} \frac{d\theta}{\cos\theta \sqrt{a^2 + b^2 \tan^2\theta}} \end{aligned} \tag{5.74}$$

Let $t = b\tan\theta$ we have the following differential

$$dt = b\sec^2\theta d\theta$$

Since $\sin\theta = \sqrt{1 + \tan t}$ by the Pythagorean trigonometric identity, we have the differential

$$\begin{aligned} dt &= \frac{b}{\cos\theta} \sec\theta d\theta \\ &= \frac{b}{\cos\theta}\sqrt{1+\tan^2\theta} d\theta \\ &= \frac{b}{\cos\theta}\sqrt{1+\left(\frac{t}{b}\right)^2} d\theta \\ &= \frac{d\theta}{\cos\theta}\sqrt{b^2+t^2} \end{aligned} \tag{5.75}$$

and thus we have

$$\frac{d\theta}{\cos\theta} = \frac{dt}{\sqrt{b^2+t^2}}$$

Now $F(a,b)$ becomes

$$\begin{aligned} F(a,b) &= \frac{2}{\pi}\int_0^\infty \frac{1}{\sqrt{a^2+t^2}} \frac{dt}{\sqrt{b^2+t^2}} \\ &= \frac{2}{\pi}\int_0^\infty \frac{dt}{\sqrt{(a^2+t^2)(b^2+t^2)}} \\ &= \frac{1}{\pi}\int_{-\infty}^\infty \frac{dt}{\sqrt{(a^2+t^2)(b^2+t^2)}} \end{aligned} \tag{5.76}$$

Let $u = \frac{1}{2}\left(t - \frac{ab}{t}\right)$ and we have the differential

$$du = \frac{1}{2}\left(1+\frac{ab}{t^2}\right) dt.$$

Note that

$$\begin{aligned} \frac{2u}{t} = \frac{t}{t} - \frac{ab}{t^2} &= 1 - \frac{ab}{t} \\ \implies \frac{ab}{t^2} &= 1 - \frac{2u}{t} \\ \implies 1 + \frac{ab}{t^2} &= 2 - \frac{2u}{t} \\ &= 2\left(1 - \frac{u}{t}\right). \end{aligned} \tag{5.77}$$

Since $1 + \frac{ab}{t^2} > 0$, we have

$$1 + \frac{ab}{t^2} = 2|1 - \frac{u}{t}|.$$

And therefore

$$\begin{aligned} \frac{du}{dt} &= \frac{1}{2}2|1 - \frac{u}{t}| \\ du &= \frac{dt}{|1 - \frac{u}{t}|}. \end{aligned} \tag{5.78}$$

In equation (5.76), we handle the integral as

$$\frac{1}{\pi}\int_{-\infty}^{\infty}\frac{dt}{\sqrt{(a^2+t^2)(b^2+t^2)}} = \frac{1}{\pi}\left(\int_{-\infty}^{0}\frac{dt}{\sqrt{(a^2+t^2)(b^2+t^2)}} + \int_{0}^{\infty}\frac{dt}{\sqrt{(a^2+t^2)(b^2+t^2)}}\right). \tag{5.79}$$

Substituting u in above integrals, we obtain

$$\begin{aligned} F(a,b) &= \frac{1}{\pi}\left(\int_{-\infty}^{\infty}\frac{du}{|1-\frac{u}{t}|\sqrt{a^2b^2+(a^2+b^2)t^2+t^4}} + \int_{-\infty}^{\infty}\frac{du}{|1-\frac{u}{t}|\sqrt{a^2b^2+(a^2+b^2)t^2+t^4}}\right) \\ &= \frac{2}{\pi}\int_{-\infty}^{\infty}\frac{du}{|1-\frac{u}{t}|\sqrt{a^2b^2+(a^2+b^2)t^2+t^4}} \end{aligned} \tag{5.80}$$

Notice that

$$\begin{aligned} u &= \frac{1}{2}\left(t - \frac{ab}{t}\right) \\ \implies u^2 &= \frac{1}{4}\left(t^2 - 2ab + \frac{a^2b^2}{t^2}\right) \\ \implies u^2 &= \frac{t^4 - 2abt^2 + a^2b^2}{4t^2} \\ \implies 4u^2t^2 &= t^4 - 2abt^2 + a^2b^2 \\ \implies a^2b^2 + t^4 &= 4u^2t^2 + 2abt^2 \end{aligned} \tag{5.81}$$

And again start with u such that $u = \frac{1}{2}\left(t - \frac{ab}{t}\right)$, we can solve for t to obtain

$$\begin{aligned}
2ut &= t^2 - ab \\
t^2 - 2ut &= ab \\
t^2 - 2ut - ab &= 0 \\
t &= \frac{1}{2}\left(2u \pm \sqrt{4u^2 + 4ab}\right) \\
&= u \pm \sqrt{u^2 + ab} \\
t - u &= \pm\sqrt{u^2 + ab}.
\end{aligned} \tag{5.82}$$

Substitute expressions from equation (5.81) and equation (5.82) into the function $F(a, b)$, we obtain

$$\begin{aligned}
F(a, b) &= \frac{2}{\pi}\int_{-\infty}^{\infty} \frac{du}{|1 - \frac{u}{t}|\sqrt{4u^2t^2 + 2abt^2 + (a^2 + b^2)t^2}} \\
&= \frac{2}{\pi}\int_{-\infty}^{\infty} \frac{du}{|t - u|\sqrt{4u^2 + (a + b)^2}} \\
&= \frac{2}{\pi}\int_{-\infty}^{\infty} \frac{du}{\sqrt{4u^2 + (a + b)^2}\sqrt{u^2 + ab}} \\
&= \frac{1}{\pi}\int_{-\infty}^{\infty} \frac{du}{\sqrt{\left(\left(\frac{a+b}{2}\right)^2 + u^2\right)(ab + u^2)}} \\
&= F\left(\frac{1}{2}(a + b), \sqrt{ab}\right).
\end{aligned} \tag{5.83}$$

The above computation yields

$$F(a, b) = F\left(\frac{1}{2}(a + b), \sqrt{ab}\right)$$

and thus we can apply the iteration of arithmetic-geometric mean as

$$\begin{aligned}
a_{i+1} &= \frac{1}{2}(a_i + b_i) \\
b_{i+1} &= \sqrt{a_i b_i}, \text{ for } i = 0, 1, 2, 3, ...
\end{aligned} \tag{5.84}$$

without changing the value of the integral. This iteration converges to and terminates at $M(a_0, b_0)$ in the limit of a_i, b_i as $i \to \infty$, that is $\lim_{i\to\infty} a_i = \lim_{i\to\infty} b_i := M(a_0, b_0)$. The convergence of complete elliptic integrals confirms that the Laplace's expression $I_{10}^{-1}(a, b, c)$ is a closed form.

In order to compute the total energy U as in equation (5.62), we will need to consider the rotational energy of the body as well. We express the position vector in cylindrical coordinates as

$$\vec{r} = z\ \hat{z} + f\left(z\right)\hat{r}. \tag{5.85}$$

Consider a generic point on the ring, as shown in Figure 5.7b, has cylindrical coordinates $\left(f\left(z\right), \phi, z\right)$, so its distance d to the axis has the relation

$$d^2 = z^2 + (f(z))^2 \sin^2(\phi). \tag{5.86}$$

And the moment of inertia around the axis of rotation I, is given by d^2. Then we obtain the rotational potential by placing a unit mass at the location rotating with angular speed ω. And thus we have the rotational energy expressed as

$$-\frac{1}{2}\omega^2\left(f^2\left(z\right)\sin^2\left(\phi\right) + z^2\right). \tag{5.87}$$

Following the notation in equation (5.2.1), we obtain

Corollary 5.2.3. *The total potential U for the rotating body, evaluated at the surface of the body, is the sum of the expressions in equations* (5.71) *and* (5.87)*:*

$$U = -2\pi G\rho \int_{-z_0}^{z_0} dz'\, f(z') I_{10}^{-1}(f(z'), f(z), |z - z'|) - \frac{1}{2}\omega^2(f^2(z)\sin^2\phi + z^2). \tag{5.88}$$

Notice that the negative sign for the last two terms constitute the sign of the repulsive centrifugal force. In conclusion, equation (5.88) can be used in two ways. First, if the explicit shape (i.e. asteroid shape) is known, then the gravitational acceleration $g = -\nabla U$, on the surface of the object can be computed. Second, an optimal shape can be obtained for a particular class of shapes (such as dumbbell shapes). This can be modeled as an isoperimetric problem in which to determine the total potential for the function that has the smallest variability for the optimal shape of the class.

The shape of equilibrium is obtained for the $f(z)$ for which U a constant, independent of z. This solution of the nonlinear integral equation, while extremely useful, is not likely to be solved exactly. Realistically we should explore the minimization problem in the parameter space of a well suited family of functions instead. In the following section, we give an example of such a procedure.

5.3 Gravitational Potential of Dumbbell Shaped Body Derived by Variational Approach

Here we investigate the gravitational potential of dumb-bell shapes, with the goal of determining which dumb-bell shapes can be attained under the effect of gravitational and rotational forces as shown in the Section 5.2. As a follow up of the previous section, we consider to apply the result of Section 5.2 on finding the total potential of a dumb-bell shaped body in a cylindrical system with symmetry. Surprisingly, the problem can be substantially reduced to a relatively simpler integral.

Consider the shape of dumb-bell, we aim to explore how the shape would affect the potential energy U. We aim to apply the variational principle to the problem— specifically, we consider the problem as mentioned and propose a function to describe the dumb-bell shape of the body. This function introduces the body's shape with parameters and thus its corresponding gravitational potential parametrically. For each rotational speed ω, the parameters of the function is varied. By computing the gravitational potential with respect to each particular dumb-bell shape (depending on parameters), we obtain the particular parameters that provide us the potential that is approximately constant for the fixed ω. Therefore, we obtain an approximate equipotential surface for some fixed ω. For a given body shape, $f(z)$, equation (5.88) gives the total potential U. Now taking dumb-bell shapes into consideration, we choose to explore the family of

$$F(z) = \gamma\sqrt{\left(1-(\frac{z}{z_0})^2\right)\left(1+\frac{\beta}{1-\beta}(\frac{z}{z_0})^2\right)}, \tag{5.89}$$

where $z \in [-z_0, z_0]$, by considering the surface of revolution around the z-axis. The parameter γ gives the value $F(0)$, representing the height of the saddle point, while the parameter β controls the convexity. Let $z = z_0\eta$, we have the dimensionless formula

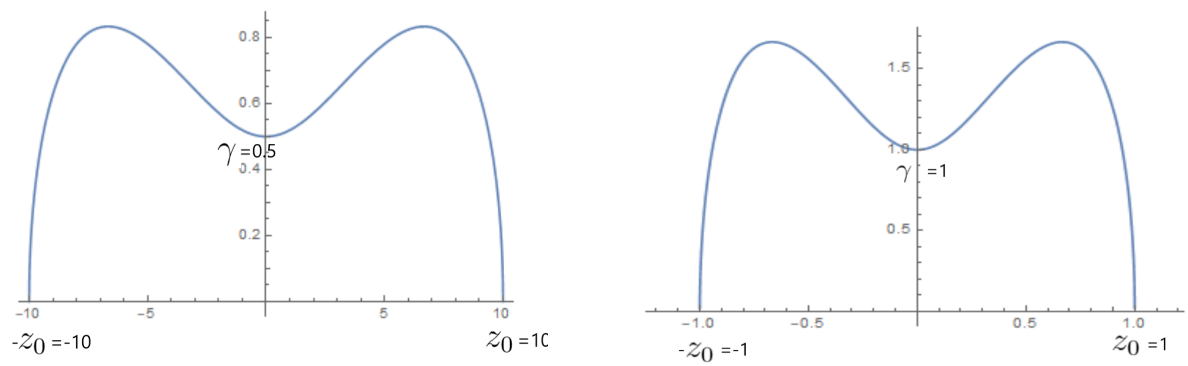

(a) The function $F(z)$ at z_0 equals 10, γ equals 0.5 and β equals 0.9.

(b) The function $F(z)$ at z_0 and γ both equal 1 (i.e. $f(z)$) and β equals 0.9.

Figure 5.6: Graphs of the functions of F(z).

defined by

$$f(\eta) = \sqrt{\left(1-\eta^2\right)\left(1+\frac{\beta}{1-\beta}\eta^2\right)} \tag{5.90}$$

where $\eta \in [-1, 1]$ and thus

$$\begin{aligned} F(z) &= \gamma\sqrt{\left(1-(\frac{z}{z_0})^2\right)\left(1+\frac{\beta}{1-\beta}(\frac{z}{z_0})^2\right)} \\ &= \gamma\sqrt{\left(1-\eta^2\right)\left(1+\frac{\beta}{1-\beta}\eta^2\right)} \end{aligned} \tag{5.91}$$

$$\begin{aligned} &:= \gamma f(\eta), \text{ for } \eta = \frac{z}{z_0} \\ F(z) &= \gamma f\left(\frac{z}{z_0}\right) \end{aligned} \tag{5.92}$$

Note that $f(\eta)$ is the formula of dimensionless (i.e.$z_0 = 1$ and $\gamma = 1$) case. Equation (5.91) demonstrates the relationship between the formulas of dimensionless and non-dimensionless case; the two cases differ only by a rescaling. It is both practical for us to use while performing numerical analysis. In the following context, we are going to use the notation $f(z)$ for the considered function for the surface.

With the symmetry assumptions with respect to the x- and z-axes as well as the parametrization in $alpha$ and β, we obtain a dumb-bell shaped body, which rotates with constant angular speed ω around the Cartesian x-axis.

Ideally, we want the total potential U being constant. We evaluate U for some fixed values of z. By plotting the total potential against z for different γ and β, we aim to find the γ and β that provide us a shape with the total potential that is approximately constant while varying z, for each fixed ω (i.e. the rotation speed).

Consider the dumb-bell shaped celestial body to be symmetric with respect to the $z-$ axis (generated by the surface of revolution) as shown below.

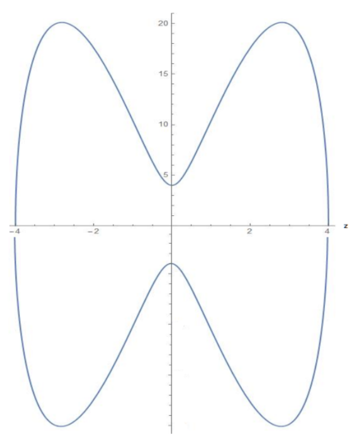

(a) A dumb-bell shape is formed with symmetry on the $z-$ axis.

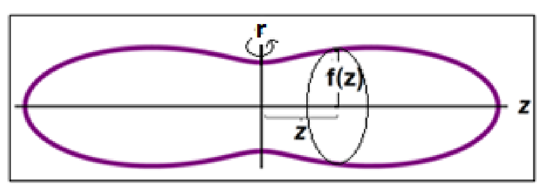

(b) Sagittal section of body of revolution around the z-axis. All points inside the object are within $|z| \leqslant z_0$. For a fixed z, points are in a circular disc of radius r_{max}.

Figure 5.7: Graphs of the functions of F(z).

In the Section 5.2, we have equation (5.88) as the total potential at the surface of an object. A problem that immediately arise from the equation is that, at the surface of the object, the gravitational potential Φ depends only on z while the rotational potential additionally depends on ϕ. Walking along the ring of Figure (5.7b), Φ remains constant while the rotational potential has $\sin^2\phi$ of dependence. Clearly the potential cannot be constant on the family (5.89). Nevertheless, the practical problem of a real celestial body must be interpreted in the context of rotating not with respect to a fixed axes, but secularly with respect to all axes perpendicular to z. Under these conditions and owing to the $\sin^2\phi$ factor, oblate shapes will develop perpendicular to z. However these shapes will eventually develop in other directions, as the axis of rotation rotates. Hence, we should consider the celestial bodies that after long times compared with the rotational period $\frac{2\pi}{\omega}$, have cross sections averaged in ϕ.Therefore, it is physically sensible to remove the ϕ-dependence, and we do so by considering the effective total potential

$$U_{eff} = \frac{1}{2\pi}\int_0^{2\pi} U\left(z,\phi\right)d\phi. \tag{5.93}$$

It yields

$$U_{eff} = -2\pi G\rho\int_{-z_0}^{z_0} f\left(z'\right)L\left(f\left(z'\right),f\left(z\right),\left|z-z'\right|\right)dz' - \frac{1}{4}f^2\left(z\right)\omega^2 - \frac{1}{2}z^2\omega^2 \tag{5.94}$$

Finding the $f(z)$ that produces a potential U_{eff} with the least variability for our family of curves as in equation (5.89) would be the next task. Replacing $f(z)$ in equation (5.94) by equation (5.89) and performing the integral numerically, we obtain numerical values of the function $U_{eff}(z,\beta,\gamma)$. We then search, among all pairs of parameters (β,γ), that which produces, for a given ω a potential U_{eff} with the least variability in z. For the increment of ω as 0.1, the potential at each location of z is computed for each of the fixed γ and β. We use the standard deviation of the potential over absolute value of its mean, i.e. $\frac{\sigma}{|\mu|}$ for further evaluation. This quantity is known as the coefficient of variation. It does not only show the extent of variability in relation to the mean, but also is a dimensionless quantity for comparison and therefore it is very practical for us to compare the variability of different data sets. In our case, we use it for measuring the variability of the total potential of all z given by different parameters in this isoperimetric problem; it provides us the comparison for the best parameters, which control the shape of the body. Our goal is to find the dumbbell shape that provide relatively constant on the potential energy. We record the lowest values of $\frac{\sigma}{|\mu|}$ for the results given by each pair of γ and β. The results suggest different interesting dumbbell shape for the body as in Figure 5.8, 5.9 and 5.10. Some of the shapes obtained below are 'visually' similar to the observed shapes of some asteroids and comets, such as 624 Hektor, 103P/Hartley and 8P/Tuttle.

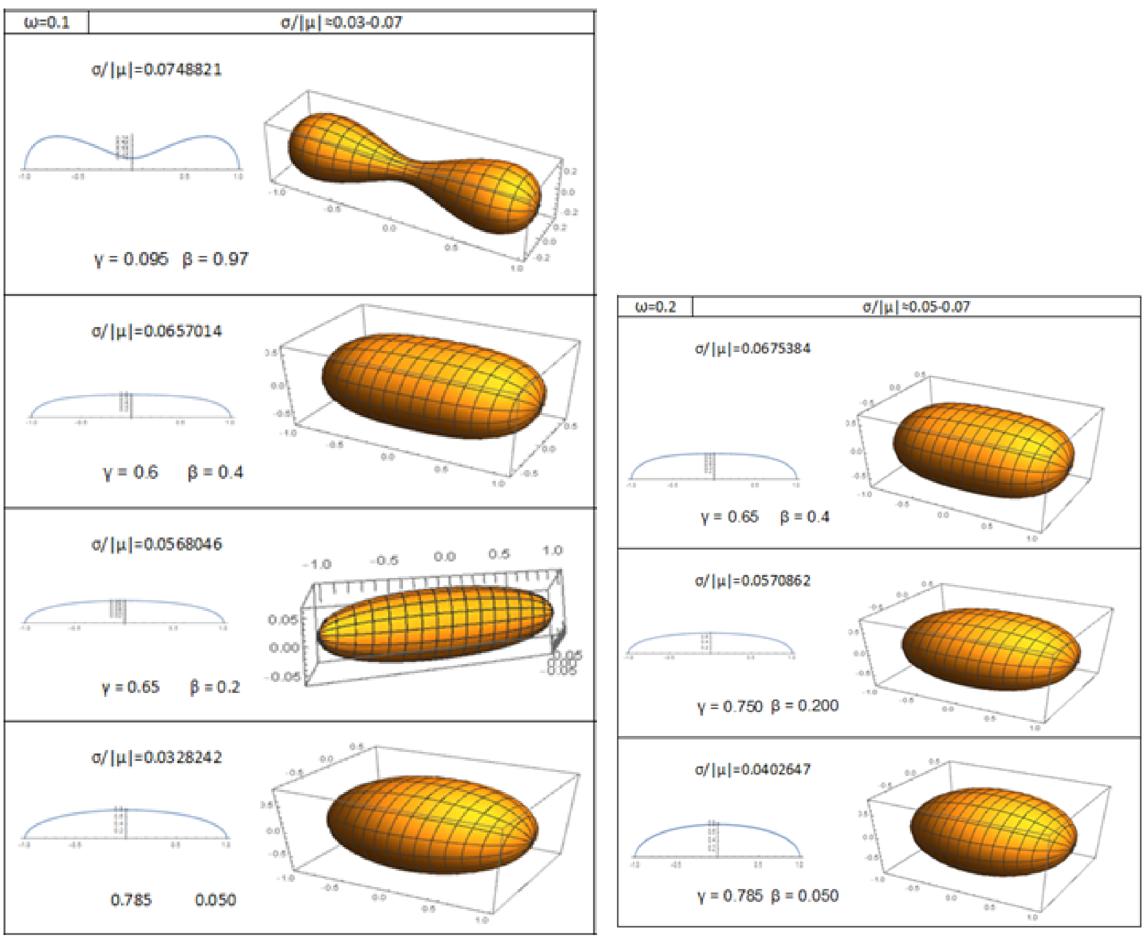

Figure 5.8: Approximate equilibrium shapes for $\omega = 0.1$ and $\omega = 0.2$.

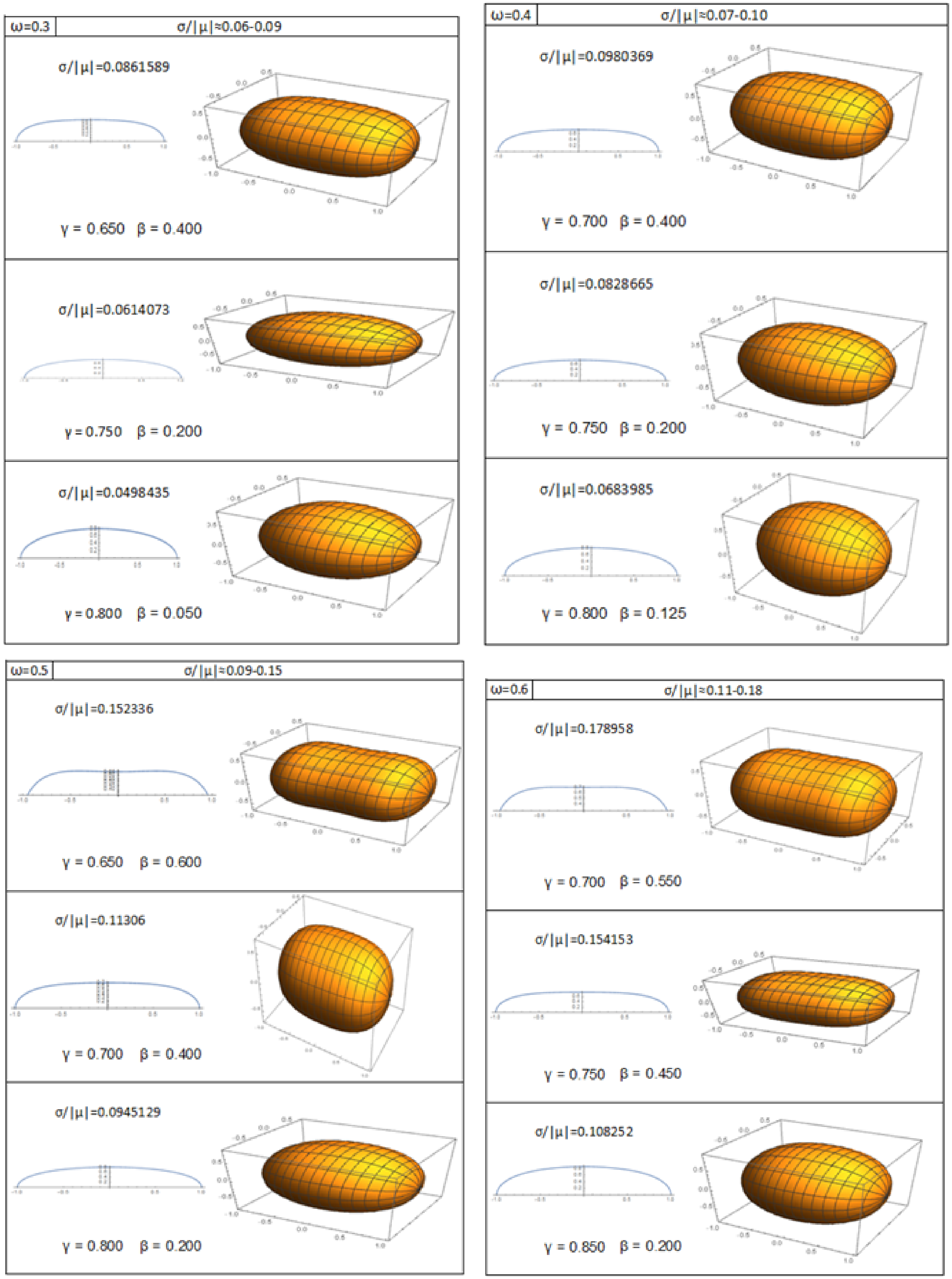

Figure 5.9: Approximate equilibrium shapes for $\omega = 0.3$ and $\omega = 0.4$, $\omega = 0.5$ and $\omega = 0.6$.

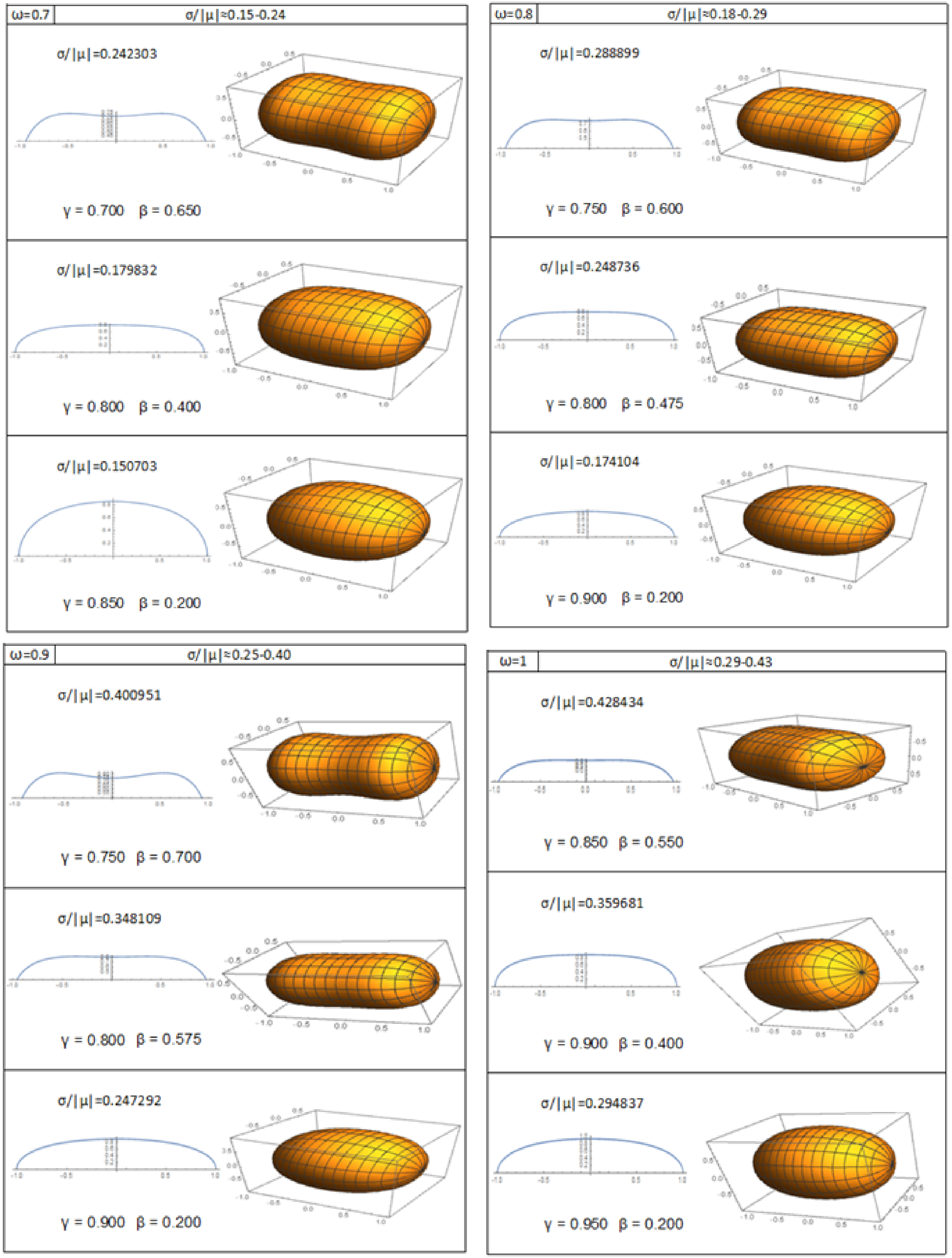

Figure 5.10: Approximate equilibrium shapes for $\omega = 0.7$ and $\omega = 0.8$, $\omega = 0.9$ and $\omega = 1$.

5.4 Conclusions

In this chapter, we consider the gravitational potential generated by an axisymmetric body that rotates around an axis perpendicular to the symmetry axis and derive a relatively simple and useful formula in terms of elliptic integrals. In addition, we formulate an isoperimetric problem that was applied to finding approximate equilibrium shapes based on the principle of minimizing the variations of the potential on the surface. As an example to astrodynamics, we consider a two-parameter family of dumbbell shapes. Depending on the rotational speed, we compute numerically their shapes with choices of parameters. With numerical computation and analysis, we obtain the parameters for each of the rotational speed that the gravitational potential at the surface is approximately constant.

There also exist exact equilibrium solutions of dumbbell shape as shown in [EHS82]; we notice that such dumbbell shapes are not given by closed form equations. Contrarily, we provide a family of dumbbell shapes that are given by simple, explicit formulas which only depend on $2-$parameters. We remark that these only correspond to approximate equipotential surfaces. The family of dumbbell of our choice could be potentially utilized to find first approximations for irregular shaped asteroids and comets. Furthermore, we can derive formulas for the gravitational potential generated by such shapes at any point in space.

Our approach can be extended to modeling the gravitational potential generated by other families of shapes (depending on more parameters), as well as shapes that are not generated as solids of revolution.

Chapter 6

Electrostatic N-Body Problem and the Poisson Boltzmann equation

In this chapter, we consider a colloidal system. We first give some background information about colloidal system and the Poisson-Boltzmann equation. Then the solutions to the electrostatic potential surrounding a pair of spherical colloidal particles is obtained by using a variational principle to the non-linear Poisson-Boltzmann equation in three dimensions. We consider the Poisson-Boltzmann action integral for the electrostatic potential produced by charged colloidal particles and we propose an analytical ansatz solution, which is controlled by two parameters. The solution to the Poisson-Boltzmann action integral introduces the density and its corresponding electrostatic potential for different fixed parameter. Then we minimize the Poisson Boltzmann action with respect to the parameter, for the fixed potential and fixed separation distance. Furthermore, we study the obtained results and approximate the parameters as functions of tip particle separation and boundary electrostatic potential are obtained by using polynomial-exponential relationship. Provided with this information, we compute tip-particle energy separation and study the stability properties based on the shape of the energy-separation curves.

6.1 Background

6.1.1 Colloidal System

A colloidal system, which is is one of the three primary types of mixtures in chemistry, is a liquid system in which very small particles of one substance are distributed evenly (relatively even) throughout another substance. In this chapter, we focus in a system with particles ranging from 1 to 1000 nano-meters in diameter. In general, there are different types of colloidal systems, such as the solid–liquid dispersions (i.e.suspensions), the liquid–liquid dispersions (i.e.emulsions), and the gas–liquid dispersions (i.e.foams). They also appear in our daily life; paints, milk, proteins as well as fog are some examples of colloids [BS15] [EW94]. Considering a colloidal system, one of the central problems is to determine the stability of colloidal particles. When the particles approach each other, the interaction leads to the rearrangement of charges in the ambient medium, outside the colloidal particles. For instance, these interactions could be determined by the surface charge on the particles and electrolyte concentration. Thus the characteristics of surface charges play an important role on the stability of colloidal particles and thus we note that the effect of the electrical double layers controls electrostatic stabilization. Mathematically, the details of the pair-wise energy as a function of separation of colloidal particles determine the colloidal stability. Thus the number of valleys of such energy curve determines the separations of possible equilibrium or meta-equilibrium.

6.1.2 Poisson-Boltzmann Equation

The electric behaviors and/or the electrostatic stabilization of a suspension of charged colloidal particles in an electrolyte solution depend strongly on the distributions of electrolyte ions and of the electric potential around the particle. Considering the electric potential in solution, the Poisson-Boltzmann is very useful that it consists of the Poisson

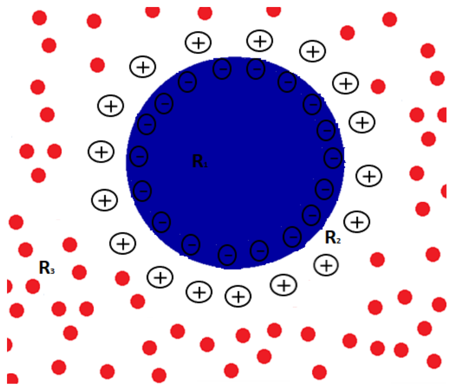

Figure 6.1: A particle with negaitive charges on the surface. It attracts positively charged ions while the red mobile ions are either positively or negatively charged.

equation of electrostatics with the Boltzmann distribution. The PB equation is typically obtained by combining Poisson's equation [Jac] and the Boltzmann factor [Hil60] for the distribution of electrostatic energies at a given temperature. This distribution is important as it determines the interaction between particles in solution. In this section, we aim to derive the Poisson-Boltzmann equation [Hol93].

If a charge distribution $\rho(\vec{r}) = (x, y, z)$ is defined, at the point $\mathbf{r}$, with ϵ as a dielectric constant, we have the Poisson's equation as

$$\nabla^2 \varphi(\mathbf{r}) = -\frac{4\pi}{\epsilon}\rho(\mathbf{r}), \tag{6.1}$$

where $\nabla^2 \varphi(\mathbf{r})$ is the Laplace operator $\nabla^2 \varphi(\mathbf{r}) = \frac{\partial^2 \varphi}{\partial x^2} + \frac{\partial^2 \varphi}{\partial y^2} + \frac{\partial^2 \varphi}{\partial z^2}$. It expresses the relationship between a charge distribution $\rho(\mathbf{r})$ and the electrical potential $\varphi(\mathbf{r})$.

Let R_1 be the region contained a particular ion of the solution. In Figure 6.1, the particle for which we are interested to determine the electrostatic potential from far is located in the region R_1. There is a layer of opposite charged ions attracted to the particle; this layer is refer as R_2. And region R_3 is simply refer as the solvent that contains mobile ions outside the double layer (as shown in Figure 6.1). In the simple case that all mobile ions are univalent, we can refer them as positive and negative ions with charge $+e_c$ and $-e_c$, where e_c is the charge of an electron. Notice that in the three region R_i, for $i = 1, 2, 3$, the electrostatic potential satisfies Gauss' law [Hol93] and we have that in the differential form yields a Poisson's equation as

$$\nabla^2 \varphi(\mathbf{r}) = -\frac{4\pi}{\epsilon}\rho(\mathbf{r}), \tag{6.2}$$

at the point $\mathbf{r}$, where ϵ is the dielectric constant. In order to use the equation (6.1) to determine the potential $\varphi(\mathbf{r})$ in the regions, the charge density functions $\rho(\mathbf{r})$ must be defined for each of the region. Consider the region R_1. For the particle that is represented by a series of N charges c_i at positions r_i, where $c_i = z_i e_c$, $z_i \in \mathbb{R}$, and $i = 1, ..., N$, we can compute the potential in the region R_1 as

$$\varphi_1(\mathbf{r}) = \sum_{i=1}^{N} \frac{c_i}{\epsilon_1 |r - r_i|}, \tag{6.3}$$

where ϵ_1 is the dielectric constant for region 1.

Recall the free space Green's function for the Laplace's equation in $\mathbb{R}^3$,

$$G(\mathbf{r}, \mathbf{r}') = \frac{1}{4\pi} \frac{1}{|\mathbf{r} - \mathbf{r}'|} \tag{6.4}$$

where $\mathbf{r} = (x, y, z)$ is a point in $\mathbb{R}^3$. It is a solution to the equation

$$\bigtriangledown^2 G(\mathbf{r}, \mathbf{r}') = \delta(\mathbf{r} - \mathbf{r}') \tag{6.5}$$

where δ is the Dirac delta function. Now we apply the Laplacian to both side of equation (6.3), we obtain

$$\bigtriangledown^2 \varphi(\mathbf{r}) = \sum_{i=1}^{N} \frac{-4\pi c_i}{\epsilon} \delta(\mathbf{r} - \mathbf{r}_i) \tag{6.6}$$

where δ is the Dirac delta function.

Consider the region R_2. Since it consists of the double layer around the particle, there is no mobile charges of the solvent are present and thus the charge density is given by

$\rho(\mathbf{r}) = 0$. Hence, we have

$$\bigtriangledown^2 \varphi_2(\mathbf{r}) = 0 \tag{6.7}$$

Consider the region R_3. Assuming the bulk concentration of ions is M per cubic centimeter for each of the two ions present, one with charge of $+e_c$, while the other with charge of $-e_c$. The distance between the particle and the ions around play an important role; the amount of positive and negative ions in cubic centimeter differs when getting close to the particle in R_1. In the Debye-Hückel theory, we have the assumption that the concentration of one type of ion close by the particle in R_1 to its concentration far from the region R_1 is encountered by the Boltzmann distribution law:

$$e^{-W_i(\mathbf{r})/[k_B T]}, \tag{6.8}$$

where T is the absolute temperature, k_B is Boltzmann's constant, and $W_i(\mathbf{r})$ is the work required to move the ion of type i from $|r| = \infty, (i.e. \varphi(\mathbf{r}) = 0)$ to the point $\mathbf{r}$. In our simple model, it consists of only two types of ions and we have the required work for the positive ions as

$$W_1(\mathbf{r}) = +e_c \varphi(\mathbf{r})$$

while the required work for the negative ions is given by

$$W_2(\mathbf{r}) = -e_c \varphi(\mathbf{r})$$

Consider the Boltzmann distribution law now, we have $M_+ = Me^{-e_c \varphi(\mathbf{r})/[k_B T]}$, $M_- = Me^{+e_c \varphi(\mathbf{r})/[k_B T]}$, where we assume that $M_+ = M_- = M$ far from the region R_1. Thus, the charge density

$$\begin{aligned}\rho(\mathbf{r}) =&M_+e_c - M_-e_c \\ =&Me_ce^{-e_c\varphi(\mathbf{r})/[k_BT]} - Me_ce^{e_c\varphi(\mathbf{r})/[k_BT]} \\ =&-2Me_c\sinh\left(\frac{e_c\varphi(\mathbf{r})}{k_BT}\right)\end{aligned} \tag{6.9}$$

describes the amount of electric charge at any point in R_3. With this charge density, the Gauss' law for R_3 becomes:

$$\bigtriangledown^2\varphi(R) = -(\frac{8\pi Me_c}{\epsilon})\sinh(\frac{e\varphi(\mathbf{r})}{k_BT}), \tag{6.10}$$

where M is the ion bulk concentration of electrolyte, T is the absolute temperature, e the ion charge magnitude of anions and cations, ϵ is the dielectric constant of the surrounding fluid and k_B is the Boltzmann's constant. The equation (6.10) is known as the non-linear Poisson-Boltzmann equation. It introduces the Boltzmann distribution of ions, which provides the distribution of the electric potential in solution with charged ions present. Being a second-order partial differential equation, the nonline Posson Boltzmann equation has an exact known solution only for one-dimensional geometries. We note that in three dimensions the exact nonlinear Poisson Boltzmann equation is not amenable to analytical solutions, not even for a simple case of having a single colloidal particle in the electrolyte. In higher dimensions, Posson Boltzmann equation is commonly solved numerically. For instance, in the case of having the colloidal particle charge or voltage low, the Poisson Boltzmann equation can be linearized, in which case solutions for spherical [BR73] and cylindrical [BIS08] geometries have also been obtained. We also note that in three dimensions there are analytical and numerical approaches to the nonlinear Poisson Boltzmann equation for the geometry of sphere-plane as in [HC92], [CHS94], [PSCH95] and [Zyp06]. In the next section, we present a method to handle the full nonlinear PB equation in three-dimensions for interacting particles.

6.2 Colloidal System between an Atomic Force Microscope Probe and a Charged Particle

The theoretical prediction of the force between an Atomic Force Microscope probe and a charged particle has been an open problem for scientists and technologists. Particularly, we are interested in the case when both of the Atomic Force Microscope probes are immersed in an electrolytic environment [ZE13]. This problem is of interest due to the importance of understanding the electrostatics biological matters, in which water is inherently present [McL89]. Recently, Atomic Force Microscope has indeed become the de facto metrological tool to probe organic and inorganic matter from the micron down to the nanometer length scales [MVG$^+$16]. In order to measure the interaction forces between the colloidal particles and the electrolyte, we introduce the probe technique; it relies on the use of the Atomic Force Microscope. It has the ability to probe in size ranging from microns to nanomaters because of the sensing element located on the tip and its climax ranges in size of those length-scales.While immersing in an electrolyte, the tip can gain surface charge due to pH. On the other hand, it mayof the Atomic Force Microscope also develop a diffuse charge layer due to the presence of ions in solution [JELZ11]. There is a natural connection between the measurement of Atomic Force Microscopes in liquid and colloidal science while the scientific interest is on the interaction between colloidal particles and their corresponding stability. The Atomic Force Microscope in solution is our main concern and interest, but the results obtained in this chapter are readily usable in the system of colloids. For the example of application in this chapter, we focus on a liquid system in which 1- 1000nm particles are submerged in an ionic solution. As one of the primary type of mixtures in Chemistry, colloidal systems arouse the concern of their stability. In other words, we are interested if the system coagulates or remain indefinitely stable under known conditions, such as concentration.

The presence of charge at their surfaces is the key to determine the stability of colloids; the electrical double layer controls electrostatic stabilization. The rearrangement of charges in the ambient liquid, outside of the colloidal particles occur due to the interaction between particles when they approach each other. Indeed, these interactions are known to depend on the surface charge on the particles and electrolyte concentration. The stability of colloidal systems is fascinating theoretically, and critical for industrial applications.

Consider the pairwise energy as a function of separation of colloidal particles; we can then determine the stability of the colloidal systems [VO48]. In addition, the valleys of such function determine the separations of the possible equilibrium. There are different approaches for obtaining the energy: (i) solve the Poisson-Boltzmann equation, which yields the charge density and electrostatic potential in the liquid surrounding the colloidal particles and (ii) solve the linearized PB equation under some conditions so as to obtain the solutions for certain germetries such as spherical geometry as in [BR73] and cylindrical geometry as in [BIS08]. In the case of a particular geometry of sphere-plane, we notice that in there are analytical and numerical approaches to the nonlinear Poisson Boltzmann equation in the three dimensions as in [HC92], [CHS94], [PSCH95] and [Zyp06].

As a method to tackle the full nonlinear PB equation in three-dimensions for interacting particles, we introduce and present an analytical method— based on the choice of a parametric trial family of functions, we approximate the solution. Consider the two particles with interaction, we introduce an ansatz for the charge density function and the corresponding electrostatic potential parametrically. Then we use the variational method to minimize the Poisson Boltzmann functional with respect to the parameters.

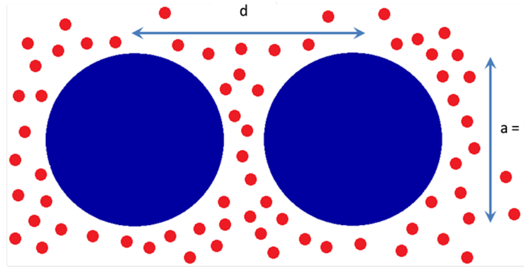

Figure 6.2: Two colloidal particles (large, blue) separated by a distance d. The small red particles represent the ions dissolved in water and are treated as a continuum in the Poisson-Boltzmann approach. These ions could be different, we show them here with the same color for graphical simplicity.

6.3 Electrostatics Potential Produced by a Pair of Colloids

Consider a colloidal particle as shown in Figure 6.1. The schematics of the system of interest— the two charged spherical colloidal particles of unit diameter are separated by a distance d, is shown in Figure (6.2). We remark that the unit of length throughout this section is the particles diameter, or the tip diameter of Atomic Force Microscope. Notice that equation (6.10) can be written as the dimensionless form [McL89] by defining the dimensionless electrostatic potential $\varphi(\mathbf{r}) = \frac{e}{k_B T}\Phi(\mathbf{R})$ and the dimensionless position vector $\mathbf{r} = \sqrt{\frac{8\pi n e^2}{k_B T \epsilon}}\mathbf{R}$,

$$\bigtriangledown^2 \varphi = -\sinh \varphi \tag{6.11}$$

where φ represents the dimensionless electrostatic potential. In equation (6.11) the function φ is a function of $\mathbf{r}$. Since n has units of inverse volume, and ϵ is the absolute dielectric constant of the surrounding fluid, $\frac{8\pi n e^2}{k_B T \epsilon}$ has units of inverse area. Indeed equation (6.11) can be derived from a variational principle, by applying Euler-Lagrange to the action

$$I = \int_{Space} [\frac{1}{2} \mid \bigtriangledown \varphi \mid^2 + \cosh(\varphi) - 1] dV \tag{6.12}$$

where V is the volume. The minimum of I occurs for the function φ that satisfies the Euler-Lagrange equation, which gives rise Equation (6.11). Let z be the axis joining the centers of the two colloidal particles. The axial symmetry of the problem allow us to rewrite the action in cylindrical coordinates as

$$4\pi \int_0^\infty \int_0^\infty [\frac{1}{2} \mid \bigtriangledown\varphi \mid^2 + \cosh(\varphi) - 1]\eta d\eta dz \tag{6.13}$$

where η is the radial polar coordinate in the $xy-$ plane, while the angular polar integration is readily performed and gives 2π. The additional factor of 2 comes from integrating z in half space and multiplying by 2 due to mirror symmetry. For further evaluation, we propose the following ansatz for the density and corresponding electrostatic potential which depends on the parameter k,

$$\varphi(\eta, z) = \varphi_0 e^{-\frac{k}{2}[\sqrt{(z-\frac{d}{2})^2+\eta^2}-\frac{1}{2}][\sqrt{(z+\frac{d}{2})^2+\eta^2}-\frac{1}{2}]} \tag{6.14}$$

where φ_0 is the Dirichlet boundary condition, d is the center-to-center separation between the two spherical colloids and k is a constant that can be interpreted as an inverse Debye length times the radius of the interacting particles. The intuitive justifications for the functional form are: (1) its exponential decay characteristic of ionic screening, (2) that at the surface of the colloids $\varphi(\eta, z) = \varphi_0$ satisfied the proper boundary conditions , and (3) that the electrostatic potential between the two colloids tends to zero as d goes to infinity. Furthermore, a contour plot of the potential around the colloidal particles with respect to different k is shown in Figure 6.3. There are a few reasons of choosing this potential: (1) the potential rapidly approach its bulk value away from the spheres, (2) the electrostatic potential satisfies the Dirichlet boundary conditions, meaning to have a constant value at the surface of the colloidal particles To find the sought solution to the dimensionless Poisson Boltzmann equation (6.11), we minimize the PB action functional with respect to the parameter k. For each of the fixed potential φ_0 and fixed separations d, we find

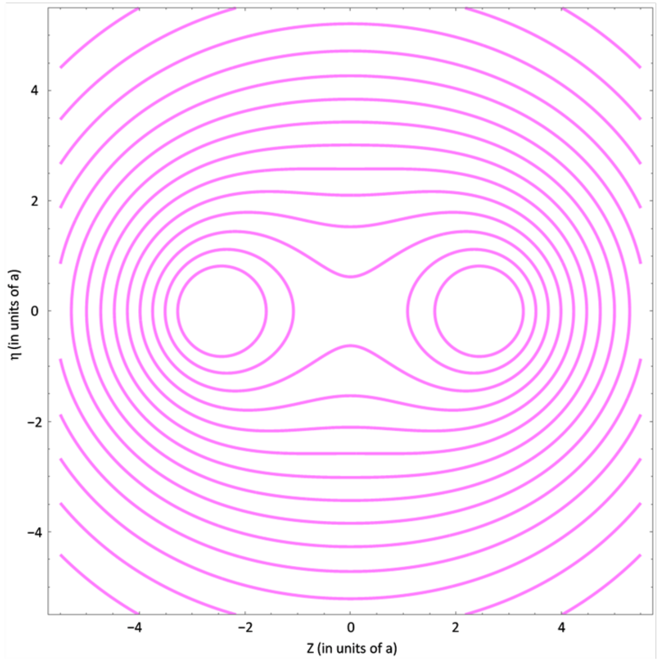

Figure 6.3: Contour plot of $\varphi(\eta, z)$. The potential is constant φ_0 at the surfaces of the particles, becomes spherical far away while decaying to zero.

the constant k (i.e. minimum point $k = k(\varphi_0, d)$) for the proposed $\varphi(x, y)$ that minimizes the action. The obtained data suggests that there is an approximately linear relationship between the best constant k_{best}, and the separation d (with small separations) for each boundary condition φ_0. Such a relationship is shown in Figure 6.4. Furthermore, it leads us to study the relationship between the linear relationship and the boundary condition φ_0. The polynomial approximations for the functions that relate the linear parameters (i.e.the slopes and $\eta-$intercepts) and the boundary conditions are obtained and shown in Figure 6.5. Consider the large separations between the colloidal particles, we find that the best constant k converges to 0.1 for all of the boundary conditions φ_0. We remark that at large separations, we should obtain a simple superposition the potential around a single sphere. So the feature for the best constant k that mentioned should be universal regardless of the model used. As shown in Figure 6.6, the functional forms for the k_{best} can be described by a simple function as follows

$$k_{best} = (A(\varphi) - 0.1)e^{\frac{B(\varphi)}{A(\varphi)-0.1}d} + 0.1 \tag{6.15}$$

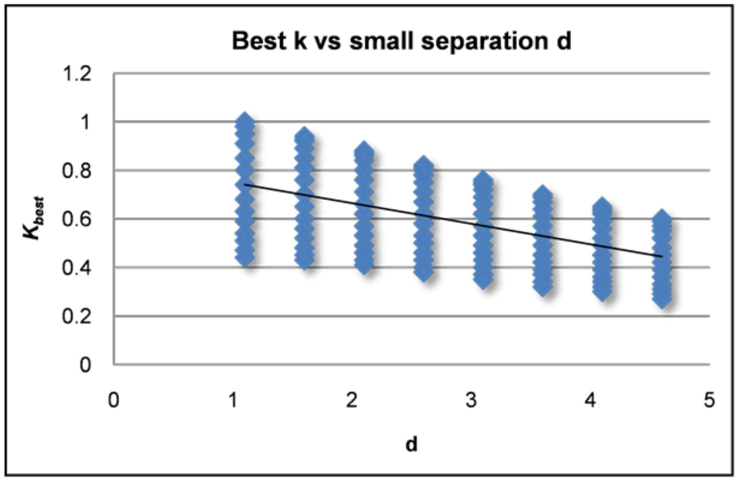

Figure 6.4: Graphs of k_{best} as a function of small separation d, as φ_0 is changed. It shows an approximately linear relationship between k_{best} and small separation d for each φ_0. The black line is drawn to show the average trend between k_{best} and φ_0.

where $A(\varphi)$ is the polynomial approximation between the linear parameter-η-intercepts and φ_0, $B(\varphi)$ is the polynomial approximation between the other linear parameter-slope and φ_0, and d is the center-to-center separation between the two colloids.

6.4 Colloid Interaction Energy

Indeed, the charge distribution cocurs in the whole space that surrounds the colloidal particles. Thus we have the energy as a function of separation d [HC92] given by

$$E_\varphi(d) = \frac{1}{2}\int_{Space} d\mathbf{r}\rho_\varphi(d)V_\varphi(d) \tag{6.16}$$

where we recall that ρ is density and φ is voltage, which are now known from Section 6.3. In order to obtain the colloid interaction energy, the integral (6.16) is evaluated for the corresponding optimal value of k for each of boundary conditions. In fact, equation (6.16) provides the sought sphere-sphere energy-separation curves. These curves are shown in Figure 6.7. The shape of the curves lead us to the conclusions regarding the stability properties predicted by this theory.

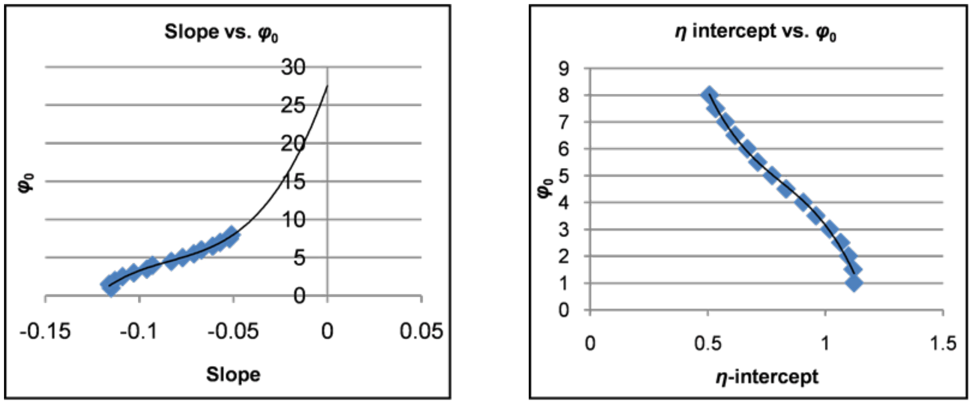

Figure 6.5: (a) Polynomial approximation between the linear parameter-slope and the boundary conditions. This is the slope of k_{best} vs. d (Figure 6.4). (b) Polynomial approximation between the η-intercept and the boundary condition. This is the η-intercept of k_{best} vs d (Figure 6.4).

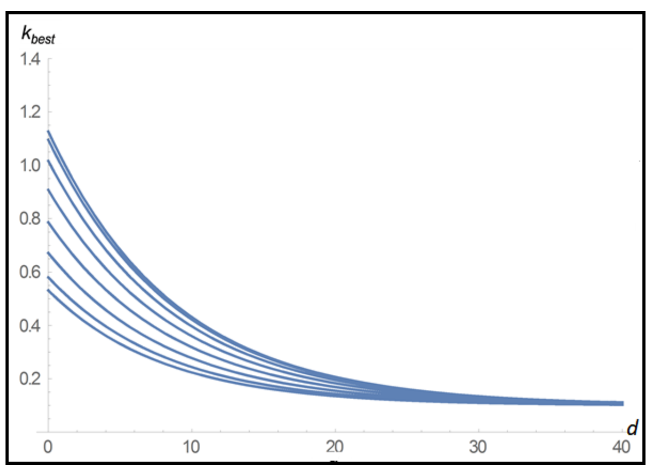

Figure 6.6: With Equation (6.15), curves of k_best as functions of separation d for different boundary condition are sketched. While in Figure 6.4, we show k_{best} vs d only for small d, here we show the whole range of d values, from small to large.

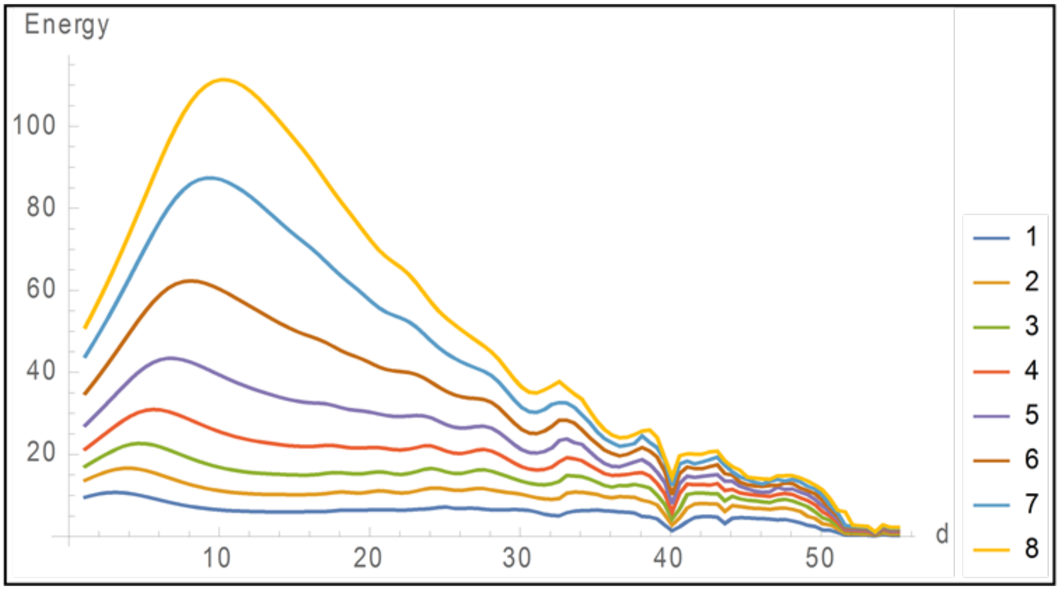

Figure 6.7: The energy-separation curves for φ_0 from 1 to 8.

6.5 Conclusions

In this chapter, we consider the problem of colloidal system that consists of two colloidal particles and we handle the problem by developing a method to tackle the full non-linear Poisson Boltzmann equation in three dimensions for interacting particles. The major quantitative result of this application is shown on Figure 6.7; it shows that the particles attract each other at small separations for all boundary conditions φ_0. We note that this result is consistent with all the published experimental results in the literature as in [IA78]. Furthermore, our results indicate that the energy decreases monotonically for large φ_0 due to the repulsion at large separations. In the case for small φ_0, there are plateaus which suggest the existence of secondary minima [PSCH95]. It is noticeable that there are local minima for all values of φ_0 at distances larger than 30. However, they cannot be expected to represent experimental behavior since they correspond to the distances that is too much larger than the size of the particles. From Figure 6.7, we also remark that the peak positions of the energy curves shift to larger distances as φ_0 increases, which is the same as our expectation. Lastly, in Figure 6.6 we see that the behavior of the screening parameter has a strong dependence on distances and its value reduced by more than 50 percent. This behavior is one of the observations shown in experimental measurements [PSCH95]. Regarding to the contribution to the Atomic Force Microscope community, the results in this chapter are practical by comparing the experimental forces to the derivative of the curves shown in Figure 6.7. In this work, our model here in this chapter is limited to particles of the same size. However, it is clear that the extension of our model to having colloidal particles of two different radii correspond to adding a second parameter to Equation (6.14). With this modification and a proper choice of theoretical curve, by choosing the proper theoretical curve, we can infer the charge of the particle interacting with the Atomic Force Microscope tip.

Bibliography

[Abr90] Marek A Abramowicz. Centrifugal force-a few surprises. *Monthly Notices of the Royal astronomical society*, 245:733, 1990.

[AGST12] John A Arredondo, Jianguang Guo, Cristina Stoica, and Claudia Tamayo. On the restricted three body problem with oblate primaries. *Astrophysics and Space Science*, 341(2):315–322, 2012.

[AH12] Kendall Atkinson and Weimin Han. *Spherical harmonics and approximations on the unit sphere: an introduction*, volume 2044. Springer Science & Business Media, 2012.

[APC13] John Alexander Arredondo and Ernesto Perez-Chavela. Central configurations in the Schwarzschild three body problem. *Qualitative theory of dynamical systems*, 12(1):183–206, 2013.

[APHS16] Md Chand Asique, Umakant Prasad, M. R. Hassan, and Md Sanam Suraj. On the photogravitational R4BP when the third primary is a triaxial rigid body. *Astrophysics and Space Science*, 361(12):379, Nov 2016.

[AW99] George B Arfken and Hans J Weber. Mathematical methods for physicists, 1999.

[Bal94] Georges Balmino. Gravitational potential harmonics from the shape of an homogeneous body. *Celestial Mechanics and Dynamical Astronomy*, 60(3):331–364, 1994.

[BDVV+04] William E Boyce, Richard C DiPrima, Hugo Villagómez Velázquez, et al. *Elementary differential equations and boundary value problems. Ecuaciones diferenciales y problemas con valores en la frontera.* 2004.

[Bel18] Edward Belbruno. *Capture dynamics and chaotic motions in celestial mechanics: With applications to the construction of low energy transfers.* Princeton University Press, 2018.

[BF13] Paul F Byrd and Morris D Friedman. *Handbook of elliptic integrals for engineers and physicists*, volume 67. Springer, 2013.

[BGG15] Jaime Burgos-García and Marian Gidea. Hill's approximation in a restricted four-body problem. *Celestial Mechanics and Dynamical Astronomy*, 122(2):117–141, 2015.

[BIS08] Klemen Bohinc, Aleš Iglič, and Tomaž Slivnik. Linearized poisson boltzmann theory in cylindrical geometry. *Elektrotehniški vestnik*, 1(75):82–85, 2008.

[Boy97a] W. Boyce. Comment on a formula for the gravitational harmonic coefficients of a triaxial ellipsoid. *Celestial Mechanics and Dynamical Astronomy*, 67:107–110, February 1997.

[Boy97b] William Boyce. Comment on a formula for the gravitational harmonic coefficients of a triaxial ellipsoid. *Celestial Mechanics and Dynamical Astronomy*, 67(2):107–110, 1997.

[BP13] A.N. Baltagiannis and K.E. Papadakis. Periodic solutions in the Sun–Jupiter–Trojan asteroid–Spacecraft system. *Planetary and Space Science*, 75:148–157, 2013.

[BR73] Stephen L Brenner and Robert E Roberts. Variational solution of the poisson-boltzmann equation for a spherical colloidal particle. *The Journal of Physical Chemistry*, 77(20):2367–2370, 1973.

[BS15] K Birdi and S. *Handbook of surface and colloid chemistry*. CRC press, 2015.

[BS16] Nakone Bello and Jagadish Singh. On the stability of triangular points in the relativistic R3BP with oblate primaries and bigger radiating. *Advances in Space Research*, 57(2):576–587, 2016.

[BU18] Nakone Bello and Aishetu Umar. On the stability of triangular points in the relativistic R3BP when the bigger primary is oblate and the smaller one radiating with application on Cen X-4 binary system. *Results in Physics*, 9:1067–1076, 2018.

[Cel10] Alessandra Celletti. *Stability and chaos in celestial mechanics*. Springer Science & Business Media, 2010.

[CG18] Alessandra Celletti and Catalin Gales. Dynamics of resonances and equilibria of Low Earth Objects. *SIAM Journal on Applied Dynamical Systems*, 17(1):203–235, 2018.

[CHS94] Kwong-Yu Chan, Douglas Henderson, and Frank Stenger. Nonlinear poisson-boltzmann equation in a model of a scanning tunneling microscope. *Numerical Methods for Partial Differential Equations*, 10(6):689–702, 1994.

[CLPC04] Montserrat Corbera, Jaume Llibre, and Ernesto Pérez-Chavela. Equilibrium points and central configurations for the Lennard-Jones 2- and 3-body problems. *Celestial Mechanics and Dynamical Astronomy*, 89(3):235–266, Apr 2004.

[Dan89] JMA Danby. Book review: Fundamentals of celestial mechanics, /willmann-bell, 1988. *The Observatory*, 109:211, 1989.

[Des15] Pascal Descamps. Dumb-bell-shaped equilibrium figures for fiducial contact-binary asteroids and EKBOs. *Icarus*, 245:64 – 79, 2015.

[DLZ12] R. Dvorak, C. Lhotka, and L. Zhou. The orbit of 2010 TK7: possible regions of stability for other Earth Trojan asteroids. *Astronomy & Astrophysics*, 541:A127, 2012.

[Eas93] Robert W Easton. Introduction to hamiltonian dynamical systems and the n-body problem (kr meyer and gr hall). *SIAM Review*, 35(4):659–659, 1993.

[EHS82] Yoshiharu Eriguchi, Izumi Hachisu, and Daiichiro Sugimoto. Dumb-bell-shape equilibria and mass-shedding pear-shape of selfgravitating incompressible fluid. *Progress of theoretical physics*, 67(4):1068–1075, 1982.

[EW94] D Fennell Evans and Haåkan Wennerström. colloidal domain. 1994.

[G$^+$09] Peter Goldreich et al. Tidal evolution of rubble piles. *The Astrophysical Journal*, 691(1):54, 2009.

[Gei16] Hansjörg Geiges. *The geometry of celestial mechanics*, volume 83. Cambridge University Press, 2016.

[GN12] Marian Gidea and Constantin P Niculescu. A Brief Account on Lagrange's Algebraic Identity. *The Mathematical Intelligencer*, 34(3):55–61, 2012.

[Hal95] Leon M Hall. Special functions. *Available in: http://web. mst. edu/˜ lmhall/SPFNS/spfns. pdf*, 1995.

[HC92] Douglas Henderson and Kwong-Yu Chan. Potential distribution in the solution interface of a scanning tunneling microscope. *Journal of Electroanalytical Chemistry*, 330(1-2):395–406, 1992.

[Hil78] G. W. Hill. Researches in the lunar theory. *American Journal of Mathematics*, 1(1):5–26, 1878.

[Hil60] TL Hill. An introduction to statistical thermodynamics, adison-wesley. *Reading, MA*, 1960.

[Hol93] Michael Jay Holst. Multilevel methods for the poisson-boltzmann equation. *PhDT*, 1993.

[IA78] Jacob N Israelachvili and Gayle E Adams. Measurement of forces between two mica surfaces in aqueous electrolyte solutions in the range 0–100 nm. *Journal of the Chemical Society, Faraday Transactions 1: Physical Chemistry in Condensed Phases*, 74:975–1001, 1978.

[Jac] JD Jackson. Classical electrodynamics (john willey, 1998). *Section*, 8:352–356.

[JELZ11] Keith E Jarmusik, Steven J Eppell, Daniel J Lacks, and Fredy R Zypman. Obtaining charge distributions on geometrically generic nanostructures using scanning force microscopy. *Langmuir*, 27(5):1803–1810, 2011.

[Joh11] Wm Robert Johnston. Asteroids with satellites. *URL: http://www. johnstonsarchive. net/astro/asteroidmoons. html (accessed 31 October 2017)*, 2011.

[JPL] JPL Solar System Dynamics. `https://ssd.jpl.nasa.gov/`. Accessed: 2018-08-01.

[JV97] Angel Jorba and Jordi Villanueva. On the persistence of lower dimensional invariant tori under quasi-periodic perturbations. *Journal of Nonlinear Science*, 7(5):427–473, 1997.

[Kau66] William M Kaula. Theory of satellite geodesy, blaisdell publ. *Co., Waltham, Mass*, 1966.

[KBES12] JR Kuhn, R Bush, M Emilio, and IF Scholl. The precise solar shape and its variability. *Science*, 337(6102):1638–1640, 2012.

[KIB12] Eduardo Kausel and Mirza Irfan Baig. Laplace transform of products of bessel functions: a visitation of earlier formulas. *Quarterly of applied mathematics*, 70(1):77–97, 2012.

[Kre09] Erwin Kreyszig. Advanced engineering mathematics, 10th eddition, 2009.

[LC15] C. Lhotka and A. Celletti. The effect of Poynting-Robertson drag on the triangular Lagrangian points. *Icarus*, 250:249–261, 2015.

[MBW+06] F. Marchis, J. Berthier, M.H. Wong, P. Descamps, D. Hestroffer, F. Colas, I. de Pater, and F. Vachier. Search of binary Jupiter-Trojan asteroids with laser guide star AO systems: A moon around 624 Hektor. In *Bulletin of the American Astronomical Society*, volume 38, page 615, 2006.

[McC63] S.W. McCuskey. *Introduction to celestial mechanics*. Addison-Wesley Series in Aerospace Science. Addison-Wesley, 1963.

[McL89] Stuart McLaughlin. The electrostatic properties of membranes. *Annual review of biophysics and biophysical chemistry*, 18(1):113–136, 1989.

[MDCR+14] F. Marchis, J. Durech, J. Castillo-Rogez, F. Vachier, M. Cuk, J. Berthier, M.H. Wong, P. Kalas, G. Duchene, M.A. Van Dam, et al. The puzzling mutual orbit of the binary Trojan asteroid (624) Hektor. *The Astrophysical journal letters*, 783(2):L37, 2014.

[Mei07] James D Meiss. *Differential dynamical systems*. SIAM, 2007.

[MRPD01] V. V. Markellos, A. E. Roy, E. A. Perdios, and C. N. Douskos. A Hill problem with oblate primaries and effect of oblateness on Hill stability of orbits. *Astrophysics and Space Science*, 278:295–304, 2001.

[MS] TM MacRobert and N Sneddon. Spherical harmonics, 1967.

[MS82] Kenneth R. Meyer and Dieter S. Schmidt. Hill's lunar equations and the three-body problem. *Journal of Differential Equations*, 44(2):263 – 272, 1982.

[MVG+16] Uroš Maver, Tomaž Velnar, Miran Gaberšček, Odon Planinšek, and Matjaž Finšgar. Recent progressive use of atomic force microscopy in biomedical applications. *TrAC Trends in Analytical Chemistry*, 80:96–111, 2016.

[PA13] Jeffrey S Parker and Rodney L Anderson. Targeting low-energy transfers to low lunar orbit. *Acta Astronautica*, 84:1–14, 2013.

[PSCH95] O Pecina, W Schmickler, KY Chan, and DJ Henderson. A model for the effective barrier height observed with a scanning tunneling microscope. *Journal of Electroanalytical Chemistry*, 396(1-2):303–307, 1995.

[Sch16] Daniel J Scheeres. *Orbital motion in strongly perturbed environments: applications to asteroid, comet and planetary satellite orbiters*. Springer, 2016.

[SR76] Ram Krishan Sharma and PV Subba Rao. Stationary solutions and their characteristic exponents in the restricted three-body problem when the more massive primary is an oblate spheroid. *Celestial Mechanics*, 13(2):137–149, 1976.

[Sve18] Drazen Svehla. *Geometrical Theory of Satellite Orbits and Gravity Field*. Springer, 2018.

[T$^+$09] Paolo Tanga et al. Thermal inertia of main belt asteroids smaller than 100 km from iras data. *Planetary and Space Science*, 57(2):259–265, 2009.

[Taf85] Laurence G Taft. Celestial mechanics. *John Wiley and Sons, New York*, 1:437, 1985.

[VO48] EJW Verwey and J Th G Overbeek. Theory of stability of lyophobic colloids' elsevier publishing" co, 1948.

[WB06] James O Wilkes and Stacy G Birmingham. *Fluid Mechanics for Chemical Engineers with Microfluidics and CFD.* Pearson Education, 2006.

[WW02] Edmund Taylor Whittaker and George Neville Watson. *A Course of Modern Analysis: An Introduction to the General Theory of Infinite Series and of Analytic Functions, with an Account of the Principal Transcendental Functions*. University Press, 1902.

[WWZ18] Nan Wu, Xuefeng Wang, and Li-Yong Zhou. Comment on "Out-of-plane equilibrium points in the restricted three-body problem with oblateness (research note)". *Astronomy & Astrophysics*, 614:A67, 2018.

[ZE13] Fredy R Zypman and Steven J Eppell. Electrostatic force curves in finite-size-ion electrolytes. *Langmuir*, 29(38):11908–11914, 2013.

[Zyp06] FR Zypman. Exact expressions for colloidal plane–particle interaction forces and energies with applications to atomic force microscopy. *Journal of Physics: Condensed Matter*, 18(10):2795, 2006.

Appendix I

Some Related Results to Chapter 5

Mass Formula

To find the relationship between the mass and the parameters γ and β, we start with

$$\begin{aligned}\text{Mass} &= \text{Volume} \times \text{density} \\ &= 2 \times \int_0^{z_0} \pi F^2(z) dz \times \rho \\ &= 2\pi\rho \int_0^{z_0} F^2(z) dz\end{aligned} \tag{6.17}$$

Consider the family of function that we proposed to solve the above integral.

$$F(z) = \gamma \sqrt{\left(1 - \left(\frac{z}{z_0}\right)^2\right)\left(1 + \frac{\beta}{1-\beta}\left(\frac{z}{z_0}\right)^2\right)} \text{ , for } 0 < \beta < 1$$

We solve the integral in equation 6.17 for a formula:

$$\begin{aligned}
\int_0^{z_0} F^2(z)dz &= \int_0^{z_0} \gamma^2\left(\left[1-\left(\frac{z}{z_0}\right)^2\right]\left[1+\frac{\beta}{1-\beta}\left(\frac{z}{z_0}\right)^2\right]\right)dz \\
&= \int_0^{z_0} \gamma^2\left(1-\left(\frac{z}{z_0}\right)^2+\frac{\beta}{1-\beta}\left(\frac{z}{z_0}\right)^2-\frac{\beta}{1-\beta}\left(\frac{z}{z_0}\right)^4\right)dz \\
&= \gamma^2\int_0^{z_0} \left(1-\left(\frac{z}{z_0}\right)^2+\frac{\beta}{1-\beta}\left(\frac{z}{z_0}\right)^2-\frac{\beta}{1-\beta}\left(\frac{z}{z_0}\right)^4\right)dz \\
&= \gamma^2-\left(z+\frac{2\beta-1}{3(1-\beta)}\frac{z^3}{z_0^2}-\frac{\beta}{5(1-\beta)}\frac{z^5}{z_0^4}\right)\Bigg|_0^{z_0} \\
&= \gamma^2\left(z_0+\frac{(2\beta-1)z_0}{3(1-\beta)}-\frac{\beta z_0}{5(1-\beta)}\right) \\
&= \gamma^2 z_0\left(1-\frac{2\beta-1}{3(1-\beta)}-\frac{\beta}{5(1-\beta)}\right)
\end{aligned} \tag{6.18}$$

Therefore, we have the mass formula

$$\text{Mass} = 2\pi\rho\gamma^2 z_0\left(1-\frac{2\beta-1}{3(1-\beta)}-\frac{\beta}{5(1-\beta)}\right) \tag{6.19}$$

Potential at z_0

To find the constant Φ_0, that is the gravitational potential energy at z_0. Fig. 6.8 shows

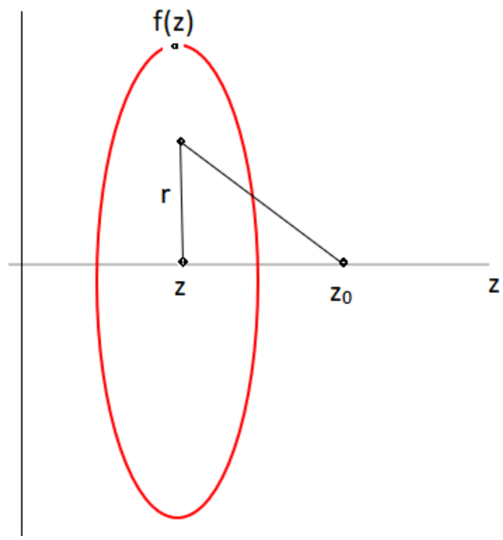

Figure 6.8: For each z and its corresponding $f(z)$, we can locate a point vertically from z such that the length r is less than $f(z)$. Connecting the point to z_0, a right triangle formed. The distance between the point to z_0 is easily obtained by Pythagorean theorem. Since the potential energy is expressed as an integral based on the length of the two vectors $-G\rho\int d^3\vec{r'}\frac{1}{|r-r'|}$ and thus the potential at z_0 can be obtained easily.

that the potential at z_0 can be easily obtained.

$$\begin{aligned}
\Phi_0 &= -2\pi\rho G\int_{-z_0}^{z_0}\int_0^{F(z)} rdrdz\frac{1}{\sqrt{r^2+(z-z_0)^2}} \\
&= -2\pi\rho G\int_{-z_0}^{z_0}\frac{1}{2}\int_0^{F(z)} 2rdrdz(r^2+(z-z_0)^2)^{-1/2} \\
&= -2\pi\rho G\int_{-z_0}^{z_0}\frac{1}{2}\frac{(r^2+(z-z_0)^2)^{1/2}}{\frac{1}{2}}\Bigg|_0^{F(z)} dz \\
&= -2\pi\rho G\int_{-z_0}^{z_0}(\sqrt{F^2(z)+(z-z_0)^2}-\sqrt{0+(z-z_0)^2}dz \\
&= -2\pi\rho G\int_{-z_0}^{z_0}(\sqrt{F^2(z)+(z-z_0)^2}-(z-z_0))dz \\
&= -2\pi\rho G z_0^2\int_{-1}^{1}(\sqrt{(\frac{\gamma}{z_0})^2 f^2(\eta)+(\eta-1)^2}-(\eta-1)d\eta
\end{aligned} \tag{6.20}$$

$$\begin{aligned}
&= -2\pi\rho G z_0^2\alpha^2 \int_{-1}^{1} (\sqrt{(f^2(\eta) + z_0^2(\eta-1)^2} - \frac{\eta-1}{\alpha^2} d\eta \\
&= -2\pi\rho G z_0^2\alpha^2 \int_{-1}^{1} (\sqrt{(f^2(\eta) + (\eta-1)^2}) d\eta + \frac{2}{\alpha^2} \\
&= -2\pi\rho G z_0^2\alpha^2 \int_{-1}^{1} \left(\sqrt{\left(1-\eta^2\right)\left(1+\frac{\beta}{1-\beta}\eta^2\right) + (\eta-1)^2}\right) d\eta + \frac{2}{\alpha^2} \\
&= -2\pi\rho G z_0^2\alpha^2 \left[\sqrt{\frac{1}{1-\beta}} \int_{-1}^{1} d\eta \sqrt{(1-\eta)^2(1-\beta) + (1-\beta+\beta\eta^2)(1-\eta^2)}\right]
\end{aligned} \tag{6.21}$$

Let $G = (1-\eta^2)(1-\beta+\beta\eta^2)$. We aim to solve the integral

$$\int_{-1}^{1} \sqrt{G + (1-\beta)(1-\eta)^2} d\eta. \tag{6.22}$$

Although the integral is not elemental, we apply numerical approach for solving it. Consider the expression of $\sqrt{G + (1-\beta)(1-\eta)^2}$ as a power series of β up to degree 8^{th}. Notice that the integral is indeed finite and regular for $0 \leqslant \beta \leqslant 1$. Hence, we can solve the integral numerically. First, for $\beta = 0$ we have a simplified integral (6.22) as follows:

$$\begin{aligned}
\int_{-1}^{1} (1-\eta^2) + (1-\eta)^2 dz &= \int -1^1 \sqrt{1-\eta^2+1-2\eta+\eta^2} d\eta \\
&= \int_{-1}^{1} \sqrt{1-2\eta+1} d\eta \\
&= \int_{-1}^{1} \sqrt{2-2\eta} d\eta \\
&= -\frac{1}{2} \int_{-1}^{1} 2\sqrt{2-2\eta} d\eta \\
&= -\frac{1}{2}\frac{2}{3}(2-2\eta)^{3/2}\Big|_{-1}^{1} \\
&= -\frac{1}{3}\left[(2-2(1))^{3/2} - (2-2(-1))^{3/2}\right] \\
&= \frac{8}{3}
\end{aligned} \tag{6.23}$$

Next, for $\beta = 1$ we have a simplified integral (6.22) as follows:

$$\int_{-1}^{1} \sqrt{(1-\eta^2)\eta^2} d\eta = \int_{-1}^{1} \eta\sqrt{1-\eta^2} d\eta \tag{6.24}$$

Let $\sqrt{1-\eta^2}$ be $\cos\theta$, we have

$$\int_{-1}^{1} \sqrt{(1-\eta^2)\eta^2} d\eta = \int \cos^2\theta \sin\theta d\theta \tag{6.25}$$

Taking integration by parts, we obtain

$$\begin{aligned} \int \cos^2\theta \sin\theta d\theta &= -\cos^3\theta - 2\int \cos^2 \sin\theta d\theta \\ \Longrightarrow 3\int \cos^2\theta \sin\theta d\theta &= -\cos^3\theta \\ \Longrightarrow \int \cos^2\theta \sin\theta d\theta &= -\frac{1}{3}\cos^3\theta \\ &= -\frac{1}{3}(\sqrt{1-\eta^2})^3 \end{aligned} \tag{6.26}$$

Since the integral (6.24) is evaluating a symmetric function from -1 to 1 and thus we will have to split the integral for further computation.

$$\begin{aligned} \int_{-1}^{1} \sqrt{(1-\eta^2)\eta^2} d\eta &= \int_{-1}^{0} \sqrt{(1-\eta^2)\eta^2} dz + \int_{0}^{1} \sqrt{(1-\eta^2)\eta^2} d\eta \\ &= -\frac{1}{3}(\sqrt{1-\eta^2})^3\Big|_{-1}^{0} - \frac{1}{3}(\sqrt{1-\eta^2})^3\Big|_{0}^{1} \\ &= 0 + \frac{1}{3} + \frac{1}{3} - 0 \\ &= \frac{2}{3} \\ &= \left(\frac{8}{3}\right)\left(\frac{1}{4}\right) \end{aligned} \tag{6.27}$$

Now, back to the integral (6.22). As $\beta = 0$, we have the solution to the integral (6.22) as $\frac{8}{3}$. Thus we consider the power series of $\sqrt{G + (1-\beta)(1-\eta)^2}$ with an coefficient of $\frac{3}{8}$. Hence, we have

$$
\begin{aligned}
&\int_{-1}^{1}\frac{3}{8}\sqrt{F+(1-\beta)(1-\eta)^2}d\eta\\
=&\int_{-1}^{1}\Bigg(\frac{3\sqrt{1-\eta}}{4\sqrt{2}}+\frac{3\sqrt{1-\eta}(\eta-1)(2+2\eta+\eta^2)\beta}{16\sqrt{2}}\\
&-\frac{3\sqrt{1-\eta}(\eta-1)(2+2\eta+\eta^2)^2\beta^2}{128\sqrt{2}}+\frac{3\sqrt{1-\eta}(\eta-1)^3(2+2\eta+\eta^2)^3\beta^3}{512\sqrt{2}}\\
&-\frac{15\sqrt{1-\eta}(\eta-1)^4(2+2\eta+\eta^2)^4\beta^4}{8192\sqrt{2}}+\frac{21\sqrt{1-\eta}(\eta-1)^5(2+2\eta+\eta^2)^5\beta^5}{32768\sqrt{2}}\\
&-\frac{63\sqrt{1-\eta}(\eta-1)^6(2-2\eta+\eta^2)^6\beta^6}{262144\sqrt{2}}+\frac{99\sqrt{1-\eta}(\eta-1)^7(2+2\eta+\eta^2)^7\beta^7}{1048576\sqrt{2}}\\
&-\frac{1287\sqrt{1-\eta}(\eta-1)^8(2+2\eta+\eta^2)^8\beta^8}{33554432\sqrt{2}}+\text{H.O.T}\Bigg)d\eta\\
=&\frac{3}{8}\Bigg[1-\frac{19\beta}{42}-\frac{12643\beta^2}{120120}-\frac{3846727\beta^3}{77597520}-\frac{1258610741\beta^4}{42833831040}-\frac{215565834613\beta^5}{11002175458560}\\
&-\frac{7621848478843\beta^6}{542773989288960}-\frac{1838899975043737\beta^7}{173983735112079360}-\frac{4065005867152492813\beta^8}{493150205493069250560}+\mathscr{O}(\beta^9)\Bigg]
\end{aligned}
\tag{6.28}
$$

To find the coefficient for β^9, we simply use the fact that value to the integral (6.22) is $\frac{2}{3}$.

For $\beta = 1$, we have

$$
\begin{aligned}
\frac{3}{8}\int_{-1}^{1}\sqrt{G+(1-\beta)(1-\eta)^2}d\eta &= \frac{3}{8}\\
\Longrightarrow \int_{-1}^{1}\sqrt{G+(1-\beta)(1-\eta)^2}d\eta &= \frac{1}{4}\\
\Longrightarrow \frac{3}{8}\Bigg[1-\frac{19\beta}{42}-\frac{12643\beta^2}{120120}-\frac{3846727\beta^3}{77597520}-\frac{1258610741\beta^4}{42833831040}&\\
-\frac{215565834613\beta^5}{11002175458560}-\frac{7621848478843\beta^6}{542773989288960}-\frac{1838899975043737\beta^7}{173983735112079360}&\\
-\frac{4065005867152492813\beta^8}{493150205493069250560} &= \frac{1}{4}\\
\Longrightarrow \text{coefficient of}\beta^9 &= \frac{316456352318138813}{5191054794663886848}
\end{aligned}
$$

And therefore for we have the 9^{th} degree polynomial solution to the integral (6.22) as

$$\frac{3}{8}\Bigg[1-\frac{19\beta}{42}-\frac{12643\beta^2}{120120}-\frac{3846727\beta^3}{77597520}-\frac{1258610741\beta^4}{42833831040}-\frac{215565834613\beta^5}{11002175458560}$$
$$-\frac{7621848478843\beta^6}{542773989288960}-\frac{1838899975043737\beta^7}{173983735112079360}-\frac{406500586715249281 3\beta^8}{493150205493069250560}$$
$$+\frac{316456352318138813\beta^9}{5191054794663886848}\Bigg]. \tag{6.29}$$

Thus it provides the polynomial up to degree 9^{th} as a numerical solution to the integral that we intended to solve.